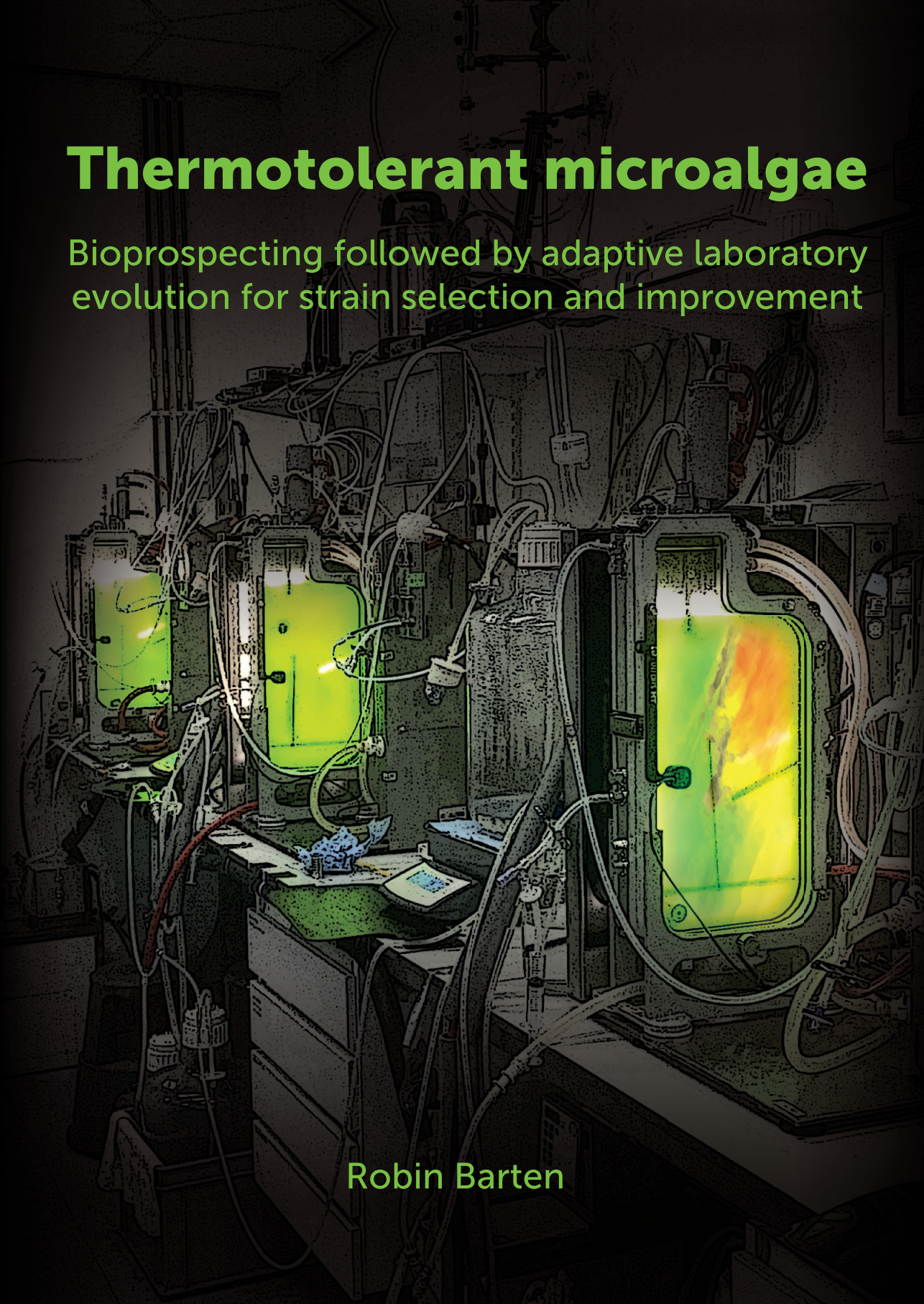# Thermotolerant microalgae

Bioprospecting followed by adaptive laboratory evolution for strain selection and improvement

Robin Barten

Propositions

1. Thermotolerant microalgae are the strongest solution to culture overheating caused by solar irradiance
   (this thesis)

2. Adaptive laboratory evolution is the best method to improve microalgal strain robustness
   (this thesis).

3. An annual science retreat should be a compulsory part of the TSP for PhD candidates.

4. Strict enforcement of proposition criteria inhibits their creative purpose.

5. It is in human nature to always strive for more luxury despite its environmental footprint.

6. Peanut butter tastes better in the Caribbean.

7. Efficiency is about cutting corners.

Propositions belonging to the thesis entitled

Thermotolerant microalgae - Bioprospecting followed by adaptive laboratory evolution for strain selection and improvement

Robin Barten
Wageningen, 7 September 2022

Thermotolerant microalgae

Bioprospecting followed by adaptive laboratory evolution for strain selection and improvement

Robin Barten

Thesis committee

Promotors
Prof. Dr. M.J. Barbosa
Personal Chair, Bioprocess Engineering Group
Wageningen University & Research

Prof. Dr. R.H. Wijffels
Professor of Bioprocess Engineering
Wageningen University & Research

Other members
Prof. Dr J.A.G.M de Visser, Wageningen University & Research
Dr D. Van de Waal, Netherlands Institute of Ecology, Wageningen
Dr C. Sagt, DSM, Delft
Prof. Dr M.C. Posewitz, Colorado School of Mines, USA

This research was conducted under the auspices of the Graduate School Food Technology Agrobiotechnology Nutrition and Health Science.

Thermotolerant microalgae

Bioprospecting followed by adaptive laboratory evolution for strain selection and improvement

Robin Barten

Thesis
Submitted in fulfilment of the requirements for the degree of doctor
at Wageningen University
by the authority of the Rector Magnificus,
Prof. Dr A.P.J. Mol,
in the presence of the
Thesis Committee appointed by the Academic Board
to be defended in public
on Friday 7 September 2022
at 4 p.m. in the Aula

Table of contents

Chapter 1

General introduction and thesis outline

1.1. The potential of microalgae

Microalgae have been recognized as a promising nutrient-rich "crop" for decades now [1]. Microalgal biomass is rich in protein, fatty acids and carbohydrates [2]. Furthermore, microalgal biomass contains valuable components such as pigments, omega-3 fatty acids and sterols. Potential applications of microalgal biomass are found in food, feed, and chemical processes. A major advantage of microalgae over traditional food crops is the high yield on light, which means that microalgal biomass can be produced with areal productivities that significantly outperform traditional food crops [3].

Despite the potential of microalgal biomass, it is currently only produced for niche markets. Production of microalgal biomass is expensive, which hinders commercial implementation on the market for bulk products. Techno-economic analysis project theoretical production costs of 3.4 euro per kg for commercial-scale (>10 ha) [4]. However, commercial facilities at such a scale are currently non-existent. The cost price of microalgal biomass has to be reduced significantly before it becomes commercially attractive for the bulk market [2]. Several targets for cost price reduction were determined through these techno-economic models. Examples of such targets are increased photosynthetic efficiency and higher tolerance to stressful temperatures. In addition, technical process improvements such as scale-up for benefits of increased facility size, a reduced light path, reduced airflow, use of flue gas, reduced cleaning frequency, use of wastewater, and reduced inoculum size would reduce process costs [4].

The highest areal biomass productivities can be reached in regions with long periods of high solar irradiance levels. However, due to high solar irradiance, the microalgal photobioreactor cultures heat to temperatures above 45°C [5]. Such high temperatures affect microalgal productivity and can lead to culture collapse. Most currently used microalgal species have a temperature optimum between 20°C to 30°C [6]. The temperature in photobioreactors is controlled through cooling to prevent a negative impact on microalgal productivity. Photobioreactor cooling is expensive and has a significant environmental impact. It should therefore be avoided as much as possible. To illustrate the impact of cooling on process operational costs, techno-economic model simulations revealed that a cost reduction of 31% can be achieved when algal species can maintain high growth rates up to 45°C, instead of 30°C, using the south of Spain as a cultivation location [4].

With this thesis, we addressed the impact of heat on productivity and physiology of microalgae. We studied the effect of supra-optimal temperature on microalgal physiology both in the short and long term. Robust thermotolerant microalgal strains were proposed as a solution to reduce cooling costs for microalgal production. The island of Bonaire was chosen a model location for research on microalgal cultivation in saline water under high light and high-temperature conditions. Seasonal fluctuations are minimal on this island as Bonaire is located in the Caribbean Sea, on the equator. The absence of significant seasonal fluctuations allows for continuous operation of cultivation systems under "summer" conditions. Daytime temperatures range from 28°C to 36°C. The solar day lasts 12 hours with an average daily irradiance of ~40 $mol.m^{-2}.d^{-1}$.

1

1.2. The effect of temperature on microalgal productivity and physiology

1.2.1. The impact of temperature on microalgal growth

Each species has its own specific minimal (T_{min}), optimal (T_{opt}), and maximal (T_{max}) temperature for growth (Figure 1.1) [6, 7]. The growth rate at temperatures around the optimal growth temperature presents a plateau where small fluctuations have little effect on growth. For efficient growth and, therefore, maximal productivity, the culture must remain near the optimal growth temperature during daytime. A temperature below or above the optimal growth temperature reduces microalgal growth. Below T_{min} the growth rate becomes negative, which results in decay. Cells will eventually die when the temperature remains lower than T_{min} due to the inability for growth and cell stress. Similar effects are observed when the temperature increases above T_{max}. However, high temperatures have a more disastrous impact and cells will die rapidly when high temperatures are sustained [6].
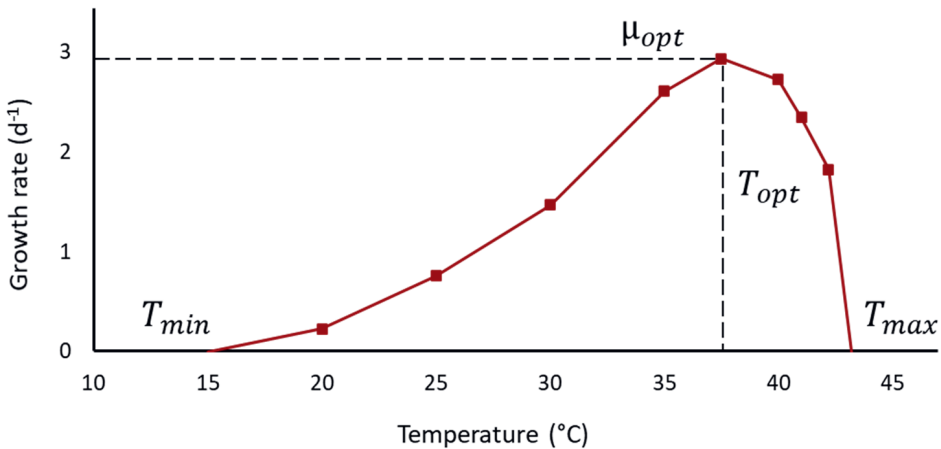
Figure 1.1: *Temperature effect on the growth rate of Picochlorum sp. BPE23 (**Chapter 7**). Cells were grown under a continuous irradiance of 200 μmol.m⁻².s⁻¹. The minimal temperature (T_{min}), Maximal temperature (T_{max}), optimal temperature (T_{opt}), and optimal growth rate ($μ_{opt}$) are displayed in the graph.*

## 2.2. Microalgal growth parameters to simulate growth in models

Mathematical growth models can simulate microalgal growth under specific conditions that can be used to assess the potential of specific bioreactor configurations of microalgal strains. A model is only accurate when the input parameters are accurate. Such parameters have to be obtained through dedicated laboratory experiments. Examples of biological growth parameters that are important for growth models are: μ_{opt}, T_{min}, T_{max}, T_{opt}, but also the specific maintenance rate (μ_e), maximal specific growth rate (μ_{max}), maximal biomass yield on light are ($Y_{x,ph}$), and specific absorption cross-sectional area. Depending on the modeled situation, more parameters have to be determined.

1.2.3. The microalgal heat stress response

Exposure to supra-optimal temperature disrupts cellular homeostasis. Different microalgae express different coping mechanisms. However, when generalizing few effects on cellular physiology are: destabilization of the cell membrane due to increased membrane fluidity, changes in enzymatic activity due to deformation of enzymes, errors in protein folding (Figure 1.2)[8-10]. The induced stress response causes system-wide changes that result in decreased cellular fitness. Microalgal cells have evolved protecting mechanisms to prevent permanent cellular damage and even cell death. The initial stress response within hours of being triggered involves minimizing cell damage. Whereafter cellular acclimation is initiated over the following days.

Several protection and acclimation mechanisms are activated in response to the disturbed cellular homeostasis due to heat stress. Heat shock proteins are produced that perform a chaperoning function [11, 12]. Chaperoned enzymes temporarily gain protection to denaturation up to higher temperatures. Proteases degrade denatured proteins to prevent the accumulation of denatured protein products within the cell. As a consequence of decreased capacity of the central metabolism to process energy into biomass, an energy surplus is present from the photosynthetic machinery with the formation of harmful reactive oxygen species (ROS) as a result [13]. Quenching and ROS scavenging mechanisms are activated to prevent ROS accumulation. Production of filtering pigments ensures lower light availability for the photosystems, whereas antioxidants such as carotenoids and enzymes (catalase, superoxide dismutase, and peroxidase) degrade produced ROS

[14, 15]. Reduction of the energy inflow is not instantaneous. Therefore, the energy surplus is temporarily transferred to storage compounds such as lipids and carbohydrates, which serve as a temporary electron sink [8, 12]. Temperature increases fluidity of all cell membranes, affecting their functionality as a barrier and binding enzymes and protein complexes. To stabilize membranes, the fatty acid and sterol composition are remodeled.
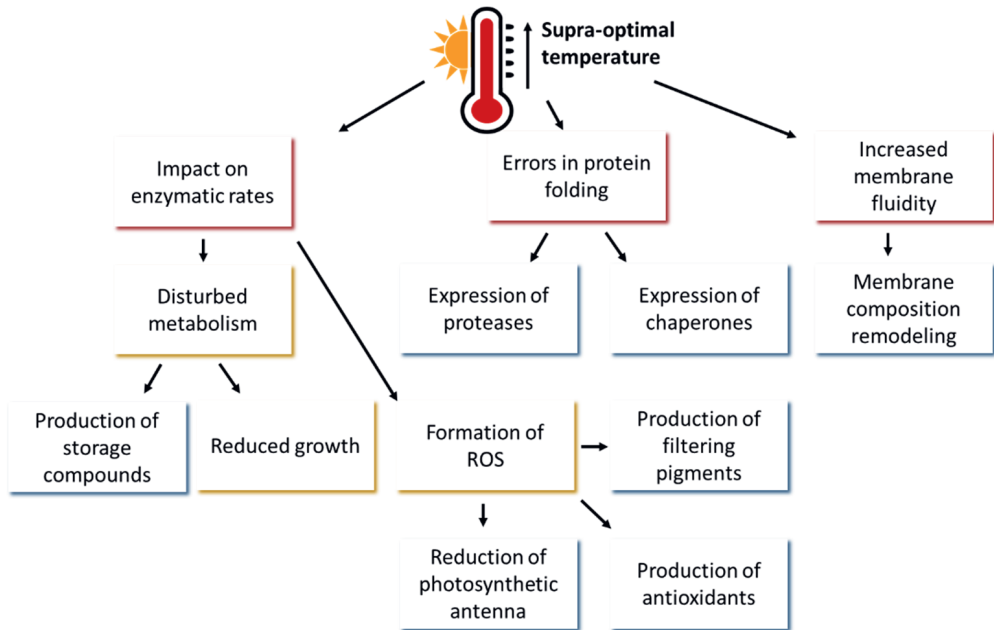

Figure 1.2: *The impact of supra-optimal temperature on microalgal physiology combined with the microalgal protection mechanism and its acclimation response. Boxes in red display the impact of supra-optimal temperature on the cell, boxes in yellow display the consequence of this impact, boxes in blue display the cellular response to counteract the adverse effects.*

1.3. Selection and improvement of robust microalgae

1.3.1. Bioprospecting

Bioprospecting is done to obtain new and novel microalgal species with specific growth characteristics and the desired biomass composition. Successful bioprospecting projects depend on careful and efficient selection to obtain strains with the desired traits. Sampling locations with extreme growth conditions increase the chance to find species that grow optimally under such conditions (Figure 1.3). To increase the chance of obtaining strains with desired growth characteristics, it is best to perform an enrichment procedure before isolating individual strains. For example, if thermotolerant strains are desired then the bioprospected sample should be grown under high temperatures for multiple generations to eliminate all non-thermotolerant strains and give thermotolerant species the opportunity to become more dominant in the cell culture. A wide variety of species have been isolated with robustness against stress factors such as high or low salinity levels, temperature, pH, light, or toxic compounds [16-18]. In addition, combining selection for growth parameters with selection based on biomass composition can yield more interesting strains. Growth experiments, fluorescence associated cell sorting and chromatography-based methods are popular techniques to characterize microalgal potential. Special attention is often given to lipid content, fatty acid content and pigment composition because their value [16]. Also, proteins, carbohydrates and unique compounds are of interest for commercialization [2].
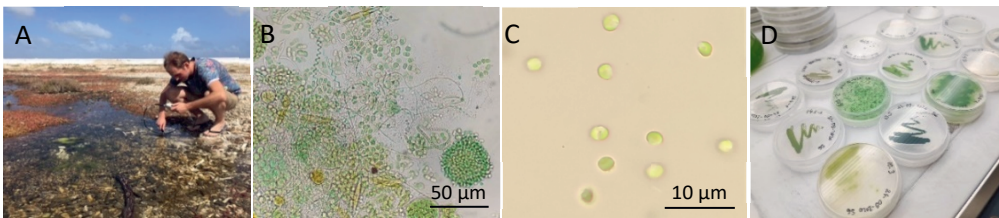
Figure 1.3: *(A) Bioprospecting by sampling in warm saline water bodies on Bonaire. (B) Microscopic image of a mixed cell culture at the start of the enrichment phase. (C) Microscopic image of isolated Picochlorum sp. BPE23 cells. (D) Isolated microalgal strains conserved on agar plates.*

1.3.2. Picochlorum

In this thesis microalgae were bioprospected on Bonaire with the intention for cultivation photobioreactors that reach temperatures of 45°C to 50°C. *Picochlorum sp. BPE23* was selected from the generated culture collection due to its high growth rate in combination with its effortless growth in photobioreactor systems. Species of Picochlorum are trending because of its robustness and high growth rate. This diploid green microalga falls within the taxon of *Chlorophyceae*. Currently, 5 assembled genomes are available. Species of *Picochlorum* are known for being robust and commonly exhibit tolerance to high light levels, have a high upper-temperature tolerance of up to 47.5°C under diel cycles, and have a high tolerance to fluctuating salinity levels in a range of 3.5 to 105 ppt [19-21]. Furthermore, species of *Picochlorum* exhibit growth rates of up to 8 d^{-1} which is unique in the field of microalgae [21]. While wildtype strains of *Picochlorum* produce fatty acids and carbohydrates, its main biomass component is protein (**Chapter 2**). Adverse growth conditions such as nitrogen depletion or temperature stress induce accumulation of storage compounds [22]. However, other commonly used microalgal species such as *Nannochloropsis* and *Neochloris* naturally accumulate higher levels of such compounds.

1.3.3. Adaptive laboratory evolution

Strain improvement is inevitable when optimizing the microalgal cultivation process. Adaptive laboratory evolution (ALE) is a technique to improve microbial phenotypes by utilizing natural genetic mutations. As such, no prior genetic knowledge is required for strain improvement. By the introduction of selective pressure, the growth rate of the microalgae will reduce. Mutated cells with improved physiology arise due to the gain in fitness under the applied stress conditions. Cell cultures are typically grown in periodically diluted photobioreactors or erlenmeyers to ensure continuous selection takes place.

ALE was adopted to improve microalgal growth characteristics over the past years [23]. This technique is especially suitable to promote robustness in microorganisms due to the inherent selection for growth rate under specific growth conditions. Microalgal cultivations benefit significantly from fast-growing robust strains because microalgal cultivation at commercial-scale is prone to environmental influences. Common targets for phototrophic microalgal ALE experiments are strain

characteristics related to a tolerance to a specific compound or culture conditions. Examples of such characteristics are: (1) tolerance to flue gas, (2) tolerance to high or low temperatures, (3) tolerance to high CO_2 levels, (4) tolerance to high salinity levels, (5) tolerance to high or low pH, tolerance to high light, (7) tolerance to toxic compounds such as herbicides, and (8) specific growth rate [23-25].

Cells acclimate to a new homeostatic phase after exposure to stressful conditions, and given time, also adapt genetically. Whereas phenotypic acclimation takes place over a few generations, genetic adaptation takes significantly longer. In the case of *Picochlorum costavermella*, a mutational rate of $10.12 \cdot 10^{-10}$ nucleotide per generation leads to 74 generations for a single mutation to emerge [26]. However, the large number of cells present in cell cultures increases the chance for beneficial mutations. In addition, the mutational rate increases under stressful conditions [27]. Typical ALE experiments last for several months in which hundreds of generations are cultivated. ALE experiments commonly are not extended into the range of a thousand generations as each consecutive mutation has a reduced positive effect on physiology. ALE experiments with thousands of generations showed that such prolonged selection pressure for growth under a single stress factor commonly produces specialist phenotypes [28]. The number of generations required before new phenotypes emerge in a mixed culture can lead to ALE experiments that last for multiple months, or years for species with a low growth rate.

ALE experiments have a high success rate, making them increasingly popular within the field of biotechnology. In addition, generation of strains with improved growth characteristics, comparison of the evolved strains with the parental strain allows for the identification of adaptation mechanisms [29, 30]. Identification of adaptation mechanisms through a multi-omics approach is already being done in model organisms such as *Escherichia coli* and *Saccharomyces cerevisiae*. However, the full potential of ALE has not been utilized yet in microalgal ALE studies. Most studies only report growth and biomass composition changes, occasionally assisted by transcriptomics changes [23]. As such, microalgal evolutionary mechanisms to supra-optimal temperature are currently unknown.

1.4. Aim and thesis outline

In this thesis, we aimed to reduce cooling costs for microalgal biomass production by utilizing thermo-tolerant species. To achieve this, thermo-tolerant species were bioprospected and consecutively improved through ALE. We studied and elucidated cellular coping mechanisms in response to supra-optimal temperature for the selected microalgae: *Picochlorum sp. BPE23*. For this purpose, we subjected *Picochlorum sp. BPE23* to various temperature regimes in different time frames, from hours to months (Figure 1.4).

In **chapter 2**, we performed a bioprospecting project on Bonaire to isolate thermo-tolerant microalgal and cyanobacterial species. A selection procedure with high temperature was performed to screen for species that grew optimally in photobioreactors in the Bonairean climate. Capability to grow under mid-day peak temperatures of up to 45°C were desired. For this, we assessed the growth rate over a temperature range of 25°C to 45°C. These temperatures were maintained continuously while the day/night cycle was simulated as a 12/12 block. In addition to the growth rate, the microalgal biomass composition was characterized.

In **chapter 3**, the selected strain, *Picochlorum sp. BPE23*, was subjected to 4 diel cycles with different mid-day peak temperatures to mimic growth conditions in a photobioreactor on Bonaire with different levels of cooling. We monitored the cell physiology over a period of 24 hours by 2-hourly sampling.

To evaluate the potential of *Picochlorum sp. BPE23* as a commercial production strain, the growth parameters: maximal specific growth rate, maintenance rate, yield on light, and specific absorbing cross-sectional area were determined experimentally in **chapter 4**. In addition, growth parameters were also determined for two relevant industrial microalgal species *Nannochloropsis sp.* and *Neochloris oleoabundans* for comparison. Growth predictions were performed using a pre-existing microalgal growth model in combination with the newly obtained growth parameters. Productivity and photosynthetic efficiency were predicted for cultivation in flat-panel photobioreactors using the light conditions as found on Bonaire.

In **Chapter 5**, the physiologic response of *Picochlorum sp. BPE23* was studied after exposure to a supra-optimal temperature of 42°C for an extended period of 120 hours, whereas the optimal growth temperature of *Picochlorum sp. BPE23* is 38°C. We elucidated the protection and acclimation mechanisms that *Picochlorum sp.*

BPE23 utilizes to cope with supra-optimal temperature. To do so, the following strain characteristics were studied: growth characteristics (cell volume, cell number, growth rate quantum yield), cell composition (fatty acids and pigments) and transcriptional changes.

Adaptive laboratory evolution experiments were done to improve the thermal tolerance of *Picochlorum sp. BPE23*. In **chapter 6**, improvement of tolerance to high diel peak temperatures was addressed. ALE was performed using circadian temperature and light cycles. The mid-day peak temperature was 47.5°C at the start of the ALE experiment, whereas the cell culture grew at 49 °C at the end. Clones isolated from the ALE cell culture were subjected to strain characterization experiments in which growth and physiology were studied over a range of diel peak temperatures.

In addition to ALE with natural diel cycles, a second ALE experiment was performed using continuous light and temperature (**chapter 7**). The temperature was shifted from 42 °C to 44.6 °C in small steps over 322 days. The temperature shifts were done when the cell culture fitness level (i.e., growth rate) had stabilized. After isolation of clones from the stable cell culture at 44.6°C, growth rates were screened over a temperature range from 20 °C to 45 °C. To elucidate mechanism behind the increased thermal tolerance, two selected clones and the wildtype strain were characterized. We applied a multi-omics approach involving whole-genome sequencing, transcriptomics, growth kinetics, and biomass composition analysis.

Finally, **chapter 8** concludes this thesis with a general discussion. Current challenges related to climatological influence on commercial microalgal production processes are discussed. Bioprospection and adaptive laboratory evolution are presented to make microalgal strains more robust to fluctuating and stressful growth conditions.

Chapter 2
Bioprospection and characterization
- Tolerance to temperature
- Growth rate
- Biomass composition

Chapter 3
Growth parameter estimation
- Maximal growth rate
- Maintenance coefficient
- Yield on light
- Absorption cross-sectional area
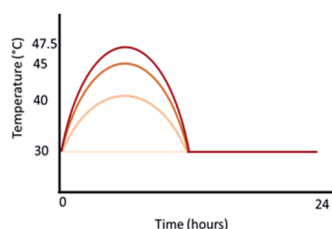
Chapter 4
Diel cycles over a 24-hour period
- Growth rate
- physiology
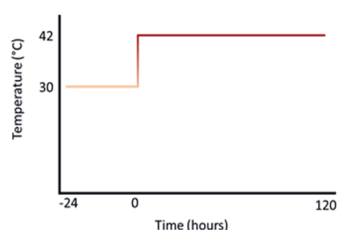
Chapter 5
Effect of a heat shock on physiology
- Growth rate
- Transcriptome
- Pigmentation
- Fatty acid composition
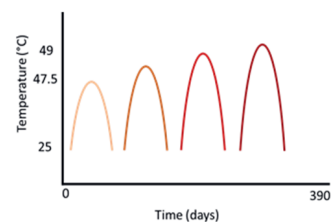
Chapter 6
ALE to increase tolerance to diel temperature cycles
- Tipping point
- Growth
- Cell size
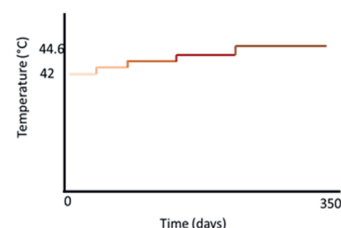
Chapter 7
ALE to shift the upper temperature limit under continuous temperature stress
- Growth
- Composition
- Transcriptome
- Genome

Figure 1.4: *The temperature regimes that were applied to study microalgal growth in the chapters of this thesis.*
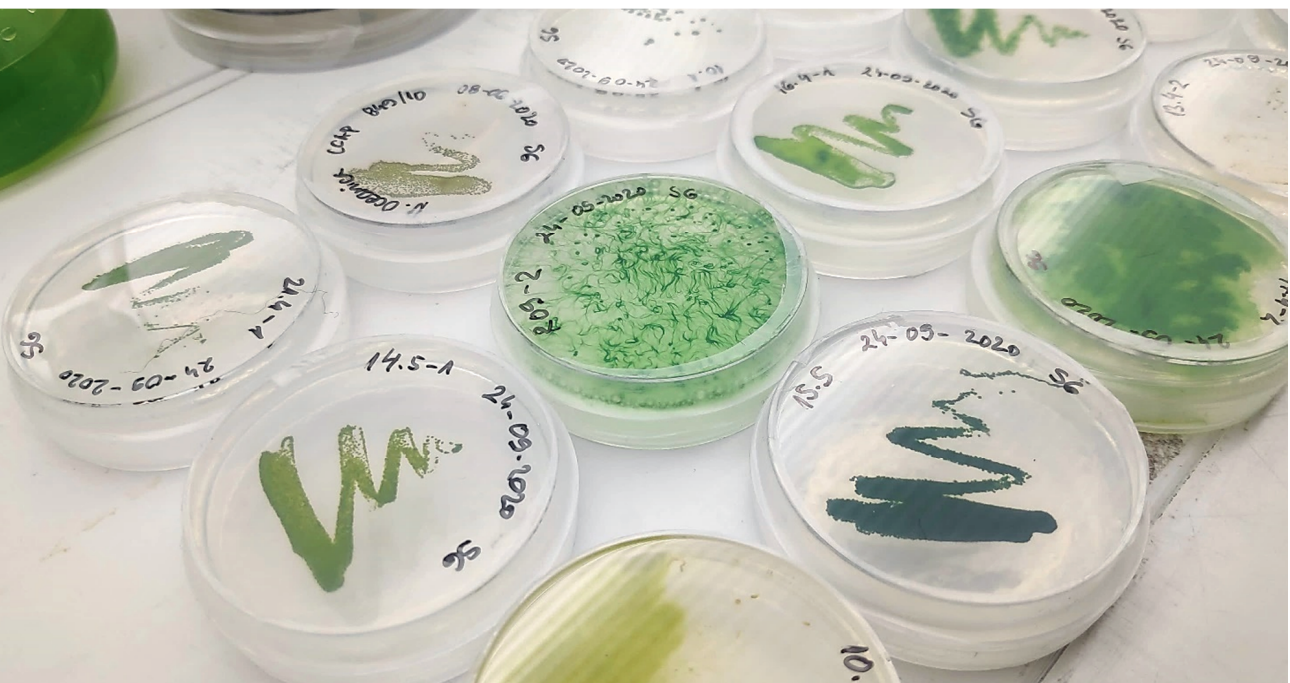
Chapter 2

Bioprospecting and characterization of temperature tolerant microalgae from Bonaire

Abstract

Control of temperature is a major challenge for industrial microalgae production in photobioreactors outdoors. Strains with tolerance for high temperatures can reduce the cost of production as active temperature control is not required. In this study, marine photoautotrophic microorganisms were isolated to reduce the need for control of high temperature.

Twenty-two samples were taken from different saline waters on the Caribbean island Bonaire. During strain enrichment, a temperature of 40°C was used as selective pressure and strains with the highest growth rate were selected. We isolated and identified 59 strains, after which 5 were selected for characterization on growth rate and biomass composition. *Picochlorum sp.* and *Leptolyngbya sp.* showed optimal growth at 40°C and 35°C with a growth rate of 0.12 h^{-1} during daytime, respectively. The strains contain 62.1% and 68.2% of protein and have varying fatty acid compositions suitable for application as edible oil and biofuel.

2.1. Introduction

Microalgae are recognised as a promising alternative to traditional crops. They are unicellular photosynthetic microorganisms which can be grown in photobioreactors. Applications are found in food, feed, biofuel, bioplastics, cosmetics and nutraceuticals industries [31, 32]. Cultivation of microalgae can be done anywhere, as long as basic requirements for growth, such as sufficient light and nutrients, and tolerable temperatures are met. The ability to grow microalgae in photobioreactors and open ponds removes the requirement for arable land and creates opportunities for production in desert regions [1, 33]. Sustainable and cost-effective production of microalgae should be done in places offering high solar irradiance, constant climatological conditions and seawater availability [2]. The Caribbean island Bonaire has been presented as a location which meets all these requirements [34].

The culture inside photobioreactors, when not controlled, can reach peak temperatures up to 50 °C due to high irradiation levels [35, 36]. The optimal growth temperature for most industrial microalgal strains is commonly between 20°C and 30°C [6, 37]. At temperatures higher than their optimum growth temperature, microalgae suffer from enzyme degradation and failure of the photosynthetic system as a result of heat stress [13, 37]. One major cost factor for microalgae cultivation in photobioreactors is cooling during day-time to avoid losses of productivity and culture collapses [38]. Currently applied methods for cooling involve bioreactor shading, spraying with water, use of a heat exchanger or reactor submersion in water [39]. Each of these methods has the disadvantage of either increasing process costs or decreasing productivity. Removing the requirement for bioreactor cooling would result in a significant decrease in production costs. Microalgae species which can tolerate peak temperature of 45°C instead of 30°C when grown in flat panel photobioreactors would decrease production costs by 31%, as calculated by the techno-economic model of [4].

The microalgal biodiversity around the world is large, with 72,500 species known and an estimated 1 million species still to be discovered [40]. This significant untapped potential harbours organisms with beneficial traits for growth and production in regions around the equator. Such regions commonly harbour a constant climate all year round, high light intensities, and high temperatures. Bioprospecting of new microalgae species for both research and industrial applications has been performed in many regions of the world [16, 18, 41-43]. In

most of these studies, the aim was to isolate strains for production of specific compounds, such as lipids, protein or carbohydrates, without considering process conditions. As a result, process control is currently more expensive than it could be. More attention must be given to process-oriented bioprospecting to reduce temperature control requirements. In this study, the tropical island of Bonaire is presented as a blueprint for microalgae production in other regions with comparable climatological conditions. The temperature of a photobioreactor on Bonaire will fluctuate between 27°C and 50°C in a diel pattern, depending on the time of the day and weather conditions [35, 36]. To reach the highest possible productivity under these conditions, the ideal strain must have a high growth rate over this temperature range.

The focus of the present study was to isolate robust microalgal strains which grow at temperatures higher than current industrial strains. Water bodies on Bonaire were sampled to isolate indigenous strains. We selected strains after a strain enrichment to find strains with high growth rates at 40°C. After this initial selection, the growth kinetics were studied for 5 strains at different temperatures and a light intensity of 300 $\mu mol.m^{-2}.s^{-1}$. These strains were then screened for their chemical composition to identify potential commercial applications.

2.2. Materials and methods

2.2.1. Bioprospecting and strain identification

2.2.1.1. Collection, enrichment, isolation of microalgae

Water samples were collected from twenty-two ocean and inland saline waterbodies at 16 different locations on Bonaire (Figure 2.1). Sampling was performed on March 2018 and October 2018. Samples were transferred into pH 7.4 HEPES ($C_8H_{18}N_2O_4S$) buffered artificial seawater enriched with nutrients, resulting in the following concentrations (in mM): NaCl, 419.5; Na_2SO_4, 22.5; $CaCl_2 \cdot 2H_2O$, 5.4; K_2SO_4, 4.9; $MgCl_2 \cdot 6H_2O$, 48.2; $C_8H_{18}N_2O_4S$, 20; $NaNO_3$, 24.94; KH_2PO_4, 1.69; $Na_2EDTA \cdot 2H_2O$, $2.8 \cdot 10^{-1}$; $FeSO_4 \cdot 7H_2O$ $1.1 \cdot 10^{-1}$; $MnCl_2 \cdot 2H_2O$, $1.1 \cdot 10^{-2}$; $ZnSO_4 \cdot 7H_2O$, $2.3 \cdot 10^{-3}$; $Co(NO_3)_2 \cdot 6H_2O$, $2.4 \cdot 10^{-4}$; $CuSO_4 \cdot 5H_2O$, $9.6 \cdot 10^{-5}$; $Na_2MoO_4 \cdot 2H_2O$, $1.0 \cdot 10^{-3}$. The cultures were incubated in a 2% CO_2 enriched shaking incubator (Multitron, Infors HT, Switzerland) at a rotational speed of 125 rpm

Figure 2.1: *Sampling locations on Bonaire.*

and relative humidity of 60%. The circadian cycle comprehended 12 hours of day-time at 40°C and 12 hours of night-time at 30°C. Wide spectrum white fluorescent light (Philips master TL-D reflex, color temperature 840) was set at an intensity of 140 µmol.m^{-2}.s^{-1} during the daytime. An enrichment phase was used to increase the number of cells which were able to grow under the enforced growth conditions. The cultures were diluted twice weekly in fresh culture medium at 3% v/v for 2-4 weeks until only a few species remained in the culture. Isolation of single species was performed by serial dilution on agar enriched growth medium. Colonies were selected for transfer to liquid medium based on colony size and microscopic observations.
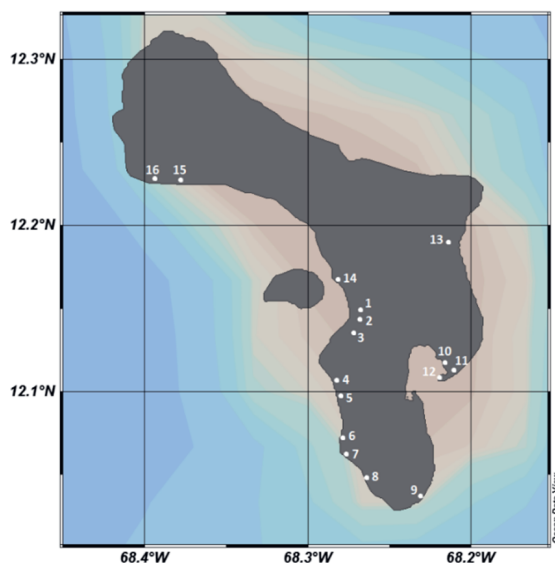
2.2.1.2. Phylogenetic analysis of isolated strains

Isolated microalgae were identified by PCR and sequencing of the 16S rRNA gene (rDNA) in cyanobacteria and 18S rRNA gene (rDNA) for microalgae. DNA was extracted from pelleted microalgae and prepared for direct PCR according to recommendations of the manufacturer of the Phire Plant Direct PCR Kit (Finnzymes, Woburn, MA, USA). Primers specific for cyanobacterial 16S rRNA gene (rDNA) amplification were used as described by Nübel et al [44]. A DNA product of approximately 700bp was generated using the CYA106F and CYA781R (a+b) primers. 18S rRNA gene (rDNA) amplification was performed using FW primer 5' CCT GGT TGA TCC TGC CAG 3' and RV primer 5' (A/T)TG ATC CTT C(T/C)G CAG GTT CA 3' with a melting temperature of 64.9 °C [45]. A DNA product of approximately 1500 bp was generated using these 18s rRNA gene (rDNA) primers. PCR products were sequenced using Sanger sequencing. The sequence ends were trimmed off manually, after which identification of the microalgae was performed through the NCBI BLAST. The closest named species is presented as determined using NCBI BLAST. The isolated strains are presented at a genus level in this article as more detailed identification is necessary to identify at a species level.

2.2.2. Characterization

2.2.2.1. Maximum growth rate

Cells were grown in a stirred incubator (Algaebator, 'ontwikkel-werkplaats' Wageningen University, The Netherlands, Wageningen). A daily sequencing batch mode was applied for cultivation, in which 100 ml microalgae cultures were diluted daily to a set cell density to avoid light limitation. Warm white LED light (BXRA W1200, Bridgelux, USA, Livermore) was provided at the bottom of a 250 ml erlenmeyer and controlled at 300 $\mu mol.m^{-2}.s^{-1}$ in a 12/12 h day/night cycle. A 2% v/v CO_2 enriched headspace was created to ensure a non-limiting carbon concentration. Optical density measurements at 750nm (OD_{750}) were used to determine the dilution factor for starting the daily sequencing batch culture. Cultures were diluted daily to an OD_{750} of 0.1 directly after the onset of the dark period. Duplicate cultures were grown in sequencing batch mode at 20, 25, 30, 35, 40 and 45 °C, until the growth rate between days stabilized, at which the culture was considered to be at steady-state.

Data from minimally 3 consecutive days at steady-state was used to calculate the maximum growth rate under each culture condition studied. Cultures were considered in steady state when the deviation of the growth rate between days was <10%. The growth rate was calculated as seen in Equation 2.1. N_{t0} and N_{tx} represents the OD_{750} value directly after dilution (t_{t0} in h^{-1}) and 24 hours after dilution (t_{tx} in h^{-1}). The growth rate (u_x in h^{-1}) was calculated only considering the illuminated hours.

$$u_x = \frac{\ln(N_{tx}) - \ln(N_{t0})}{t_{tx} - t_{t0}}$$

Equation 2.1

2.2.2.2. Biomass and composition

Biomass samples for compositional analysis were taken in a separate batch cultivation experiment. The growth conditions were as described in '2.2.1. Maximum growth rate' except for the dilution and harvesting procedure. Algae were harvested during the linear growth phase, either when a biomass concentration of 2.5 g.l^{-1} was reached, or after 14 days of growth. The biomass was centrifuged at 4000g for 5 minutes, washed twice with 0.5 M ammonium formate, and stored at -20 °C. Afterwards, samples were lyophilised for 24 hours.

2.2.2.3. Fatty acid composition and content

Total fatty acid content was determined through gas chromatography. 10 mg of lyophilised biomass was disintegrated by bead beating. Fatty acids were extracted in a 2:2.5 V/V% chloroform/methanol mixture containing a C15:0 TAG internal standard (T4257, Sigma Aldrich). Extraction, transesterification and gas chromatography analysis was done as described by de Winter et al [46].

2.2.2.4. Protein content

Total protein content was measured in 2 mg lyophilised microalgae biomass by total nitrogen analysis ('Kjehldahl method'). A conversion factor for nitrogen to protein of 4.78 was used [47]. Biological replicate samples (n = 2) were each analysed in triplicate (n = 3).

2.2.2.5. Carbohydrate content

Total carbohydrate was quantified as described by Dubois et al. (1956) and Klok et al. (2013) [48, 49]. A phenol-sulfuric acid mixture was added to the 5 mg of lyophilised biomass. Carbohydrate content was analysed on biological duplicate samples (n=2) which were each measured with technical duplication (n = 2). The absorbance was measured at 483 nm. Glucose monohydrate and starch were used as reference and positive control, respectively.

2.2.3.1. Data analysis and statistics

The reported values for each experiment are the mean of individual biological replicates. Statistical analysis of the growth rate experiments was performed using a two-tailed student's t-test in Excel on biological replicate samples (n ≥ 6). The statistical treatment on the data on fatty acid composition was based on the standard error of two biological replicates (n = 2). The statistical treatment on the data of the carbohydrate and protein content was done using a two-tailed students t-test in Excel on the sum of the technical and biological replicates.

2.3. Results and discussion

2.3.1 Bioprospecting and strain Identification

The waters of Bonaire represent a wide range of environmental conditions. Isolated saline water bodies of different pH levels (pH 6.8 – 10), salinities (15 – 150 ppt) and temperatures (26.3 – 35.5 °C) harbour a rich variety of microorganisms. Twenty-two water samples were taken on Bonaire. The biodiversity was high in all bioprospected samples, independent of sampling location. Every culture contained a wide variety of species at the very beginning of the enrichment phase. This variety was greatly reduced by the stringent selective pressure applied on fast growth at 40°C during daytime and 30°C during the night.

Fifty-nine monoalgal colonies were selected for colony picking and upscaling to liquid cultures. Forty out of the fifty-nine strains showed growth in liquid cultures. These strains were identified through PCR amplification and sequencing of the 16/18s rRNA genes (16/18S rDNA). Some strains showed nearly identical 16/18s rRNA gene (16/18S rDNA) sequences. As a result, these strains gave an identical hit during the NCBI blast search. Therefore, in the case of an identical 16/18s rRNA gene (16/18S rDNA) sequence identity, these strain were named only once for data presentation in this paper (Table 2.1). In this way, the number of different identified species was reduced to 18. Especially the genus *Picochlorum* was highly present with 16 out of 40 sequenced isolates associated with it. The 16 strains of *Picochlorum* were identified and clustered into 3 different species (Table 2.1).

Percentage-wise the isolated species were identified as cyanobacteria (55.6%), Chlorophyta (33.3%), and bacillariophyta (11.1%). The large presence of cyanobacteria was expected as these species commonly thrive under higher temperatures [41]. Bacillariophyta are commonly found in colder regions [16, 50].

Table 2.1: *Isolated species as found through NCBI online database using nucleotide BLAST. Date accessed: 11.01.2019. Origin corresponds to the sampling location as shown in Figure 2.1: sampling locations on Bonaire.*

division	Closest named species (Genbank)	Isolate	Origin (location)	GenBank accession no.	Identity
Bacillariophyta	Halamphora subtropica (MG027330.1)	BPE42	Saline Puddle (4)	MN907400	100.00%
Bacillariophyta	Stauroneis latistauros (KY054994.1)	BPE48	Saltwater Lake (15)	MN907403	96.59%
Chlorophyta	Dunaliella polymorpha (KY923056.1)	BPE46	Salt plains (5)	MN907401	99.44%
Chlorophyta	Dunaliella primolecta (KR607494.1)	BPE47	Salt plains (5)	MN907402	99.91%
Chlorophyta	Picochlorum maculatum (KU561155.1)	BPE21	Estuary (14)	MN907398	99.63%
Chlorophyta	Picochlorum oklahomense (KY054988.1)	BPE16	Saltwater lake (16)	MN907397	98.96%
Chlorophyta	Picochlorum sp. (KF495093.1)	BPE23	Bay (13)	MN907399	97.21%
Chlorophyta	Tetraselmis sp. (KC820794.1)	BPE14	Saltwater lake (16)	MN907396	99.25%
Cyanobacteria	Candidatus Pleurinema perforans (KX388631.1)	BPE18	Ocean coast (16)	MN909718	99.18%
Cyanobacteria	Leptolyngbya sp. (EU249119.1)	BPE10	Saline pond (8)	MN909716	99.84%
Cyanobacteria	Leptolyngbya sp. (KC695850.1)	BPE12	Salt marsh (2)	MN909717	96.03%
Cyanobacteria	Phormidium lucidum (GU186899.1)	BPE39	Unknown	MN909720	100.00%
Cyanobacteria	Plectonema cf. battersii (AJ621837.1)	BPE55	Saltwater lake (16)	MN909721	99.83%
Cyanobacteria	Romeria sp. (KU951673.1)	BPE57	Saline Puddle (15)	MN909722	98.04%
Cyanobacteria	Synechococcus elongatus (AY946243.1)	BPE37	Unknown	MN909719	99.18%
Cyanobacteria	Synechococcus sp. (AB862161.1)	BPE58	Saline Puddle (15)	MN909723	99.00%
Cyanobacteria	Unidentified (JN434813.1)	BPE53	Saltwater Lake (15)	MN906016	98.68%
Cyanobacteria	Unidentified (KC002930.1)	BPE59	Saltwater lake (16)	MN906017	94.56%

2.3.2. Growth kinetics at varying temperatures

Five isolated species were selected from the list of species provided in Table 2.1, based on visual observations of the cell cultures for two weeks. The criteria for selection were based on the potential for upscaling. Considering the ability to grow to a high density in cell suspension without forming biofilm or flocs. Photobioreactor productivity decreases due to biofilm formation, as a large fraction of the incident light is absorbed by this oversaturated layer of microalgae. Cleaning of biofilms is time-consuming and therefore undesirable, which makes it an important selection criterium. The ability to grow at high cell densities was observed for most species that were also able to grow without forming biofilms.

A high growth rate is important to start photobioreactors quickly and to prevent contamination. In addition, a high growth rate will lead to a faster upscale trajectory and will result in high bioreactor productivity [6, 51]. To determine the growth rate of the selected microalgae, they were cultured in repeated batch mode at a daily starting cell density of 0.03 g.L^{-1}. The low cell density was chosen to assess
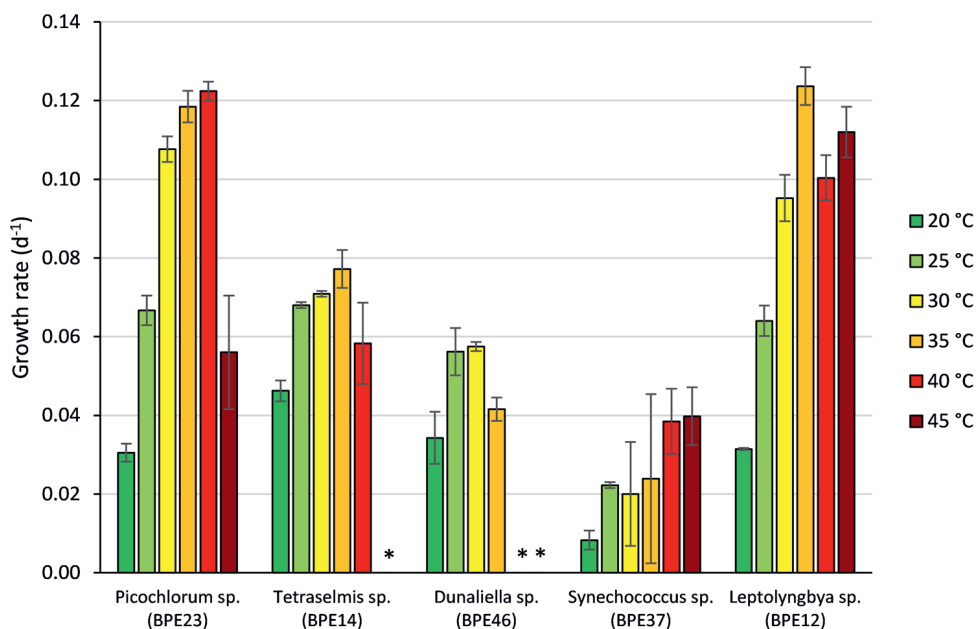
Figure 2.2: *Maximal growth rate (u_x in h^{-1}) at temperatures ranging from 20°C to 45°C with 5°C intervals of five isolated microalgae and cyanobacteria. Cultures were grown in repeated batch mode at temperatures ranging from 20°C to 45°C with 5°C intervals. Incident light intensity was 300 µmol.m^{-2}.s^{-1}. Data points represent the average ± SD of n ≥ 6 biological replicates. *, no growth observed.*

their growth rate without the effect of cell shading. The cultures required five days under repeated batch cultivation to reach a stable growth rate, which was considered a steady-state. Reproducible growth rates were then observed between replicate cultures. Growth rates of the selected species at temperatures from 20 to 45°C are presented in Figure 2.2. The relevance of these data is not only found in the maximum rate of growth but especially in the temperature at which the maximum growth is reached.

As previously mentioned, The strains of the genus *Picochlorum* were well represented among the identified strains. To reduce the number of strains before performing elaborated growth experiments 6 strains were chosen for a preliminary short growth study. These subspecies of *Picochlorum sp.* were subjected to the repeated batch growth experiment at 35°C. *Picochlorum sp. CTM20019 BPE23* was found to possess the highest growth rate (data not shown). Accordingly, this strain was selected for the more detailed growth studies, shown in Figure 2.2.

This study aimed to find strains with a high growth rate from 25°C to 45°C in combination with a light intensity of 300 µmol.m^{-2}.s^{-1}. Based on these criteria, *Leptolyngbya sp.* (BPE12) and *Picochlorum sp. BPE23* were the best performers. A maximum growth rates up to 0.12 h^{-1} was observed for these strains at 35°C and 40°C. *Picochlorum* species have recently gained attention because of their high growth rates, sometimes in combination with high thermo- and halotolerance [21, 43].

Tetraselmis sp. (BPE14), showed growth up to 40°C with an observed growth rate of 0.08 h^{-1} at 35°C. Most of the other reported *Tetraselmis* species have a temperature optimum around 25°C [52]. *Tetraselmis* strains with a temperature tolerance up to 40°C have been reported before [53]. However, no growth rates were reported which complicates good comparison.

Dunaliella sp. (BPE46) and *Tetraselmis sp*. (BPE14) grew under temperatures up to 35°C and 40°C, respectively. *Picochlorum sp. BPE23*, *Synechococcus sp.* (BPE37) and *Leptolyngbya sp.* (BPE12) showed growth up to 45°C, which was the maximum temperature studied. While for *Picochlorum sp. BPE23* a decrease in growth rate was observed when the temperature was increased from 40°C to 45°C, this was not observed for *Synechococcus sp.* (BPE37) and *Leptolyngbya sp.* (BPE12). It is, therefore, speculated that the optimum temperature of these strains may be beyond 45°C. This is demonstrated by *Synechococcus elongatus*, which is closely

related to *Synechococcus sp.* (BPE37). This species is capable of active growth up to 60°C with an optimum at 55°C [54],

For *Synechococcus sp.* (BPE37) it was found that growth was not optimal due to excessive light stress as under dense culture conditions the observed growth rate of *Synechococcus sp.* (BPE37) was comparable to the growth rate of *Leptolyngbya sp.* (BPE12) and *Picochlorum sp. BPE23* (data not shown) [55].

2.3.3. Biomass composition

Industrial microalgal production strains must produce components with economical applications and value. The selected strains were analysed for protein, carbohydrate and fatty acid levels during the linear growth phase, shown in Figure 2.3. These three major groups comprise up to 86.5% of microalgal biomass in our study and are currently the most relevant bulk products. *Synechococcus sp.* BPE37 and *Leptolyngbya sp.* (BPE12) show a protein content of 62.1% and 68.2% of total
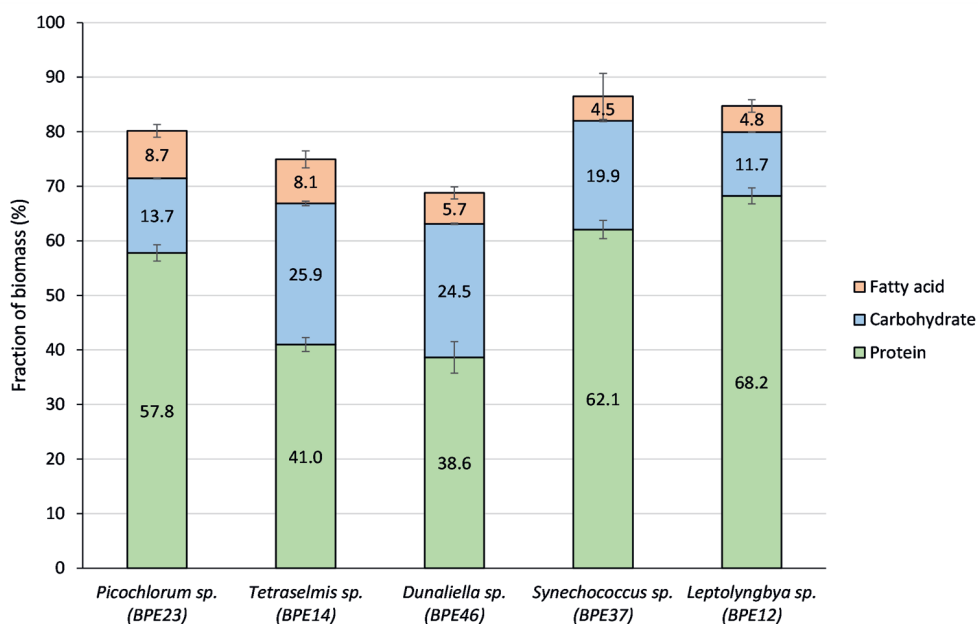
Figure 2.3: *Protein, carbohydrate and fatty acid content of three microalgae and two cyanobacterial strains during the linear growth phase. Fatty acid content represents the average ± standard error of n = 2 biological replicates. The carbohydrate and protein content data represent the average ± standard deviation of the technical replication, in addition to the biological replication with n = 2 and n = 3, respectively.*

biomass, respectively. Compared to the microalgal strains *Tetraselmis sp*. (BPE14) and *Dunaliella sp.* (BPE46) this is significantly higher. This is partly because the microalgal strains *Tetraselmis sp*. (BPE14) and *Dunaliella sp.* (BPE46) have a higher carbohydrate content 25.9 and 24.5%, respectively. Microalgae accumulate storage compounds as a stress response to nutrient depletion [56, 57]. The cells within our research were grown under nutrient replete conditions. Due to the absence of a nutrient starvation phase, a low fatty acid content was expected. Lipid bodies are absent under these conditions. Therefore the majority of measured fatty acids must be in a membrane-bound state.

The composition of fatty acids largely determines their economic value. This gives relevance to the analysis of fatty acid composition for our species [56, 57]. Microalgae and cyanobacteria found in high-temperature regions are commonly composed of short-chain saturated fatty acids (SFAs). This is the result of a lower need for high membrane fluidity which is provided by unsaturated fatty acids. It was found that fatty acid composition varied significantly amongst species. Both cyanobacteria, *Leptolyngbya sp.* (BPE12) and *Synechococcus sp.* (BPE37) show low saturation levels for C16 and C18 fatty acids, which is comparable to palm oil.

Picochlorum sp. BPE23 is composed of 64% of polyunsaturated fatty acids (PUFAs) with the most significant fatty acids being palmitic acid (C16:0), linoleic acid (C18:2), and α-linoleic acid (C18:3). The level of fatty acid unsaturation is high compared to algae strains in literature and commercial oils (Table 2.2) [56]. Research papers on other strains of *Picochlorum* report variable fatty acid compositions with 20-29% SFA, 34-62%MUFA and 36-51%PUFA [58, 59]. One commercial oil with fatty acid chain lengths comparable to *Picochlorum sp. BPE23*, is rapeseed oil, with the exception that the level of fatty acid unsaturation is higher in *Picochlorum sp. BPE23*. *Dunaliella sp.* (BPE46) registered a very comparable fatty acid profile as *Picochlorum sp. BPE23*, with a higher C18:3 content at the cost of C18:2. *Tetraselmis sp*. (BPE14) shows a large number of different fatty acids, including the omega 3 fatty acids eicosatrienoic acid (C20:3-N3) and eicosapentaenoic acid (C20:5-N3) which can be used as a fish oil replacement. Other major fatty acid groups include C16:0, C18:2, and C18:3.

The high level of fatty acid unsaturation of the *Tetraselmis sp*. (BPE14), *Picochlorum sp. BPE23* and *Dunaliella sp.* (BPE46) make these strains suitable for edible oil production. Especially the unsaturated Omega-3 and Omega-6 fatty acids are of interest within this group. The beneficial fatty acid composition combined with the

microalgae's high protein content makes these strains an interesting food and feed production platform.

Table 2.2: *Fatty acid composition of five isolated microalgal and cyanobacterial strains from Bonaire. The fatty acid content was calculated and expressed as a percentage of total fatty acid in the cell. Cultures were grown in batch mode at 35°C. Incident light intensity was 300 µmol.m^{-2}.s^{-1}. Cells were harvested in the linear growth phase. Fatty acid compositions for Rapeseed and palm oil were obtained from literature [60]. Data points represent the average of n = 2 biological replicates. The average relative error for all tests was 4.16%.*

	Picochlorum sp. BPE23	Tetraselmis sp. BPE14	Dunaliella sp. BPE46	Synechococcus sp. BPE37	Leptolyngbya sp. BPE12	Rapeseed oil	palm oil
C13:0	1.38	1.29	1.10				
C14:0	1.67	4.50	1.66	2.49			
C14:1 cis-9	1.59	1.80	1.10	1.06			
C16:0	24.82	23.80	29.15	46.56	41.83	7-19	51
C16:1	1.39	2.47	0.99	10.45	10.55		
C16:2				1.32	1.27		
C16:3	8.56	2.27	2.16	1.72	1.05		
C17:0		11.56	5.32				
C18:0	1.25	1.05	1.73	3.06	2.83		
C18:1	3.89	7.20	5.41	15.96	27.50	22-70	39
C18:2	33.06	16.59	20.81	11.82	14.96	12-21	10
C18:3	22.39	18.15	30.57	5.55		3-11	
C19:0		2.53					
C20:1		1.88					
C20:3-n3		1.80					
C20:5-n3		3.10					
Saturated fatty acids	29.12	44.74	38.96	52.11	44.67	7-19	51
Monounsaturated fatty acids	6.87	13.36	7.50	27.47	38.05	22-70	39
Polyunsaturated Fatty acids	64.01	41.91	53.54	20.41	17.28	15-23	10

2.4. Conclusions

To reduce process costs and improve yields when cultivating microalgae in tropical regions there is a need for thermo-tolerant species. Process-oriented strain selection was performed to isolate photoautotrophic microorganisms with a temperature optimum between 30°C and 45°C. Two ideal species were found, *Picochlorum sp. BPE23* and *Leptolyngbya sp.* (BPE12)*, which showed growth up to 45°C, with a maximum growth rate of 0.12 h^{-1} between 35°C and 40°C. Measurements on biomass composition indicate applicability for food because of the high protein content and as a replacement for palm tree oil, fish oil and rapeseed oil.

Data Availability

Sequencing data of the 18s gene identification can be found in the NCBI nucleotide sequence repository under the reference of MN907396 : MN907403[accn]. Sequencing data of the 16s gene identification can be found in the NCBI nucleotide sequence repository under the reference of MN909716 : MN909723[accn] and MN906016 : MN906017[accn]. Other data used to support the findings of this study are available from the corresponding author upon request. Microalgae strains were cryopreserved and stored at Wageningen University facilities. These are available from the corresponding author upon request.
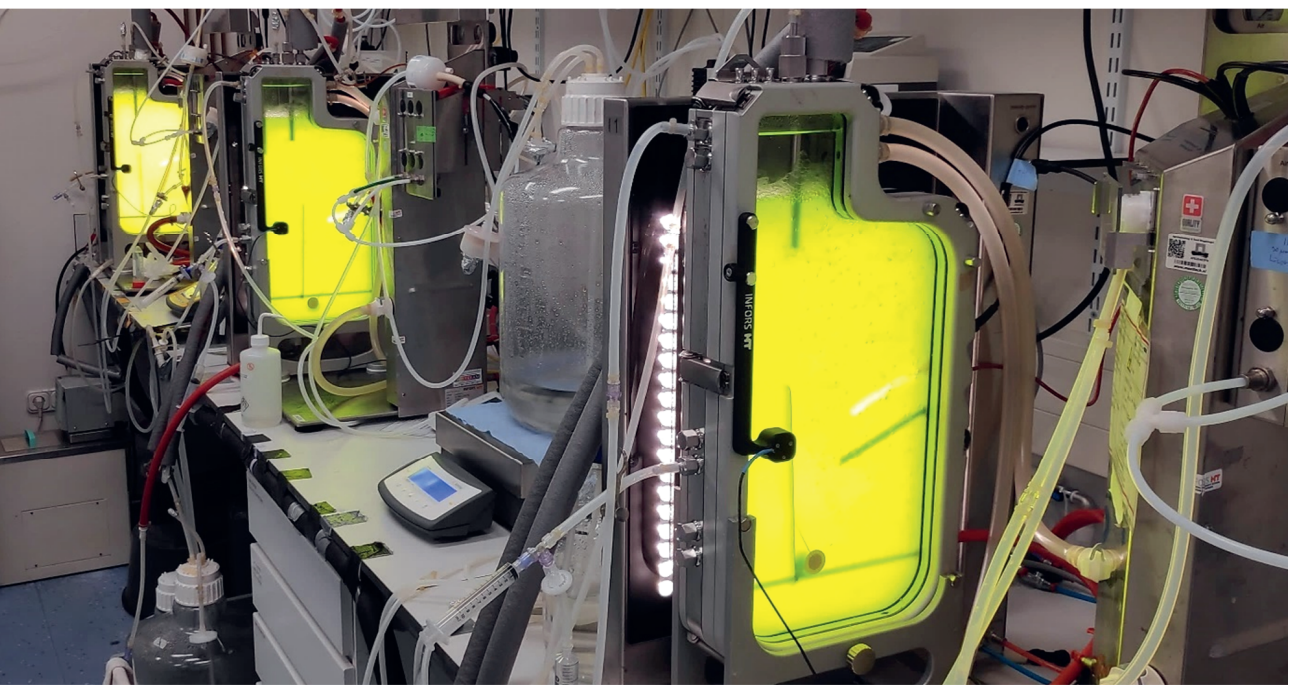
Chapter 3

Towards industrial production of microalgae without temperature control: The effect of diel temperature fluctuations on microalgal physiology

Abstract

Regions that offer high levels of sunlight are ideal to produce microalgae. However, as a result of high light intensities, the temperature in photobioreactors can reach temperatures up to 50°C. Control of temperature is essential to avoid losses on biomass productivity but should be limited to a minimum to avoid high energy requirements for cooling. Our objective is to develop a production process in which cooling is not required. We studied the behaviour of thermotolerant microalgae *Picochlorum sp. BPE23* under four diel temperature regimes, with peak temperatures from 30°C up to a maximum of 47.5°C. The highest growth rate of 0.17 h^{-1} was obtained when applying a daytime peak temperature of 40°C. Operating photobioreactors in tropical regions, with a maximal peak temperature of 40°C, up from 30°C, reduces microalgae production costs by 26.2%, based on simulations with a pre-existing techno-economic model. Cell pigmentation was downregulated under increasingly stressful temperatures. The fatty acid composition of cell membranes was altered under increasing temperatures to contain shorter fatty acids with a higher level of saturation. Our findings show that the level of temperature control impacts the biomass yield and composition of the microalgae.

3.1. Introduction

Microalgae are photosynthetic microorganisms that can be grown using sunlight as an energy source. These microalgae contain high levels of protein, lipids, pigments and carbohydrates and are therefore interesting for the production of a wide range of products such as food, feed, biofuels, cosmetics and bioplastics [2, 61]. Stable climate and high light intensities are favourable conditions to achieve yearly high productivities [4]. Cultivation of microalgae is best done in photobioreactors, where high process control, high cell densities and high productivities can be obtained [1, 4, 62]. However, the disadvantages of such systems compared to traditional open ponds are higher capital and operational costs, and the absence of natural cooling through water evaporation. As a result of exposure to high light intensities, the culture temperature in a photobioreactor can increase up to 50°C [18, 36]. This exceeds the optimum temperature of most industrial microalgae, which is between 20°C and 30°C [6, 63]. As a consequence, this will result in losses of productivity or even culture collapse. While mechanical cooling, shading or spraying of water can offer a solution, applying these cooling methods should be avoided as much as possible due to their negative economic and environmental impact [4]. These high temperatures only occur for a few hours each day, at midday. However, this still affects most microalgae severely. Microalgal species that tolerate and remain productive under such high temperatures can significantly reduce process costs. If species are able to grow optimally at a diel peak temperature of 40°C instead of 30°C then production costs decrease by 26.2%, while a peak temperature of 45°C would reduce production costs by 28.4%, as calculated by the techno-economic model of Ruiz et al., using climatological conditions as found in Curacao [4].

At peak temperatures exceeding the microalgae's lethal growth temperature, microalgal cells will die quickly due to denaturation, dissociation, and destabilisation of nucleic acid structures, proteins, and cell membranes [6, 11]. Also temperatures below the lethal, but above the optimal growth temperature cause cell stress. To survive, cells have to rebalance their composition. Membrane fluidity is elevated at higher temperatures, which is rebalanced by alterations in sterol composition and by fatty acid remodelling. Higher saturation levels are favourable at increased temperature [64, 65]. Photosynthesis is impaired severely as temperatures past the optimum growth temperature unbalance the energy equilibrium within the cell. Excessive energy which cannot be transferred into the photoelectron transfer chain is dissipated by which reactive oxygen species (ROS)

are formed [66]. ROS are highly reactive and cause damage to DNA, proteins and membrane lipids. As a response, photoprotective pigments are produced to filter light, to support in non-photochemical quenching and to scavenge ROS [67]. Examples of these photoprotective pigments that can be found in green algae are lutein, carotene and the xanthophyll cycle pigments: zeaxanthin, antheraxanthin and violaxanthin [61]. The mentioned adaptation mechanisms protect against changes in environmental conditions both throughout seasons and during shorter periods [68-70].

The temperature in a photobioreactor fluctuates if no cooling is applied [6, 71-74]. However, most studies done in the field of microalgae cultivation are done under stable temperatures [6, 65, 75]. A stable temperature does not reflect the situation in photobioreactors at industrial scale. To understand the physiology of microalgae in representative industrial settings, a fluctuating diel temperature regime should be used. Research on the effect of diel, above optimal temperature fluctuations on microalgae growth and composition are therefore very relevant to both academia and industry. The objective of this study is to develop a microalgal production process in which photobioreactor cooling can be greatly reduced or avoided, in order to improve the sustainability and economics of the process. In this research paper, we study the response of the green temperature-tolerant microalgae strain *Picochlorum sp. BPE23* to diel fluctuating temperatures [76]. The interest and number of studies on *Picochlorum sp.* species have recently increased due to their robustness and tolerance for high light, temperature and salinity levels, also in combination with fluctuating conditions [20, 21, 77, 78]. *Picochlorum sp. BPE23* was selected for our study because of its high growth rate in combination with its thermotolerance [7]. To the authors' knowledge, this is the first study in which Picochlorum is subjected to simulated industrial growth conditions with a diel temperature profile. To compare different temperature scenarios, four diurnal temperature cycles with maximal peak temperatures of 30°C, 40°C, 45°C and 47.5°C during daytime and a constant 30°C during night-time were studied in highly controlled flat panel photobioreactors. These temperature profiles were based on temperatures that can be found in photobioreactors on Bonaire, as a reference for regions that harbour similar climatological conditions, since these are favourable for microalgae growth [4]. This study provides insight on the physiological response of the green microalgae *Picochlorum sp. BPE23* to diel temperature cycles in a photobioreactor production process, up to lethal temperatures.

3.2. Materials and methods

3.2.1. Microalgae cultivation

3.2.1.1. Microalgae and growth medium.

The green microalga *Picochlorum sp. BPE23*, belonging to the phylum *Chlorophyceae*, was used for this research [7]. For photobioreactor cultivation, a filter-sterilized growth medium was created using artificial seawater, enriched with 20 ml of nutrient solution and 1 ml of trace element solution per kilogram of growth medium. The artificial seawater was created using 24.5 g.l^{-1} NaCl, 3.2 g.l^{-1} Na$_2$SO$_4$, 0.8 g.l^{-1} CaCl$_2$·2H$_2$O, 0.85 g.l^{-1} K$_2$SO$_4$ and 9.8 g.l^{-1} MgCl$_2$·6H$_2$O. The nutrient solution contained 106 g.l^{-1} NaNO$_3$, 11.5 g.l^{-1} KH$_2$PO$_4$ and 3 g.l^{-1} Na$_2$EDTA·2H$_2$O. The trace element solution contained 45 g.l^{-1} Na$_2$EDTA·2H$_2$O, 30 g.l^{-1} FeSO$_4$·7H$_2$O, 1.71 g.l^{-1} MnCl$_2$·2H$_2$O, 0.66 g.l^{-1} ZnSO$_4$·7H$_2$O, 0.07 g.l^{-1} Co(NO$_3$)$_2$·6H$_2$O, 0.02 g.l^{-1} CuSO$_4$·5H$_2$O and 0.24 g.l^{-1} Na$_2$MoO$_4$·2H$_2$O. During inoculum preparation, HEPES buffer was added at a final concentration of 4.77 g.l^{-1}. The pH of the growth medium was set to 7.4 both for inoculum and photobioreactor cultivation.

3.2.1.2. Inoculum preparation and photobioreactor inoculation

The inoculum for all experiments was prepared in 250 ml erlenmeyers with a liquid volume of 100 ml. Light was set at ~100 µmol.m^{-2}.s^{-1}. The CO$_2$ level in the atmosphere was regulated at 2% and the relative humidity at 60%. A day/night cycle of 12/12 hours was applied with 40°C during daytime and 30°C during night-time.

The flat panel photobioreactor was inoculated with microalgae biomass at a concentration of 0.1 g.l^{-1}. Bicarbonate was added at a concentration of 0.168 g.l^{-1} at the moment of inoculation to ensure sufficient carbon. To avoid light stress during the initial batch growth phase, the light level was set at 200 µmol.m^{-2}.s^{-1} and increased periodically with steps of 200 µmol.m^{-2}.s^{-1} until a level of 813 µmol.m^{-2}.s^{-1} was reached after two days. The bioreactor was operated in batch mode until an outgoing light level of 35 µmol.m^{-2}.s^{-1} (PAR) was reached, after which photobioreactor dilution was started.

3.2.1.3. Photobioreactor setup and experimental conditions

Cell cultivation experiments were done in heat sterilized flat-panel photobioreactors with a 1.8 liter working volume, a 20.7 mm light path and a 0.08 m^2 surface area for irradiation (Labfors 5 Lux, Infors HT, Switzerland). A gas mixture was sparged at the bottom of the flat panel photobioreactor, consisting of 480 ml.min^{-1} fresh air and 500 ml.min^{-1} recycled gas. Extra CO_2 was added to the gas stream on-demand with a maximum flow rate of 25 ml.min^{-1} to compensate for pH changes as a result of CO_2 and NO^{-3} consumption. Illumination was done from one side by 260 warm white LED lights with a spectrum of 450-620 nm. The incoming light level was set constant at 813 µmol.m^{-2}.s^{-1} under a 12/12 h/h day/night cycle. The outgoing light level was maintained at 35 µmol.m^{-2}.s^{-1} (PAR) by light-controlled dilution of the cell culture (turbidostat mode). The culture dilution rate was determined by logging the feed addition.

Temperature was controlled in a sinusoid pattern during day time to mimic outdoor temperature fluctuations as can be found near the equator. Four peak temperatures were applied: 30°C, 40°C, 45°C, and 47.5°C. These are displayed in
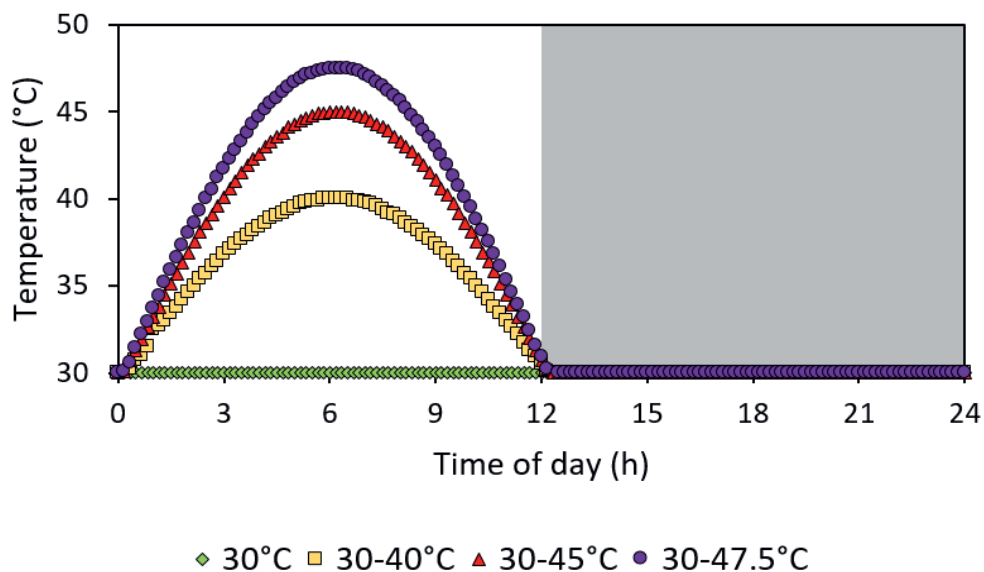
Figure 3.1: *The temperature and light profile as measured in the flat panel photobioreactor during microalgae cultivation. The night and the peak culture temperature, found 6 hours after 'sunrise' are displayed in the legend. The x axis displays hours after 'sunrise', with day and night time indicated in white and grey background, respectively*

Figure 3.1 as measured in the photobioreactor. The temperature during night time was kept constant at 30°C.

3.2.1.4. Sampling regime

Microalgae were grown until a cycling steady state was reached. Cultures were determined to be in a cycling steady state when the deviation between days, for all measured on-line and off-line parameters was less than 15% for a period of at least 3 days. In the situation where peak temperatures of 45°C and 47.5°C were applied, a period of adaptation and stabilization of several weeks was required before a cycling steady state situation was reached. Once cultures reached this state, samples were taken for at least two days (n = 2). Two flat panel photobioreactors were operated with a shifted time-schedule which differed 12 hours. Sampling was done every two hours for a period of 14 hours. The data of the two different algae growth schedules were connected and overlaid to allow for an analysis of 24 hours of cultivation, which represents a full day of growth.

3.2.2. Offline measurements

3.2.2.1. Biomass concentration

The biomass concentration (in g.l^{-1}) was measured in duplicate by dry weight determination. Empty Whatman glass microfiber filters (θ 55 mm, pore size 0.7 μm) were dried overnight at 95°C and placed in a desiccator for 2 hours. Filters were then weighed and placed in the mild vacuum filtration setup. Cell culture containing 1 to 10 mg of microalgae biomass was diluted in 25 ml 0.5 M ammonium formate and filtered. The filter was washed twice with 25 ml 0.5 M ammonium formate to remove residual salts. The wet filter was dried overnight at 95°C, placed in a desiccator for 2 hours, and weighed. Biomass concentration was calculated from the difference in filter weight before and after filtration and drying.

3.2.2.2 Cell size and cell number

Cell size and cell number were determined in duplicate with the Multisizer III (Beckman Coulter Inc., USA, 50 μm aperture). Samples were diluted in two steps before analysis, initially by dilution of 5x in fresh medium, followed by dilution of 100x in Coulter Isoton II.

3.2.2.3. Quantum yield

The cell culture's quantum yield (F_v/F_m), representing the maximum photosynthetic capacity of photosystem II was determined. Cells were measured after dark adaption at room temperature for 15 minutes (AquaPen-C 100, PSI; excitation light 455 nm (blue), saturating light pulse: 3000 $\mu mol.m^{-2}.s^{-1}$).

3.2.3. Compositional analysis

3.2.3.1. Harvest and Lyophilising

Biomass samples for compositional analysis were taken every 2 hours, at the same moment as when offline measurements were performed. Microalgae cells were pelleted by centrifugation at 4000g for 5 minutes and washed with 0.5M ammonium formate. The centrifugation/washing cycle was repeated twice more after which the cell pellet was frozen at -20 °C. Samples were then lyophilised for 24 hours and stored at -20 °C until further processing.

3.2.3.2. Pigment analysis

Pigment extraction was done using 10 mg of lyophilized biomass. Cells were disrupted by bead beating (Precellys 24, Bertin Technologies, France) at 5000 rpm for three cycles of 90 seconds with 60 second breaks on ice between each cycle. The extraction was done through five washing steps with methanol containing 0.1% butylhydroxytoluene. Separation, identification and quantification of pigments were performed using a Shimadzu (U)HPLC system (Nexera X2, Shimadzu, Japan), equipped with a pump, degasser, oven (25°C), autosampler, and photodiode array (PDA) detector. Separation of pigments was achieved using a YMC Carotenoid C30 column (250x4.6mm 5 µm ID) coupled to a YMC C30 guard column (20x4mm, 5 µm ID)(YMC, Japan) at 25°C with a flow rate of 1 $ml.min^{-1}$. A sample injection volume of 20µL was used. The mobile phases consisted of Methanol (A), water/methanol (20/80 (v/v%)) containing 0.2% ammonium acetate (B), tert-methyl butyl ether (C) (all solvents were purchased at Sigma Aldrich). The elution protocol started with 0-12 min isocratic A:95% B:5% C:0%, with at 12 min a step to A:80%, B:5%, C:15%, followed by a linear gradient 12-30min to A:30%, B:5%, C:65%, finally followed by a conditioning phase 30-40 min at the initial concentration. Analytical HPLC standards for Antheraxanthin, Chlorophyll-a, Chlorophyll-b, Lutein, Violaxanthin, Zeaxanthin had a purity of >99% (Carotenature, Switzerland).

3.2.3.3. Fatty acids analysis

Fatty acids within the triacylglycerol (TAG) and polar lipids (PL) fraction were quantified through GC-FID analysis [79]. 10 mg of lyophilised biomass was disrupted by bead beating. The fatty acids were extracted from the disrupted biomass in a mixture of chloroform/methanol (1:1.25, v:v) containing Glyceryl tripentadecanoate (C19:0 TAG) (T4257, Sigma-Aldrich) and 1,2-didecanoyl-sn-glycero-3-phospho-(1'-rac-glycerol) (sodium salt) C10:0 PG (840434, Avanti Polar Lipids Inc) as internal standards for the TAG and the PL fraction, respectively. Separation of TAG and PL was done by the use of Sep-Pak Vac silica cartridge (6 cc, 1000 mg; Waters). TAGs were eluted from the column with a solution of hexane:diethylether (7:1, v:v) and the PL were eluted with a solution of methanol:acetone:hexane (2:2:1, v:v:v). The extracts were methylated for 3 hours at 70°C in methanol containing 5% H_2SO_4.

3.2.4. Data and statistical analysis

The error of the cell diameter, cell density, dry weight, quantum yield data, displayed per hour, was calculated using the average deviation of both technical and biological duplicate measurements. The error on the reactor dilution rate data per hour was calculated using the standard deviation, while the dilution rate data per day was calculated by propagation of errors as calculated per hour through the standard deviation. The error for the fatty acid groups and pigment species, as displayed as an average per growth condition, was calculated by the standard deviation of eight (fatty acids) and fourteen (pigments) samples which were taken throughout the day from biological duplicates. The error on the total average fatty acid content over the entire day was calculated by propagation of errors through the error as calculated by the standard deviation for each of the fatty acid groups.

3.3. Results and discussion

3.3.1. Growth and cell size

Diurnal growth conditions were applied to the microalgae culture with 4 different peak temperatures as shown in Figure 2.1. These temperature profiles were selected to mimic temperature conditions as found in outdoor photobioreactors placed under Caribbean climatological conditions. Cell density was maintained at a stable level through adaptive dilution based on light transmission through the cell culture (turbidostat mode).

Table 3.1: *Average dilution rate (d^{-1}) and quantum yield (Fv/Fm) of the cell cultures at different diel temperatures. Data corresponds to the average ± SD of 24 hours of data acquisition (N=2)*

Diel temperature (°C)	Dilution rate (d^{-1})	Quantum yield (Fv/Fm)
30	1.05±0.02	0.73±0.01
30-40	1.22±0.06	0.70±0.02
30-45	0.61±0.03	0.68±0.02
30-47.5	0.29±0.02	0.67±0.02

The measured dilution rates throughout the day are displayed as average per day in Table 3.1 and per hour in Figure 3.2. The culture grown at a stable temperature of 30°C shows a daily dilution rate of 1.05 ± 0.02 d^{-1} with a peak growth rate of 0.13 h^{-1} at 6 hours after sunrise. The maximum growth rate was found when a diel oscillation between 30°C and 40°C was applied. In this scenario, the peak in growth (0.17 h^{-1}) was found 6 hours after sunrise, in similarity to the experiment under a stable temperature of 30°C. The daily growth rate was 1.22 ± 0.06 d^{-1}. The growth rate of these two cultures follow a sinusoid pattern while the cultures grown with diel peak temperatures of 45°C and 47.5°C clearly show different profiles. These cultures show a decrease in growth rate during midday, which becomes more severe as temperature increases. The daily dilution rate was found to be respectively, 0.61 ± 0.03 d^{-1} and 0.28 ± 0.02 d^{-1} at 45°C and 47.5°C. With 47.5°C being the maximum peak day-temperature at which *Picochlorum sp. BPE23* showed active growth, as cells died when a diel peak temperature of 48°C was applied (data not shown). While *Picochlorum sp. BPE23* was able to grow when a diel peak temperature of 47.5°C was applied, the productivity was found with a diel peak temperature of 40°C. Allowing an increased maximum temperature during the operation of a photobioreactor located in tropical regions, can lead to a cost
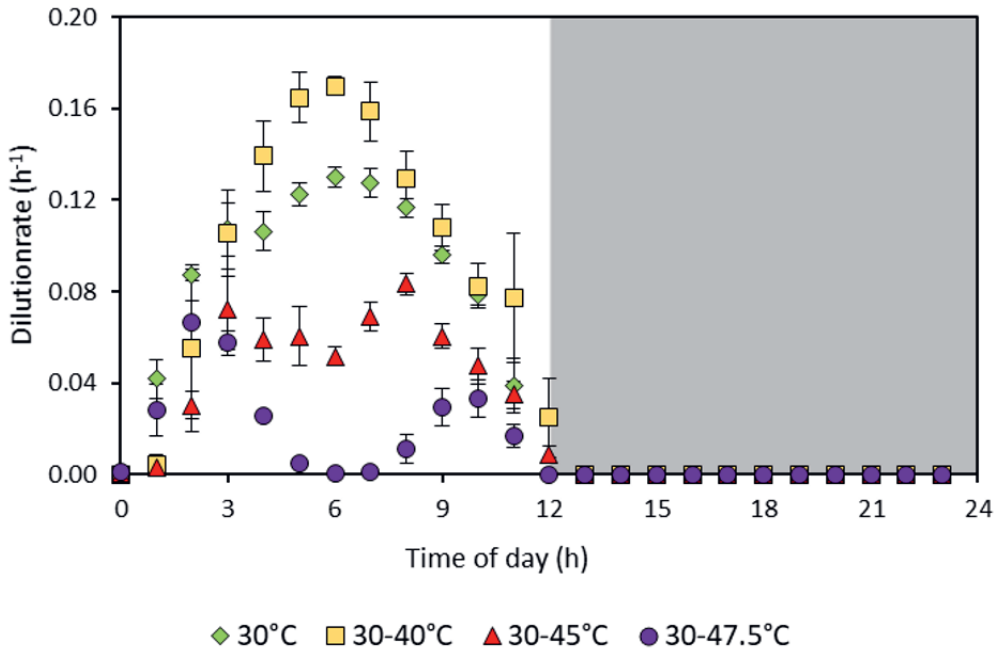
Figure 3.2: *Measured dilution rates (h^{-1}) of the microalgal cell culture. The night and the peak culture temperature, 6 hours after 'sunrise' are displayed in the legend. The x axis displays hours after 'sunrise', with day and night periods indicated in white and grey background, respectively.*

reduction of 26.2%, based on techno-economic model simulations using the model as described by [4]. For these model simulations Bonaire was chosen as model location for light and temperature, seawater at a temperature of 27°C was chosen as cooling medium, and a photosynthetic efficiency of 2.6% was assumed. The ability to grow optimally at 40°C is a major improvement compared to other industrially applied species which commonly exhibit optimal growth temperatures of 20-30°C [6].

The sinusoid trend observed for the dilution rate throughout the day found for two of the cultures (Figure 3.2) is not solely due to changing temperatures as this trend is also observed with the stable temperature of 30°C (Figure 3.2). All cultures show a slight delay before dilution starts directly after sunrise, due to the need to recover from nightly biomass losses associated to cell maintenance (Figure 3.4a) [80]. Interestingly, the dilution rate declines from midday to sunset despite light being supplied at a continuous level throughout the 12 hours daytime. It is thought that the cell cycle plays a role in the observed growth pattern, as is shown by cell size (Figure 3.3) [81].

49
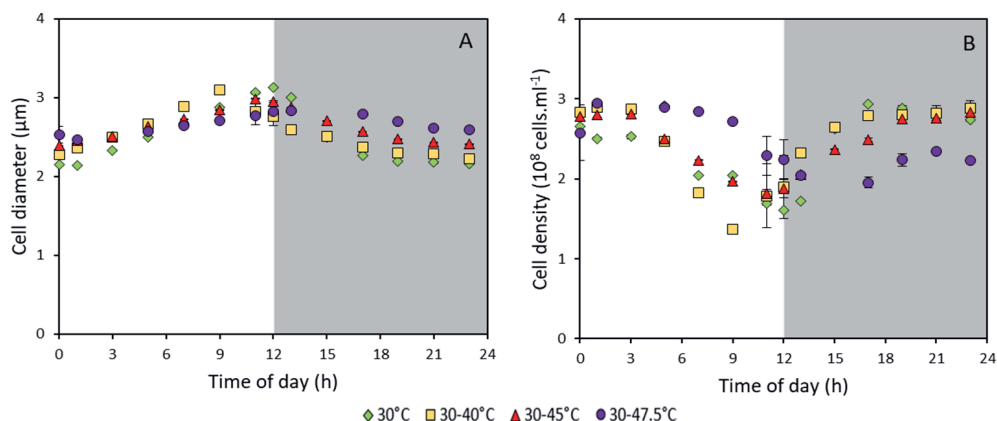
Figure 3.3: *cell diameter (a) and cell density values (b) over time in the microalgal cell culture during 24 hours of cultivation. The night and the peak culture temperature, found 6 hours after 'sunrise' are displayed in the legend. The x axis displays hours after 'sunrise', with day and night periods indicated in white and grey background, respectively. Data is composed of the average ± average deviation of both biological and technical duplicate measurements.*

An increase in cell size is observed from sunrise to sunset (Figure 3.3a). Cell division was initiated around sunset as indicated by the rapid decrease in cell size. Cell division of the culture was concluded within 8 hours after the first cell division event was observed, based on the increase in cell number (Figure 3.3b). For the culture grown at the diel cycle of 30-40°C, the onset of cell division was observed sooner than for the other cultures. The cell division took place at a cell diameter 3.2 μm which is the same size at which cell division occurred in the culture grown at the diel cycle of 30°C. Cultures grown under non-optimal conditions such as 30-45°C and 30-47.5°C, show reduced increase in cell size during the day. Furthermore, these cultures showed less cell division events during the night. Interestingly, the cell size continued to increase at a steady rate throughout daytime, even at a stressful peak temperature of 47.5°C. This contradicts the observations for the reactor dilution rate in which a reduction in growth was observed from 3 to 9 hours after sunrise. This continuing cell size increase is partly explained by the accumulation of storage compounds such as fatty acids (Figure 3.6). In addition, It was found that due to depigmentation of microalgae biomass the concentration of microalgae (in g.L^{-1}) within the photobioreactor kept growing despite the halted reactor dilution (Figure 3.4a and Figure 3.5).

A decrease in biomass concentration was observed in the night for every culture which is accounted for by respiration and maintenance requirements of the culture
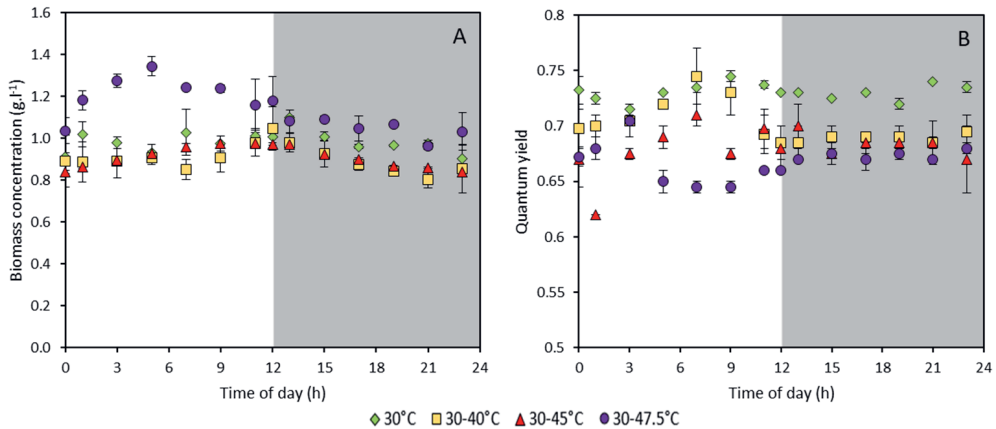
Figure 3.4: *Biomass concentration (a) and Quantum yield (b) values of the microalgal cell culture during 24 hours of cultivation. The night and the peak culture temperature, found 6 hours after 'sunrise' are displayed in the legend. The x axis displays hours after 'sunrise', with day and night periods indicated in white and grey background, respectively. Data is composed of the average ± average deviation of both biological and technical duplicate measurements.*

(Figure 3.4a). Based on literature, the rate of biomass decrease during night was expected to increase with increasing growth rate during daytime, and thus when the cells have a more active metabolism [80]. However, this was not observed in our data, in which the decline in biomass is the same for each condition. During daytime the biomass concentration remains stable between $0.8 - 1.0$ g.l^{-1} for all cultures, except for the culture grown with a peak temperature of 47.5°C in which the biomass concentration was 1.34 g.l^{-1}. This was caused by depigmentation of the cell due to temperature stress. This influenced the turbidostat control of the flat panel photobioreactor. Species of *Picochlorum* can rapidly adapt their photosystems to modulate the photon uptake rate [70]. Under stressful temperatures as seen in this experiment, *Picochlorum sp. BPE23* downregulated its photon uptake capacity accordingly, meaning that higher biomass concentrations were required to maintain the absorbed light level constant at 35 µmol.m^{-2}.s^{-1}.

Quantum yield, as a measure for the efficiency with which light energy is converted into assimilated carbon, was measured throughout the day (Table 3.1, Figure 3.4b). This analysis can serve as a qualitative indicator for cell health. We generally observe that quantum yield values for non-stressed cultures of *Picochlorum* range between 0.7 to 0.75. The algae grown at 30°C exhibited an average quantum yield of 0.73 ± 0.01. The algae cultures grown at diel cycles of 30-40°C and 30-45° showed

an increasing trend that continued until the peak temperature at mid-day was reached. While the culture grown at the diel cycle of 30-47.5°C showed a decrease, 5 hours after sunrise, when a temperature of 46°C was reached.

3.3.2. Pigment composition

The role of pigments in cells is diverse. Their role in photosynthesis involves light harvesting, photoprotection, ROS scavenging, excess energy dissipation, and structure stabilization [61, 82]. In addition, each pigment can fulfil multiple functions within the cell. Primary and secondary carotenoids synthesis is shown to be affected by exposure to temperature stress conditions, and significantly enhanced by the presence of ROS [66]. The concentration of six pigments present in the microalgae was measured throughout the day for all four experimental conditions (Figure 3.5).

Overall, pigment concentrations were highest for microalgae grown at 30-40°C. The cells showed decreasing levels of chlorophyll when diel peak temperatures
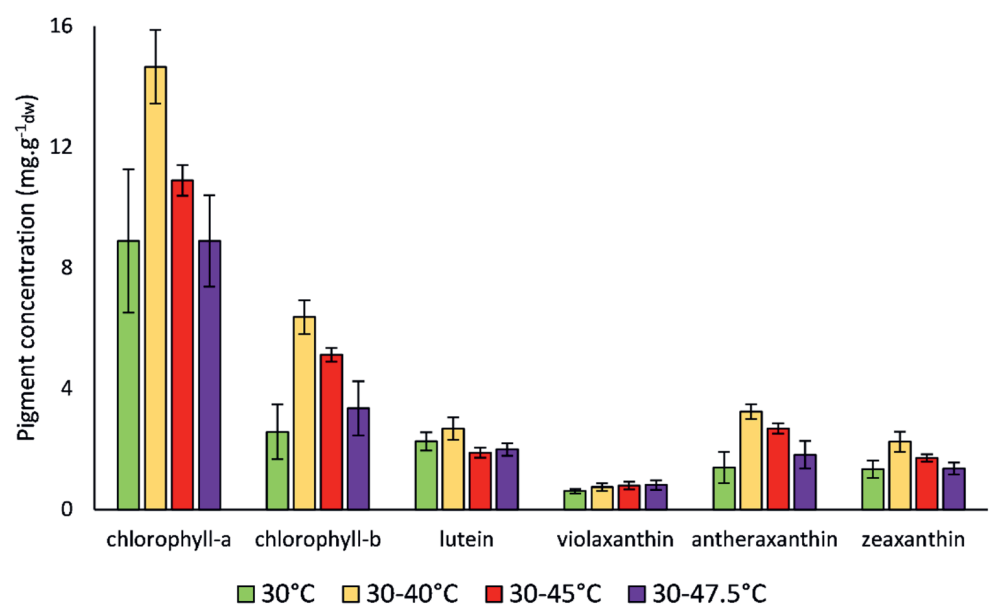
Figure 3.5: *Average pigment concentration of microalgae cells throughout the day under different temperature conditions. Every point represents the average of 14 samples measured throughout the day which were obtained as biological duplicate. The night and the peak culture temperature, found 6 hours after 'sunrise' are given in the legend.*

increased up to 45°C and 47.5°C, but also when a stable temperature of 30°C was applied. Modification of the pigment composition is often seen during adaptation to new environmental conditions [68-70]. When the growth rate decreases as a result of non-optimal growth temperatures, the cell is unable to utilize all the energy that is absorbed by the photosystems. Primary light-harvesting pigments are downregulated to prevent cell damage as a result of an energy overflow within the metabolism. Excess energy within the metabolism results in the formation of harmful ROS which is neutralised by scavenging compounds with an antioxidant function [83]. Three of these compounds present in *Picochlorum sp. BPE23* are the xanthophyll cycle pigments violaxanthin, antheraxanthin and zeaxanthin. With zeaxanthin being the most efficient ROS scavenger, followed by antheraxanthin and violaxanthin, respectively. The xanthophyll cycle serves as an important short term stress acclimation mechanism in higher plants, while its importance varies significantly amongst algae species [84]. As stressful temperatures have a disturbing effect on the electron transport chain, oversaturation of the photosystem likely caused excess energy in the microalgae cells grown at 30-47.5°C [61]. Increased concentrations of all xanthophyll cycle pigments, but especially zeaxanthin were expected to protect against cell damage [68, 69]. However, the opposite was observed (Figure 3.5), all measured pigments, including the pigments which are known as strong ROS scavengers, showed lower levels when stress conditions increased. The xanthophyll cycle appears to have an insignificant role in protecting against stressful diurnal temperature cycles in *Picochlorum sp. BPE23*, in similarity with other green microalgae species (Chlorophyceae) such as *Chlorella*, *Scenedesmus* and *Haematococcus* [84]. These pigments must, therefore, have a different function. The most obvious being involvement in light-harvesting complexes, which are hypothesised to be downregulated to decrease the energy inflow into the disrupted metabolism based on Dimier et al and Polle et al [70, 85]. This hypothesis is strengthened by the fact that the ratio of chlorophyll per zeaxanthin is stable at 1.5±0.05 under all temperature conditions [67]. Two exceptions on this decrease in pigment concentration are lutein and violaxanthin which are found at constant levels throughout all experimental conditions. These pigments must therefore fulfil a function other than light-harvesting, such as light-filtering or as an antioxidant [61].

3.3.3. Fatty acid composition

Fatty acid levels of the polar lipid fraction (PL) and triacylglycerol fraction (TAG) were measured throughout the day and presented as averaged content due to the absence of apparent trends within a cultivation day (Figure 3.6). The total lipid content was found highest for 30-45°C, at 186 mg.g^{-1}. The lipid content at 30-47.5°C was 162 mg.g^{-1} and the content at 30°C and 30-40°C was 149 and 152 mg.g^{-1}, respectively. Lipids in the polar lipid fraction show a decrease with increasing temperature. TAG is found at the highest concentration at 30-45°C. The content of C16:0, C16:3 and C18:3 in the polar lipid fraction decreases largely with increasing temperatures (Figure 3.6b). While C16:2 and C18:2 fractions show an increase. This increase in double unsaturated fatty acids is at the cost of triple unsaturated fatty acids. Comparable trends are found in literature, in which most species, including species of *Nannochloropsis*, *Rhodomonas* and *Isocrysis*, show increasing fatty acid saturation with increasing temperature [65, 86]. Changes in temperature may have a disruptive effect on the stability of the cell membrane due to changes in membrane fluidity. Remodelling of cell membrane components such as fatty acids and sterols is done to counteract this effect. With increasing fluidity, the level of saturated fatty acids in the cell membrane was upregulated at the cost of unsaturated fatty acids to maximize hydrophobic interactions, restoring membrane stability [87].

In the TAG fraction, the total amount of fatty acids increases with increasing temperature (Figure 3.6c). Indicating a larger reserve of lipids under more stressful conditions. This is mainly due to an increase of the fatty acids C16:0, C16:2 and C18:2. The other fatty acid groups show a comparable pattern, at a lower concentration. The effect of temperature on the level of TAG differs from species to species, some species show an increase in TAG with increasing temperature, while other species exhibit a decreased amount [65, 75]. In agreement with our data, studies on *Arabidopsis* and *Dunaliella* show increased TAG content with increased temperature [72, 87]. In both studies this was mainly caused by increased levels of saturated fatty acids. Correspondingly, increased temperature caused a decrease of the fatty acid 18:3 in *Arabidopsis* [87].
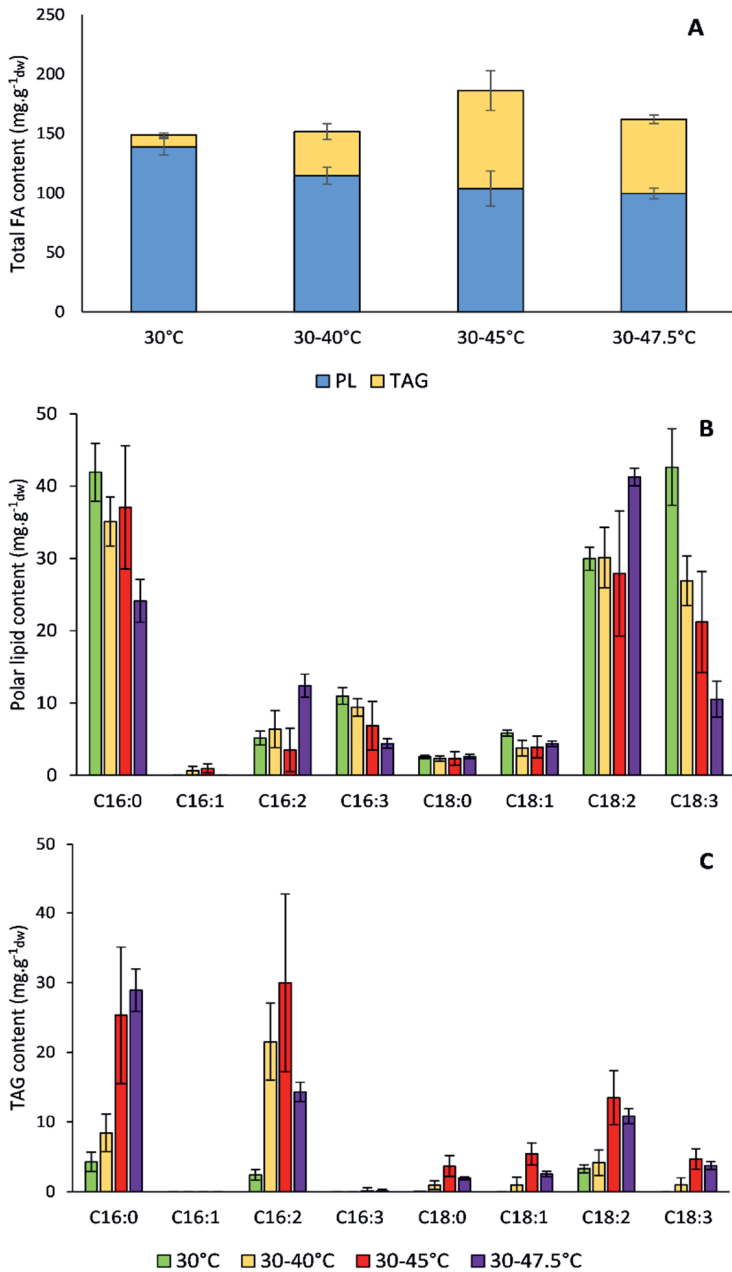
Figure 3.6: *(A) Polar lipid fraction (PL) and Triacylglycerol fraction (TAG) content in the biomass of Picochlorum sp. BPE23. (B) Effect of temperature on the Polar lipid content of Picochlorum sp. BPE23. (C) TAG content of Picochlorum sp. BPE23. The night and the peak culture temperature, found 6 hours after 'sunrise' are displayed in the legend. Data is presented as the average ± SD fatty acid content over a day using 8 timepoints within the day (biological replication: N = 2).*

3.4. Conclusions

Studies on the physiological response of microalgae to fluctuating temperatures as found in industrial production systems are scarce. Our objective is to develop a microalgae production process in which cooling could be avoided. Therefore *Picochlorum sp. BPE23* was subjected to four diel temperature cycles and its physiological response was studied. Temperature was found to affect the growth and biomass composition of microalgae severely. When exposed to temperatures other than the optimum growth temperature which was found at 40°C during daytime, a decrease in total pigment content was observed. Additionally, the fatty acid composition showed a tendency towards higher saturation levels with increasing temperature. Our study shows that the highest productivity of *Picochlorum sp. BPE23* is reached when the daytime temperature increased to a maximum of 40°C. Growth rate and productivity decreased with an increased diel peak temperature and under a continuous diel temperature of 30°C. Despite the reduced productivity, *Picochlorum sp. BPE23* was able to grow when exposed to a maximum diel temperature of 47.5°C. The ability to grow optimally at maximum diel temperature of 40°C instead of 30°C, can reduce costs for industrial microalgae production in tropical regions by 26.2%.

Chapter 4

Growth parameter estimation and model simulation for three industrially relevant microalgae: *Picochlorum, Nannochloropsis, and Neochloris*

Abstract

Multiple models have been developed in the field to simulate growth and product accumulation of microalgal cultures. These models heavily depend on the accurate estimation of growth parameters. In this paper growth parameters are presented for three industrially relevant microalgae species: *Nannochloropsis sp*., *Neochloris oleoabundans*, and *Picochlorum sp*. *BPE23*. Dedicated growth experiments were done in photobioreactors to determine the maximal biomass yield on light and maintenance rate, while oxygen evolution experiments were performed to estimate the maximal specific growth rate. *Picochlorum sp.* exhibited the highest specific growth rate of 4.98 ± 0.24 d^{-1} and the lowest specific maintenance rate of 0.079 d^{-1}, whereas *N. oleoabundans* showed the highest biomass yield on light of 1.78 $g_x.mol_{ph}^{-1}$. The measured growth parameters were used in a simple kinetic growth model for verification. When simulating growth under light conditions as found at Bonaire (12°N, 68°W), *Picochlorum sp.* displayed the highest areal biomass productivity of 32.2 $g.m^{-2}.d^{-1}$ and photosynthetic efficiency of 2.8%. The presented growth parameters show to be accurate compared to experimental data and can be used for model calibration by scientists and industrial communities in the field.

4.1. Introduction

Microalgae are a promising sustainable platform to produce proteins, lipids, carbohydrates and pigments. However, commercialization is still limited by high production costs [1, 31, 88]. These costs need to be significantly reduced to create a profitable business model. The production of microalgae commonly takes place in cultivation systems, such as raceway ponds and photobioreactors [62]. Many studies attempt at optimizing the microalgae production process through a variety of measures. Verification of the impact of these measures and optimization of the production process is commonly done through mathematical simulations before upscaling to pilot and production scale [89].

Many mathematical models have been developed, and are still being developed, to predict biomass productivity in photobioreactors [4, 88, 90, 91]. Applications of these models are for example: predictions on the impact of different photobioreactor designs, predictions on different operation modes, and predictions of the effect of different climatological conditions [89, 92]. One thing that all these models have in common is their dependency on accurate input parameters. Examples of important biological parameters for modeling microalgal growth are the maximal specific growth rate, the maximal biomass yield on light (i.e. intrinsic photosynthetic efficiency), and the specific maintenance rate of the microalgal species. However, to determine these model parameters for microalgae accurately and systematically is labor intensive. Such growth parameters are seldomly determined for microalgal species. Not only due to the required time, but also due to the knowledge gap regarding simple methodology to estimate these parameters. The efficiency and rate at which microalgae convert light into biomass differ significantly between species [93-95]. Considering this, growth parameters need to be determined anew for each species. As a result, there is a lack of reliable estimates of growth parameters to make accurate model predictions to simulate the impact of innovative methods on upscaling of algal cultivation [89].

The present study provides microalgal growth model parameters for three microalgae species that are of industrial interest: *Picochlorum sp., Neochloris oleoabundans,* and *Nannochloropsis sp*. [7, 96, 97]. The maximal photosynthetic efficiency (i.e. biomass yield on light), maintenance rate, and maximal specific growth rate were determined for each microalga in dedicated laboratory scale experiments. Flat-panel photobioreactors and a biological oxygen monitor device were used as reliable and quantifiable systems to measure these parameters. An

already existing and validated kinetic growth model was then applied to simulate and compare microalgae productivity at an ideal low-latitude location using the newly obtained growth parameters [90]. The model parameters can be used by others as input data in other mathematical models to simulate microalgal cultivation systems.

4.2. Material and methods

This study applied cell cultivation in flat-panel photobioreactors and a biological oxygen monitor to determine growth parameters for three selected microalgae. These growth parameters then were used as input data in a microalgae growth model to assess and compare the productivity of the three microalgae species.

4.2.1. Cell cultivation
4.2.1.1. Pre-culture and growth media

Picochlorum sp. BPE23 was isolated from a saltwater body of Bonaire (12°N, 68°W) and pre-cultivated in shake flasks in an orbital shaker incubator (Multitron, Infors HT) with a 12/12 h day/night cycle and an average light intensity of 100 μmol_{ph} m^{-2} s^{-1} [7]. The temperature was 40 °C during the day and 30 °C during the night. The incubator's relative air humidity was set to 60% and enriched with 2% CO_2. Cells were cultured in artificial seawater enriched with nutrients and trace elements. Salts, nutrients and trace elements were provided at the following concentrations (in g.L^{-1}): NaCl, 24.5; $MgCl_2.6H_2O$, 9.80; Na_2SO_4, 3.20; CH_4N_2O (urea), 2.12; K_2SO_4, 0.85; $CaCL_2.2H_2O$, 0.80; KH_2PO_4, 0.23; $Na_2EDTA·2H_2O$, 0.105; Na_2EDTA, 0.06; $FeSO_4.7H_2O$, 0.0396; $MnCl_2·2H_2O$, $1.71·10^{-3}$; $ZnSO_4.7H_2O$, $6.60·10^{-4}$; $Na_2Mo_4·2H_2O$, $2.42·10^{-4}$; $Co(NO_3)_2·6H_2O$, $7.00·10^{-5}$; $NiSO_4·6H_2O$, $2.63·10^{-5}$; $CuSO_4·5H_2O$, $2.40·10^{-5}$; K_2CrO_4, $1.94·10^{-5}$; Na_3VO_4, $1.84·10^{-5}$; H_2SeO_3, $1.29·10^{-5}$. HEPES (4.77 g.L^{-1}) was added as a pH buffer to shake flask cultures. The medium pH was adjusted to 7.0 after which it was filter sterilized before use. Antifoam B (J.T.Baker, Avantor, USA) was added at a concentration of 0.5 mL.L^{-1} from a 1% w/w% stock. Sodium bicarbonate ($NaHCO_3$)(0.168 g.L^{-1}) was added during the inoculation to provide sufficient CO_2 at the start of the cultivation.

Neochloris oleoabundans UTEX1185 and *Nannochloropsis* sp. CCAP 211/78 pre-cultures were cultivated in an orbital shaker incubator (Multitron, Infors HT), and illuminated with 50 μmol_{ph} m^{-2}s^{-1}. Temperature was set to 25 °C, and the headspace was enriched with 2% CO_2. *Neochloris oleoabundans* and *Nannochloropsis* sp. were cultivated on filtered natural seawater (Oosterschelde, The Netherlands) enriched with the following nutrients and trace elements (in g.L^{-1}): KH_2PO_4, 0.23; Na_2EDTA, 0.21; $Fe_2SO_4·7H_2O$, 0.03; $MnCl_2·2H_2O$, $1.62·10^{-3}$; $ZnSO_4·7H_2O$, $6.61·10^{-4}$; $Co(NO_3)_2·6H_2O$, $6.98·10^{-4}$; $CuSO_4·5H_2O$, $2.50·10^{-4}$; $Na_2MoO_4·2H_2O$, $2.66·10^{-3}$. HEPES (4.77 g.L^{-1}) and Na_2EDTA (1.86 g.L^{-1}) were added to the seawater as a pH buffer to

Erlenmeyer cultures. The medium pH was adjusted to 7.5 followed by heat sterilization (20 minutes at 121˚C). The nutrient and trace element solution was first autoclaved, and then filtrated through a sterile filter (0.20 μm). Sodium nitrate (2.13 g.L^{-1}) was used as nitrogen source to cultivate *Nannochloropsis* sp. CCAP 211/78, whereas urea (1.50 g.L^{-1}) was used for *Neochloris oleoabundans*.

4.2.1.2. Photobioreactor operation to estimate yield on light and maintenance rate

Microalgae were cultivated in sterilized flat panel photobioreactors (Algaemist, Technical Development Studio, WUR) with a 0.38 L working volume and a 14 mm optical depth [98]. Flat panel photobioreactors were chosen for these experiments as these systems allow for the most accurate light calibration which is essential for accurate estimation of growth parameters. Photobioreactors were operated in chemostat mode at different dilution rates to determine the growth parameters: maximal yield of biomass on light (Y_{xphm}) and specific maintenance rate (μ_e). The photobioreactor was continuously illuminated (24/24h) with warm white LED lamps (Bridgelux, BXRA W1200). Optimal growth temperatures were chosen for each microalgae species [7, 99]. The CO_2 level in the photobioreactor was non-limiting, as controlled by the pH level through on-demand CO_2 supplementation. The outgoing light was measured with an external LI-COR SA-190 Quantum sensor (PAR-range 400-700 nm). Photobioreactor harvest was collected in darkness at 4 °C and weighed daily to monitor the photobioreactor dilution rate.

Table 4.1: *Experimental settings applied in the chemostat experiments to determine the maximal biomass yield on light and the maintenance rate.*

Organism	Nannochloropsis sp. CCAP 211/78	Neochloris oleoabundans	Picochlorum sp. BPE23
Applied dilution rates (d^{-1})	0.1, 0.2, 0.4, 0.5, 0.6	0.4, 0.5, 0.6, 0.7, 0.8, 0.9, 1.2	0.18, 0.27, 0.31, 0.35, 0.48, 0.48, 0.57, 0.69, 0.90
Incident light intensity (μmol$_{ph}$.m^{-2}.s^{-1})	100	100	100
Temperature (˚C)	25	30	39
Air flow rate (vesselvolume.min^{-1})	2	2	1

The photobioreactor was operated until a steady state was reached. The steady state was defined as followed: the variation on the measurements of optical density and dilution rate should remain <15% for at least three days. After reaching this steady state, measurements were performed daily for an additional seven days after which the average of the steady state was taken for data presentation.

4.2.1.3. Biological oxygen monitor to estimate maximal photosynthetic rates

The maximal specific growth rate (μ_{max}) was indirectly estimated by monitoring the photosynthetic oxygen production rate with a liquid phase biological oxygen monitor (BOM) (Oxytherm[+], Hansatech). An exponentially growing cell culture was diluted to a density of 0.1 to 0.4 g.L^{-1} in 2.4 mL volume and inserted into the measurement cuvette of the BOM. This low cell density was selected to minimize in-culture cell shading. The medium was buffered at pH 7 with 20 mM HEPES and enriched with 50 mM sodium bicarbonate. Oxygen was stripped from the cell culture with nitrogen gas before closure of the cuvette. The microalgal culture was first exposed to darkness followed by increasing light levels while the oxygen concentration in the liquid was continuously recorded to generate a photosynthesis irradiance curve (PI curve). During this sequence the suspension was continuously mixed by a magnetic stirring bar and temperature was controlled at the optimal growth temperature (Table 4.1). Applied light levels are displayed in supplementary material 4.6. The increase in dissolved oxygen over time was then used to calculate the specific growth rate.

4.2.2. Analysis
4.2.2.1. Dry weight

The biomass concentration (in g.L^{-1}) was measured in duplicate as dry weight. Empty Whatman glass microfiber filters (θ 55 mm, pore size 0.7 μm) were dried overnight at 95 °C and placed in a desiccator for 2 hours. Filters were then weighed and placed in a mild vacuum filtration setup. Culture containing 1 to 10 mg of microalgae biomass was diluted in 25 mL 0.5 M ammonium formate and filtered. The filter was washed twice with 25 mL 0.5 M ammonium formate to remove residual salts. The wet filter was dried overnight at 95 °C, placed in a desiccator for

2 hours, and weighed. Biomass concentration was calculated from the difference in filter weight before and after filtration, and the volume of the sample.

4.2.2.2. Absorption cross-section

The average dry-weight specific optical cross section (m^2.g^{-1}) was measured with an UV-VIS/double-beam spectrophotometer (Shimadzu UV-2600, Japan, light path: 2 mm), equipped with an integrating sphere module (ISR-2600). Absorbance was measured from 400 to 700 nm with a step size of 1 nm.

4.2.3. Calculations

The μ: specific growth rate (d^{-1}) was determined over a range of incident irradiance levels (Supplementary material 4.6) using the biological oxygen monitor and Equation 4.1. With r_o: the oxygen production rate (mol.L^{-1}.d^{-1}), x_{ox}: the ratio of oxygen per biomass produced (mol.mol^{-1}), and $C_{xcuvette}$: biomass concentration in the culture chamber (mol.L^{-1}). A molecular weight for microalgal biomass of 24 g.mol^{-1} was adopted from the literature [90]. The ratio in mole of oxygen per mole of biomass (x_{ox}) was 1.11 for urea, and 1.44 for nitrate, as nitrogen source [93]. μ_{max} was found at the light intensity where μ was largest.

$$\mu = \frac{r_o}{x_{ox} \cdot C_{xcuvette}} \qquad\qquad \text{Equation 4.1}$$

The maximal biomass yield on light and the maintenance rate were determined by chemostat experiments under light limited conditions. First the specific growth rate, μ (d^{-1}), was calculated through the photobioreactor dilution rate (d^{-1}) using Equation 4.2. With: M_h: harvest mass, (g.d^{-1}), V_r: photobioreactor volume (0.38 L), and ρ: culture medium density (1030 g.L^{-1}).

$$\mu = D = \frac{M_h}{V_r \rho} \qquad\qquad \text{Equation 4.2}$$

Through Equation 4.3, which is based on Pirt's law, a linear regression was made for the photobioreactor experiments by varying the reactor dilution rate. With as a result μ and q$_{ph}$: the specific photon consumption rate (Figure 4.1) [93, 100]. The equation was built on the assumption that all absorbed photons are used at maximal efficiency because of the application of light limitation and absence of photo saturation. This assumption is only valid under low light conditions as in the

performed experiments, and evidenced by a linear correlation between μ and q_{ph} [101, 102]. The slope in this regression is equal to $\frac{1}{Y_{xphm}}$ and the intercept with the y-axis $m_s = \frac{\mu_e}{Y_{xphm}}$.

$$q_{ph} = \frac{\mu}{Y_{xphm}} - \frac{\mu_e}{Y_{xphm}} = \frac{I_{phin} - I_{phout}}{C_x \, d} \qquad \text{Equation 4.3}$$

4.2.4. Model simulations

The obtained biological parameters (i.e. Y_{xphm}, μ_e, and μ_{max}) for *Picochlorum sp.*, *Nannochloropsis sp.*, and *N. oleoabundans* were used in an existing kinetic model for microalgal growth under light limited conditions [90] in order to simulate and compare their potential biomass productivities in a flat panel photobioreactor. This model was validated and proved to be accurate for simulating microalgal growth on lab-scale [90, 103]. The model calculations are based on the Lambert-Beer law, the photosynthesis model of Jassby and Platt, and the aerobic chemoheterotrophic growth model of Pirt, and were applied to calculate the biomass productivity in case of chemostat operation as an example to showcase the measured biological growth parameters [101, 104]. It must be noted that the obtained parameters can also be used in other microalgal growth models that may be more sophisticated or in which non-ideal growth conditions are simulated.

In our simulations, it was assumed that the photobioreactor is located on the Caribbean island Bonaire (12°N, 68°W) as an example case. Irradiance data was obtained from Meteonorm 7.1, a global climate database, in which measured irradiance over recent decades at the nearby weather station on Curacao is used to generate hourly data for a typical year. Of this data, day 172 was considered (Supplementary material 4.2), which is equal to the summer solstice, i.e. the longest day in the northern hemisphere. Based on the irradiance values, light intensities on day 172 were simulated as a sinus function in which a maximum intensity of 1900 $\mu mol_{ph}.m^{-2}.s^{-1}$ is reached at noon, sunrise occurs at 6:00 am and sunset occurs at 6:00 pm.

Using the simulated light intensity, the Lambert-Beer law is applied in the model to compute the light gradient over the depth of a flat horizontal photobioreactor (Rquation 4.4). The Lambert-Beer law is a simple and commonly used method to model light. For the purpose of verifying the estimated growth parameters in flat

panel photobioreactor systems the applied method provides sufficient accuracy. In research where the aim is to provide more accurate growth estimations for complicated reactor designs or weather patterns, more refined light models may be required, which include variation in the direction of light and light scattering (e.g. ray tracing or Monte-Carlo simulations).

The applied model takes into account the spectrum of the sun, the depth of the photobioreactor, the absorption cross section of the microalgae, and the biomass concentration of the culture.

$$I_{ph}(z) = \sum_{\lambda=700}^{\lambda=400} I_{ph,\lambda}(0) \cdot e^{-a_{x,\lambda} \cdot C_x \cdot z} \cdot \Delta\lambda \qquad \text{Equation 4.4}$$

In which $I_{ph}(z)$ is the light intensity at depth z in the cell culture (mol$_{ph}$.m^{-2}.s^{-1}), $I_{ph,\lambda}(0)$ is the light intensity for each wavelength in the PAR-region at the illuminated surface of the cell culture (mol$_{ph}$.m^{-2}.s^{-1}), $a_{x,\lambda}$ is the wavelength-dependent absorption cross section (m^2.mol$_x$$^{-1}$), C_x is the biomass concentration (mol$_x$.m^{-3}), z is the distance from the illuminated reactor surface to depth z in the culture (m), and λ is the wavelength of the light in the PAR-region (nm).

In our simulations, it was assumed that the depth of the reactor is equal to 0.015 m. This is an arbitrary choice and lies within a normal range for flat panel photobioreactors. The optical depth of the reactor ultimately influences the biomass concentration and can be further optimized at a later stage. The volume of the reactor itself does not influence the model results. For the absorption cross sections $a_{x,\lambda}$ of the microalgae, values for wavelengths between 400-700 nm were obtained from experiments in this study and from literature for low light conditions (Supplementary material 4.3).

From the light gradient within the reactor, the model ultimately calculates the average specific growth rate (Equation 4.5), based on the photosynthesis model of Jassby and Platt and the aerobic chemoheterotrophic growth model of Pirt.

$$\mu = \mu_m \cdot \tanh\left(\frac{Y_{xphm} \cdot a_x \cdot I_{ph}}{\mu_m}\right) - \mu_e \qquad \text{Equation 4.5}$$

In which μ is the average specific growth rate (s^{-1}), μ_m is the maximum specific growth rate (s^{-1}), Y_{xphm} is the maximum biomass yield on light (mol$_x$.molph^{-1}), and μ_e is the maintenance rate (s^{-1}).

The areal biomass productivity and the biomass yield on light were calculated by the model for chemostat operation conditions where the dilution was set for the

hours between sunrise and sunset. A period of 10 identical days was simulated, which was found to be sufficient to reach a pseudo steady-state characterized by a repetitive cyclic pattern of the biomass concentration. For each of the microalgae, a dilution rate was chosen that results in the highest biomass productivity, namely 0.68 d^{-1} for *Picochlorum sp.*, 0.47 d^{-1} for *N. oleoabundans*, and 0.44 d^{-1} for *Nannochloropsis sp.* (Supplementary material 4.4).

The changes in biomass concentration in the photobioreactor as well as the harvested biomass were computed for every minute of the simulated period, based on Equation 4.6 and 4.7.

$$\frac{d}{dt} C_x(t) = (\mu(C_x(t), t) - D(t)) \cdot C_x(t) \qquad \text{Equation 4.6}$$

$$\frac{d}{dt} M_x(t) = D(t) \cdot C_x(t) \qquad \text{Equation 4.7}$$

In which D is the dilution rate (s^{-1}) and M_x is the harvested biomass (mol.m^{-3}).

Since the average specific growth rate μ itself is a function of the biomass concentration in the photobioreactor, a Runge-Kutta method was adopted to solve the differential equations for C_x and M_x over the simulated period of 10 days. The initial biomass concentrations were chosen to be 2.9 g.L^{-1} for *Picochlorum sp.*, 3.6 g.L^{-1} for *N. oleoabundans*, and 3.6 g.L^{-1} for *Nannochloropsis sp,* which were found to be near the final steady-state concentrations*.*

Ultimately, the areal biomass productivity and the observed biomass yield on light on the tenth day were considered. These were calculated using Equation 4.8 and 4.9.

$$r_{x,area} = \left(C_x(t_{d10}) - C_x(t_{d9})\right) + \left(M_x(t_{d10}) - M_x(t_{d9})\right) \cdot l \qquad \text{Equation 4.8}$$

$$Y_{x/ph} = \frac{r_{x,area}}{I_{ph}} \qquad \text{Equation 4.9}$$

In which $r_{x,area}$ is the areal biomass productivity (mol.m^{-2}.d^{-1}), I is the photobioreactor depth (m), $Y_{x/ph}$ is the observed biomass yield on light (mol$_x$.mol$_{ph}$$^{-1}$), and I_{ph} is the total available irradiance during the simulated day (mol$_{ph}$). From the areal biomass productivity and the available irradiance, the photosynthetic efficiency was also determined as described in supplementary material 4.5.

4.3. Results and discussion

4.3.1. Biomass yield on light and specific maintenance rate

The maximal biomass yield on light and specific maintenance rate were determined through light limited chemostat experiments for the microalgae *Picochlorum sp. BPE23, Nannochloropsis sp.* and *Neochloris oleoabundans*. Currently, the most accurate method for estimation of the maximal yield on light and the specific maintenance rate is based on the application of chemostat-operated photobioreactors. In this situation, a steady state will be reached, allowing for measurements on a culture that does not change over time. This approach is essential for photoautotrophic growth due to the extra dimension of light. Changing biomass concentrations during phototrophic batch growth will cause changing substrate (i.e., light) levels due to in-culture cell shading. In comparison, for heterotrophic growth, steady-state conditions are of less importance as changing biomass concentrations will not directly affect substrate availability, and therefore, batch experiments are often used to determine the biomass yield on substrate. A low incident irradiance level of 100 $\mu mol_{ph}\, m^{-2}\, s^{-1}$ was set to ensure that all light was used for growth without energy wastage through light dissipation in the photosynthetic complexes. The specific photon consumption: q_{ph} rate was plotted as a function of the reactor dilution rate, and thus as the specific growth rate (μ) (Equation 4.2) for each of the performed experiments (Figure 4.1). This resulted in a linear relation between the different runs. The linear relation observed for each of the microalgae confirms that light limited conditions were achieved, as light saturated cells would have resulted in a negative exponential relationship
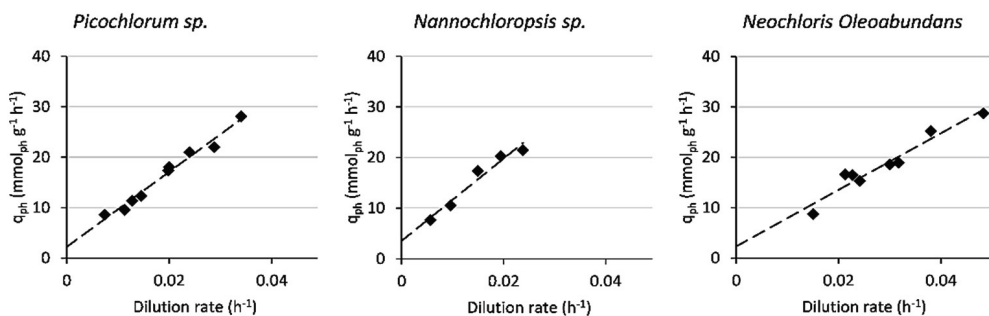
Figure 4.1: *Specific photon consumption rate as a function of the photobioreactor dilution rate for three microalgae species, Picochlorum sp. BPE23, Nannochloropsis sp., and Neochloris oleoabundans. Each data point is the average ± S.D. of seven days of steady-state growth. A linear regression was plotted to indicate the intercept with the y-axis.*

[101, 102]. Therefore, we conclude that almost all energy was utilized for growth and that energy dissipation as a result of photosystem oversaturation was minimal. A linear regression was made for each dataset (Figure 4.1). The inverse of these regression lines' slopes represents the maximal biomass yield on light (Y_{xphm}). The specific maintenance rate (μ_e) of the microalgae species was deducted from the point at which the regression line intercepts the y-axis.

An overview of the obtained model parameters is presented in Table 4.2. The maximal biomass yield on light for *Picochlorum sp. BPE23* was determined to be 1.38 $g_x.mol_{ph}^{-1}$. For *Nannochloropsis sp.* a lower yield on light of 1.23 $g_x.mol_{ph}^{-1}$ was measured, while for *N. oleoabundans* a higher yield on light of 1.78 $g_x.mol_{ph}^{-1}$ was measured. The maximal theoretical yield on light is 1.5 and 1.8 $g_x.mol_{ph}^{-1}$ for growth on nitrate and urea, respectively [105]. In practice, microalgal species show a yield on light ranging from 1.0 to 1.8 $g_x.mol_{ph}^{-1}$, depending on species. The model organisms *Chlamydomonas reinhardtii* and *Chlorella sorokiniana* display a yield on light of 1.25 and 1.80 $g_x.mol_{ph}^{-1}$, respectively [93, 106], while *Dunaliella salina* and *Tetradesmus obliquus* present a yield on light of 1.00 and 1.15 $g_x.mol_{ph}^{-1}$ [95, 107]. A study done on *Nannochloropsis salina* shows a yield on light of 1.68 $g_x.mol_{ph}^{-1}$, which is high compared to the yield on light of 1.23 $g_x.mol_{ph}^{-1}$ that we found for *Nannochloropsis sp.* in our study [94].

The maximal yield on light varies significantly between species, and even between strains. The cause for the variation is difficult to pinpoint and would require in-depth study of each strains' energy metabolism. To a certain extent the yield on light is influenced by the biomass composition, which can cause a small error in the estimated growth parameters. Also the efficiency in energy transfer and carbon fixation can lead to differences in photosynthetic efficiency [108]. Another potential cause is the absorption of light by filtering pigments, which reduces the available photons for biomass formation [61].

Table 4.2: *Values for the maximal biomass yield on light (Y_{xphm}) and maintenance rate (μ_e), as found through photobioreactor experiments.*

Organism	Y_{xphm} ($g_x.mol_{ph}^{-1}$)	μ_e (d^{-1})
Picochlorum sp. BPE23	1.38	0.079
Nannochloropsis sp. CCAP 211/78	1.23	0.099
Neochloris oleoabundans	1.78	0.104

The specific maintenance rate (μ_e) was estimated experimentally. *Picochlorum sp. BPE23* showed a specific maintenance rate of 0.079 d^{-1}, whereas *Nannochloropsis sp.* and *N. oleoabundans* showed a specific maintenance rate of 0.099 d^{-1} and 0.104 d^{-1}, respectively. This maintenance rate equals the rate at which microalgal biomass decreases when irradiated, and in darkness. To facilitate maintenance during dark periods, microalgae provide energy from reserves through respiration. The estimated specific maintenance rates in our study are average to low compared to values found in literature. Few microalgal species from the class of *Chlorophyceae* such as *Chlorella pyrenoidosa*, *Dunaliella tetriolecta*, and *Nannochloropsis atomus* exhibit specific maintenance rates of 0.08, 0.18, and 0.14 d^{-1}, respectively [108].

4.3.2. Maximal growth rate

The microalgal net specific oxygen production rate (q_o) was measured for *Picochlorum sp. BPE23*, *Nannochloropsis sp.*, and *Neochloris oleoabundans* when grown on urea and nitrate, using a range of light intensities (Figure 4.2). From the specific oxygen production rate we estimated the maximal specific growth rate (μ_{max}) based on biomass stoichiometry (Table 4.3) [93]. Estimating the maximum specific growth rate directly through growth experiments is complicated. Conditions at which microalgae growth at their maximal growth rate are complicated to maintain in a steady state situation throughout an experiment while measuring biomass concentrations. In addition, growing microalgae at low biomass density with a high incident irradiance destabilizes the cell culture which causes stress responses such as biofilm formation, auto flocculation, and sedimentation. As a result, we chose to monitor the specific oxygen production rate as a proxy for the specific growth rate. Monitoring biological oxygen production is a quick and efficient method estimate microalgal specific growth rates under different culture conditions. *Picochlorum sp. BPE23* showed the highest specific oxygen production rate out of the three microalgal species, both when grown on urea and on nitrate. *Picochlorum sp. BPE23 reached* this highest specific oxygen production rate at a light intensity of 1500 umol.m^{-2}.s^{-1}. The specific oxygen production rate decreased with increasing light intensities above 1500 umol.m^{-2}.s^{-1}. For *Nannochloropsis sp.* and *Neochloris oleoabundans* a decrease of the specific oxygen production rate was not observed. This decreasing specific oxygen production rate in *Picochlorum sp. BPE23* may have been caused by photoinhibition. However, a more likely reason
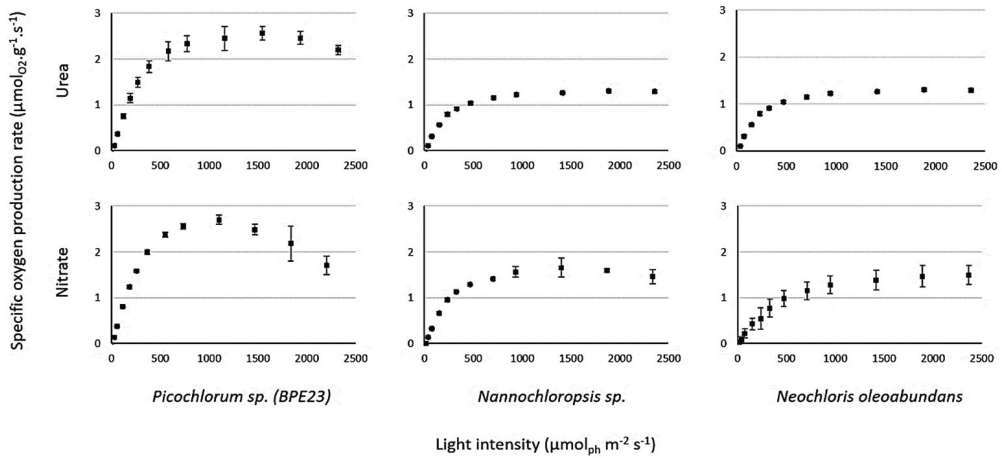
Figure 4.2: *PI curves for Picochlorum sp. BPE23, Neochloris oleoabundans, and Nannochloropsis sp., grown with either urea or nitrate as nitrogen source. The y-axis displays the specific oxygen production rate ($\mu mol_{O2}.g^{-1}.s^{-1}$) at different light levels, measured by the biological oxygen monitor (BOM). Data represent the average ± S.D. of at least 3 biological replicates.*

for this decline is the oxygen concentration in the liquid phase which reached values above air saturation in these specific experiments (Supplementary material 4.1). These high and oversaturating oxygen concentrations resulted in the formation of gas bubbles which was further stimulated by the rapid mixing of the culture in the biological oxygen monitor. Such gas bubbles serve as a sink for oxygen, leading to a decrease of the dissolved oxygen level in the liquid phase, causing an underestimation of oxygen production rates. For measurements with *Neochloris* and *Nannochloropsis* the oxygen concentration in the liquid phase never surpassed the level of air saturation.

The maximal specific growth rate was then estimated using the highest value of the specific oxygen production rate for each species and growth condition. For *Picochlorum sp. BPE23* grown on urea a maximum specific growth rate of 4.98±0.24 d^{-1} was calculated, and when grown on nitrate a growth rate of 3.79±0.06 d^{-1} was calculated. *Nannochloropsis* displayed a maximal specific growth rate of 2.10±0.19 d^{-1} with urea as a nitrogen source and 2.48±0.24 d^{-1} with nitrate as nitrogen source. *Neochloris* displayed a maximal specific growth rate of 2.45±0.05 d^{-1} when grown on urea and 2.44±0.45 d^{-1} when grown on nitrate. Comparable maximal specific growth rates have been reported in the literature [99, 109]. Urea and nitrate are both commonly used nitrogen sources for microalgal production. Stoichiometrically maximal specific growth rates using urea should be higher than for nitrate, as

nitrate is more reduced than urea and therefore requires a larger investment of energy for conversion to protein [93]. However, only *Picochlorum sp. BPE23* grew faster on urea than on nitrate. While in theory urea is energetically favorable, in practice it is unpredictable which nitrogen source yields higher specific maximal growth rates [110, 111]. Species of *Picochlorum* are known for their high growth rate; Weissman et al. found a growth rate for *Picochlorum Celeri* of 7.9 - 8.16 d^{-1} [21, 78]. Such high growth rates are rarely found in microalgae, as most microalgae show a maximal specific growth rate of 1 d^{-1} to 3 d^{-1} [6, 62, 89]. The specific growth rate of strains within a genus can differ significantly, as seen by the difference in maximal specific growth rate for *Picochlorum Celeri* and *Picochlorum sp. BPE23*. The variation between species with regard to substrate preference and growth characteristics is why growth parameters have to be determined anew for each strain.

Table 4.3: *Values for the estimated maximal specific growth rate (μ_{max}) based on biological oxygen evolution experiments.*

Organism	μ_{max}(d^{-1})(urea)	μ_{max}(d^{-1})(Nitrate)
Picochlorum sp. BPE23	4.98±0.24	3.79±0.06
Nannochloropsis sp. CCAP 211/78	2.10±0.19	2.48±0.24
Neochloris oleoabundans	2.45±0.05	2.44±0.45

4.3.3. Model simulations

As an example, the biological parameters obtained for *Picochlorum sp. BPE23, Nannochloropsis sp.*, and *N. oleoabundans* were used in a microalgal growth model to simulate their potential biomass productivity in a flat panel photobioreactor under chemostat operation conditions (Figure 4.3). In these simulations, the Caribbean island Bonaire was considered, which is a low-latitude location with high irradiance throughout the year. Irradiance levels on day 172 of the year, corresponding to the longest day in the northern hemisphere, were used in the model. Based on generated irradiance data (Supplementary material 4.2), assumed operation conditions, obtained biological parameters (Table 4.2 and 4.3), and respective absorption coefficients (Supplementary material 4.3), the areal biomass
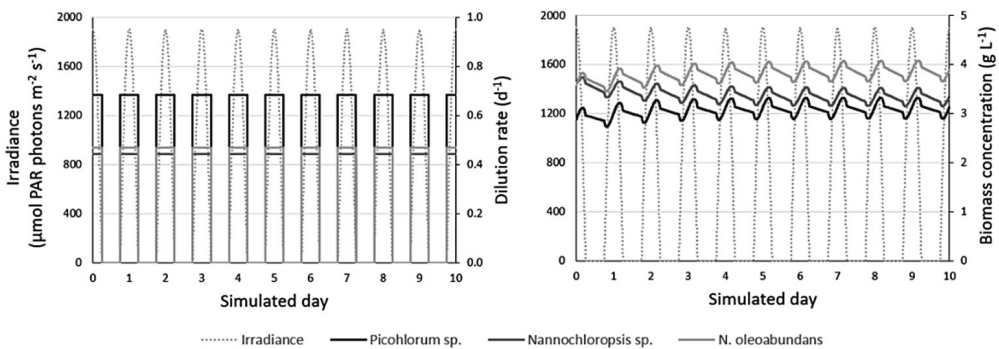
Figure 4.3: *The irradiance levels, dilution rates, and biomass concentrations of the microalgae during the simulated period of 10 identical days.*

productivity and biomass yield on light were computed for the microalgae. Ten identical days were simulated, during which a pseudo-steady state is reached (Figure 4.3). The last day was considered to calculate the biomass productivity of the microalgae.

Our simulations show that *Picochlorum sp.* achieves the highest areal biomass productivities (Table 4.4); productivities of 32.2 $g.m^{-2}.d^{-1}$ were computed, whereas for *N. oleoabundans* and *Nannochloropsis* values of 27.4 and 22.4 $g.m^{-2}.d^{-1}$ were found, respectively. Considering the simulated available sunlight on day 172, namely 52.3 $mol_{ph}.m^{-2}.d^{-1}$, these productivities correspond to the following photosynthetic efficiencies (PE) normalized to the complete solar spectrum (Supplementary material 5): 2.8% for *Picochlorum sp.*, 2.4% for *N. oleoabundans*, and 2.0% for *Nannochloropsis sp.* (Table 4.4 and Supplementary material 4.5).

These values are in a similar range or slightly higher compared to photosynthetic efficiencies reported for outdoor photobioreactor experiments [4, 62]. For instance, in the Netherlands, average photosynthetic efficiencies of 1.1-2.4% and areal productivities of 9.7-20.5 g.m^{-2}.d^{-1} were achieved with *Nannochloropsis sp.* in outdoor photobioreactors during several weeks in the summer [62]. It should be noted that studies are difficult to compare directly due to the differences in location, microalgae species, and cultivation conditions.

Table 4.4: *Model results for the areal biomass productivity ($r_{x,area}$) and the photosynthetic efficiency (PE) of the microalgae when grown in a photobioreactor on Bonaire. For the simulations of Picochlorum sp. BPE23, Nannochloropsis sp., and Neochloris oleoabundans, the obtained biological parameters in this study (Table 4.2 and 4.3) were used, whereas for Picochlorum celeri a hypothetical simulation was done using its μmax of 7.9 d^{-1} [21] in combination with the biological parameters of Picochlorum sp. BPE23.*

Organism	$r_{x,area}$ (g m^{-2} d^{-1})	PE (%)
Picochlorum sp. BPE23	32.2	2.8
Nannochloropsis sp. CCAP 211/78	27.4	2.4
Neochloris oleoabundans	22.4	2.0
Picochlorum celeri	40.6	3.5

The model results illustrate that, in a photobioreactor at a low-latitude location such as Bonaire, *Picochlorum sp.* is able to achieve the highest biomass productivities, followed by *N. oleoabundans* and *Nannochloropsis sp*. The differences between the microalgae are largely a result of their maximum specific growth rate; in this study the maximum specific growth rate for *Picochlorum sp.* was found to be more than double that of *Nannochloropsis sp.* and *N. oleoabundans* when grown on urea (Table 4.3). Other studies show even higher values for *Picochlorum* species. For example, Krishnan et al. 2021 found an exceptional maximum specific growth rate of 7.9 d^{-1} for *Picochlorum celeri* when grown at a relatively high temperature of 33 °C and constant light of 900 μmol.m^{-2}.s^{-1} in a salt water medium [78]. To discern the effect of such a high maximum growth rate on the final biomass productivity, simulations were performed with the microalgal growth model in which a maximal growth rate of 7.9 d^{-1} was considered in combination with the other measured growth parameters of *Picochlorum sp.* These simulations resulted in high biomass productivities of 40.6 g.m^{-2}.d^{-1} at a

location such as Bonaire (Table 4.4). This productivity corresponds to a photosynthetic efficiency of 3.5% (Table 4.4). The results illustrate the potential of fast-growing microalgae such as *Picochlorum* to improve biomass productivities and photosynthetic efficiencies.

Our model allows estimation of potential biomass productivities that can be reached based on the determined biological parameters of the microalgae and the irradiance conditions at a low-latitude location. To model and compare reliable estimates of biomass productivity of different algal species under solar conditions, it is essential to accurately determine the biological parameters of each microalgae strain, including the maximum growth rate, maximum biomass yield on light, and maintenance rate, as was done in this study. These parameters can ultimately be used in different models to study and optimize microalgae production.

4.4. Concluding remarks

The growth parameters biomass yield on light, specific maintenance rate and maximal specific growth rate were measured for the microalgae *Picochlorum sp.*, *N. oleoabundans,* and *Nannochloropsis sp.* using urea and nitrate as nitrogen sources. *Picochlorum sp.* exhibited the highest maximal specific growth rate with 4.98 ± 0.24 d^{-1}, and the lowest specific maintenance rate of 0.079 d^{-1}. *N. oleoabundans* displayed the highest yield on light of 1.78 $g_x.mol_{ph}^{-1}$.

A simple growth model was applied to compare biomass productivities at a high-irradiance location. Based on these model simulations, *Picochlorum sp.* was found to achieve the highest biomass productivity, followed by *N. oleoabundans* and *Nannochloropsis sp.* The measured growth parameters are of significant relevance as they can be applied in more extensive models without further modification, can help to compare microalgal species, and help to manage expectations on the productivities of microalgae cultivation.

4.5. Supplementary materials

4.5.1. Supplementary material 4.1

Effect of oxygen concentration in the liquid phase on the growth rate of *Picochlorum sp. BPE23*. Experiments were performed by monitoring of biological oxygen production (2.1.3. Biological oxygen monitor). The decrease in growth rate was calculated as the difference between the maximal specific growth rate and the growth rate which was measured at the end of the experiment.
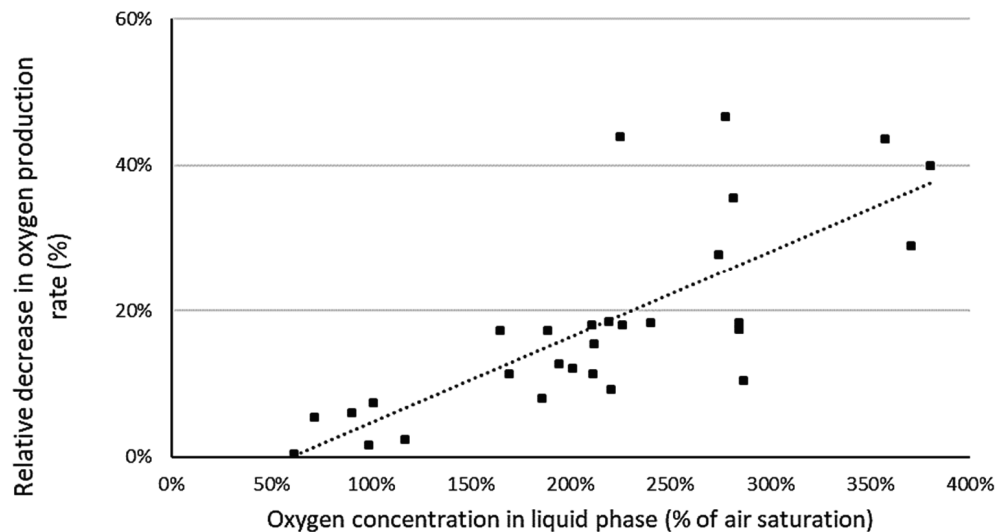
Supplementary figure A4.1: *The effect of the oxygen concentration on the relative oxygen production rate of Picochlorum sp. BPE23 during oxygen evolution experiments.*

4.5.2. Supplementary material 4.2

Irradiance levels on Bonaire during day 172. Values in $W.m^{-2}$ were obtained from Meteonorm 7.1, based on the measured irradiance at the nearby weather station on Curacao over recent decades. Those values were converted to values in $J\text{-}PAR.m^{-2}.s^{-1}$ and $\mu mol_{-ph}m^{-2}.s^{-1}$ with conversion factors of 0.425 $J\text{-}PAR.J\text{-}sunlight^{-1}$ and 4.6 $\mu mol_{-ph}.J\text{-}PAR^{-1}$.

Supplementary table A4.1: *Irradiance data from Meteonorm 7.1.*

Hour	Light intensity		
[h]	$[W.m^{-2} =$ $J\text{-}sunlight.s^{-1}.m^{-2}]$	$J\text{-}PAR.m^{-2}.s^{-1}$	$[\mu mol_{-ph}.m^{-2}.s^{-1}]$
6	0	0	0
7	13	6	25
8	210	89	411
9	439	187	859
10	647	275	1266
11	822	349	1608
12	928	394	1816
13	971	413	1900
14	945	402	1849
15	849	361	1661
16	688	292	1346
17	478	203	935
18	252	107	493
19	27	11	53
20	0	0	0

4.5.3. Supplementary material 4.3

The absorption cross section was measured for *Picochlorum sp. BPE23*, and obtained from literature for *Nannochloropsis sp.,* and *Neochloris oleoabundans*. The absorption cross section was used for the model simulations.

Supplementary table A4.2: *Absorption spectra for Picochlorum sp. BPE23 for Nannochloropsis sp., and Neochloris oleoabundans.*

	Picochl orum sp. BPE23	Nannochl oropsis sp. CCAP 211/78	Neochlo ris oleoabu ndans		Picochl orum sp. BPE23	Nannochl oropsis sp. CCAP 211/78	Neochlo ris oleoabu ndans
	This study	Benvenuti et al. 2014	Klok et al. 2013		This study	Benvenuti et al. 2014	Klok et al. 2013
Wavel ength [nm]	Absorp tion [m^2.mo l^{-1}]	Absorptio n [m^2.mol^{-1}]	Absorpti on [m^2.mol^{-1}]	Wavel ength [nm]	Absorp tion [m^2.mo l^{-1}]	Absorptio n [m^2.mol^{-1}]	Absorpti on [m^2.mol^{-1}]
400	7.7	6.2	5.8	551	1.3	0.9	0.8
401	7.7	6.5	5.8	552	1.3	0.9	0.8
402	7.9	6.5	5.9	553	1.2	0.8	0.8
403	7.9	6.5	6.1	554	1.2	0.9	0.8
404	8.1	6.5	6.2	555	1.3	0.8	0.8
405	8.2	6.8	6.3	556	1.3	0.8	0.8
406	8.3	6.9	6.4	557	1.3	0.8	0.8
407	8.4	7	6.5	558	1.3	0.8	0.8
408	8.6	7	6.6	559	1.3	0.8	0.8
409	8.7	7.1	6.7	560	1.3	0.9	0.8
410	8.8	7.3	6.8	561	1.3	0.8	0.8
411	9	7.5	6.9	562	1.3	0.8	0.8
412	9.1	7.5	7	563	1.3	0.8	0.9
413	9.2	7.6	7.1	564	1.4	0.8	0.9
414	9.2	7.6	7.2	565	1.4	0.8	0.9
415	9.3	7.6	7.3	566	1.4	0.9	0.9
416	9.5	7.7	7.3	567	1.4	0.8	0.9
417	9.3	7.8	7.4	568	1.4	0.9	1
418	9.5	7.9	7.5	569	1.5	0.9	1
419	9.5	8	7.5	570	1.5	0.9	1

420	9.7	8	7.6	571	1.5	0.9	1
421	9.6	8	7.6	572	1.5	0.9	1
422	9.7	8	7.7	573	1.7	0.9	1.1
423	9.7	8	7.7	574	1.7	1	1.1
424	9.9	8.2	7.8	575	1.8	1	1.1
425	9.9	8.1	7.8	576	1.8	1	1.1
426	10	8.2	7.9	577	1.8	1	1.2
427	10	8.4	8	578	1.8	1	1.2
428	10.1	8.4	8	579	1.8	1	1.2
429	10.1	8.4	8.1	580	1.9	1.1	1.2
430	10.2	8.4	8.2	581	1.9	1.1	1.2
431	10.4	8.6	8.3	582	1.9	1.1	1.3
432	10.4	8.5	8.4	583	1.9	1.1	1.3
433	10.4	8.8	8.4	584	1.9	1.1	1.3
434	10.5	8.7	8.5	585	2	1.1	1.3
435	10.5	8.8	8.5	586	2	1.2	1.3
436	10.5	8.8	8.5	587	2	1.2	1.4
437	10.6	8.8	8.5	588	2	1.2	1.4
438	10.5	8.7	8.5	589	2	1.2	1.4
439	10.5	8.7	8.5	590	2	1.2	1.4
440	10.4	8.7	8.5	591	2.2	1.2	1.4
441	10.4	8.7	8.4	592	2.2	1.2	1.5
442	10.2	8.6	8.3	593	2.2	1.2	1.5
443	10.1	8.4	8.2	594	2.2	1.2	1.5
444	10	8.4	8.1	595	2.2	1.2	1.5
445	9.9	8.3	8	596	2.2	1.2	1.5
446	9.6	8	7.8	597	2.2	1.2	1.5
447	9.5	7.8	7.7	598	2.2	1.2	1.5
448	9.2	7.7	7.5	599	2.2	1.3	1.6
449	9.1	7.5	7.4	600	2.3	1.2	1.6
450	9	7.4	7.2	601	2.3	1.3	1.6
451	8.7	7.2	7.1	602	2.3	1.3	1.6
452	8.6	7	6.9	603	2.3	1.3	1.6
453	8.4	7	6.8	604	2.3	1.3	1.7
454	8.3	6.7	6.7	605	2.3	1.4	1.7
455	8.3	6.5	6.6	606	2.3	1.5	1.7
456	8.3	6.5	6.6	607	2.3	1.4	1.7

4

457	8.2	6.4	6.5	608	2.4	1.5	1.8
458	8.2	6.3	6.5	609	2.4	1.6	1.8
459	8.1	6.3	6.4	610	2.4	1.6	1.8
460	8.1	6.2	6.4	611	2.4	1.6	1.8
461	8.1	6.2	6.4	612	2.6	1.7	1.9
462	8.1	6.1	6.3	613	2.6	1.7	1.9
463	8.1	6	6.3	614	2.7	1.8	1.9
464	8.2	6	6.3	615	2.7	1.8	2
465	8.2	5.9	6.3	616	2.7	1.9	2
466	8.2	5.8	6.3	617	2.7	1.9	2
467	8.2	5.7	6.3	618	2.8	1.9	2
468	8.2	5.8	6.3	619	2.8	2	2.1
469	8.1	5.6	6.3	620	2.8	2	2.1
470	8.2	5.6	6.3	621	2.8	2	2.1
471	8.2	5.5	6.3	622	2.8	2.1	2.1
472	8.2	5.5	6.3	623	2.8	2.1	2.1
473	8.2	5.6	6.3	624	2.8	2.1	2.1
474	8.2	5.5	6.3	625	2.8	2.1	2.1
475	8.2	5.5	6.3	626	2.8	2.2	2.2
476	8.2	5.5	6.3	627	2.9	2.1	2.2
477	8.2	5.5	6.3	628	2.9	2.2	2.2
478	8.2	5.5	6.3	629	2.9	2.2	2.2
479	8.2	5.5	6.2	630	2.8	2.1	2.2
480	8.2	5.6	6.2	631	2.8	2.1	2.2
481	8.1	5.6	6.2	632	2.9	2.1	2.2
482	8.1	5.6	6.2	633	2.8	2.1	2.2
483	8.1	5.7	6.1	634	2.9	2.1	2.2
484	8.1	5.7	6.1	635	2.9	2.1	2.2
485	7.9	5.7	6.1	636	2.9	2	2.2
486	7.8	5.7	6	637	3.1	2	2.2
487	7.8	5.7	6	638	3.1	2	2.3
488	7.7	5.6	5.9	639	3.1	1.9	2.3
489	7.6	5.7	5.8	640	3.3	1.9	2.3
490	7.3	5.6	5.7	641	3.3	1.9	2.4
491	7.2	5.5	5.6	642	3.5	1.8	2.4
492	7	5.5	5.5	643	3.7	1.8	2.5
493	6.9	5.4	5.4	644	3.8	1.8	2.6

494	6.7	5.4	5.3	645	4	1.8	2.7
495	6.5	5.3	5.1	646	4.2	1.7	2.8
496	6.4	5.3	5	647	4.4	1.8	2.9
497	6.1	5.2	4.9	648	4.5	1.8	3
498	6	5.1	4.7	649	4.6	1.9	3.1
499	5.8	5	4.5	650	4.6	1.9	3.2
500	5.6	4.9	4.4	651	4.7	2	3.3
501	5.4	4.8	4.2	652	4.7	2	3.4
502	5.1	4.7	4	653	4.7	2.2	3.4
503	4.9	4.6	3.9	654	4.7	2.3	3.5
504	4.7	4.4	3.7	655	4.7	2.4	3.6
505	4.5	4.3	3.5	656	4.7	2.6	3.7
506	4.4	4.2	3.4	657	4.9	2.8	3.8
507	4.1	4.1	3.2	658	5	3	3.9
508	4	3.9	3	659	5.1	3.3	4
509	3.7	3.8	2.9	660	5.2	3.5	4.2
510	3.6	3.7	2.7	661	5.5	3.7	4.3
511	3.5	3.5	2.6	662	5.8	4	4.5
512	3.2	3.4	2.5	663	5.9	4.3	4.7
513	3.1	3.4	2.3	664	6.1	4.5	4.9
514	2.9	3.1	2.2	665	6.3	4.8	5.1
515	2.7	3	2.1	666	6.7	5	5.3
516	2.6	2.9	2	667	6.8	5.3	5.5
517	2.4	2.8	1.9	668	7	5.5	5.6
518	2.2	2.7	1.8	669	7.2	5.7	5.8
519	2.2	2.5	1.7	670	7.4	5.9	5.9
520	2	2.5	1.6	671	7.6	6.2	6
521	1.9	2.3	1.5	672	7.7	6.4	6.1
522	1.9	2.2	1.5	673	7.8	6.5	6.2
523	1.8	2.1	1.4	674	7.9	6.7	6.3
524	1.8	2.1	1.3	675	7.9	6.8	6.3
525	1.7	1.9	1.3	676	7.9	6.9	6.3
526	1.7	1.9	1.2	677	7.9	7	6.3
527	1.5	1.8	1.2	678	8.1	7	6.3
528	1.5	1.8	1.2	679	7.9	7	6.3
529	1.5	1.7	1.1	680	8.1	7	6.3
530	1.4	1.6	1.1	681	7.9	6.9	6.2

4

531	1.4	1.6	1.1	682	7.8	6.7	6.1
532	1.4	1.6	1	683	7.4	6.6	5.9
533	1.4	1.5	1	684	7.2	6.3	5.7
534	1.3	1.4	1	685	6.8	6	5.5
535	1.3	1.4	1	686	6.3	5.7	5.2
536	1.3	1.3	1	687	5.8	5.3	4.8
537	1.4	1.3	1	688	5.1	4.9	4.5
538	1.3	1.2	0.9	689	4.6	4.5	4.1
539	1.3	1.2	0.9	690	4.1	4.1	3.8
540	1.3	1.2	0.9	691	3.6	3.6	3.4
541	1.3	1.2	0.9	692	3.2	3.3	3.1
542	1.3	1.1	0.9	693	2.7	2.9	2.8
543	1.3	1.1	0.9	694	2.3	2.5	2.5
544	1.3	1.1	0.9	695	2	2.2	2.2
545	1.3	1.1	0.9	696	1.8	1.9	1.9
546	1.2	1	0.9	697	1.5	1.7	1.7
547	1.3	1	0.9	698	1.4	1.5	1.5
548	1.3	0.9	0.8	699	1.3	1.3	1.3
549	1.3	0.9	0.8	700	1.2	1.1	1.2
550	1.3	0.9	0.8				

4.5.4. Supplementary material 4.4

Simulation results for each microalgae strain to determine the optimal dilution rate from the calculated biomass productivity and yield on light.

Supplementary table A4.3: *Model simulation results*

Picochlorum sp. BPE23

Cx0		Dilution rate		Biomass productivity		Biomass yield on light
[mol.m^{-3}]	[g.L^{-1}]	[s^{-1}]	[d^{-1}]	[g.L^{-1}.d^{-1}]	[g.m^{-2}.d^{-1}]	[g$_x$.mol$_{ph}$$^{-1}$]
120	2.9	1.67E-05	0.72	2.146	32.2	0.616
120	2.9	1.39E-05	0.60	2.140	32.1	0.614
120	2.9	1.94E-05	0.84	2.129	31.9	0.611
120	2.9	1.53E-05	0.66	2.146	32.2	0.616
120	2.9	1.58E-05	0.68	2.147	32.2	0.616
120	2.9	1.61E-05	0.70	2.147	32.2	0.616
120	2.9	1.64E-05	0.71	2.146	32.2	0.616
120	2.9	1.56E-05	0.67	2.147	32.2	0.616
120	2.9	1.11E-05	0.48	2.105	31.6	0.604
120	2.9	2.22E-05	0.96	2.095	31.4	0.601

Neochloris oleoabundans

Cx0		Dilution rate		Biomass productivity		Biomass yield on light
[mol.m^{-3}]	[g.L^{-1}]	[s^{-1}]	[d^{-1}]	[g.L^{-1}.d^{-1}]	[g.m^{-2}.d^{-1}]	[g$_x$.mol$_{ph}$$^{-1}$]
100	2.4	1.67E-05	0.72	1.676	25.1	0.481
120	2.9	1.39E-05	0.60	1.782	26.7	0.512
100	2.4	1.94E-05	0.84	1.505	22.6	0.432
120	2.9	1.11E-05	0.48	1.826	27.4	0.524
150	3.6	8.33E-06	0.36	1.799	27.0	0.516
150	3.6	9.72E-06	0.42	1.822	27.3	0.523
150	3.6	1.06E-05	0.46	1.827	27.4	0.524
150	3.6	1.08E-05	0.47	1.827	27.4	0.524
150	3.6	1.03E-05	0.44	1.826	27.4	0.524

4

Nannochloropsis sp. CCAP 211/78

Cx0		Dilution rate		Biomass productivity		Biomass yield on light
[mol.m^{-3}]	[g.L^{-1}]	[s^{-1}]	[d^{-1}]	[g.L^{-1}.d^{-1}]	[g.m^{-2}.d^{-1}]	[g$_x$.mol$_{ph}^{-1}$]
100	2.4	1.67E-05	0.72	1.335	20.0	0.383
100	2.4	1.39E-05	0.60	1.437	21.6	0.412
100	2.4	1.94E-05	0.84	1.182	17.7	0.339
70	1.7	1.94E-05	0.84	1.178	17.7	0.338
100	2.4	1.11E-05	0.48	1.487	22.3	0.427
150	3.6	8.33E-06	0.36	1.476	22.1	0.424
150	3.6	9.72E-06	0.42	1.491	22.4	0.428
150	3.6	1.03E-05	0.44	1.491	22.4	0.428
150	3.6	1.00E-05	0.43	1.491	22.4	0.428
150	3.6	1.06E-05	0.46	1.491	22.4	0.428
150	3.6	1.08E-05	0.47	1.49	22.4	0.428

Picochlorum celeri

Cx0		Dilution rate		Biomass productivity		Biomass yield on light
[mol.m^{-3}]	[g.L^{-1}]	[s^{-1}]	[d^{-1}]	[g.L^{-1}.d^{-1}]	[g.m^{-2}.d^{-1}]	[g$_x$.mol$_{ph}^{-1}$]
120	2.9	2.22E-05	0.96	2.700	40.5	0.775
120	2.9	2.50E-05	1.08	2.683	40.2	0.770
120	2.9	1.94E-05	0.84	2.704	40.6	0.776
120	2.9	1.67E-05	0.72	2.692	40.4	0.773
120	2.9	2.08E-05	0.90	2.704	40.6	0.776
120	2.9	2.03E-05	0.88	2.704	40.6	0.776
120	2.9	2.00E-05	0.86	2.704	40.6	0.776
120	2.9	2.14E-05	0.92	2.703	40.5	0.776

4.5.5. Supplementary material 4.5

The photosynthetic efficiencies were determined by first calculating the available amount of light energy from the available photons. This light energy was calculated with a conversion factor of 4.6 µmol PAR photons / J PAR photons, which resulted in a value of $1.1 \cdot 10^7$ J PAR photons m^{-2} d^{-1}. Then, the energy content of the produced biomass was calculated. For the latter, the following conversion factors were used: 24 $g.mol_x^{-1}$ and $5.59 \cdot 10^5$ $J.mol\text{-}biomass^{-1}$ [112]. The photosynthetic efficiencies could then be calculated as the fraction of the energy content of the produced biomass over the available light energy. A distinction is made between the light energy in the PAR-range and the complete sunlight spectrum. It was assumed that the PAR-fraction constitutes to 42.5% of the complete sunlight spectrum.

Supplementary table A4.4: *The calculated biomass productivity and photosynthetic efficiency of the microalgal cultures in a photobioreactor on Bonaire.*

	Biomass productivity and energy content			Photosynthetic efficiency		
	$[g.m^{-2}.d^{-1}]$	$[mol.m^{-2}d^{-1}]$	$[J.m^{-2}d^{-1}]$	PAR-range (%)	Sunlight (%)	$[g\text{-}biomass.mol\text{-}ph^{-1}]$
Picochlorum sp. BPE23	32	1.3	$7.5 \cdot 10^5$	6.6	2.8	0.62
Neochloris oleoabundans	27	1.1	$6.4 \cdot 10^5$	5.6	2.4	0.52
Nannochloropsis sp.	22	0.93	$5.2 \cdot 10^5$	4.6	2.0	0.43
Picochlorum celeri	41	1.7	$9.4 \cdot 10^5$	8.3	3.5	0.78

4

4.5.6. Supplementary material 4.6

Supplementary table A4.5: *The biological oxygen monitor experiment was performed using the following light conditions*

Light level ($u_{molph}.m^{-2}.s^{-1}$)	Time interval (minutes)
0	6
10	4
20	3
40	2
80	2
160	1
250	1
350	1
500	1
750	1
1000	1
1500	1
2000	1
2500	1

Chapter 5

Short-term physiologic response of the green microalga *Picochlorum sp. BPE23* to supra-optimal temperature

Abstract

Photobioreactors heat up significantly during the day due to irradiation by sunlight. High temperatures affect cell physiology negatively, causing reduced growth and productivity. To elucidate the microalgal response to stressful supra-optimal temperature, we studied the physiology of *Picochlorum sp. BPE23* after increasing the growth temperature from 30°C to 42°C, whereas 38°C is its optimal growth temperature. Cell growth, cell composition and mRNA expression patterns were regularly analyzed for 120h after increasing the temperature. The supra-optimal temperature caused cell cycle arrest for 8h, with concomitant changes in metabolic activity. Accumulation of fatty acids was observed during this period to store unspent energy which was otherwise used for growth. In addition, the microalgae changed their pigment and fatty acid composition. For example, palmitic acid (C16:0) content in the polar fatty acid fraction increased by 30%, hypothetically to reduce membrane fluidity to counteract the effect of increased temperature. After the relief of cell cycle arrest, the metabolic activity of *Picochlorum sp. BPE23* reduced significantly over time. A strong response in gene expression was observed directly after the increase in temperature, which was dampened in the remainder of the experiment. mRNA expression levels associated with pathways associated with genes acting in photosynthesis, carbon fixation, ribosome, citrate cycle, and biosynthesis of metabolites and amino acids were downregulated, whereas the proteasome, autophagy and endocytosis were upregulated.

5.1. Introduction

Photobioreactors heat up significantly as a result of irradiation by sunlight, leading to shifts in temperature throughout the day up to levels that can be stressful for microalgae. Heat stress poses a significant challenge in the cultivation of microalgae for the production of food, feed and chemicals. Non-optimal temperatures reduce microalgal growth, thereby reducing productivity and photosynthetic efficiency [6]. The effect of excessive heat on the cellular physiology has been studied in photosynthetic model organisms such as *Arabidopsis thaliana* and *Chlamydomonas reinhardtii*. While many aspects of the response to heat have been studied, much still has to be learned on how exactly microalgae cope with heat [8, 12, 13]. In addition, detailed research on the effect of heat stress on other photosynthetic (micro)organisms, is scarce.

Many cellular processes are impacted by supra-optimal temperature which ultimately unbalances cellular homeostasis [11]. Several effects are; failure of correct protein folding and protein complex assembly, destabilization of cell membranes through increased membrane fluidity, a reduction in photosynthesis, changes in DNA replication and repair, changes in enzymatic activity, and reduced metabolic activity [8-10]. As a response to temperature-induced physiological changes, heat shock factors (HSF's) and heat shock proteins (HSP's) are expressed to mediate and protect against adverse effects through chaperoning after exposure to heat stress [11, 12, 113]. Excessive heat kills microalgae quickly due to denaturation of proteins and destabilization of membranes. However, in this paper we will focus on a supra-optimal temperature. Supra optimal temperatures fall between the optimal and maximal temperature for growth. Here, growth rate is reduced, but cells still survive.

Photosynthesis, carbon fixation and the central energy metabolism form a delicate system with consecutive enzymatic reactions [13, 114]. Photosystem II is considered the most thermosensitive complex within the photosynthetic pathway while several components of the carbon fixation pathway are thermosensitive [8]. However, Photosystem II is not considered a bottleneck between the optimal and lethal growth temperature [114]. When one or more reactions in the energy metabolism are inhibited by temperature, the entire energy flux through the pathway will slow down. This ultimately results in excessive energy in the photosystems, which will overflow and lead to the formation of harmful reactive oxygen species (ROS) [13]. To prevent the accumulation of ROS, cells suppress

photosynthesis by downregulation of key genes. Next to suppression of photosynthesis to prevent ROS formation, mechanisms for ROS scavenging are activated. ROS scavenging in microalgae is done through several mechanisms: enzymatically (by catalases, superoxide dismutases, and peroxidases) and by production of antioxidants for ROS scavenging such as carotenoids [14, 15]. A third protection mechanism, to prevent formation of ROS, is *de novo* production and accumulation of energy storage compounds such as lipids and carbohydrates as an energy sink [8, 12]. As a result of the before mentioned impact of temperature and the response mechanisms, growth rate decreases [115, 116].

In this study, we investigated the effect of supra-optimal temperature on the physiology of *Picochlorum sp. BPE23* to elucidate how this microalga copes and acclimates to temperature stress. *Picochlorum sp. BPE23* exhibits a high maximal growth rate of 5 d^{-1} under non-limiting growth conditions which together with its robustness and its relatively small genome size of ~13 Mbp makes it an interesting model platform for both fundamental studies, and industrial application [7, 21, 43, 78]. This chlorophyte has a cell size of 3-4 μm. Currently, five genome assemblies for various species of *Picochlorum* are available and tools for genetic modification have been developed [43]. A temperature increase from 30°C to 42°C was studied, which is 4°C above the optimal growth temperature of this strain [7]. To elucidate the effect of the temperature shift to 42°C, the growth rate, cell volume, quantum yield, pigment composition, fatty acid composition, and mRNA expression were periodically measured for 120 hours. The results show how *Picochlorum sp. BPE23* copes with the immediate adverse effects of supra-optimal temperatures to prevent cell damage and how the onset to acclimatization to this temperature takes place.

5.2. Materials and methods:

5.2.1. Cell cultivation

5.2.1.1. Growth media and inoculum preparation

Picochlorum sp. BPE23, isolated from a saltwater body of Bonaire was pre-cultivated in shake flasks in an orbital shaker incubator (Multitron, Infors HT) with a 12/12 h day/night cycle and a light intensity of 100 μmol_{ph} m^{-2} s^{-1} [7]. The temperature was 30°C during night and 40°C during day. Furthermore, the relative humidity of the air in the incubator was set to 60% and enriched with 2% CO_2. Cells were cultured in artificial seawater enriched with nutrients and trace elements. Elements were provided at the following concentrations (in g.L^{-1}): NaCl, 24.5; MgCl$_2$.6H$_2$O, 9.80; Na$_2$SO$_4$, 3.20; NaNO$_3$ 2.12; K$_2$SO$_4$, 0.85; CaCL$_2$.2H$_2$O, 0.80; KH$_2$PO$_4$, 0.23; Na$_2$EDTA·2H$_2$O, 0.105; Na$_2$EDTA, 0.06; FeSO$_4$·7H$_2$O, 0.0396; MnCl$_2$·2H$_2$O, 1.71·10^{-3}; ZnSO$_4$·7H$_2$O, 6.60·10^{-4}; Na$_2$Mo$_4$·2H$_2$O, 2.42·10^{-4}; Co(NO$_3$)$_2$·6H$_2$O, 7.00·10^{-5}; NiSO$_4$·6H$_2$O, 2.63·10^{-5}; CuSO$_4$·5H$_2$O, 2.40·10^{-5}; K$_2$CrO$_4$, 1.94·10^{-5}; Na$_3$VO$_4$, 1.84·10^{-5}; H$_2$SeO$_3$, 1.29·10^{-5}. HEPES (4.77 g.L^{-1}) was added for shake flask cultures as a pH buffer. The medium pH was adjusted to 7.4 after and filter sterilized before use. During photobioreactor cultivation, Antifoam B (J.T.Baker, Avantor, USA) was added at a concentration of 0.5 mL.L^{-1} out of a 1% w/w% stock. In addition, 0.168 g.L^{-1} Sodium bicarbonate (NaHCO$_3$) was added at the time of inoculation to provide sufficient CO_2 at the start of the cultivation. The photobioreactor was inoculated at a starting OD density of 0.2.

5.2.1.2. Photobioreactor operation

Microalgae were cultivated in heat-sterilized flat panel photobioreactors (Labfors 5 Lux, Infors HT, Switzerland) with a working volume of 1.8 L, an optical depth of 20.7 mm and a surface area for irradiation of 0.08 m^2. Continuous irradiation (24/24h) was applied from one side by 260 warm white LED lamps at 813 μmol_{ph}.m^{-2}.s^{-1} (PAR). To remove variation in gene expression due to the circadian cycle we grew the microalgae under continuous irradiation while maintaining all other growth conditions stable at the same time. The biomass density was maintained at approximately 2.3 g.L^{-1} by continuous light controlled dilution of the cell culture (turbidostat mode). The turbidostat control was set to maintain an outgoing light level of 10 μmol_{ph}.m^{-2}.s^{-1} (PAR). The dilution rate of the photobioreactor was logged continuously by weighing the ingoing medium vessel. Compressed air was supplied

at a rate of 980 mL.min^{-1}. CO_2 was provided on-demand by pH-controlled addition. The pH level in the photobioreactor was set at 7. The photobioreactor temperature was set at 30°C from the start of cell cultivation. When steady state was reached, the temperature was increased to 42°C in one step, which took approximately 15 minutes. Samples were taken daily at 0h, 1h, 4h, 8h, 24h after the temperature increase, and once a day for every day onwards to monitor changes in cell physiology.

5.2.2. Biomass analysis

5.2.2.1. Dry weight

Biomass concentration (g.L^{-1}) was measured in duplicate by dry weight determination. Empty Whatman glass microfiber filters (θ 55 mm, pore size 0.7 μm) were dried overnight at 95°C and placed in a desiccator for 2h. Filters were then weighed and placed in the mild vacuum filtration setup. Cell culture containing 1 to 10 mg of microalgae biomass was diluted in 25 ml 0.5 M ammonium formate and filtered. The filter was washed twice with 25 ml 0.5 M ammonium formate to remove residual salts. The wet filter was dried overnight at 95°C, placed in a desiccator for 2h, and weighed. Biomass concentration was calculated from the difference in filter weight before and after filtration and drying.

5.2.2.2. Cell volume and number

Cell size and cell number were measured in duplicate with the Multisizer III (Beckman Coulter Inc., USA, 50 μm aperture). Samples were diluted in two steps before analysis, initially by dilution of 5x in fresh medium, followed by dilution of 100x in Coulter Isoton II. Cell volume was then derived from the cell size by assuming that cells were shaped spherical.

5.2.2.3. Quantum yield

The cell culture's quantum yield (F_v/F_m), representing the maximum photosynthetic capacity of photosystem II was determined. Cells were measured after dark adaption at room temperature for 15 min (AquaPen-C 100, PSI; excitation light 455 nm (blue), saturating light pulse: 3000 μmol.m^{-2}.s^{-1}).

5.2.2.4. Biomass harvest and lyophilizing

Biomass samples for compositional analysis were taken at the same moment as when offline measurements were performed. Microalgae cells were pelleted by centrifugation at 4000g for 5 min and washed with 0.5M ammonium formate. The centrifugation/washing cycle was repeated twice more after which the cell pellet was frozen at -20 °C. Samples were then lyophilised for 24h and stored at -20 °C until further processing.

5.2.2.5. Pigment analysis

Pigment content was determined through extraction and HPLC analysis [117]. 10 mg of lyophilized biomass was disrupted by bead beating (Precellys 24, Bertin Technologies, France) at 5000 rpm for three cycles of 90 seconds with 60-second breaks on ice between each cycle. The extraction was done through five washing steps with methanol containing 0.1% butylhydroxytoluene. Separation, identification and quantification of pigments were performed using a Shimadzu (U)HPLC system (Nexera X2, Shimadzu, Japan), equipped with a pump, degasser, oven (25°C), autosampler, and photodiode array (PDA) detector. Separation of pigments was achieved using a YMC Carotenoid C30 column (250x4.6mm 5 µm ID) coupled to a YMC C30 guard column (20x4mm, 5 µm ID)(YMC, Japan) at 25°C with a flow rate of 1 ml.min^{-1}. A sample injection volume of 20µL was used. The mobile phases consisted of Methanol (A), water/methanol (20/80 (v/v%)) containing 0.2% ammonium acetate (B), tert-methyl butyl ether (C) (all solvents were purchased at Sigma Aldrich). The elution protocol started with 0-12 min isocratic A:95% B:5% C:0%, with at 12 min a step to A:80%, B:5%, C:15%, followed by a linear gradient 12-30min to A:30%, B:5%, C:65%, finally followed by a conditioning phase 30-40 min at the initial concentration. Analytical HPLC standards for chlorophyll-a, chlorophyll-b, β-carotene, canthaxanthin, violaxanthin, antheraxanthin, zeaxanthin, and lutein had a purity of >99% (Carotenature, Switzerland).

5.2.2.6. Fatty acid analysis

Fatty acids within the triacylglycerol (TAG) and polar lipids (PL) fraction were quantified through GC-FID analysis according to [79]. 10 mg of lyophilised biomass

5

was disrupted by bead beating. The fatty acids were extracted from the disrupted biomass in a mixture of chloroform/methanol (1:1.25, v:v) containing Glyceryl tripentadecanoate (C15:0 TAG) (T4257, Sigma-Aldrich) and 1,2-didecanoyl-sn-glycero-3-phospho-(1'-rac-glycerol) (sodium salt) C10:0 PG (840434, Avanti Polar Lipids Inc) as internal standards for the TAG and the PL fraction, respectively. Separation of TAG and PL was done by use of Sep-Pak Vac silica cartridge (6 cc, 1000 mg; Waters). TAG was eluted from the column with a solution of hexane:diethylether (7:1, v:v) and the PL were eluted with a solution of methanol:acetone:hexane (2:2:1, v:v:v). The extracts were methylated for 3h at 70°C in methanol containing 5% H_2SO_4.

5.2.3. Transcriptome analysis

5.2.3.1. mRNA extraction and sequencing

mRNA-Seq analysis was done for samples taken at 0h, 1h, 4h, 8h, 24h and 120h after the temperature increase from 30°C to 42°C. Biomass was directly put on ice and centrifuged for 5 minutes at 4255 g at 2°C. The cell pellet was then immediately frozen in liquid nitrogen and stored at -80°C until further processing. mRNA was extracted from ~200 ul frozen cell pellet by automated mRNA extraction (Maxwell® 16 LEV simplyRNA, Promega, USA). Extracted mRNA was tested for integrity (Qsep100, GCbiotech, Netherlands) and quantity (Qubit fluorometer, ThermoFisher, USA). Sequencing libraries were prepared using the NEB Next® Ultra™ mRNA Library Prep Kit. Fragments of the mRNA library in the size range of 250-300 bp were sequenced using the Illumina Novoseq PE150 platform, yielding paired-end reads of 150 nt (Novogene, China). The quality of mRNA-Seq reads was assessed using FastQC v0.11.5 [118].

5.2.3.2. Transcript assembly and annotation

Paired-end reads were mapped to the genome of *Picochlorum sp. SENEW3* (assembly ASM87641v1) using HISAT2 v2.2.1 with the -very--sensitive pre-set [19, 119]. Transcript were assembled and predicted using StringTie v2.1.4, which was guided by the structural annotation of *Picochlorum sp. SENEW3*. StringTie's prepDE3 python script was used to extract gene counts and predict genes *de novo*. Functional annotation was initiated by a BLASTP search of the translated *Picochlorum sp. BPE23* coding sequences against the protein sequences of

Arabidopsis thaliana with an E-value threshold of 1E^{-10}. Unannotated genes were filtered and orthology inference was conducted using OrthoFinder v2.5.2 against the protein sequences of the microalgae *Auxenochlorella protothecoides*, *Chlorella variabilis*, *Chlamydomonas reinhardtii*, and *Helicosporidium sp*. Ortholog gene identifiers were then matched to their gene description. Functional annotation was concluded by matching unannotated genes to their inferred domains, as derived from Pico-PLAZA.

5.2.3.3. Differential expression analysis and GO, and KEGG enrichment analysis

Pairwise differential expression (DE) analysis was performed using the DESeq2 v1.30.0. R package. Sample-level quality control consisted of pairwise correlation clustering, hierarchical clustering, and Principal Component Analysis (PCA). Fold change values were generated on a log2 scale (LFC). Two designs for data display were implemented; first, where a control condition after 0h was used for each sample to compare DE between stressed and non-stressed growth. Second, where the previous sampling moment was used as a control condition to compare DE over time. Genes with a false discovery rate (FDR) adjusted *p*-value ≤ 0.05 and an LFC > 1 were considered as significantly differentially expressed.

Arabidopsis thaliana gene identifiers that matched to *Picochlorum sp. BPE23* genes were linked to their corresponding DE-analysis results and used for GO and KEGG pathway enrichment analysis [120]. Enrichment analyses were conducted by use of clusterProfiler v3.18.1. and org.At.tain.db v3.12.0. packages. GO-terms and KEGG pathways with an FDR-adjusted p-value ≤ 0.05 and a positive or negative enrichment score were considered as significantly enriched and visualized with the ggplots2 package.

5.2.3.4. Network interference analysis

Weighted gene co-expression network analysis (WGCNA) was conducted by applying the WGCNA R package v1.69. [121]. The correlation network was inferred from a correlation matrix of normalized counts. The optimal value of power was determined through scale-free topology analysis. The network was restricted to genes with informative connectivity, referring to a connectivity higher than the

median connectivity of the entire network. Modules were then constructed with average linkage hierarchical clustering using distances in the topological overlap construction. Networks were constructed in a hybrid adaptive tree with a deepSplit of 1, a power of 12, a minimum cluster size of 30, a cut height of 0.8, and no PAM-like stage filtering. Subsequently, the gene with the highest eigengene-based connectivity was identified for each module and considered the module's hub gene. Furthermore, modules were annotated with GO-terms and KEGG pathways to infer functional properties.

5.3. Results

5.3.1. Temperature increase to supra-optimal level leads to cell-cycle arrest and decreased growth

The effect of the increase in temperature from 30°C to 42°C for a time span of 120h on *Picochlorum sp. BPE23* can be seen in Figure 5.1. The specific growth rate, quantum yield, and cell volume were measured over time, before and after temperature increase. At the onset of temperature increase (t=0), the cell culture was at steady state, in a photobioreactor operated in turbidostat mode. Since only temperature was changed, it is safely assumed that the observed changes in the culture are solely due to the temperature shift. Two distinct responses were observed; an immediate short-term response, followed by a long-term response in which the microalgae gradually acclimated.

One hour after the temperature shift all monitored growth parameters had changed (Figure 5.1). The specific growth rate decreased during the first hour, followed by a temporary increase to higher levels than those observed at 30°C. It remained high until 8h after the temperature shift point at which it started to
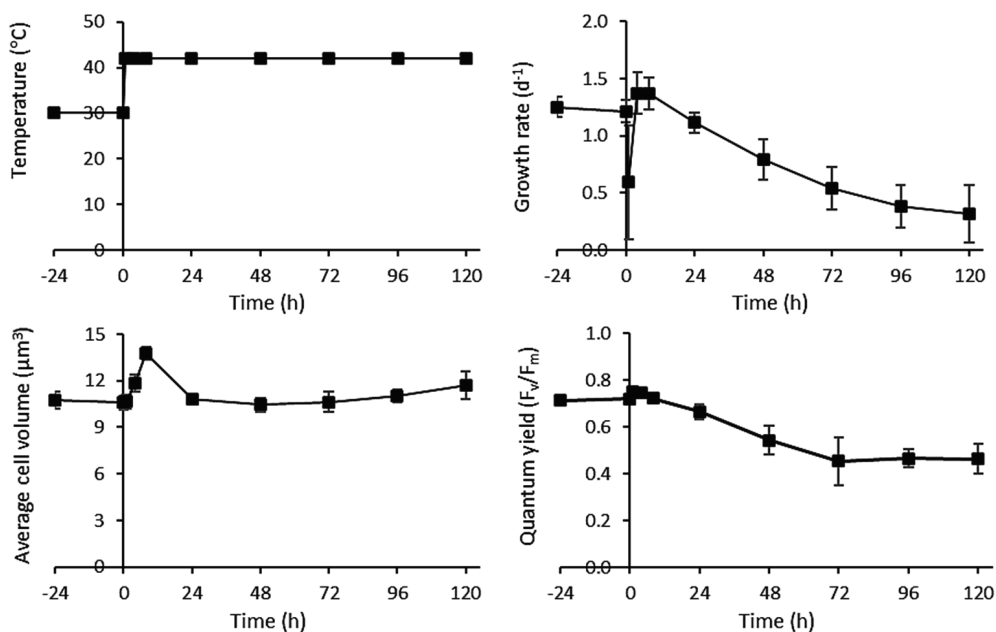
Figure 5.1: *Effect of temperature increase to supra-optimal value, on the specific growth rate (d^{-1}), quantum yield (F$_v$/F$_m$), and average cell volume (μm^3.cell^{-1}) in Picochlorum sp. BPE23. Temperature was increased from steady state growth at 30°C to 42°C at Time=0h. Data represents the mean ± standard deviation of biological triplicate experiments.*

decrease until the end of the experiment (120 h). During the first 8h the average cell volume increased by 30%, from 10.6 μm³ to 13.76 μm³. The combination of a decreased growth rate and an increase in cell volume due to halted cell division indicates a cell cycle arrest. The cell cycle arrest was released after 8h and cell volume returned to the initial value after 24h. The cell volume gradually kept increasing from 24h after the temperature shift until the end of the experiment.

Quantum yield (F_v/F_m) is a measure for the maximum photosynthetic capacity of photosystem II and can be used to monitor photo inhibitory damage in response to stress, in this study as a result of high temperature [122]. The observed quantum yield shortly increased from 0.72 to 0.75 at 42°C, after which a gradual decrease was observed to a level of 0.45 at 72h and remained stable until the end of the experiment (120h).

5.3.2. Pigment content increased after exposure to supra-optimal temperature

Pigment content was measured over time and is displayed in Figure 5.2. The pigment concentrations were also measured through optical density measurements which show a comparable trend (Supplementary material 5.4). The concentration of chlorophyll-a and chlorophyll-b decreased slightly in the first hour after the temperature shift. However, from 4h onwards an increase in concentration was observed with a peak at 72h. The concentration for both
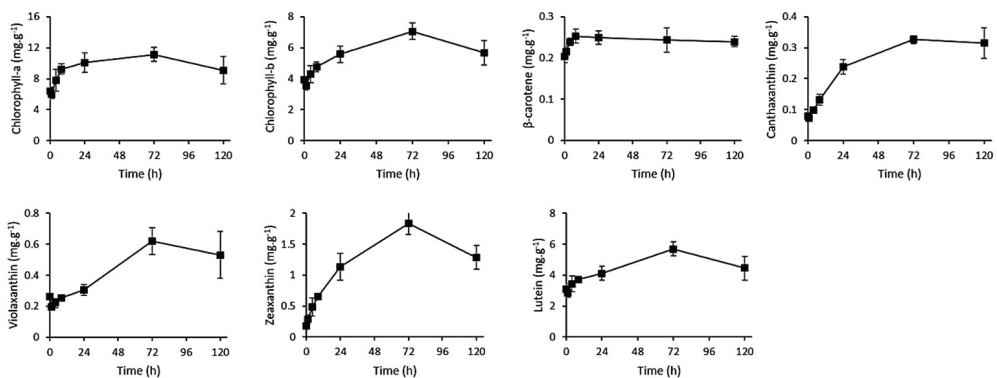

Figure 5.2: *Concentrations of chlorophyll-a, chlorophyll-b, β-carotene, canthaxanthin, violaxanthin, zeaxanthin, and lutein in algal biomass as measured over time, starting at the moment of the temperature increase from 30°C to 42°C. Data represents the mean ± standard deviation of biological triplicate experiments.*

chlorophyll-a and chlorophyll-b increased with a factor of 1.75, indicating an upregulation of photosystems. The ratio between chlorophyll-a and chlorophyll-b increased slightly between 8 and 24 hours, but returned to the values as found at the start of the experiment at 72 hours.

Carotenoids, in addition to a light-harvesting function within the photosystems, also have a photoprotective role in non-photochemical quenching, ROS scavenging, and/or filtering of light [83]. The xanthophyll pigments Violaxanthin and Zeaxanthin show a peak concentration at 72h after temperature increase. Antheraxanthin was measured but not detected. The concentration of zeaxanthin increased directly after exposure to supra-optimal temperature, from 0.18 $mg.g^{-1}$ to 1.84 $mg.g^{-1}$ after 72h, whereas the concentration of violaxanthin initially decreases after one hour, followed by a gradual increase during the first 24h. Xanthophyll pigments accommodate energy dissipation through non-photochemical quenching [83]. Also, β-carotene, Canthaxanthin and Lutein, known as strong antioxidants, were found at increased concentrations in stressed cells after exposure to supra-optimal temperatures [83].

5

5.3.3. *Picochlorum sp. BPE23 accumulated fatty acids as a response to the increased temperature*

Fatty acids can be distributed into two general groups; neutral and polar, which are present as lipid bodies and in the cell membranes, respectively (Figure 5.3). The concentration of neutral fatty acids increased from 3.0 mg.g^{-1} at 0h to 11.5 mg.g^{-1} at 24h, whereas the total content of polar fatty acids increased from 79.0 mg.g^{-1} to 88 mg.g^{-1}. Within the neutral fatty acids, all fatty acid species showed an increased concentration at approximately the same ratio. In the polar fatty acids the increase in content was mainly caused by C16:0 content, which C16:0 increased from 21.0 mg.g^{-1} after 0h to 30.0 mg.g^{-1} after 72h. At the same time, a decrease in C16:3 was observed over time.
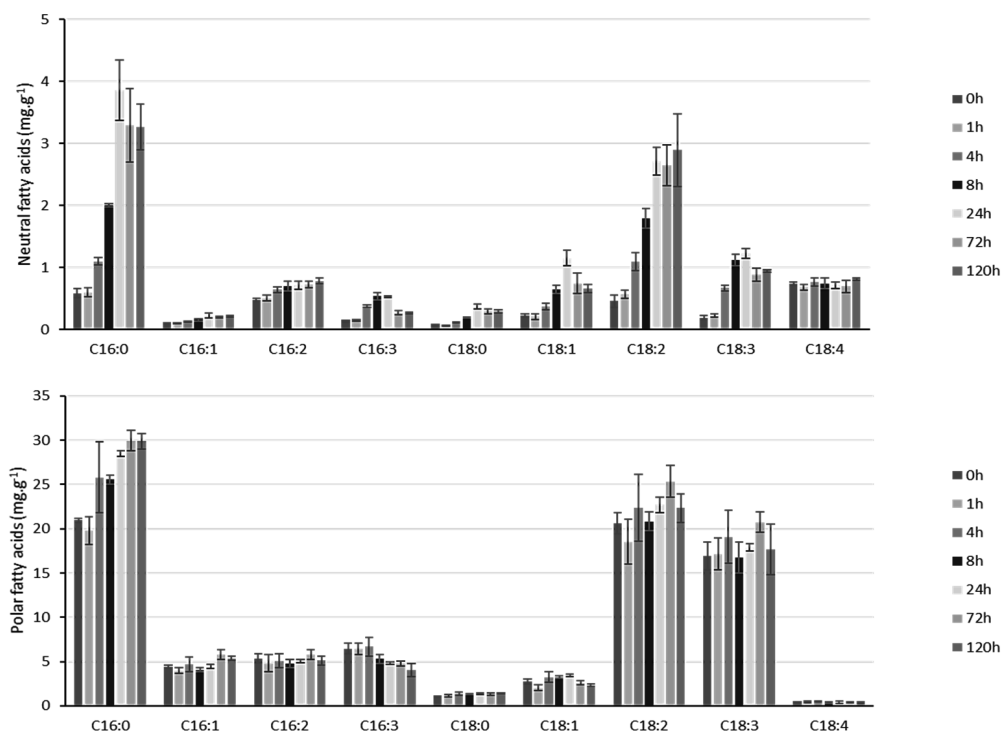
Figure 5.3*: Neutral fatty acid and polar fatty acid concentrations as measured over time, starting at the moment of the temperature increase from 30°C to 42°C. Data represents the mean ± standard deviation of biological triplicate experiments.*

5.3.4. A large transcriptional change was observed after the increase in temperature

Comparative transcriptome analysis provided further insight into the stress response of *Picochlorum sp. BPE23* to supra-optimal temperatures. In total 6990 genes were identified in the transcriptome, of which 5930 were annotated through BLASTP and Orthofinder search and inferring domains. In addition, 55 novel genes
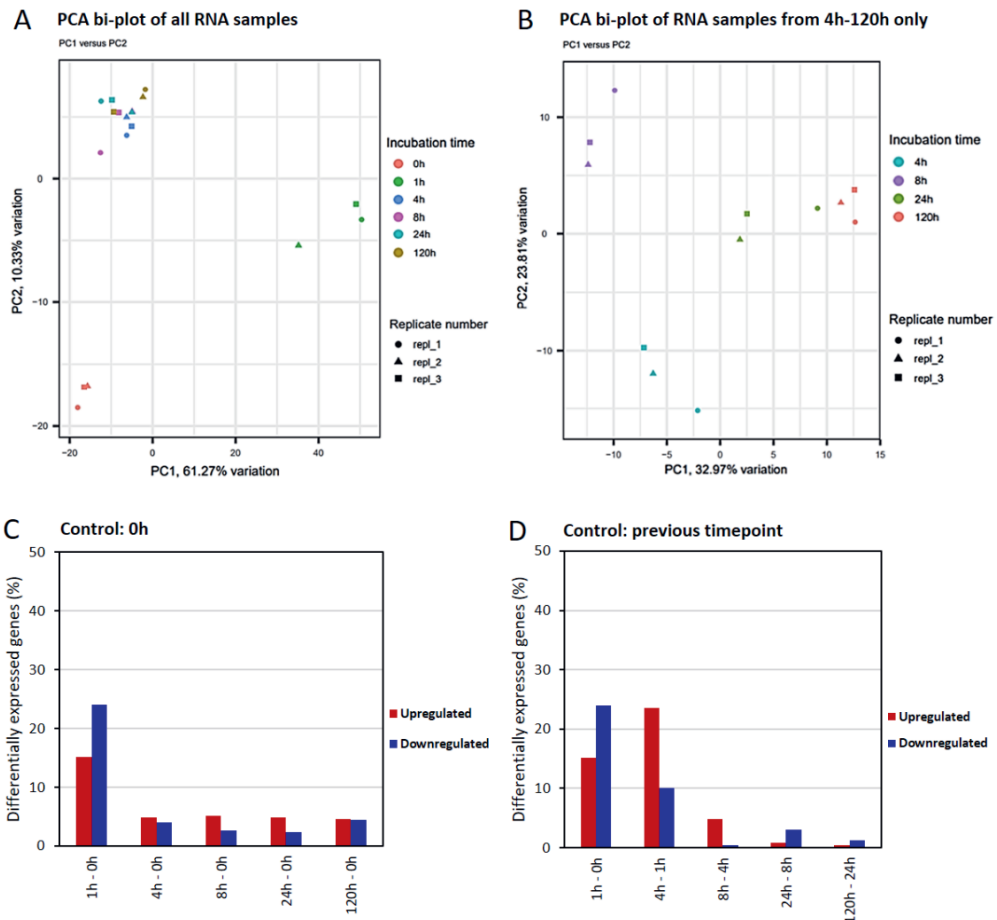
Figure 5.4: *(A/B): PCA bi-plots of the RNA-Seq samples collected at 0h, 1h, 4h, 8h, 24h and 120h and for samples collected at 4h, 8h, 24h and 120h after the increase in temperature from 30°C to 42°C. The first two PCs are displayed. (C/D) Percentage of DEGs over time, observed in Picochlorum sp. BPE23 after an increase in temperature from 30°C to 42°C. The total pool of genes was 6990. The time after temperature shift is displayed on the x-axis, as is the sampling time that was used as control. Up-regulated genes are indicated in green whereas down-regulated DEGs are indicated in red. DEGs were selected based on an FDR-adjusted p-value ≤ 0.05 and an absolute log2 fold change value > 1.*

were identified. 4427 of these genes matched to *A. thaliana* proteins (62.8%). Iteratively, the remaining unidentified genes were matched to other species of which 678 genes matched to *C. Variabilis* orthologs (9.6%), 116 genes matched to *A. protothecoides* orthologs (1.6%), 3 genes matched to *Helicosporidium sp.* orthologs (0.04%) and 60 genes matched to *C. reinhardtii* orthologs (0.9%). 643 out of the remaining 1761 genes had a domain annotation (9.1%).

Differential gene expression levels and enrichment analyses are displayed in two ways in Figure 5.4C/5.4D, 5.5, and 5.6. The left-hand side of Figure 5.4 shows the number of genes that are differentially expressed in the individual timepoints compared to the control condition at timepoint zero, which represents steady state growth at 30°C. The right-hand side of the figure shows the number of genes that are differentially expressed between consecutive timepoints.

39% of all genes showed an log2 fold change value larger than 1 after 1h, which was largely reversed between 1h and 4h (Figure 5.4). The number of differentially expressed genes (DEGs) decreased from 4h to 8h, and subsequently to 24h after the temperature increase. This indicates that the initial heat stress subsided and that *Picochlorum sp. BPE23* was reverting to a stable state once again. Between 24h and 120h only 2% of genes were differentially expressed. The changes in log2 fold change after 8h, 24h and 120h look very similar when compared to 0 h. However, when compared to the previous sampling time then differences in expression levels can be observed.

A PCA was conducted to identify similarities among biological replicates (Figure 5.4). mRNA expression at 0h and 1h showed a significant distance from samples taken at 4h, 8h, 24h, and 120h. A second PCA was then done using only samples at 4h, 8h, 24h, and 120h. The samples taken at 4h, 8h, 24h, and 120h cluster together by biological triplicate and display distance to sample moments as expected. The clustering of biological replicates confirms that samples were processed and sequenced correctly.

5.3.5. Temperature stress affects protein processing, HSP expression, and DNA replication

KEGG pathway enrichment was performed to identify which metabolic pathways were affected by the temperature increase (Figure 5.5). The RNA degradation pathway was upregulated directly after temperature increase. Other upregulated pathways involved in the immediate response were the proteasome, autophagy, and endocytosis pathways. Downregulated pathways were DNA replication, ribosome, and base/nucleotide excision repair. In addition, pathways in the central metabolism such as biosynthesis of amino acids, biosynthesis of secondary metabolites, and citrate cycle were downregulated 1 hour after the temperature increase. A reversal of this initial downregulation was observed after 4h. Despite the observed upregulation between sampling moments, the processes were never enriched in the upregulated pathways when compared to growth at 0h (30°C). The ribosome pathway remained enriched in the downregulated pathways compared to timepoint zero throughout the experiment. Photosynthesis pathway was downregulated after 8h. Despite enrichment in the upregulated pathways at 24h-8h, the photosynthesis was still downregulated compared to 0h. From 24 to 120h after the temperature shift, downregulation increased further.
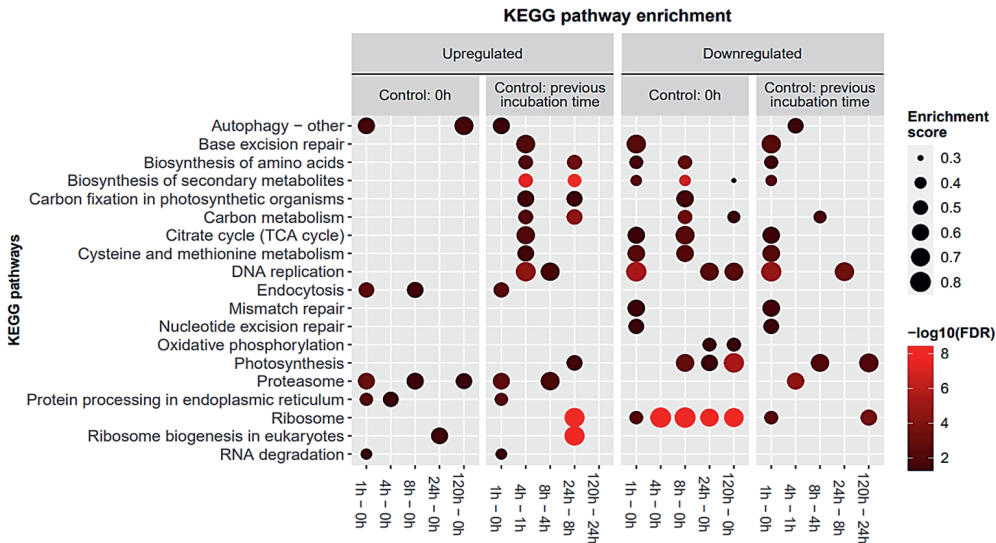

Figure 5.5: *Pathway enrichment analysis of the mRNA expression response of Picochlorum sp. BPE23 at each cultivation time after an increase in temperature from 30°C to 42°C. The dot size indicates the enrichment score of the KEGG pathway whereas the color brightness indicates significance (-log₁₀(FDR)).*

GO-term enrichment analysis was conducted in addition to the KEGG enrichment to further identify enriched cellular processes (Supplementary material 5.1). Various GO-terms related to protein processing such as Protein folding, Proteolysis and Proteasome were upregulated throughout the experiment. These GO-terms showed enrichment in the upregulated GO-terms compared to the control at 0h. In addition, cellular response to heat and heat shock protein binding show enrichment in the upregulated GO-terms. On the contrary, DNA replication, photosynthesis, peptide biosynthesis, translation, and three ribosome related GO-terms are enriched in the downregulated genes. The observations from the GO-term enrichment indicate similar changes in the mRNA expression as the observations from the KEGG pathway enrichment indicated.

5.3.6. Network analysis verifies the results of the KEGG enrichment analysis

Weighted gene co-expression network analysis (WGCNA) was performed to describe correlation patterns among genes. Genes were clustered into 18 modules based on co-expression patterns (Figure 5.6, Supplementary material 5.2). Each module was functionally annotated with GO-terms and KEGG pathways to assess differences between modules (Supplementary material 5.3). Each module displayed a unique functional annotation pattern which consisted of multiple GO-terms. The hubs were grouped roughly by similarities in functionality. The different module colours and their phylogenetic relationships are displayed in Figure 5.6. The brown, cyan, green, grey and yellow modules were made up of genes associated with proteolysis, protein ubiquitination, autophagy, endocytosis and protein processing in ER. These processes are involved in the protein-related protection response to temperature stress [12]. Furthermore, the light-green, black, green-yellow and turquoise modules were associated with processes to energy fixation and metabolism, such as ATP binding, oxidative phosphorylation, photosynthesis, thylakoid membrane, carbon fixation, glycolysis and gluconeogenesis. Other interesting modules which were affected by temperature stress are the blue, light-cyan, magenta, pink and red module. These modules are associated with RNA-, and DNA-related processes such as replication, binding and repair. Lastly, all hubs except for grey and yellow were associated to the chloroplast envelope, chloroplast stroma, and plastid.

The average module expression profile was summarised through the module's eigengene. The eigengene is a hypothetical gene that is highly correlated with expression profiles of genes in the module and can therefore function to represent the average expression of the module [121]. Genes with the highest eigengene-based connectivity were selected as hub genes, and presented together with their expression levels (Figure 5.6). The largest changes in differential expression were observed during the first hours of the experiment. The transcriptional response in the first hour after the temperature increase displayed the largest log2 fold change value, a large reversal was observed for all modules after 4h. Despite this reversal in differential expression, about half of the hub genes stay up or downregulated to a lower extent throughout the experiment. Hub genes are representative for their associated hub and therefore these hubs and their associated functions, as annotated through GO-term and KEGG pathway enrichment, hypothetically display a comparable expression pattern (Supplementary material 5.3). In general, the results from the WGCNA correspond to enrichment analysis results. Several interesting hub genes were identified which play a role in the response to an increase in temperature.

5
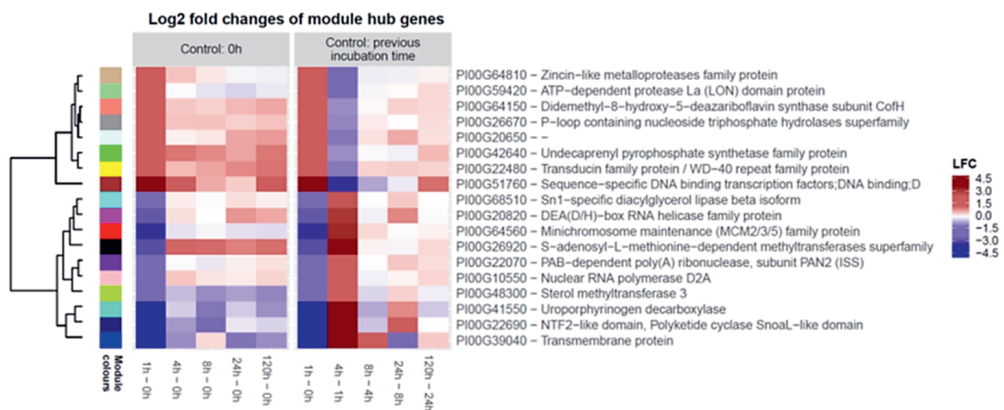
Figure 5.6: *Module hub genes associated with processes affected by temperature stress in Picochlorum sp. BPE23. Modules are defined from network inference by WGCNA of genes in the temperature-shock experiment. A heatmap represents differential expression levels of mRNA. Module color is displayed on the left. LFC represents the log2 fold change.*

5.4. Discussion

5.4.1. Cell physiology changes severely after exposure to supra-optimal temperature

In an industrial photobioreactor, temperature can raise to levels that significantly affect the growth and productivity of microalgae. Microalgae are continuously exposed to changing environmental conditions throughout the day and between days. We aimed to characterize the effect of supra-optimal temperature on the physiology of the green microalga *Picochlorum sp. BPE23*. We subjected *Picochlorum sp. BPE23* to a supra-optimal temperature of 42°C for 120h, whereas 38°C is the optimal temperature for growth [7]. Cell growth, cell volume, pigment composition, fatty acid composition and mRNA expression were measured throughout the experiment. While such long exposure to high temperature does not commonly occur in nature or in photobioreactors, this study generated knowledge on how microalgae immediately cope and eventually acclimate to supra-optimal temperatures.

Two different sequential response phases were observed after the temperature shift from 30°C to 42°C. In the first phase (0h – 8h), the cell cycle was arrested and an increase in cell volume was observed. The cell cycle resumed after 8h as cells started to divide and returned to their original cell size. During the second phase (8h – 120h), *Picochlorum sp. BPE23* acclimated towards a new homeostatic phase. The average cell volume gradually increased between 24h and 120h. This increase in cell size was unexpected as increased temperature commonly causes a decreased cell volume in other microalgal species to counteract the imbalance between catabolic and anabolic processes [6]. The growth rate and cell composition stabilized after 24h to 72h. The changes in mRNA transcription were very severe between 0h – 4h, while between 4h – 120h differential expression levels rapidly became smaller.

Interestingly, the hub gene in the red module, minichromosome maintenance (MCM2/3/5) family protein, was downregulated 5 times log2 fold during the first hours after temperature increase. The MCM complex is critical for cell division and essential for DNA replication as it is a target of various checkpoint pathways required for S-phase entry [123]. This confirms the hypothesis that the cell cycle was arrested to protect the DNA from temperature-induced damage during the replication cycle. In literature, the cell cycle of *Chlamydomonas reinhardtii* was found to be inhibited after a heat shock treatment [12, 115]. Full recovery of the

cell cycle and recovery of the cell physiology in *C. reinhardtii* was only observed after the temperature was decreased.

5.4.2. Heat shock proteins were upregulated directly after the temperature increase

A heat shock response was observed in the first hours, and to a lesser extent throughout the experiment. HSP20 and HSP70 were found among the strongest upregulated genes in the dataset. HSP70 was the main cause for enrichment in the endocytosis, protein processing and the endoplasmic reticulum pathways. Moreover, genes encoding for HSP40, HSP60, and HSP90, and HSFs showed upregulated gene expression. HSFs are transcriptional activators that regulate expression of heat shock proteins. The heat shock proteins protect cells from adverse effects of thermal stress through chaperoning and refolding of polypeptides and by stabilizing protein complexes, cellular membranes and key cellular processes [9, 11, 124]. Their regulatory role provides thermotolerance and the ability to gradually acclimate to a new environmental temperature by mediating the part of the cellular stress response that deals with protein homeostasis [125]. Next to the high upregulation of heat shock proteins, most of the other genes in the endocytosis pathway were also upregulated (~0.5-1 times log2 fold). In addition to regulation by heat shock proteins, the 5.3 times log2 fold upregulation of the ubiquitin-like superfamily protein-encoding genes is the major cause for the enrichment of the autophagy pathway and is involved in numerous stress-related functions such as the cell cycle, DNA repair, transcription, autophagy, and post-translational protein modification [126]. Proteins can still become damaged despite chaperoning and stabilization. Degradation of damaged proteins and proteins that are no longer required for cell functioning is essential to maintain cellular homeostasis [8]. The 20S proteasome alpha subunit F2 (PAF2) encoding gene was upregulated 7.5 times log2 fold and is involved in the degradation of proteins with partially unfolded regions [127].

DNA repair in microalgae is still poorly understood [8, 9]. However, heat shock proteins are known to initiate DNA repair after stressful events. HSP70 and HSP27 in particular are associated to this activity [128]. DNA replication, base excision repair, Nucleotide excision repair, and mismatch repair were enriched in the downregulated genes at 1h, whereas DNA replication was enriched in the

downregulated genes at 24h and 120h. The DNA associated network interference module (red) shows a similar pattern of downregulation, followed by almost complete reversal towards a log2 fold change value of ~0. Hypothesizing from the mRNA expression data, DNA was not damaged after exposure to supra-optimal temperatures, nor by formation of ROS.

5.4.3. Supra-optimal temperature downregulates photosynthesis but increases pigment concentrations.

The quantum yield (F_v/F_m) increased during the first hours after the temperature increase, indicating an increased efficiency of photosystem II at 42°C. After 8h, the quantum yield decreased until the end of the experiment. Moreover, between 8h – 120h, gene expression of nuclear genes encoding subunits of both photosystem I and photosystem II was enriched in the downregulated genes. mRNA expression for genes associated to both photosystems was downregulated despite the fact that photosystems are not considered a bottleneck at survivable but supra-optimal culture temperatures. In addition, several genes in the *Porphyrin and chlorophyll metabolism* show up to 4-fold downregulation, of which the most severely downregulates genes are: Coproporphyrinogen III, Uroporphyrinogen decarboxylase, and NAD(P)-binding Rossman-fold superfamily protein. Genes enriched in the turquoise hub, associated with chloroplasts, plastids, and the thylakoid membrane, showed downregulation throughout the experiment. Research on *Dunaliella bardawil* reported that photosynthesis was severely downregulated and that chlorophyll content decreased dramatically after exposure to a heat treatment of 42°C for 2h, after which temperature was returned to the optimal temperature [116]. In *Picochlorum sp. BPE23*, the mRNA transcript levels indicate overall decreased photosynthetic activity. However, an unexpected increase in chlorophyll-a and chlorophyll-b was observed nonetheless.

Downregulation of photosynthesis is done to reduce the formation of ROS [116]. When metabolism becomes unbalanced due to temperature stress the excessive energy flux from photosynthesis results in the formation of ROS. Unfortunately, too few genes in the carotenoid biosynthesis KEGG pathway gained a functional annotation. Therefore, little insight on the transcriptional response of the carotenoid biosynthesis pathway was gained. However, data on pigment concentration in the biomass show that the concentration of the carotenoids:

zeaxanthin, violaxanthin, lutein, β-carotene and canthaxanthin increased as a result of exposure to supra-optimal temperature. An increase in carotenoid content in response to temperature increase was also found in the literature for *D. bardawil* and *Haematococcus pluvialis* [116, 129]. Increased levels of carotenoids are often induced when microalgae are exposed to abiotic stress conditions such as salinity, light, and temperature for quenching of ROS [14, 130].

5.4.4. The metabolism and protein synthesis were downregulated to conserve energy.

As expected, connected to downregulation of genes associated to photosynthesis, the carbon fixation pathway and central energy metabolism were downregulated as determined through KEGG pathway enrichment. All analyses point towards downregulation of the metabolism of *Picochlorum sp.* in response to temperature stress. Lower photosynthetic activity ultimately results in depletion of the cell's energy reserves. Suppression of ribosome biogenesis reduces the energy demand of the cell through reduction of protein synthesis to conserve energy [127]. Ribosomal activity was significantly downregulated throughout the experiment. In a study with a thermosensitive *Arabidopsis Thaliana* strain it was hypothesized that the ribosomal activity was downregulated in response to stressful temperature to prevent errors in translation and protein folding [20]. Production of misfolded proteins would not only lead to wasted energy, but could also lead to formation of toxic compounds in the cell that cause further damage [113]. Therefore, reduced ribosomal activity indirectly relieves the workload of chaperones. Other protein processing related processes were affected throughout the experiment. The rate of protein synthesis was adapted to the reduced growth rate that was caused by the increased temperature. At the same time, the conserved energy was available for damage repair caused by oxidative stress and acclimation to the new temperature [9]. Downregulation of protein production and photosynthesis after temperature stress was also observed in *Picochlorum costavermella* [20]. We observed that downregulation of these vital cellular processes led to a severe decrease in growth rate.

5

5.4.5. Picochlorum sp. BPE23 accumulated fatty acids under heat stress

The concentration of neutral fatty acids is initially low (3.0 mg.g^{-1}) as cells are grown in nitrogen replete growth medium [22]. However, 24h after temperature increase, a fatty acid concentration of 11.5 mg.g^{-1} was measured. This significant 383% increase shows the funnelling of excess energy into *de novo* synthesis of lipid bodies as energy storage. In a study on *Chlamydomonas reinhardtii* and *Chlorella vulgaris* a screening was done for neutral lipid accumulation at elevated temperature, after which about 25% of the mutant strains showed similar elevated lipid accumulation [131]. Apparently, induction of neutral lipids through increased temperature is strain specific. Next to neutral lipids, also the polar membrane fatty acid concentration increased, from 79.0 mg.g^{-1} to 88.5 mg.g^{-1}. Especially C16:0 increased significantly. A study on *Chlamydomonas reinhardtii* showed that translocation of unsaturated fatty acids from cell membranes to neutral lipids happened after a temperature increase, to maintain optimal membrane fluidity [12]. Especially plastid membranes are heat sensitive, and quick modification of these membranes is necessary to keep photosynthesis running [132]. Almost all hubs found through the WGCNA analysis show gene ontology annotation to the plastid membranes, indicating that these membranes are also severely affected in *Picochlorum sp. BPE23*.

Genes in the fatty acid biosynthesis pathway exhibited downregulation as an overall trend from 0h to 1h, although the pathway itself was not significantly enriched due to the presence of few severely upregulated genes, up to 2.6 times log2 fold (Supplementary material 5.5). Pathview pathway analysis indicated increased mRNA expression of genes encoding for Malonyl-CoA synthase, which catalyses the reaction from malonate into malonyl-CoA. In addition, expression of mRNA of acyl carrier protein and long chain acyl-CoA synthase were upregulated. However, drawing accurate conclusions is challenging as the fatty acid biosynthesis pathway is only partly annotated in the used reference genome of *Picochlorum sp. SENEW3* (assembly ASM87641v1) [19]. Another possible reason for the fatty acid accumulation could be high stability of enzymes involved in fatty acid biosynthesis which resulted in the continuation of fatty acid biosynthesis, whereas other metabolic activity and cell growth decreased. Although the total increase in fatty acid content was just 18 mg.g^{-1} at 24h and 24 mg.g^{-1} at 72h, this increase corresponds to a percentual gain in fatty acid content of 22% and 38%, respectively.

The ability to induce an increased fatty acid concentration by increasing temperature for only 24h opens up the possibility to boost the lipid content of microalgal biomass before harvest.

5.5. Conclusions

In this study, the mechanisms underlying temperature stress and acclimation were determined through assessment of cell physiology and transcriptome analysis. A cell cycle arrest and a transcriptomic heat shock response were observed directly after an increase in temperature to 42°C, 4 degrees above the optimal growth temperature. During the first 8h, various regulatory and chaperoning mechanisms were differentially expressed to protect the cells from heat-induced cell damage. Between 8h - 120h after temperature increase, an acclimation process towards a new homeostatic phase started. Photosynthesis, carbon fixation, ribosomal activity, and central metabolism were downregulated, hypothetically to reduce oxidative cell damage. At the same time, pigment concentration increased significantly and the concentration of fatty acids increased by 22% over between 0h - 24h. The combination of these effects led to a decrease in growth rate throughout the experiment. This study contributes knowledge on the effect of supra-optimal temperature on the physiology of the industrially relevant green microalgae *Picochlorum sp. BPE23*.

5

5.6. Supplementary information files

5.6.1. Supplementary material 5.1
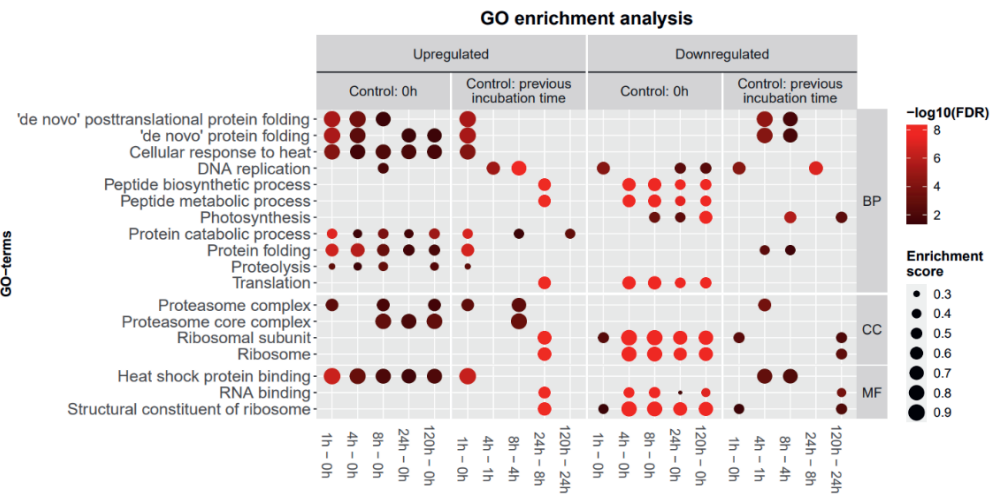
Supplementary figure 5.1: *GO enrichment analysis of the response of Picochlorum sp. BPE23 after an increase in temperature from 30°C to 42°C at different moments during the experiment. The time after the temperature shift is displayed on the x-axis, the control condition is displayed above the x-axis. GO-terms are depicted in the ontologies Biological Process (BP), Cellular Component (CC) and Molecular Function (MF). The dot size indicates the enrichment score of the GO-term whereas the color brightness indicates significance (-log10(FDR)).*

5.6.2. Supplementary material 5.2

Genes in the temperature-shock experiment were divided into eighteen modules based on co-expression patterns (Supplementary figure 5.2). Genes with the highest kME were selected and considered hub genes. The kME and functional annotations of module hub genes are displayed in Supplementary table 5.1.
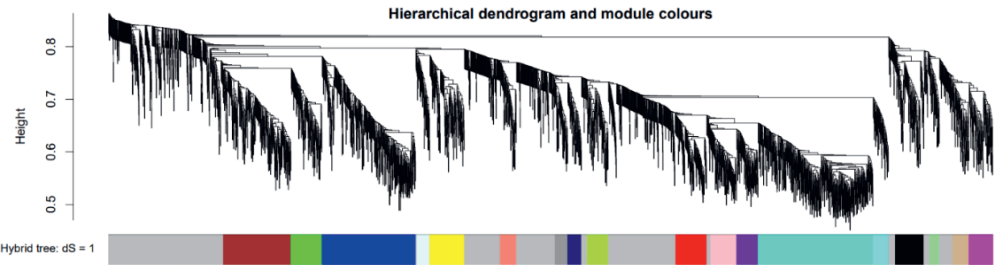
Supplementary figure 5.2: *hierarchical dendrogram and module colors of the network tree as defined by WGCNA of genes in the temperature-shock experiment. The hybrid network tree was constructed by the Dynamic Tree Cut package with a minimum module size of 30, a cut height of 0.8 and a deep split (sensitivity) of 1 out of 3.*

Supplementary table 5.1: *The module, module size, eigengene-based connectivity (kME), gene ID, gene description, type of results used to infer the description and KEGG pathway annotations of hub genes. Hub genes are defined from network inference by WGCNA of genes in the temperature-shock experiment. Unknown information is indicated with a dash.*

Module	Module size	kME	Gene ID	Gene description	Result type	KEGG pathway annotation
Black	102	0.994	PI00 G269 20	S-adenosyl-L-methionine-dependent methyltransferases superfamily protein	BLASTP result	-
Blue	334	0.996	PI00 G390 40	Transmembrane protein	BLASTP result	-
Brown	241	0.993	PI00 G517 60	Sequence-specific DNA binding, TF, DNA binding	BLASTP result	-

Cyan	55	0.990	PI00G68510	Sn1-specific diacylglycerol lipase beta isoform	Orthofinder result	-
Green	111	0.990	PI00G42640	Undecaprenyl pyrophosphate synthetase family protein	BLASTP result	Terpenoid backbone biosynthesis
Green-yellow	75	0.988	PI00G48300	Sterol methyltransferase 3	BLASTP result	Steroid biosynthesis
Grey60	45	0.992	PI00G26670	P-loop containing nucleoside triphosphate hydrolases superfamily protein	BLASTP result	-
Magenta	84	0.990	PI00G33630	DEA(D/H)-box RNA helicase family protein	BLASTP result	Spliceosome
Pink	93	0.995	PI00G10550	Nuclear RNA polymerase D2A	BLASTP result	-
Red	110	0.995	PI00G46300	Minichromosome maintenance (MCM2/3/5) family protein	BLASTP result	DNA replication
Turquoise	410	0.997	PI00G41550	Uroporphyrinogen decarboxylase	BLASTP result	Porphyrin and chlorophyll metabolism
Yellow	123	0.986	PI00G42420	Transducin family protein / WD-40 repeat family protein	BLASTP result	-

5.6.3. Supplementary material 5.3

WGCNA was conducted for describing correlation patterns among genes in the temperature-shock experiment. The network modules were functionally annotated with GO-terms (Supplementary figure 5.3), and KEGG pathways (Supplementary figure 5.4).
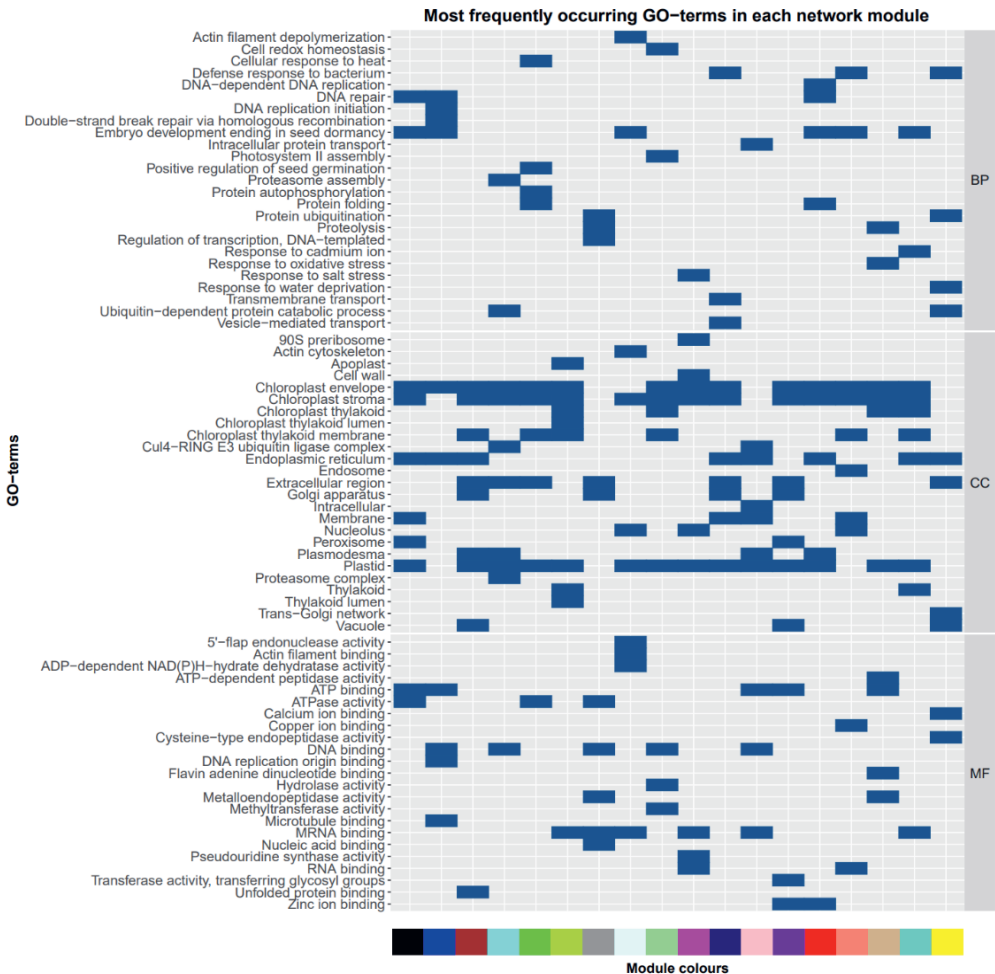
Supplementary figure 5.3: *The ten most frequently occurring GO-terms in the ontologies Biological Process (BP), Cellular Component (CC) and Molecular Function (MF) in each network module, as defined by WGCNA analysis.*

Supplementary figure 5.4: *KEGG pathway annotations of each network module, as defined by WGCNA analysis*

5.6.4. Supplementary material 5.4

The relative absorption of carotenoids (480 nm) versus biomass (750 nm) and the relative absorption of chlorophylls (680 nm) versus biomass (750 nm) were calculated and displayed in Supplementary figure 5.5. A quick decrease was observed during the first hours after the temperature increase after which an increasing trend was observed until 72 hours after the temperature step.

Optical density measured at 480, 680, and 750 nm can be used to qualitatively determine carotenoid, chlorophyll, and biomass content, respectively. The normalized 480/750 nm and 680/750 nm ratios display increased pigment content over time. This qualitative analysis agrees with the results of the quantitative pigment analysis, displayed in figure 5.2.
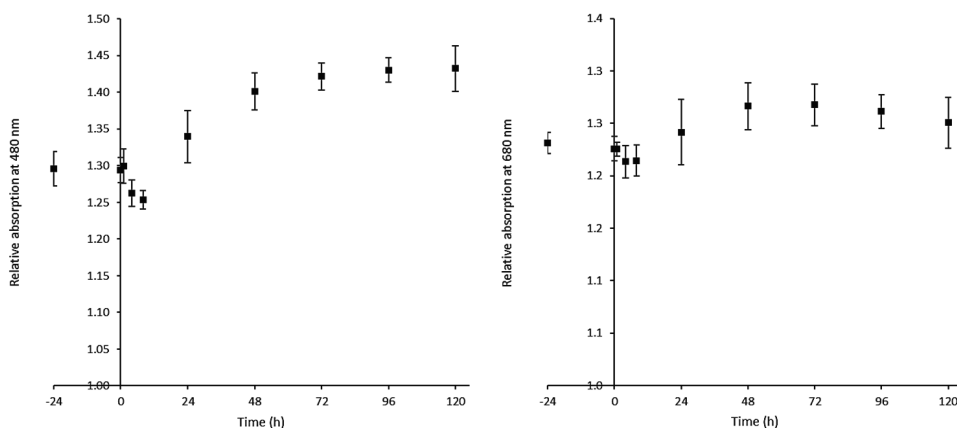
Supplementary figure 5.5: *Relative absorption values of carotenoids and chlorophylls in biomass over time.*

5.6.5. Supplementary material 5.5

Several genes from the Fatty acid biosynthesis pathway showed significant differential expression. Three of the most downregulated genes are coding for Thioesterase superfamily protein, NAD(P)-binding Rossman-fold superfamily protein, and 3-ketoacyl carrier protein synthase I and III, with a log2 fold change (LFC) of -3.1, -3.0, and -2.3 fold, respectively. Opposite, the genes encoding for Polyketide synthase enoyl reductase, acyl-activating enzyme 15, and plant stearoyl-acyl-carrier-protein desaturate were upregulated 2.6, 1.6, and 1.7 fold, respectively.
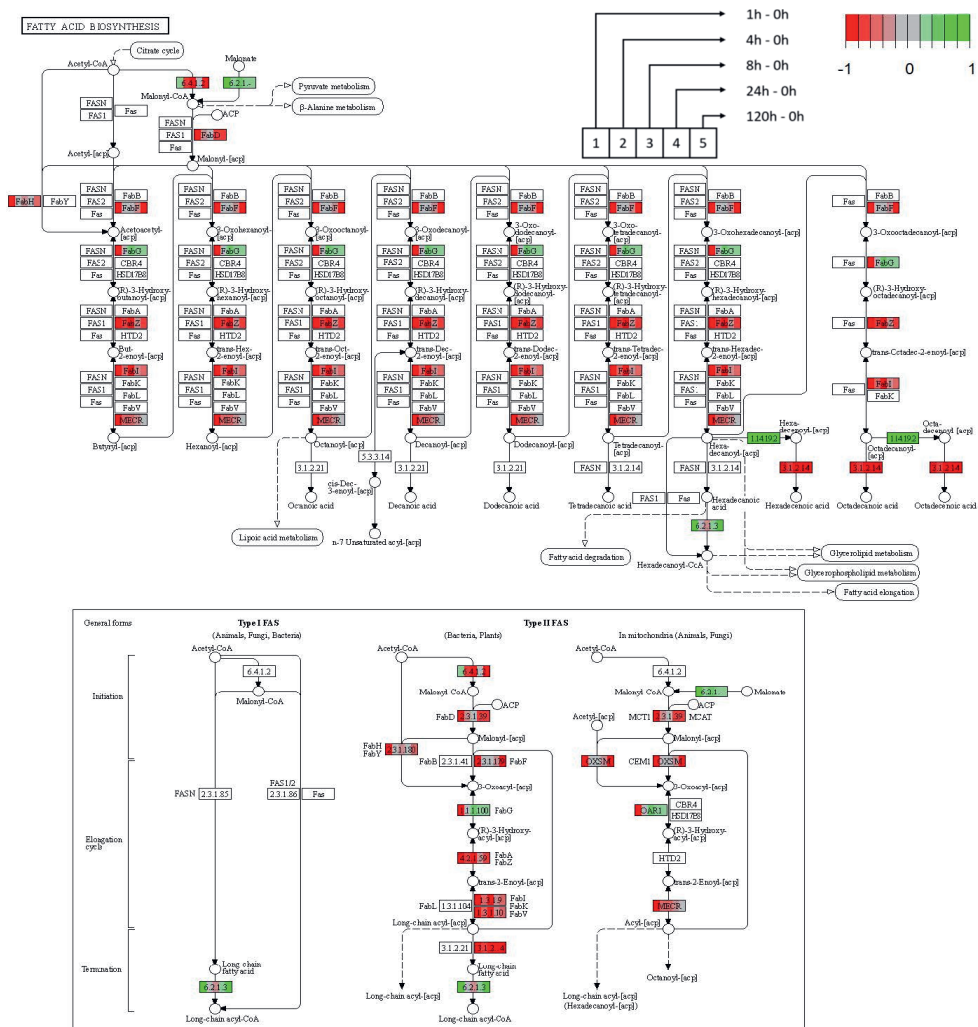
Supplementary figure 5.6: *Pathview analysis for the Fatty acid biosynthesis pathway generated through the R/Bioconductor package. Legend is displayed in the top-right corner.*
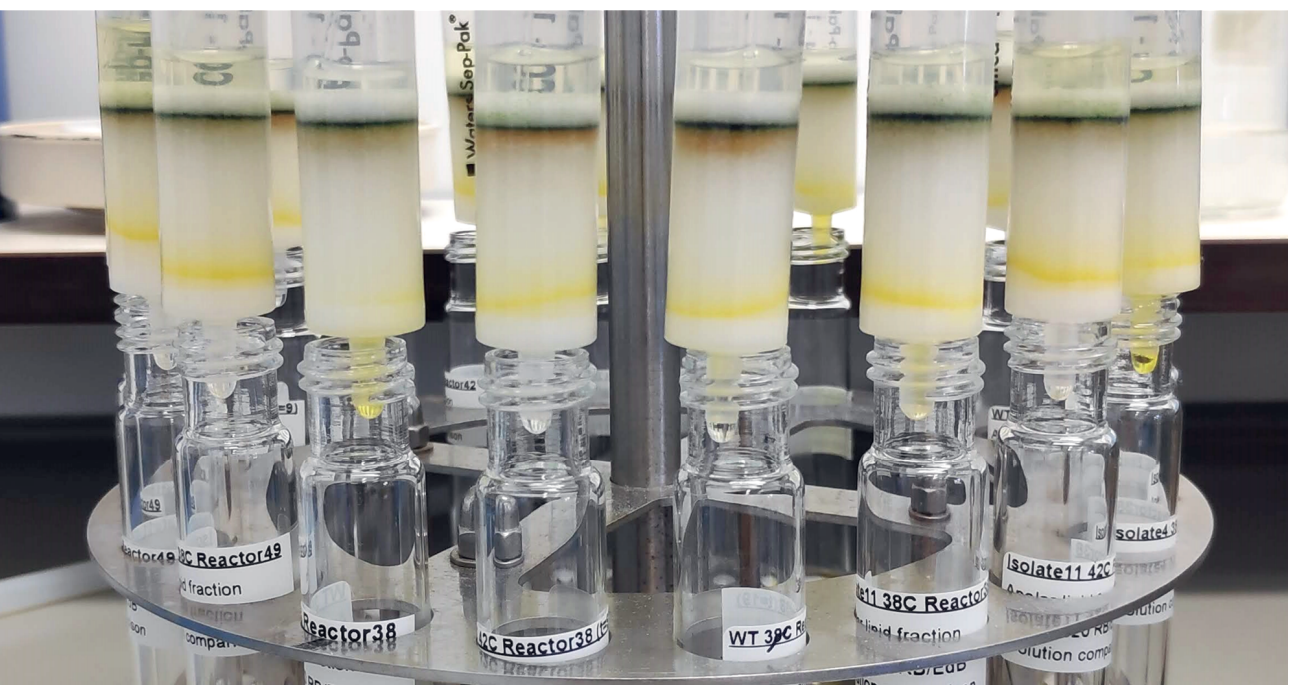
Chapter 6

Expanding the upper-temperature boundary for the microalga *Picochlorum sp. BPE23* by adaptive laboratory evolution

Abstract

Closed photobioreactors reach temperatures that reduce microalgal production or even cause culture collapses. Cooling can maintain the temperature within tolerable boundaries, but cooling is energy-intensive and expensive. More thermotolerant microalgae species can reduce dependence on traditional methods. In this study, adaptive laboratory evolution was performed for 390 days to increase the maximal tolerable temperature for the microalgae *Picochlorum sp. BPE23*. The parental wild-type strain of *Picochlorum sp. BPE23* exhibited a maximal mid-day growth temperature of 47.5°C, whereas the isolated clones grew up to 49°C. At a lower temperature of 40°C, the growth rate and absorption cross-sectional area were similar for the wild-type strain and the evolved clones. Interestingly, the clones showed a 46% increase in cell volume compared to the wild-type strain. The evolved clones with an expanded upper-temperature boundary can be applied for broader temperature control of 1.5°C, without a trade-off at lower temperatures.

6.1. Introduction

Most industrial microalgal species have a maximal growth temperature between 25°C to 35°C. However, closed photobioreactors can reach peak temperatures up to 50°C due to climatological conditions such as high light levels [6]. Such temperatures have a disastrous effect on culture viability and productivity for most microalgal species. Therefore, the temperature is actively controlled in photobioreactor systems [6]. While cooling through shading, active cooling, or spraying of water is possible, these methods are expensive and not sustainable [4]. To reduce temperature control costs, species that are naturally more resistant to otherwise stressful temperatures, preferably in combination with tolerance to diel temperature fluctuations, should be employed [6, 117]. Microalgal species that can maintain their maximal productivity rate under diel temperatures ranging from 30°C to 45°C would cause a cost reduction of 31% [4]. In addition, robust species with a high maximal growth temperature can prevent culture collapse due to photobioreactor overheating [6, 133].

Supra-optimal temperatures unbalance cellular metabolism in various ways, ultimately leading to reduced growth and productivity [7, 11]. When exposed to supra-optimal temperatures, cells initially acclimate to rebalance cellular homeostasis. Cell membranes, photosystems, and protein composition are remodeled within hours to counteract the adverse effects of increased temperature [8, 117]. Consecutively, due to the decreased metabolism and growth rate, cells allocate excess energy into storage compounds such as fatty acids and lipids [8, 12]. Acclimation will lead to a more stable cellular state, but growth will remain hindered when non-optimal growth conditions are maintained.

After prolonged exposure to supra-optimal temperature, mutants with improved phenotypes will periodically emerge due to *de novo* genetic mutations that cause fitness gains [23]. Natural genetic mutations can be exploited for strain optimization when combined with appropriate selective pressure. Adaptive laboratory evolution (ALE) has become a popular tool to select strains with improved phenotypes. Examples of traits suitable for improvement through ALE are: stress tolerance, substrate utilization, or growth rate and product yield [23, 24]. It is especially applicable to improve complex traits as no prior genetic knowledge is required. Few studies have addressed the improvement of temperature robustness in microorganisms through ALE, in which a shift in optimal or maximal growth temperature of 2°C was observed on average [134-137].

127

However, ALE studies on microalgae concerning temperature, are scarce and the exact mechanisms for adaptation are unknown [23, 24]. The green microalgae *Picochlorum costavermella* expresses a natural mutational rate of $3.23 \bullet 10^{-10}$ to $10.12 \bullet 10^{-10}$ nucleotide per generation, respectively [26, 138]. Based on the 13.3 Mbp genome size of *P. costavermella,* this would lead to 0.013 genomic mutations per cell in one generation, which would require 74 generations for a single mutation [20]. However, the mutational rate is known to increase under stressful conditions to accelerate molecular evolution for rapid adaptation to new growth conditions [27]. In addition, the large number of cells in cell cultures significantly increase the chance of beneficial mutations.

Species of *Picochlorum* are often proposed as a platform for the production of various bulk and specialty products [7, 43, 139]. In prior research, *Picochlorum sp. BPE23* was isolated, characterized and selected for its high growth rate in combination with its robustness [7]. It shows optimal growth at temperatures between 35°C and 40°C, whereas it can survive mid-day peak temperatures of 47.5°C [117]. This study reports how *Picochlorum sp. BPE23* was improved through ALE to tolerate a 1.5°C higher maximal temperature.

6.2. Materials and methods

6.2.1. Cell cultivation

6.2.1.1. Growth media and inoculum preparation

Picochlorum sp. BPE23, isolated from a saltwater body of Bonaire, was pre-cultivated in shake flasks in an orbital shaker incubator (Multitron, Infors HT) under continuous light at an intensity of 100 $\mu mol_{ph}.m^{-2}.s^{-1}$ (PAR) [7]. The temperature was set at 40°C. The relative humidity of the air in the headspace was set to 60% and enriched with 2% CO_2. Cells were cultured in artificial seawater enriched with nutrients and trace elements. Elements were provided at the following concentrations (in $g.L^{-1}$): NaCl, 24.5; $MgCl_2.6H_2O$, 9.80; Na_2SO_4, 3.20; $NaNO_3$ 2.12; K_2SO_4, 0.85; $CaCL_2.2H_2O$, 0.80; KH_2PO_4, 0.23; $Na_2EDTA \cdot 2H_2O$, 0.105; Na_2EDTA, 0.06; $FeSO_4 \cdot 7H_2O$, 0.0396; $MnCl_2 \cdot 2H_2O$, $1.71 \cdot 10^{-3}$; $ZnSO_4 \cdot 7H_2O$, $6.60 \cdot 10^{-4}$; $Na_2Mo_4 \cdot 2H_2O$, $2.42 \cdot 10^{-4}$; $Co(NO_3)_2 \cdot 6H_2O$, $7.00 \cdot 10^{-5}$; $NiSO_4 \cdot 6H_2O$, $2.63 \cdot 10^{-5}$; $CuSO_4 \cdot 5H_2O$, $2.40 \cdot 10^{-5}$; K_2CrO_4, $1.94 \cdot 10^{-5}$; Na_3VO_4, $1.84 \cdot 10^{-5}$; H_2SeO_3, $1.29 \cdot 10^{-5}$. HEPES (4.77 $g.L^{-1}$) was added for Erlenmeyer cultures as a pH buffer. The medium pH was adjusted to 7.0, after which it was filter sterilized before use through filters with a 0.2 μm pore size.

During photobioreactor cultivation, Antifoam B (J.T.Baker, Avantor, USA) was added at a concentration of 0.5 mL.L^{-1} out of a 1% w/w stock. At the start of the cultivation, 0.168 g.L^{-1} sodium bicarbonate (NaHCO$_3$) was added to provide sufficient CO$_2$. The photobioreactor was inoculated at a starting cell density of OD$_{750}$ 0.2 (±0.07 g.L^{-1}).

6.2.1.2. Adaptive laboratory evolution – photobioreactor operation

The adaptive laboratory evolution experiment was performed in a heat sterilized flat-panel photobioreactor with a 1.8 L working volume, a 20.7 mm light path and a 0.08 m^2 surface area for irradiation (Labfors 5 Lux, Infors HT, Switzerland) [117]. Illumination was done from one side by 260 warm white LED lights with a spectrum of 450-620 nm. Day-night cycles (12/12 h/h) were applied in which light was given in a sinusoid pattern. The ingoing light reached 1500 µmol$_{ph}$.m^{-2}.s^{-1} (PAR) at its peak during mid-day. The outgoing light level was set at ~1% of the ingoing light, following a sinusoid pattern similar to the ingoing light. The outgoing light was controlled by automatic dilution of the cell culture (turbidostat mode) when below the set-point. The photobioreactor was aerated through sparging of compressed air at a rate of 980 mL.min^{-1} (0.54 vesselvolume.min^{-1}). CO$_2$ was provided on-demand through pH-controlled addition. The reactor pH was set at 7. The temperature was set at 25°C during nighttime and followed a sinusoid pattern during daytime. The peak temperature was increased stepwise over a period of 403 days at the following levels, 40°C, 45°C, 47°C, 48°C, 48.5°C, 49°C, and 49.5°C. The microalgae culture was monitored closely after a temperature increase.

6.2.1.3. Culture tipping point – photobioreactor operation

The culture tipping point was measured for each temperature step throughout the evolution experiment by measuring the maximum temperature of oxygen production. When the growth of the cell culture was stable at each of the temperature steps, 400 mL of cell culture was transferred from the Laboratory evolution culture (2.1.2.) to a stand-alone Labfors photobioreactor system to reach a biomass concentration of 0.4 g.L^{-1}. Air was supplied at a rate of 980 mL.min^{-1}, and CO$_2$ was supplied at a fixed rate of 20 mL.min^{-1}. Sulfuric acid and sodium hydroxide were used to control pH. The ingoing light was set at 200 µmol$_{ph}$.m^{-2}.s^{-1} (PAR), outgoing light was set at 35 µmo$_{ph}$l.m^{-2}.s^{-1} (PAR). The Dissolved oxygen

concentration (DO) was measured online. After stabilization of the DO, the temperature was linearly increased at a rate of 5°C per hour, from 30°C to 60°C. The measured DO value was normalized on a scale of 0 to 1.

6.2.1.4. Isolation and characterization of ALE clones.

Algal clones were isolated from the ALE culture at day 390. Clone isolation was done by plating on agar, followed by colony picking. Growth characterization of the parental wild-type strain and clones was done in algaemist photobioreactors (Technical Development studio, WUR, The Netherlands), under a repeated batch mode [7]. The microalgal culture was diluted daily at sunset to an OD_{750} value of 5 (± 2 g.L^{-1}) [7]. The light was provided as a 12/12 h/h day/night cycle with light as a sinusoid with a mid-day value of 1500 μmol_{ph}.m^{-2}.s^{-1} (PAR). The temperature was set to follow a sinusoid trend. Four different midday peak temperatures were chosen: 40°C, 45°C, 47.5°C, and 49°C. Characterization experiments of the clones were performed as biological duplicates.

6.2.2. Offline measurements

6.2.2.1. Biomass concentration

The biomass concentration was determined by optical density measurements. Duplicate UV-VIS spectrophotometry measurements were performed at a wavelength of 750 nm (DR6000, Hach, USA). In addition, biomass concentration (in g.L^{-1}) was measured in duplicate by dry weight determination. Empty Whatman glass microfiber filters (θ 55 mm, pore size 0.7 µm) were dried overnight at 95°C and placed in a desiccator for 2 hours. Filters were then weighed and placed in the mild vacuum filtration setup. Cell culture containing 1 to 10 mg of microalgae biomass was diluted in 25 mL 0.5 M ammonium formate and filtered. The filter was washed twice with 25 mL 0.5 M ammonium formate to remove residual salts. The wet filter was dried overnight at 95°C, placed in a desiccator for 2 hours, and weighed. Biomass concentration was calculated from the difference in filter weight before and after filtration and drying.

6.2.2.2. Cell size and cell number

Cell size and cell number were determined in duplicate with the Multisizer III (Beckman Coulter Inc., USA, 50 μm aperture). Samples were diluted in two steps before analysis, initially by 5x dilution in fresh medium, followed by 100x dilution in Coulter Isoton II.

6.2.2.3. absorption cross-sectional area

The average dry-weight specific optical cross-section ($m^2.kg^{-1}$) was measured with a UV-VIS/double-beam spectrophotometer (Shimadzu UV-2600, Japan, light path: 2 mm), equipped with an integrating sphere module (ISR-2600). Absorbance was measured from 400 to 700 nm with a step size of 1 nm.

6

6.3. Results and Discussion

6.3.1. The maximal diel peak temperature increased over time during adaptive laboratory evolution

During an adaptive laboratory evolution experiment of 403 days, 139 generations of microalgae were grown under mimicked commercial growth conditions. The culture temperature was increased stepwise to maintain a high selective pressure after cells adapted (Figure 6.1). The parental wild-type strain, *Picochlorum sp. BPE23*, was characterized in a prior study under comparable growth conditions and the same photobioreactor setup. It exhibited a maximal growth temperature of 47.5°C [117].

The dilution rate of the photobioreactor, and therefore growth rate of the microalgae, was 0.77 d^{-1} at 40°C (Figure 6.1) [117]. As the temperature increased to 45°C, growth initially reduced to 0.55 d^{-1} but recovered over time up to 0.65 d^{-1}, indicating acclimation or adaptation. A comparable trend for this gradual culture fitness recovery was observed after each increase in temperature. The consecutive steps to 47°C, 48°C, 48.5°C, and 49°C yielded dilution rates at the end of each steady-state of 0.44, 0.30, 0.35, and 0.25 d^{-1}, respectively. The temperature step to 45°C and 47.5°C little cellular stress and acclimation was rapid. However, the increase to 48°C, 48.5°C, and 49°C induced a significant stress response directly after the increase in temperature, resulting in a temporary decrease in dilution rate.
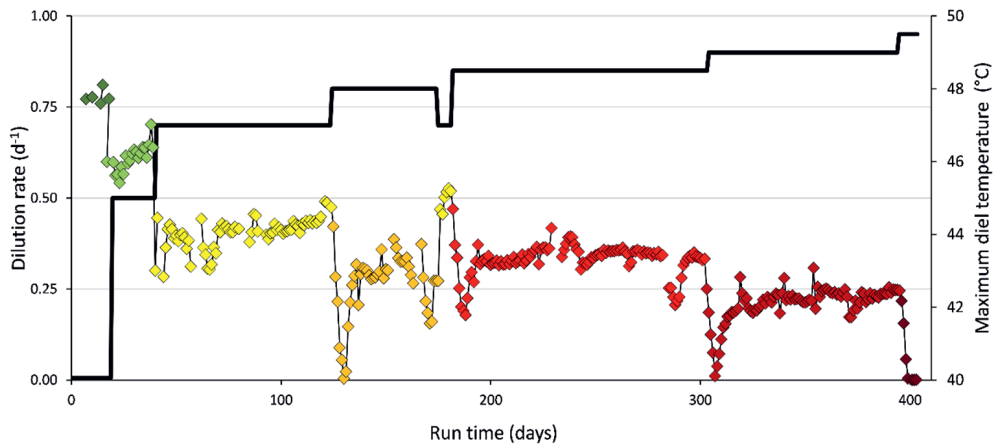

Figure 6.1: *measured dilution rate of the ALE photobioreactor over time. The dilution rate is displayed on the left y-axis, while the maximum diel temperature, found at mid-day, is displayed on the right y-axis.*

Interestingly, the dilution rate at 48.5°C was higher than the dilution rate at 48°C. We hypothesized that the microalgae adapted to higher temperatures at this point. The cell culture collapsed after the temperature increase to 49.5°C. Hypothetically adaptation to 49.5°C should be possible when the ALE experiment was extended. However, while adaptation initially occurs rapidly, it slows after several hundred generations as most simple mutations have already occurred, and more complex multi-gene mutations are required for further improvement [28].

6.3.2. Picochlorum sp. BPE23 was able to produce oxygen at increased temperatures after ALE

The maximal temperature at which the ALE culture was capable of oxygen production was determined periodically to assess whether the microalgae were successfully adapting to increased mid-day peak temperatures. Measurements were done on days 30, 120, 170, 290, and 380 as the culture was in steady-state on these selected days (Figure 6.2). Cell culture was transferred to a stand-alone photobioreactor for which temperature was increased at a rate of 5°C per hour
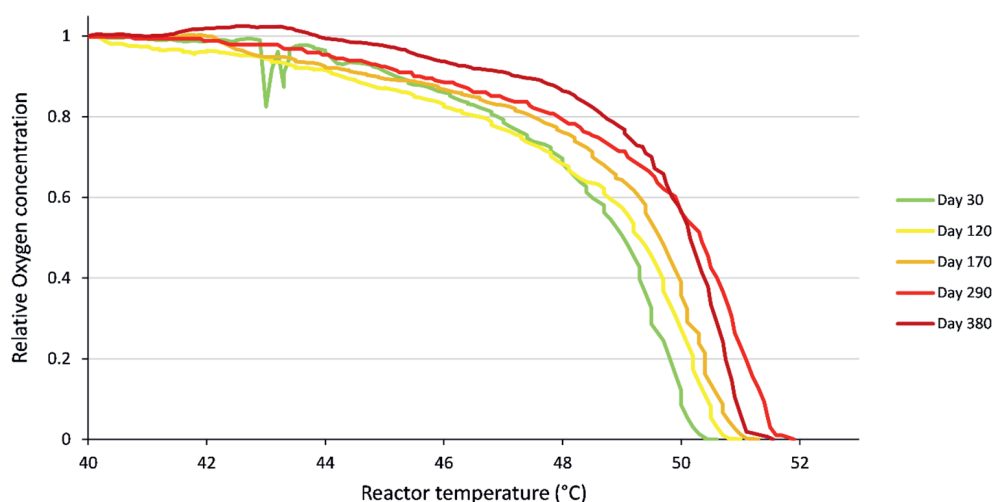
Figure 6.2: *The capability of photosynthetic oxygen production during a temperature increase. The photosynthetic oxygen production was determined in stand-alone photobioreactors in which temperature was increased by 5°C per hour, from 30°C to 60°C. Culture viability was monitored through the relative oxygen concentration which was normalized to the oxygen concentration at 40°C and displayed from 40°C to 54°C. Cell culture was taken from the ALE photobioreactor for which the day number indicates the moment at which the experiments were done during the ALE experiment.*

from 30°C to 60°C. The dissolved oxygen concentration was measured online throughout the experiment.

A gradual decrease in oxygen concentration was observed due to increasing inhibition of photosynthesis at increasing temperatures. The maximal temperature at which oxygen production was observed shifted to higher temperatures as the ALE experiment proceeded. Each consecutive experiment showed a comparable curve with a shift of ±0.5°C. The shift of ±0.5°C is directly proportional to the increase in temperature in the ALE photobioreactor. The exception to the increasing trend was the last experiment at day 380, which compared to the experiment at day 290 had a higher relative dissolved oxygen concentration up to precisely 50°C, after which the dissolved oxygen decreased with a steeper trend than was observed in the previous experiments.

The rapid decrease in dissolved oxygen is most likely caused by the denaturation of enzymes involved in photosynthetic oxygen production. Photosynthesis is a thermo-sensitive process that severely impacts the metabolism and cell growth when disrupted [8]. While photosynthesis is not the only thermosensitive process, it is a good indicator of the point at which the cells die irreversibly. As it is amongst the most thermosensitive processes and simple to measure, it provides a way to assess and compare the state of the ALE culture at different times points [8-10].

The initial increase in maximal temperature of oxygen production could be caused by short-term acclimation by exchange of photosynthetic pigment in the photosystems and by remodeling the cell membranes [117, 140]. However, because the maximal temperature of photosynthetic oxygen production increased throughout the entire experiment, we expect that genetic adaptation took place in addition to short term acclimation. Genetic adaptation can cause structural differences for enzymes by which thermal tolerance can change [141]. Photosynthesis and carbon fixation are thermosensitive cellular processes that present a bottleneck at supra-optimal temperatures [6]. Especially Rubisco was reported to limit carbon assimilation under temperature-induced cell stress [142]. We hypothesize that enzymes in these pathways have adapted to tolerate higher temperatures. This hypothesis is strengthened by the fact that the maximal temperature for oxygen production increased throughout the ALE. In addition, a compositional adaptation of the cell and thylakoid membranes is often observed in response to increased temperature to counteract the impact of temperature-induced change in membrane fluidity [117, 134].

6.3.3. Growth characterization of isolated clones

Three ALE clones were isolated at the end of the ALE experiment and subjected to growth characterization. Four diel temperature regimes were applied with different peak temperatures at mid-day (Figure 6.3). The wild-type and Clone1 show comparable growth at 40°C with a growth rate of 0.8 d^{-1}, whereas Clone2 grew faster and Clone3 grew slower at 45°C and 47.5°C. As expected, the clones were capable of growth at 49°C, while the growth rate of the wild-type strain decreased to 0 d^{-1} after 4 days at this temperature.

In previous research, a mid-day peak temperature of 40°C was reported to be optimal for wild-type *Picochlorum sp. BPE23*, whereas the maximal temperature tolerated was reported to be 47.5°C [117]. The current research shows a similar trend. The ability to grow at increased temperature makes the clones more robust,
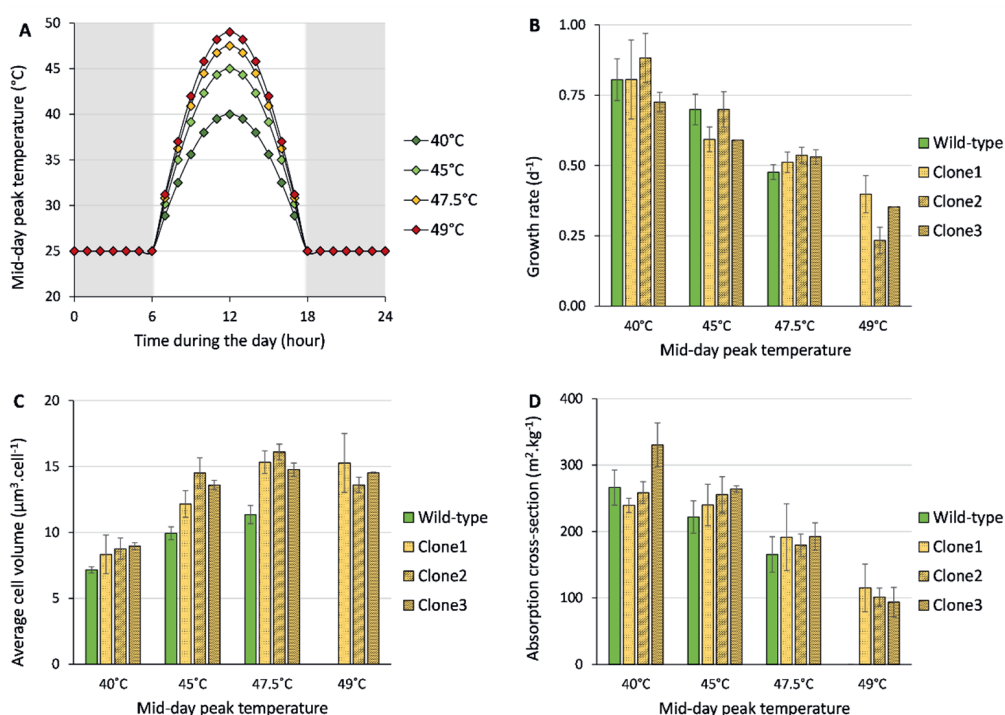
Figure 6.3: *The (A) applied temperatures for characterization, (B) specific growth rate, (C) average cell volume, and (D) specific absorption cross-sectional area as measured for wild-type strain and three ALE clones of Picochlorum sp. BPE23 during the characterization experiment. Data represent the average ± the propagated error of 3 days of steady-state growth for 2 biological duplicates photobioreactors operated in repeated batch mode.*

which is vital for maintaining a stable cell culture in commercial photobioreactors. In addition, the expanded upper-temperature boundary of 1.5°C can prevent culture crashes after periodic temperature increases. Both wild-type and clone strains could adapt to the new temperature regime within days, which indicates a rapid acclimation rate in response to changing growth conditions. Such rapid acclimation allows for less stringent process control, which can reduce operating costs.

Adaptive laboratory evolution effectively shifts temperature optima and maxima in microalgae [23, 143]. A trade-off in the lower temperature regions is commonly observed when evolving for higher temperature tolerance [134, 136]. While growth at lower temperatures (20°C to 40°C) was not characterized, the ALE clones obtained in this study did not display affected growth at the optimal growth temperature for the wild-type (40°C).

A shift in optimal temperature commonly accompanies a shift in maximal temperature due to the selective pressure in the supra-optimal temperature niche [28, 134]. However, this was not observed for *Picochlorum sp. BPE23* in this study. In an ALE study with *Tisochrysis lutea*, a shift of 3°C was observed for the optimal and maximal growth temperature [137]. *T. lutea* was able to tolerate a higher upper temperature and gained the ability to grow faster at temperatures above the optimal temperature for the wild-type.

6.3.4. The effect of temperature on the cell size of Picochlorum sp. BPE23

On day 120 of the ALE experiment, a 0.5°C temperature increase to 48°C was made that led to an increase in the average cell volume from 9 μm^3 to 13.3 μm^3 within one week time (Supplementary material 6.1). A similar pattern was observed for the clone characterization as the isolated clones showed an increased cell size compared to the parental wild-type strain (Figure 6.3). While there was a slight difference in cell size between the wild-type and clones at 40°C, the difference in cell size became more pronounced at 45°C and higher temperatures. The adaptation is assumed to be genotypic due to the persistence of the cell size increase. Just as in a previous study, an increase in cell size was observed in *Picochlorum sp. BPE23* when exposed to increasing temperature [117].

The consensus in the literature regarding whether cells increase or decrease in size during ALE under high temperatures is unclear. In theory, a decreased cell size allows for faster cell division which is beneficial for survival in continuously diluted cell culture [6, 144-146]. In addition, a larger cell surface area to cell volume ratio is considered an evolutionary benefit of small cells in a high-temperature environment where gases are less soluble [145]. Indeed, a selection for small cells was applied during a 290 generation ALE study on *Dunaliella tertiolecta*, where the obtained smaller cells were found to be more tolerant to increased temperature. [144]. We observed the opposite as cells became larger in response to increased temperature. In agreement with this, significant increases in cell size were observed during several ALE studies in *Escherichia coli* [146, 147]. In these studies, comparable patterns were observed as in our study. It was hypothesized that the mutant strains accumulated larger metabolic reserves to be capable of faster acclimation under fluctuating growth conditions. This theory fits our case and is strengthened by the fact that *Picochlorum sp. BPE23* halts cell division at mid-day when stressful peak temperatures are applied, while at the same time, larger cells with more storage compounds were observed, as shown in a previously published study [117]. The capacity to accumulate storage compounds to store energy when energy is absorbed in excess and utilize this energy when energy is lacking would be an advantage. A second and often discussed hypothesis stated that mutant cells could simply grow slower in terms of cell division but grow equally fast in terms of biomass accumulation due to larger cells [148]. This hypothesis was found to be not valid when cells were forced to grow at an equal rate in chemostat operation, as the mutant cells remained larger than the parental cells, as was also observed in our study [147]. Unfortunately, different studies contradict each other, and the exact mechanisms behind cell size adaptation remain unknown.

6.3.5. Changes in absorption cross-sectional area in response to increased temperatures

The biomass specific absorption cross-sectional area indicates the level of photosynthetic pigments in the cell since it reflects the level of light absorbed by the chromophores [98]. The absorption cross-sectional area decreased continuously throughout the ALE experiment, causing cells to become more transparent. A severe reduction event was observed around day 120 of the ALE, directly after the increase in temperature to 48°C (Supplementary material 6.2). An

average absorption cross-sectional area of 221.9 ± 18.9 was found between days 53 and 106 of the experiment, whereas an average absorption cross-sectional area of 143.4 ± 23.3 $m^2.kg^{-1}$ was found between days 348 and 393 of the ALE experiment. As a result of the lower absorption cross-sectional area, the biomass concentration increased by 20-25% due to the turbidostat operation mode, which controls reactor dilution based on light absorption (Supplementary material 6.3). Despite the decreased photobioreactor dilution rate, a larger biomass concentration caused the total productivity to remain at the same level.

Under non-optimal growth conditions, microalgae temporarily decrease their absorption cross-sectional area to decrease the energy flux from the photosystem [70, 117]. This flexibility allows growth under fluctuating environmental conditions that affect the microalgal metabolism [85]. Both wild-type and clones of *Picochlorum sp. BPE23* showed their highest absorption cross-section value at 40°C, whereas the absorption cross-section decreased with increasing temperature.

A decreased absorption cross-sectional area is reported to lead to higher biomass yields on light as light is diluted and divided amongst a larger quantity of biomass [34, 98]. As a result, less energy is dissipated into heat through photochemical quenching due to photosystem oversaturation [85]. Biomass specific absorption cross-sectional area was similar for the wild-type and the clones. Nonetheless, a difference in absorption cross-sectional area was observed at different cultivation temperatures, with lower values measured at higher temperatures (Figure 6.3). Based on the results, we conclude that the decrease in absorption cross-sectional area during ALE was a reversible acclimation effect.

6.4. Conclusion

Adaptive laboratory evolution was performed to improve the tolerance of *Picochlorum sp. BPE23* to high mid-day peak temperatures. The maximal temperature for growth was shifted from 47.5°C to 49°C over 409 days (139 generations). Periodic assessment of the maximal temperature of oxygen production revealed that the tolerance to high temperatures increased throughout the ALE procedure. During clone characterization, no trade-off in productivity was observed compared to the wild-type strain at the lowest studied mid-day temperature of 40°C. The improved clones can be applied to reduce the risk of a culture crash on sunny days at which temperature can rise to lethal levels. The clones can be applied without a trade-off at lower mid-day temperature, as low as 40°C.

The cell size and absorption cross-sectional area changed during ALE. The increase in cell size was persistent in the clones throughout the characterization experiments and became especially noticeable at supra-optimal temperatures. Due to its persistence, the cause for a cell size increase is assumed to be genotypic. Contrarily, the decreased absorption cross-sectional area was found to be reverted during later characterization experiments. This fast reversion highlights the flexibility of *Picochlorum sp. BPE23* to adapt its photosystems to new growth environments.

6

6.5. Supplementary materials

6.5.1. Supplementary material 6.1

The average cell volume was measured throughout the ALE experiment and displayed in Supplementary figure 6.1. At 120 days an increase in cell volume was observed that persisted until the end of the ALE experiment.
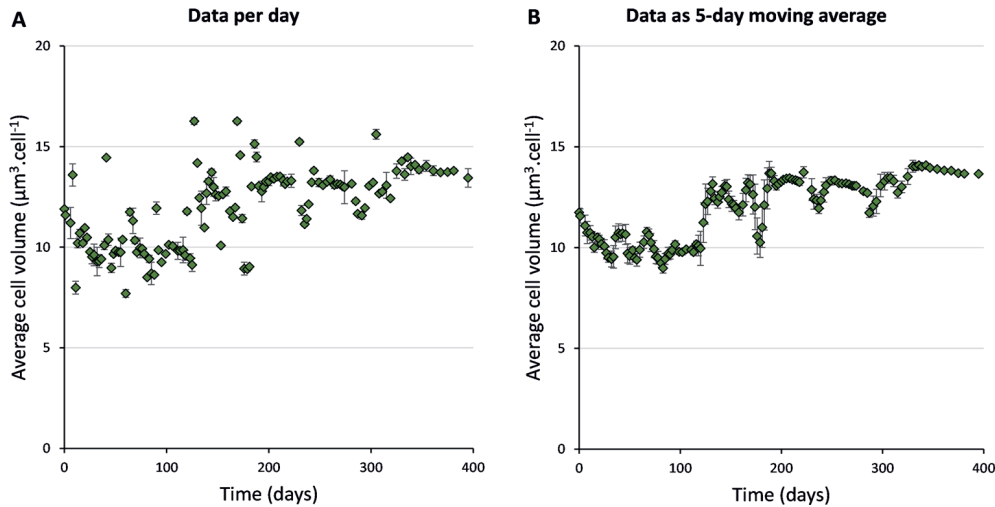
Supplementary figure 6.1: *average cell volume during the ALE experiment. Data is presented as measured per day (left), and as 5-day moving average (right). Data points represent the average ± average deviation of two technical replicates.*

6.5.2. Supplementary material 6.2

The absorption cross-sectional area of the microalgal cell culture was measured throughout the ALE experiment. The absorption cross-sectional area indicates the absorbing surface area of the cell culture. Lower pigmentation level cause lower energy uptake per cell. In addition low absorption cross-sectional area results in less in-culture cell shading. After 120 days a decreasing trend was observed up to 300 days.
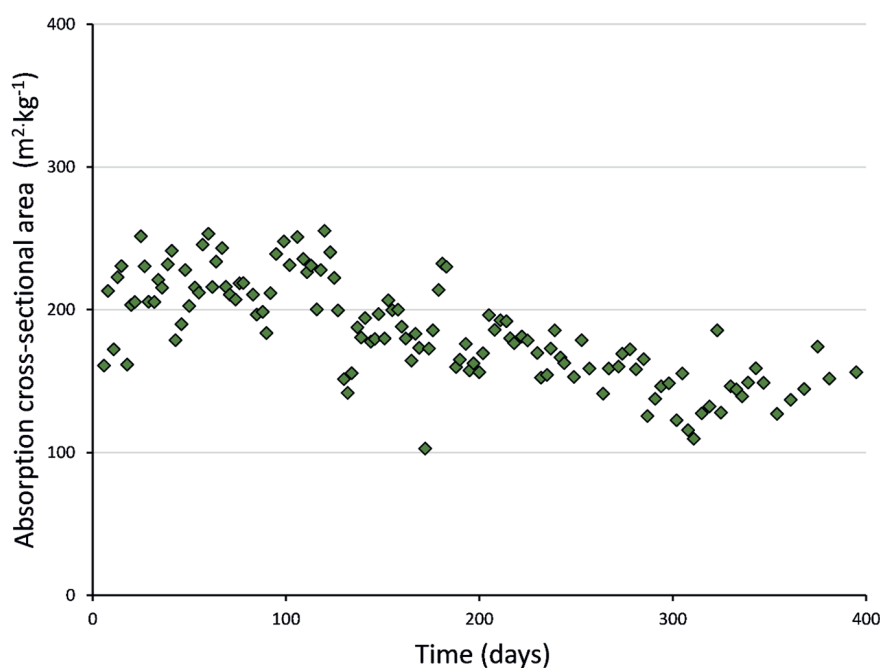
Supplementary figure 6.2: *The absorption cross-sectional area during the ALE experiment. The photobioreactor was operated in turbidostat mode.*

6.5.3. Supplementary material 6.3

The biomass concentration was ~1.5 $g.l^{-1}$ during the first 120 days of the ALE experiment. After 120 days the biomass concentration increased to ~1.8 $g.l^{-1}$, after which a gradual increase was observed throughout the remainder of the experiment. As the photobioreactor was operated in turbidostat mode, fluctuations in biomass concentration were caused by alterations in the light absorption characteristics of the biomass.

Supplementary figure 6.3: *The biomass concentration during the ALE experiment. The photobioreactor was operated in turbidostat mode. Datapoints represent the average ± average deviation of two technical replicates.*

Chapter 7

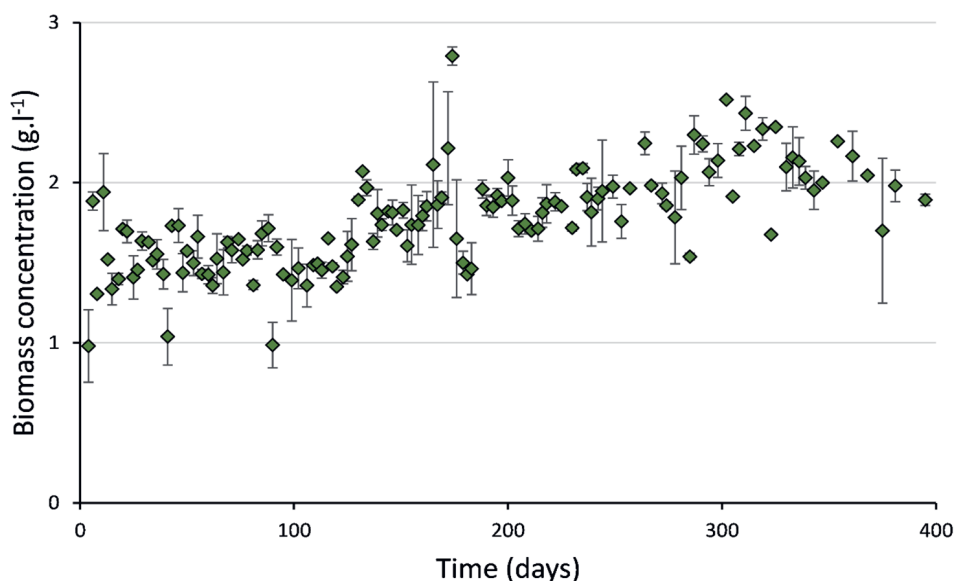**Multi-omics analysis of *Picochlorum* adaptive laboratory evolution mutants with an increased maximal growth temperature, growth rate, and yield on light**

Abstract

Adaptive laboratory evolution (ALE) is a powerful method for strain optimization towards abiotic stress factors and for identifying adaptation mechanisms. In this study, the green microalga *Picochlorum sp. BPE23* was cultured under supra-optimal temperature to force genetic adaptation. The robustness and adaptive capacity of *Picochlorum* strains turned them into an emerging model for evolutionary studies on abiotic stressors such as temperature, salinity, and light.

Mutant strains showed an expanded maximal growth temperature of 44.6 °C, whereas the maximal growth temperature of the wildtype strain was 42 °C. Moreover, at the optimal growth temperature of 38 °C the biomass yield on light was 22.3% higher and the maximal growth rate was 70.5% higher than the wildtype. Genome sequencing and transcriptome analysis were performed to elucidate the mechanisms behind the improved phenotype. A *de novo* assembled phased reference genome allowed identification of 21 genic mutations involved in various processes. Moreover, approximately half of the genome contigs were found to be duplicated or even triplicated in all mutants, suggesting a causal role in adaptation.

The developed tools and mutant strains provide a strong framework from whereupon *Picochlorum sp. BPE23* can be further developed. Moreover, the extensive strain characterization provides evidence on how microalgae evolve to supra-optimal temperature and to photobioreactor growth conditions. This study is the first to identify microalgal evolutionary mechanisms by combining ALE with genome sequencing.

7.1. Introduction

Microalgal biomass can be processed into renewable lipids, proteins, carbohydrates, and specialty chemicals [1]. Production of renewable products to replace products from finite sources becomes increasingly relevant in the battle against global warming. Despite the opportunities, microalgal production for the bulk product market is not yet competitive due to high operational costs [4, 149]. Robust microalgae would reduce photobioreactor operational costs as less cooling is required [4, 6].

Adaptive laboratory evolution (ALE) has been proposed as a high potential tool for improving robustness against a wide variety of abiotic stress factors, such as high temperature [23]. ALE was adopted just recently in microalgal biotechnology but has been proposed as a powerful way to produce genetic mutations that lead to increased fitness in stressful environments [29, 30]. ALE studies focusing on high temperature commonly yield a rapid shift in the optimal and upper growth temperature of 2-3 °C, whereafter the rate of adaptation reduces significantly [28, 134-136]. The initial rapid adaptation was hypothesized to be caused by pleiotropy [28]. Temperature as a stress factor impacts nearly every cellular process as it affects the protein configuration and membrane fluidity [150]. In addition to the general cellular metabolism, microalgae grow autotrophically through photosynthesis which is considered a thermosensitive process [6]. In prior studies, *Picochlorum sp. BPE23* was found to rapidly regulate its photosystems and the formation of storage compounds in order to align the photosynthetic energy production with the energy output to prevent the formation of harmful reactive oxygen species [117].

Significant steps in temperature tolerance are commonly generated by an accumulating of mutations in multiple genes [151]. Next to single nucleotide polymorphisms (SNPs) and genetic variants, copy number variations that are caused by partial genome duplications are hypothesized to drive evolution [152]. The extent to which copy number variation (CNV) contributes to evolution and phenotypic variation is a topic of scientific interest [153]. In *Arabidopsis thaliana*, CNVs were found to cause significant genome diversity and physiologic differences, which consecutively drove adaptation towards an applied stress factor [152]. CNVs were also proposed to drive adaptation to wastewater in *Chlorella* [154].

7

In this study we applied ALE to expand the upper-temperature boundary of the already thermotolerant microalga *Picochlorum sp. BPE23* [7]. *Picochlorum* has become one of the most relevant and promising microalgal species over the past years, also illustrated by the fact that the genome of *Picochlorum sp. SENEW3*, a closely related species, became the genome of the month in Trends in Genetics [155]. Species of *Picochlorum* have been used before in evolutionary studies on thermotolerance, halotolerance, and irradiance tolerance due to their robustness and strong adaptation capacity in combination with a small genome size of 13-14 Mb [20, 21, 43, 156]. In addition to the phenotypic characterization of growth and biomass composition, we present valuable genomic resources which can be used in future studies. Genome sequencing of both the wildtype and temperature adapted mutant strains through PacBio HiFi sequencing was performed to generate a phased genome assembly. This assembly was then used to identify genomic mutations and for the subsequent transcriptome analysis. After analysis of all data, hypotheses were formed on underlying mechanisms behind the improved phenotype of the mutants. This is the first study on microalgae that combined ALE with extensive genetic characterization of mutations to identify potential evolutionary adaptation mechanisms for thermotolerance and domestication.

7.2. Materials and methods

7.2.1. Cell cultivation

7.2.1.1. Growth media and inoculum preparation

Picochlorum sp. BPE23, isolated from a coastal bay on Bonaire, was pre-cultivated in shake flasks in an orbital shaker incubator (Multitron, Infors HT) under continuous light at an intensity of 100 µmolph m^{-2} s^{-1} photosynthetically active radiation (PAR) [7]. The temperature was set at 40 °C, the relative humidity of the air in the headspace was set to 60% and enriched with 2% CO_2. Cells were cultured in artificial seawater enriched with nutrients and trace elements. Elements were provided at the following concentrations (in g.L^{-1}): NaCl, 24.5; $MgCl_2.6H_2O$, 9.80; Na_2SO_4, 3.20; $NaNO_3$ 2.12; K_2SO_4, 0.85; $CaCL_2.2H_2O$, 0.80; KH_2PO_4, 0.23; $Na_2EDTA·2H_2O$, 0.105; Na_2EDTA, 0.06; $FeSO_4·7H_2O$, 0.0396; $MnCl_2·2H_2O$, 1.71·10^{-3}; $ZnSO_4·7H_2O$, 6.60·10^{-4}; $Na_2Mo_4·2H_2O$, 2.42·10^{-4}; $Co(NO_3)_2·6H_2O$, 7.00·10^{-5}; $NiSO_4·6H_2O$, 2.63·10^{-5}; $CuSO_4·5H_2O$, 2.40·10^{-5}; K_2CrO_4, 1.94·10^{-5}; Na_3VO_4, 1.84·10^{-5}; H_2SeO_3, 1.29·10^{-5}. HEPES (4.77 g.L^{-1}) was added to Erlenmeyer cultures as a pH

buffer. The medium pH was adjusted to 7.0, after which it was filter sterilized before use. During photobioreactor cultivation, Antifoam B (J.T.Baker, Avantor, USA) was added at a concentration of 0.5 ml.L^{-1} from a 1% w/w% stock. Also, 0.168 g.L^{-1} Sodiumbicarbonate (NaHCO$_3$) was added at inoculation to provide sufficient CO$_2$ at the start of the cultivation. The photobioreactor was inoculated at a starting cell density of OD$_{750}$ 0.2.

7.2.1.2. Adaptive laboratory evolution and mutant isolation

ALE was performed in Infors flat-panel photobioreactors [117]. The incident irradiance was set at 813 µmol.m^{-2}.s^{-1} (PAR), continuous. The outgoing light level was maintained at 10 µmol.m^{-2}.s^{-1} (PAR) by light-controlled dilution of the cell culture (turbidostat mode). The photobioreactor was aerated through sparging of compressed air at a rate of 980 ml.min^{-1}. CO2 was provided on demand through indication of an increased pH. The reactor pH was set at 7.4. Temperature was increased stepwise throughout the evolution process for 322 consecutive days as follows: 30 °C, 42 °C, 42,5 °C 43 °C, 43.5 °C, 44 °C, 44.2 °C, 44.7 °C, 44.2 °C, 44.4 °C, 44.6 °C, and 44.8 °C (supplementary material 7.1). At 44.6 °C, a sample was taken from the photobioreactor and cells were plated on agar plates followed by incubation at 42°C for one week. Colonies were picked, transferred into liquid growth medium and subjected to a growth screening using the HT24 incubating unit (Algenuity, UK). A screening temperature of 42 °C and a light intensity of 200 µmol·m^{-2}·s^{-1} (PAR) were applied. The 6 strains with the highest growth rate were selected for more elaborated growth rate and thermotolerance characterization.

7.2.1.3. Growth rate screening – Erlenmeyer cultivation

The wildtype and mutant 4, 8, 11, 14, 16, and 21 were cultured at 20 °C, 25 °C, 30 °C, 35 °C, 37.5 °C, 40 °C, 41 °C, 42.2 °C, 43.2 °C, 44 °C, and 44.6 °C to determine the maximum growth rate over a temperature range. Cells were cultured in 250 ml Erlenmeyer flasks with a liquid volume of 100 ml. Repeated batch cultivation was applied in which cultures were diluted daily to a cell concentration of OD$_{750}$ 0.05. The OD$_{750}$ was measured at 6 and 24 hours after inoculation. Broad-spectrum white fluorescent light (Philips master TL-D reflex, color temperature 840) was set at a continuous intensity of 200 µmol·m^{-2}·s^{-1} (PAR). A 2% CO$_2$ headspace was created. Data acquisition was made at steady-state [7].

7.2.1.4. Characterization of mutant strains – photobioreactor operation

Algaemist photobioreactors (Technical Development studio, WUR, The Netherlands) were used for characterization and comparison of growth characteristics and RNA expression patterns of the wildtype and two evolved strains of *Picochlorum sp. BPE23 [157]*. Cells were grown in turbidostat mode with similar growth conditions as in "paragraph 2.1.2. Adaptive laboratory evolution", with the exception that air was supplied at a rate of 200 ml.min^{-1}. Experiments were performed as biological triplicates, and samples were taken in a steady-state for both temperatures. Temperature was initially set at 38 °C until samples were taken, after which it was increased to 42 °C until a new steady-state was reached.

7.2.2. Offline measurements and analysis

The quantum yield, cell size, cell number, and biomass concentration were measured as described in [117]. Biomass harvest and biomass lyophilization, determination of pigments through HPLC, and determination of fatty acids through GC was performed as described in [150]. The photosynthesis irradiance curve and the maximal specific growth rate were measured as described in [157].

7.2.3. Genomic DNA analysis

7.2.3.1. Genome sequencing

Genomic DNA (gDNA) extraction and sequencing was performed by the genomics facility of WUR Bioscience (Wageningen, The Netherlands). gDNA of the wildtype, mut4, and mut11 was sequenced through PacBio sequencing. 50 mg washed and lyophilized biomass was used for gDNA extraction using MagMax Plant DNA kit (Applied Biosystems). Extracted gDNA was sheared using a megadisruptor device (Diagenode), aiming for a 25 kb fragment size. Barcoded SMRT bell template libraries were made for each microalgal strain using SMRT bell express template prep kit 2.0 (PacBio). gDNA was eluted in 20 μL elution buffer and pooled for size selection on a Blue Pippin instrument (Saga Sciences). The 8 to 13 kb and >=13 kb fractions were collected for each lane after which purification and concentration was performed with Ampure XP beads (Beckman Coulter). Purified SMRT bells were finally analyzed for size and used for primer annealing, polymerase binding, and purified using AMPure PB beads (SMRTLink10.1). Sequencing was done on one

SMRT cell of a PacBio Sequel IIe system with 65 pM on plate loading by diffusion with standard settings and 30 hour movie time. Data demultiplexing and HiFi read processing was done by SMRT Link 10.1.

Illumina paired-end sequencing of the wildtype, mut4, mut8, mut11, and mut16 with 150 bp reads was performed by Novogene (Novogene, United Kingdom). For library preparation, DNA was randomly fragmented to a size of 350 nt, then end polished, A-tailed, ligated with Illumina sequencing adapters, followed by PCR enrichment of P5 and P7 oligos. The PCR product was purified (AMPure XP system) and sequenced.

7.2.3.2. Genome assembly

The genome assembly of wildtype *Picochlorum sp. BPE23* was reconstructed by assembling the HiFi reads using Flye 2.9-b1768 on default settings [158]. Next, Illumina sequencing data of the wildtype strain was used to polish the Flye genome assembly with Pilon v1.24 with '--fix all' [159]. For polishing, the paired-end Illumina reads were trimmed with Trimmomatic v0.39 'ILLUMINACLIP:TruSeq3-PE.fa:2:30:10 LEADING:3 TRAILING:3 SLIDINGWINDOW:4:15 MINLEN:36' and mapped to the assembly with bwa-mem2 v2.2.1 [160, 161]. Sorting and indexing of mapping files were done with samtools v1.12 [162]. The chloroplast and mitochondrial gDNA were labeled by mapping to the assembly of *Picochlorum* sp. *'soloecismus'* strain DOE 101 with minimap2 '-xasm20' [163]. The identity of the chloroplast and mitochondrial gDNA fragments was then confirmed by a Blastn 2.11.0+ hit to the NCBI nt database [164]. Homologous contigs were identified by leveraging the location of the duplicated BUSCO genes followed by self-alignment with minimap2 v2.10 ('-k19 -w19 -A1 -B9 -O16,41 -E2,1 -s200 -z200 -X') [165]. To assess the completeness of the genome assembly, BUSCO v5.2.2 was used with the chlorophyta_odb10 set as well as KAT v2.4.1 [166, 167]. To further assess the structure of the genome assembly, it was aligned to the closely related genomes of *Picochlorum SENEW3*, *Picochlorum oklahomensis*, and *Picochlorum celeri* [156, 168]. In addition, the original HiFi data was mapped back with minimap2 v2.22. The coverage of the HiFi data was calculated using bedtools v2.30.0 [169]. HiFi and Illumina data were compared for wildtype, mut4, and mut11. Further study towards genome ploidy was performed through kmc v3.1.1 and smudgeplot v0.2.3 [170, 171].

7.2.3.3. Genome annotation

Before annotation of the wildtype genome assembly, repeats were identified in the polished assembly RepeatModeler v2.0.2 with '-LTRStruct' and subsequently masked with RepeatMasker 4.1.2-p1 [172]. The RNA-seq samples of the wildtype were mapped to the genome with hisat2 v2.2.1 to serve as RNA evidence, whereas the proteome of *Chlamydomonas reinhardtii* (GCF_000002595.2) served as protein evidence for gene prediction [119]. Gene prediction was performed with BRAKER v2.1.6 '--etpmode ' [173]. Mitochondrion and chloroplast sequence were excluded for gene prediction (but not for mapping RNA-seq). Functional annotation was done with InterProScan 5.52-86.0 [174]. The included analyses were: TIGRFAM, SUPERFAMILY, PANTHER, Gene3D, Coils, Pfam and MobiDBLite. In addition, InterPro (IPR) and Gene Ontology (GO) terms were listed. An organism specific annotation R package was created using the makeOrgPackage function from the AnnotationForge Package v1.32.0. [175]. Lastly, non-coding RNAs were identified by searching the genome with cmscan from the infernal toolkit against the Rfam database [176].

7.2.3.4. Genome analysis

Variant calling to identify mutations in the ALE strains was performed by aligning HiFi reads to the phased genome assembly with minimap v2.22 '-ax map-hifi --MD --secondary=no'. Variant were called with GATK v4.3.2.0 HaplotypeCaller, combined with CombineGVCFs and genotyped with GenotypeGVCFs [177]. Filtering variants (GATK SelectVariants) was done on QUAL<1000, homozygous REF allele for wildtype, and non-homozygous REF allele for either mutant. We used SnpEff 5.0 with the novel wildtype genome and annotation to determine the effect of the mutations on the amino acid sequence [178].

Enrichment analyses were performed with genes that had doubled or tripled coverage in mut4 or mut11 compared to the wildtype using clusterProfiler in R v4.0.4 [179]. MCScanX was used to identify syntenic blocks based on an all-vs-all BLASTP search (Wang et al., 2012).

Circos v0.69-8 was used to visually combine all data on the framework of the wildtype genome assembly [180]. Gene and repeat density were calculated in bins of 10kb.

7.2.4. mRNA extraction, sequencing and analysis

Biologically triplicate biomass samples of wildtype, mut4, and mut11 steady-state cell cultures at 38 °C and 42 °C (paragraph 2.1.4) were analyzed for mRNA levels. Biomass pre-treatment, mRNA extraction and sequencing, and data quality control were performed as described in [150]. Fragments of the mRNA library with an average size of 300 bp were sequenced using the Illumina Novoseq PE150 platform, yielding paired-end reads of 150 nt (Novogene, United Kingdom).

Paired-end reads were mapped to the phased wildtype genome using Hisat2 v 2.2.1. Transcripts were assembled using StringTie v1.3.2d. StringTie's prepDE python script was used to extract raw read counts per gene. Raw counts were normalized using DESeq2 v1.30.1. Pairwise differential expression between mutants and wildtype at different temperatures was calculated using DESeq2, setting alpha to 0.05. Enriched GO terms were detected using clusterProfiler's gseGO function and visualized using the ggplots R package.

7

7.3. Results and Discussion

7.3.1. Adaptive laboratory evolution yields an improved mutant strain

Adaptive laboratory evolution was performed for 322 days, during which 293 generations were cultivated (Supplementary material 7.1). Temperature was increased stepwise in small increments after the cell culture fitness recovered from the previous temperature step. In this way, the maximal temperature tolerated by the cell culture shifted from 42 °C to 44.6 °C at the end of the ALE trajectory.
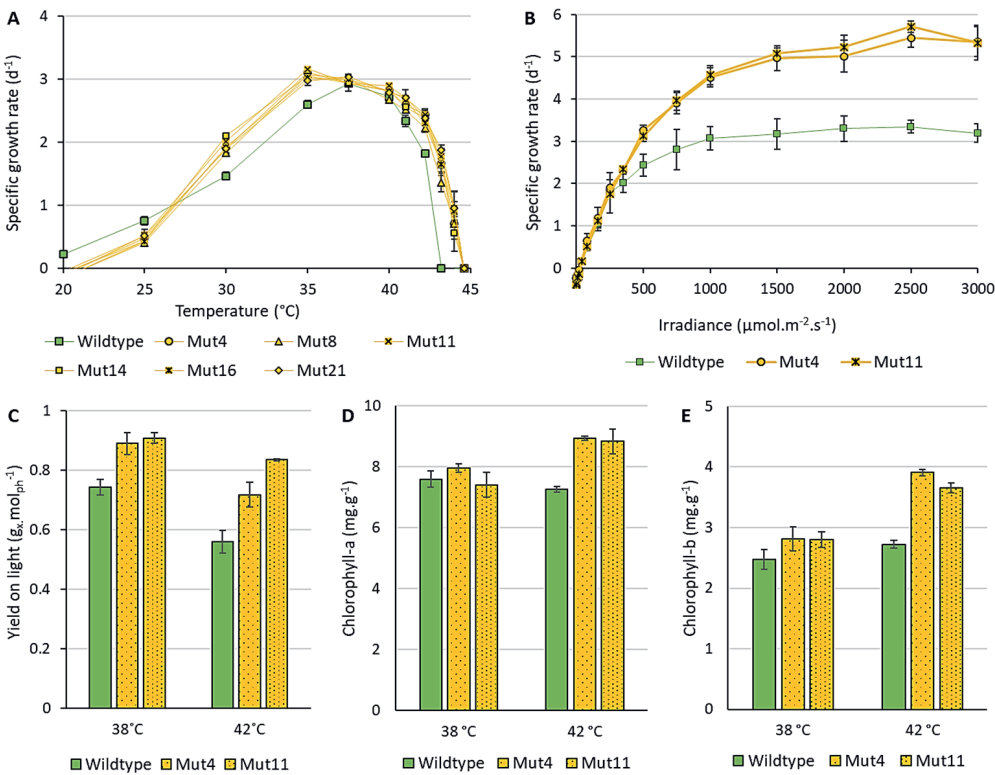
Figure 7.1: *(A) The growth rate was measured for the wildtype and six mutant strains over a temperature range from 20 °C to 44.6 °C. (B) A photosynthetic irradiance response curve at 38 °C displaying the estimated specific growth rate, as measured by photosynthetic oxygen evolution. (C) The biomass yield on light for growth at 38 °C and 42 °C, the optimal and maximal growth temperature, of the wildtype, respectively. (D) Chlorophyll-a content in the microalgal biomass. (E) Chlorophyll-b content in the microalgal biomass. The datapoints represent the average value ± the standard deviation of three biological replicates.*

After mutant isolation, six mutant strains and the wildtype strain were subjected to growth characterization over a temperature range from 20 °C to 44.6 °C (Figure 7.1A). During these screening experiments, a continuous irradiance of 200 µmol.m^{-2}.s^{-1} was applied. The mutant strains showed an expanded upper-temperature boundary which was expected based on the growth behavior of the cell culture during the ALE trajectory. ALE induced shifts in the upper-temperature boundary are commonly accompanied by a trade-off at the lower temperature boundary [181]. Such a trade-off was observed for the mutant strains as they were not able to grow at 20 °C, and in addition, showed reduced growth at 25 °C compared to the wildtype strain. Interestingly, the growth rate at 30 °C and 35 °C was higher for the mutant strains than for the wildtype strain. This increase in growth rate was not expected for these temperatures as selective pressure during ALE was on a supra-optimal temperature. Nonetheless, a broader temperature optimum is advantageous during application for commercial production in photobioreactors due to the fluctuating temperatures in such systems when not controlled. The applied light intensity of 200 µmol.m^{-2}.s^{-1} is considered a low to average intensity for microalgal cultivation. For this reason, photosynthetic irradiance curves were made under the optimal growth temperature (38 °C) to compare the maximal specific growth rates of the mutant and wildtype strains (Figure 7.1B). Mut4 and mut11 displayed a maximal specific growth rate of 5.45 ± 0.23 d^{-1} and 5.71 ± 0.14 d^{-1}, respectively, which is significantly higher than the maximal specific growth rate of the wildtype, 3.35 ± 0.15 d^{-1}. The growth rate of the wildtype strain, grown on nitrate is comparable to values reported in previous research [157].

Mut4, mut11, and the wildtype were further characterized for their growth rate and biomass yield on light in controlled photobioreactors. Biomass yield on light measured at steady-state is displayed in Figure 7.1C, whereas growth and adaptation trends prior to steady-state are presented in Supplementary material 7.2. The growth rate of the wildtype and mutant strains decreased after the temperature change from 38 °C to 42 °C, as expected based on the growth data displayed in Figure 7.1A. Interestingly, the mutant strains reached a new steady-state within days without strong growth rate decrease or a decreased quantum yield, whereas the wildtype strain required 19 days to reach a new steady-state with a significant temporary drop in growth and a decreased quantum yield. In fact, two steady-state situations were recognized for the wildtype strain, being at 9 and 19 days after the increase in temperature, with biomass yield on light values of 0.31 ±0.11 g$_x$.mol$_{ph}$$^{-1}$ and 0.56 ± 0.04 g$_x$.mol$_{ph}$$^{-1}$, respectively. In prior research,

transcriptomic and compositional analysis after a temperature increase to 42 °C revealed an immediate system-wide stress response, followed by gradual acclimation [150]. A similar response is hypothesized to have taken place in this study, whereby the first steady-state situation at day 9 is considered to be part of the acclimation phase towards the actual steady-state phase at day 19.

The concentration (in mg.g^{-1}) of both chlorophyll-a and chlorophyll-b, but also all xanthophyll cycle pigments and β-carotene did not significantly differ between wildtype and mutants at 38 °C, despite the higher biomass yield on light (Figure 7.1D/E, Supplementary material 7.4). Surprisingly both mutant strains increased their chlorophyll-a and chlorophyll-b content at 42 °C, indicating that the mutant cells actively increased their photosynthetic light absorbance in response to the temperature increase. Supra-optimal temperature commonly causes photoinhibition to prevent cellular damage through reactive oxygen species (ROS) [114]. This would lead to a severe stress response with decreased growth and reduced photosystems as a result [117]. However, the opposite was observed. Hypothesizing, the cellular machinery which copes with excessive heat may have mutated to be more active under this condition, thereby allowing more ROS formation without direct cellular damage. Such waste of light comes at the cost of a reduced photosynthetic biomass yield on light. Microalgal strains naturally exhibit different biomass yields on light. However, causes for these differences are difficult to determine, and examples in literature are mostly speculative [157]. Potential causes for the increased photosynthetic efficiency are an increased photochemical efficiency, altered antenna size and filtering pigment composition, and an altered biomass composition [6, 182].

Based on growth data and literature examples, potential mechanisms behind the expanded temperature tolerance, the increased maximal specific growth rate, and the increased biomass yield on light, are difficult to designate. To elucidate the evolutionary mechanisms underlying the observed physiologic changes, biomass samples were taken during the aforementioned steady-states to analyze mRNA expression levels, gDNA sequencing, pigment composition, and fatty acid composition.

7.3.2. Partial genome multiplication and gene variants were identified

Using the 199x coverage PacBio HiFi sequencing data with an average length of 18 kb, we produced a fully phased diploid genome assembly for wildtype *Picochlorum sp. BPE23*. The assembled contigs, with a total length of 28,372,001 bp, are displayed in Figure 7.2. For contig 1A the long sequencing reads bridged a repeat area, whereas contig 1B1 and 1B2 were not connected. Contig U1, U2, and U3 contain unassigned repeat areas. The plastid and mitochondrial genomes were both assembled in one contig. In the assembly 14,247 genes were identified that code for 14,443 predicted transcripts, of which 12,283 were annotated with at least one functional protein domain. This is the second phased genome for a species of *Picochlorum* [168].

In addition, mut4 and mut11 were sequenced (PacBio HiFi) with a coverage of 231x, and 315x and an average read length of 17 kb, to characterize genomic differences with the wildtype. Interestingly both mutant strains show a double, or even higher coverage of the baseline signal for specific genomic regions, indicating multiplication of at least 2-fold for nearly half the genome (Figure 7.2, track 5 and 6). The sequencing coverage of the wildtype strain was constant over nearly the complete genome, indicating accurate assembly and no polyploidy. Both mutants exhibited identical genomic multiplication patterns. The genomes of mut8 and mut16 were sequenced using Illumina PE150 and showed the same genome multiplication patterns (Supplementary material 7.5). Microscopic karyotyping is suggested as a follow-up method to study how the partial genome multiplication materialized. Hypothetically whole chromosomes or chromosome arms were duplicated.

7

While multiplication of genes with particular functions might be expected in the mutants, GO-term enrichment did not reveal any significant gene functions. Even the seemingly narrow peaks on contig 5B and 8A with 3 to 4 times genetic multiplication contain genes with a large variety in gene functionality. Copy number variation is hypothesized to drive adaptation and evolution, as shown in *Arabidopsis thaliana* [152]. Multiple gene copies give mutational freedom as a
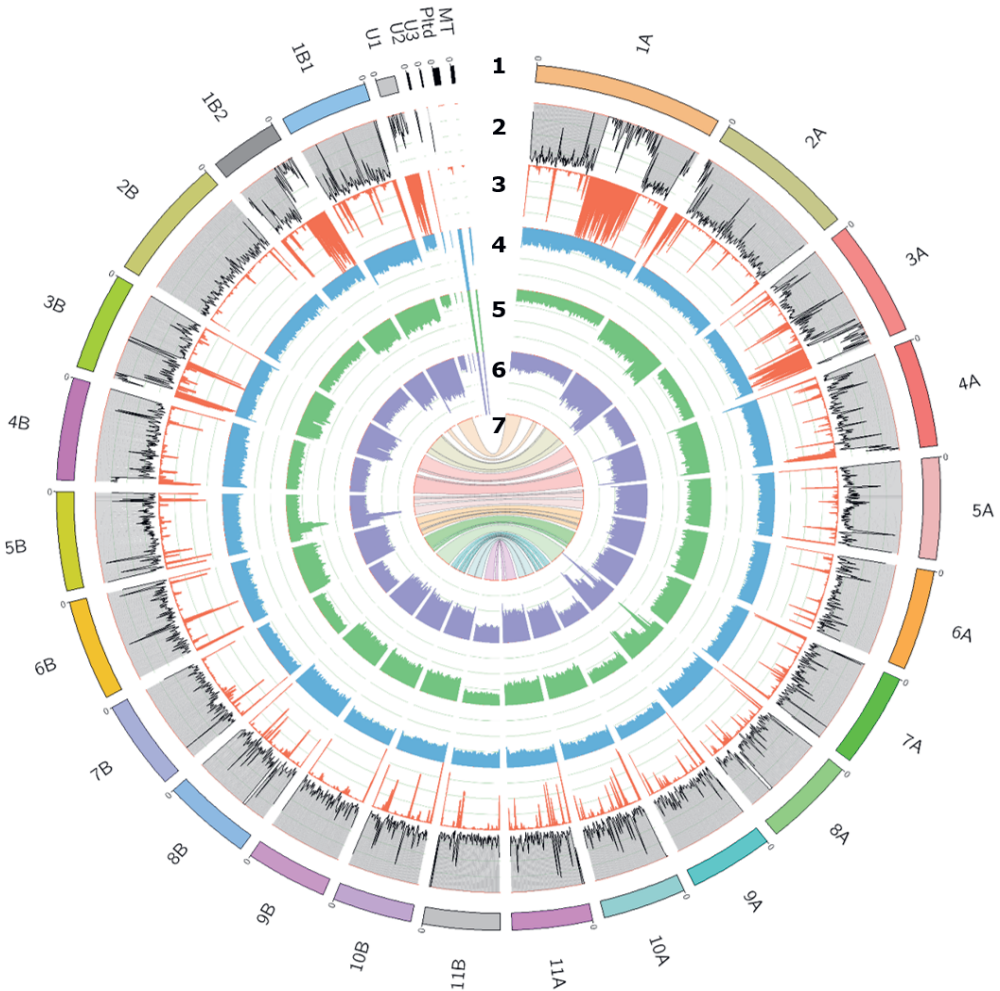
Figure 7.2 *Circos plot to illustrate the phased genome for the wildtype strain and two mutant strains of Picochlorum sp. BPE23. Items displayed from the outer to the inner layer are: (1) assembled contigs, (2) genes density, (3) repeat density, (4) coverage of wildtype sequencing reads, (5) coverage of mut4 sequencing reads, (6) coverage of mut11 sequencing reads, (7) contig synteny map. Contig coding: MT - mitochondrial DNA, Pltd - plastid, U1, U2, U3 - unassigned repeat areas. Syntenic contigs are displayed with A and B.*

defective mutation does not immediately result in decreased fitness or cell death, allowing for accumulation of mutations. In a thermotolerance ALE study with *S. cerevisiae*, large genetic duplications were observed in 5 out of 7 mutant strains [134]. However, these genetic duplications were said to have little effect on thermotolerance and the thermotolerant phenotype was dedicated largely to gene mutations. There is the consensus that after significant genome multiplication, a large number of the non-beneficial duplicated gene copies is lost over time [183]. In a different study with *S. cerevisiae*, such chromosomal duplications disappeared over time as they were unstable and imposed an energetic burden on the cell [184]. The authors speculate that large genetic duplications are acquired as a crude solution to stress, after which more subtle and efficient mutations are accumulated over time that make the chromosomal duplication obsolete.

As all mutant strains show similar growth and thermotolerance patterns, we hypothesize that the improved phenotype originated from mutations that both strains have in common. An overview of in-gene SNPs and InDels are presented in Table 7.1. In total, 220 mutations were identified of which 154 were intergenic mutations shared by both mutants and 45 were found in only one mutant. In addition, 15 gene mutations were shared by both mutants and 6 were found in only 1 mutant. From all mutations, 76.8% are shared between mutants, whereas 71.4% of the genic mutations are shared.

By deducing from the fact that most shared mutations are present on only one of the multiplicated gene copies, it can be concluded that the partial genomic replication took place close to the beginning of the ALE trajectory. Moreover, it is likely that the introduction of the shared mutations between the two mutant strains dates to the moment before the cell lines separated. The large number of shared mutations compared to the non-shared mutations indicate that the parental strain of mut4 and mut11 was dominant in the ALE cell culture until just before the end of the ALE trajectory.

In ALE strain improvement trajectories, the most significant gain in terms of temperature tolerance is gained at the beginning, after which additional mutations have a diminished effect on fitness improvement due to network complexity [30]. Therefore, it is likely that the shared mutations gained at the start of the ALE experiment caused the thermotolerant phenotype.

Most of the identified mutations were found in intergenic non-coding regions at the ends of a contig while few mutations were found in regions between coding

7

genes. Most intergenic DNA has no currently known function. However, some intergenic DNA stretches are known to enhance translation of nearby genes [185]. Non-coding RNA was demonstrated to regulate acclimation to heat [186]. There were a few intergenic mutations present close to coding genes. We found 249 non-coding RNAs in the assembled genome of *Picochlorum sp. BPE23* but none of the identified mutations was present in a non-coding RNA region. It is therefore unlikely that mutations in intergenic regions were responsible for the improved phenotype. However, the current state of knowledge on intergenic regions does not allow for finite conclusions of the impact of intergenic mutations.

Of the 21 mutated genes, only few showed significant up- or downregulation with log2 fold change values of 1-2 times (Table 7.1). Most mutations involve a SNP that introduces an amino acid change in the protein whereas a few mutations involve nucleotide insertions/deletions. Three genic mutations and one intronic mutation are unique to mut4 and two intronic mutations are unique to mut11 (PicoBPE23_07590 and PicoBPE23_11307). Moreover, two intronic mutations occurred at the same location in both mutants with different nucleotide substitutions. Differences between mutant strains are of special interest as mut11 showed a higher biomass yield on light at 42 °C, and performed slightly better than mut4, in general. Mut4 had extra mutations in introns of genes associated with formiminotransferace catalytic domain superfamily, pumilio RNA binding repeat, Ribosomal protein S12 methylthiotransferase RimO, and RNA recognition motif domain. Lastly, the ploidy of Polyketide synthase is 2 for mut11. None of these genes exhibit differential expression.

Table 7.1: An overview of all mutations that fall within a gene. Shared mutations are listed first, whereas unique mutations follow. Columns that require further explanation are the REF/ALT columns that display the nucleotide substitutions. The columns mut4 and mut11 display which REF/ALT variant is present on the haplotypes of the genome where 0 represents the wildtype variant and 1/2 represent the alternative variants. An mRNA differential expression heatmap is displayed showing log2 fold changes. Lastly, a putative functional gene annotation is presented. Priority was given to BlastP matches and when no good matches were found InterPro homology domain annotation was used to infer a gene function.

gene ID	Genomic position	REF	ALT	effect	mut4	mut11	Ploidy mut4 / mut11	Differential expression 38°C Mut4 / mut11	Differential expression 42°C Mut4 / mut11	Putative functional annotation (BlastP / Interpro domain)
PicoBPE23_05040	contig_4A (850888)	A	G	synonymous	0/1	0/1	2			IPR011004 (Trimeric LpxA-like superfamily)
PicoBPE23_07467	contig_6A (275034)	C	T	intronic	0/1	0/1	2			-
PicoBPE23_08649	contig_6B (1138611)	C	A	Gly273Cys	0/1	0/1	2			IPR041667 (Cupin-like domain 8)
PicoBPE23_07264	contig_5B (1135004)	C	A	Pro17Thr	1/1	1/1	1			BlastP: Superoxide dismutase / PANTHER: IPR044624 (repeat protein Mbb1-like)
PicoBPE23_04067	contig_3B (126306)	C	T	Asp353Asn	0/1	0/1	2			IPR036279 (5'-3' exonuclease, C-terminal domain superfamily)
PicoBPE23_08830	contig_7A (268737)	G	A	Pro34Ser	0/1	0/1	2			IPR006634 (TRAM/LAG1/CLN8 homology domain)
PicoBPE23_00798	contig_1B1 (69387)	C	T	Gln193*	0/1	0/1	2			IPR040122 (Importin beta family)
PicoBPE23_11836	contig_9B (455009)	C	T	synonymous	0/1	0/1	2			IPR003439 (ABC transporter-like, ATP-binding domain)
PicoBPE23_13246	contig_11A (185704)	T	C	Met277Val	0/1	0/1	2			BlastP: RNA polymerase II C-terminal domain phosphatase-like
PicoBPE23_00222	contig_1A (498474)	GGT	G	frame shift	1/1	1/1	1			IPR036955 (AP2/ERF domain superfamily)
PicoBPE23_02273	contig_2A (1365932)	T	TG,TGG	intronic	1/2	0/1	2			IPR022384 (Formiminotransferase catalytic domain superfamily)
PicoBPE23_03888	contig_3A (994228)	CATAT	C,CAT	intronic	1/1	2/2	1			IPR001313 (Pumilio RNA-binding repeat)
PicoBPE23_09102	contig_7A (770005)	T	TCAA	intronic	0/1	0/1	2			IPR038071 (UROD/MetE-like superfamily)
PicoBPE23_10084	contig_8A (331679)	C	CAT,CATAT	intronic	1/2	1/2	1			IPR026854 (Vacuolar protein sorting-associated protein 13-like, N-terminal)
PicoBPE23_01916	contig_2A (766369)	C	T	Arg401Trp	0/1	0/0	2			IPR001012: UBX domain / IPR018997: PUB domain
PicoBPE23_07590	contig_6A (491187)	G	GTA	intronic	0/0	0/1	2			IPR005840: Ribosomal protein S12 methylthiotransferase RimO
PicoBPE23_04568	contig_3B (1111698)	G	C	Met393Ile	0/1	0/0	2			IPR027806: Harbinger transposase-derived nuclease domain
PicoBPE23_10884	contig_8B (697809)	C	CAT	intronic	0/1	0/0	2			IPR001680: WD40 repeat
PicoBPE23_00982	contig_1B1 (457245)	A	G	His257Arg	0/1	0/0	1/2			BlastP: Polyketide synthase
PicoBPE23_11307	contig_9A (463100)	GATA	G	intronic	0/0	0/1	1			IPR000504:RNA recognition motif domain

7

161

7.3.3. mRNA expression levels

Principal component analysis confirmed that the mRNA expression patterns of the two mutant strains are very similar to each other, both at 38 °C and 42 °C, but clearly distinct from the mRNA expression patterns of the wildtype strain (Supplementary material 7.6). GO-term enrichment was performed to investigate
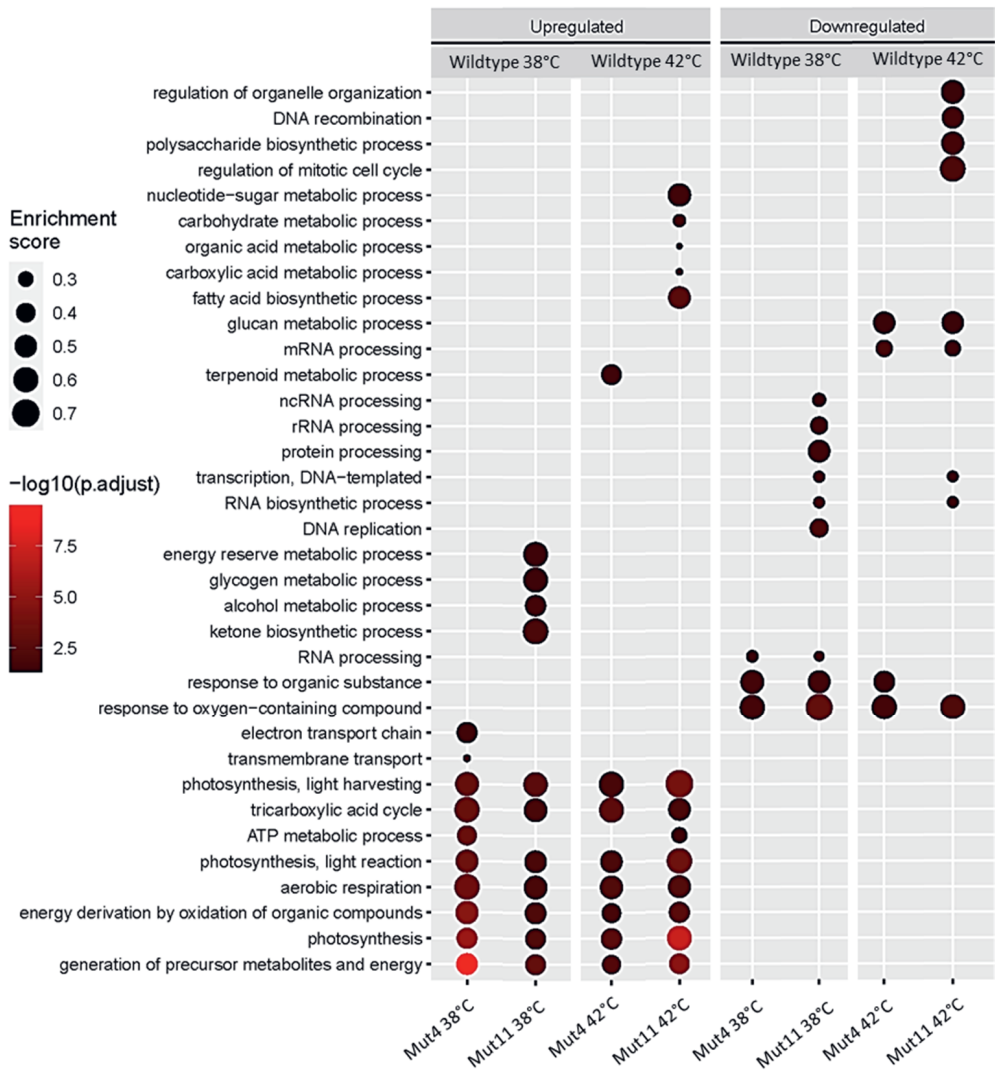
Figure 7.3: *Gene ontology enrichment analysis displaying up-, and downregulated biological processes with the wildtype strain as base expression, and the mutant strains as the variable. Double and irrelevant GO-terms were removed from the analysis. The dot size indicates the enrichment score of the GO-term whereas the color brightness indicates significance (-log10(FDR)).*

mRNA expression activity at a process scale (Figure 7.3). The mutant strains showed comparable transcription patterns, with minor differences. It must be noted that most GO-terms enriched in only one mutant strain have a *p*-value that is relatively close to the cut-off value.

Both wildtype and mutant strains suppressed processes associated to photosynthesis and the central metabolism in response to supra-optimal temperature. In addition, many RNA processing and protein processing processes were activated. Regardless of the expanded maximal growth temperature of the mutant strains, 42 °C is still a supra-optimal temperature for both the wildtype and the mutant strains by which reduced metabolic activity was expected. While photosynthesis and the metabolism were downregulated in both the wildtype and the mutant strains in response to increased temperature, the wildtype strain showed stronger downregulation.

Many biological processes associated to photosynthesis and energy metabolism were upregulated in the mutant strains compared to the wildtype, both at 38 °C and at 42 °C (Figure 7.3). The increased transcriptional activity of photosynthesis and the energy metabolism correspond to the observation that mutant cells grew faster with a higher yield on light. While not significantly upregulated as a pathway, several genes associated with nitrogen assimilation and amino-acid biosynthesis were upregulated in the mutant strains. On the other hand, the downregulation of response to oxygen-containing compounds in both mutant strains indicates a lower necessity for ROS deactivation mechanisms. Both mutant strains have downregulated mRNA processing activity. Moreover, mut11 displays downregulation of a wide variety of RNA processing associated biological processes. Among the downregulated RNA-associated biological processes was non-coding RNA, which is assumed to be involved in regulating gene activity in response to abiotic stress such as heat [187]. Moreover, mut11 shows downregulation of protein processing processes, associated to the proteasome complex, peptidase complex, and endopeptidase complex. The general perception is that protein degradation is necessary in the wildtype strain to break down damaged proteins as a result of heat stress [6, 186].

Interestingly, we did not observe significant overexpression in genes associated with a heat-shock response. In previous research, we exposed the wildtype strain of *Picochlorum sp. BPE23* to 5 days of 42 °C and monitored cell physiology whereby we observed a severe system-wide heat-shock response on a transcription, growth,

7

and cell composition level [150]. The absence of a heat-stress response in this study confirms that our approach to wait for steady state (19 days) before sampling was required to be able to compare growth of the mutant strain to the wildtype strains at an optimal and supra-optimal temperature without disturbance of a heat-shock response.

7.3.4. Adapted mechanisms underlying the physiology improvement

Both the copy number variations and the gene mutations can theoretically have caused the thermotolerant phenotype. As several hard selection events (i.e., temperature increases) were applied throughout the ALE trajectory, it is hypothesized that not one, but multiple consecutive adaptation events are responsible for the final improved phenotype. Increased selective pressure causes a wipe-out event after which part of the cell lines in the culture are eliminated [188]. Based on cell function, a selection of mutated genes is hypothesized to impact microalgal thermotolerance and growth in general. Microalgal species do not have the same annotation quality as industrialized model organisms such as *E. coli* and *S. cerevisiae*. Nonetheless, strong predictions on gene function can be made based on protein homology and protein domains.

7.3.4.1. Adaptation to temperature stress

The effect of heat on cells is system-wide but impacts some cellular components and processes more severely, whereby cells have evolved adaptation mechanisms [150]. The cell membranes are among these components as temperature affects membrane fluidity and therefore unbalance many biological processes. In response, cells remodel the cell membrane composition. Three gene mutations were associated with temperature tolerance specifically. We identified a SNP in PicoBPE23_07264 (ceramide synthase), inducing a Pro34Ser substitution. This gene encodes for the waxy sphingolipid ceramide. In *S. cerevisiae*, *de novo* synthesis of ceramide synthase was shown to be elevated after heat stress [189].

Due to heat-induced unbalancing in the photosynthetic machinery and the electron transport chain, ROS are formed causing oxidation of cellular components [6]. Photosynthetic organisms downregulate their photosystems to prevent this negative impact which naturally leads to reduced growth. Superoxide dismutase performs an important stress-relieving function by degrading reactive oxygen

species that form due to heat stress [190]. While the gene does not show differential expression changes, an increased enzymatic rate due to the Pro17Thr substitution might cause higher enzymatic activity. Also, PicoBPE23_13246, encoding for a putative RNA polymerase II C-terminal domain phosphatase-like 4, was found mutated. While intuitively one does not associate this enzyme to heat tolerance, several studies in *A. thaliana* mutator strains showcased its role in tolerance to ROS inducing abiotic stress factors such as heat through interaction with specific transcription factors and regulatory proteins [191].

7.3.4.2. Regulatory genes

Several mutations were identified in genes associated with mRNA transcription and regulation. The mRNA expression of PicoBPE23_03888, associated with mRNA stability regulation, was halved in the mutant strains indicating a lower requirement of the specific mRNA. The transcriptional activator PicoBPE_00222 was found to have undergone a frameshift mutation in both haplotype versions. A study in *A. thaliana* showed that mutagenesis of this gene caused temperature sensitivity [192]. Arguably, mutations in this gene could contribute to thermotolerance. Transcriptional activators and regulators are often found mutated in thermotolerant ALE derived mutant strains [134].

7.3.4.3. Photosynthesis, carbon fixation, and the energy metabolism

Transcriptome analysis revealed many upregulated biological processes associated with photosynthesis, carbon fixation, and energy metabolism in the mutant strains. These were upregulated both at 38 °C and 42 °C compared to the wildtype. While most differentially expressed genes had a log2 fold change below 2, a selection of genes was upregulated more severely. Both haplotype versions of RuBisCO, PicoBPE23_01132, and PicoBPE23_00347 were amongst the most upregulated transcripts with approximately 8 times higher expression. Transcript expression levels were equal for both genes while only the gene on contig 1B1 had undergone a copy number duplication, indicating that transcription was regulated based on the cellular demand for the enzyme. Comparable observations were made for other carbon fixation associated genes, and photosynthesis, glycolysis, and citric acid cycle associated genes.

7

Two genes putatively involved in photosynthesis were mutated: PicoBPE23_09102 and PicoBPE23_07264. The first gene contains a UROD domain which catalyzes a step in chlorophyll synthesis whereas the second gene is putatively involved in regulation of multiple photosystem II subunits, as shown by homology to *Chlamydomonas* [193]. However, both genes show even stronger sequence similarity to other genes, showcasing the difficulty of interpreting genetic data for non-model organisms. None of the gene mutations point exclusively at photosynthesis. While large-scale copy number variations do not directly lead to increased enzyme production due to product-regulated mRNA expression, such an event inevitably has a significant effect on cellular physiology. Ultimately, microalgae are capable of regulating energy uptake through antenna size alteration to suit the growth conditions and prevent metabolic imbalance [21, 117]. The observed upregulation of transcription photosynthesis, carbon fixation, and energy metabolism and the increased chlorophyll concentration at 42 °C could also result from pathways downstream or stress-relieving mechanisms that became more efficient under specific growth conditions, thereby allowing all energy uptake mechanisms to be upregulated by the cell.

7.3.4.4. Nitrogen metabolism and amino acid biosynthesis

We hypothesize that in addition to evolution to supra-optimal temperature, evolution took place towards growth in photobioreactor systems and to microalgal growth medium. The wildtype *Picochlorum sp. BPE23* was isolated from Bonairean waters and was not cultured extensively in the laboratory prior to ALE, by which we assume that the wildtype strain did not have mutations that benefit growth on microalgal growth medium. It is known that ALE reproducibly yields side-effect mutations that are beneficial for growth in bioreactors on a minimal medium [23]. In the case of *E. coli*, increased substrate utilization efficiency in adaptation to glucose is a recurring observation, amongst other mechanisms [151]. Light was the energy providing substrate for our photoautotrophic cultivations, whereas nitrate was added to provide nitrogen for *de novo* amino acid assimilation. Several mutations can be associated with nitrogen metabolism and amino acid biosynthesis and several genes associated with these pathways were severely overexpressed. Two mutated genes were involved in amino acid synthesis (PicoBPE23_09102 and PicoBPE23_02273). Moreover, three mutated genes were associated with the

transport of cellular compounds and proteins (PicoBPE23_00798, PicoBPE23_11836, and PicoBPE23_10084).

7.3.4.5. Confirmation of mutations

Recurring ALE mutations in microalgal strains are not yet known, but their identification becomes increasingly feasible due to the increasing number of ALE studies. Many recent ALE studies have applied genetic sequencing methods such as transcriptomics or genome resequencing to identify mutations [23]. However, these studies were performed with varying microalgal species and ALE targets. With this elaborate case study, we provide strong arguments for evolutionary mechanisms towards both temperature and growth in minimal medium. Looking forwards, more ALE studies with closely related species are required to elucidate recurring adaptation mechanisms to supra-optimal temperature and growth in photobioreactors.

To validate the hypothesized impact of the mutated genes on thermotolerance, they should be genetically engineered in the wildtype strain. Recently, genetic modification tools have been developed for a closely related strain, *Picochlorum renovo* [43]. A strong example of an efficient engineering approach to study the impact of ALE mutations on thermotolerance is demonstrated in *E. coli* by use of the MAGE technology [151]. After genetic engineering of *E. coli* with the mutations as identified after ALE, an enrichment under selective pressure was followed by resequencing of the cell culture to establish the presence of the mutated genes in the cell culture for their impact on fitness.

7.4. Conclusions

Adaptive laboratory evolution with supra-optimal temperature as a selective pressure was used to create thermotolerant strains of *Picochlorum sp. BPE23*. The mutant strains have an expanded maximal growth temperature of 44.6 °C, whereas the maximal growth temperature of the wildtype was 42 °C. The mutant strains have a superior maximal growth rate. Moreover, the mutant strains have an increased biomass yield on light at the optimal and maximal growth temperature. The mutant strains showed partial genome multiplication and 21 genic mutations. Based on protein homology, several mutations were associated with mechanisms

that could be responsible for increased growth or thermotolerance. Transcriptome analysis showed that photosynthesis and metabolic processes were upregulated in the mutant strains compared to the wildtype, while the heat-stress associated processes were downregulated. We hypothesize that evolution towards supra-optimal temperature occurred and was accompanied by evolution towards microalgal growth medium.

From an applied point of view, the improved mutant strains can replace the wildtype strain for biomass production. The biomass yield on light of mut11 increased from 0.74 $g_x.mol_{ph}^{-1}$ to 0.91 $g_x.mol_{ph}^{-1}$ at 38 °C, which directly improves biomass productivity. The broader temperature optimum of the mutant strains stimulates productivity levels over a wider temperature range, whereby less strict photobioreactor process control is required. Moreover, the maximal specific growth rate of mut11 increased from 3.35 ± 0.15 d^{-1} to 5.71 ± 0.14 d^{-1}, allowing for faster upscaling of cell cultures in addition to faster strain improvement trajectories.

With this study, a strong platform was created to enhance the development of *Picochlorum sp. BPE23*. A phased genome was assembled to enable future projects using targeted genetic strain modification and fundamental genetic research. This specific study on ALE and thermotolerance is the first example of a study using the created platform. It is also the first example of extensive genetic characterization of microalgal ALE mutant to identify evolutionary mechanisms.

Data availability

Wildtype and mutant strains of *Picochlorum sp. BPE23* are stored in liquid nitrogen and are available upon reasonable request. Moreover, genomic and transcriptomic sequencing datasets will become publicly available upon publication of the manuscript.

A web portal (https://www.bioinformatics.nl/picochlorum_bpe23), including a genome browser will become available upon publication of the manuscript for scientists to use in their research. Included items are the genomes of the wildtype, mut4, and mut11. Moreover, all mRNA sequencing data and the identified mutations are included.

7.5. Supplementary materials

7.5.1. Supplementary material 7.1
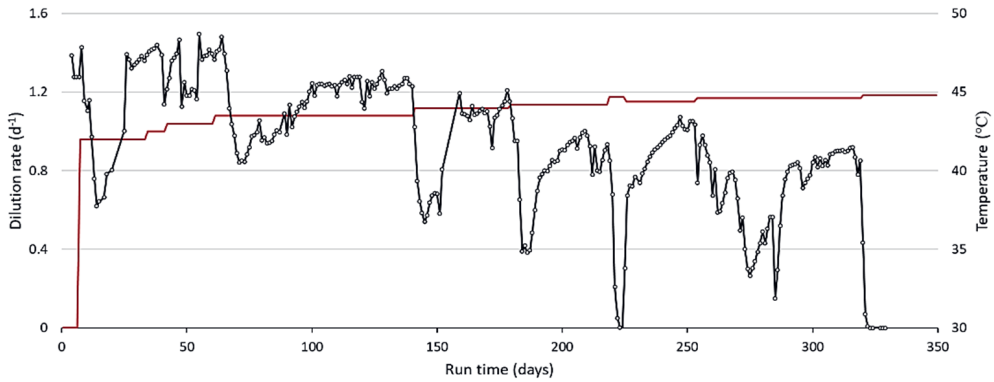
Supplementary figure 7.1: *Photobioreactor dilution rate and temperature during the adaptive laboratory evolution process. Temperature was increased step-wise, inducing fitness decreased to the microalgal cell culture.*

7.5.2. Supplementary material 7.2
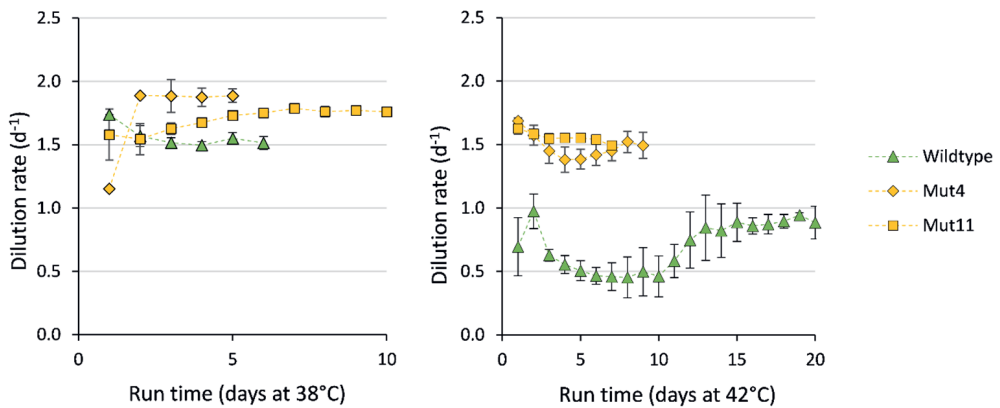
Supplementary figure 7.2: *The photobioreactor dilution rate during characterization of the wildtype, mut4, and mut11. The wildtype strain required more time to acclimate to 42 °C*

7.5.3. Supplementary material 7.3

Polar fatty acids

Polar fatty acids make up the cell membranes and thylakoid membranes. In previous research the cell membrane composition was found to be altered as a consequence of temperature stress [150]. In this study the wildtype strain contained a significantly larger amount of polar fatty acids than the mutant strains at 38 °C with a concentration of 90.4±1.84 $mg_{lipid}.g_x^{-1}$, compared to 65.2±3.13 $mg_{lipid}.g_x^{-1}$ and 67.0±1.21 $mg_{lipid}.g_x^{-1}$ for mut4 and mut11, respectively (Supplementary figure 7.3). At 42 °C the difference became smaller with values of 77.5±3.10, 76.5±0.78, and 69.83±2.85 $mg_{lipid}.g_x^{-1}$, respectively. Especially the polyunsaturated fatty acid C18:3 was present at lower concentrations in the mutant strains at both 38 °C and 42 °C. Reduction of unsaturated fatty acids such as C18:3 is done to decrease the membrane fluidity to counteract the impact of an increased temperature.
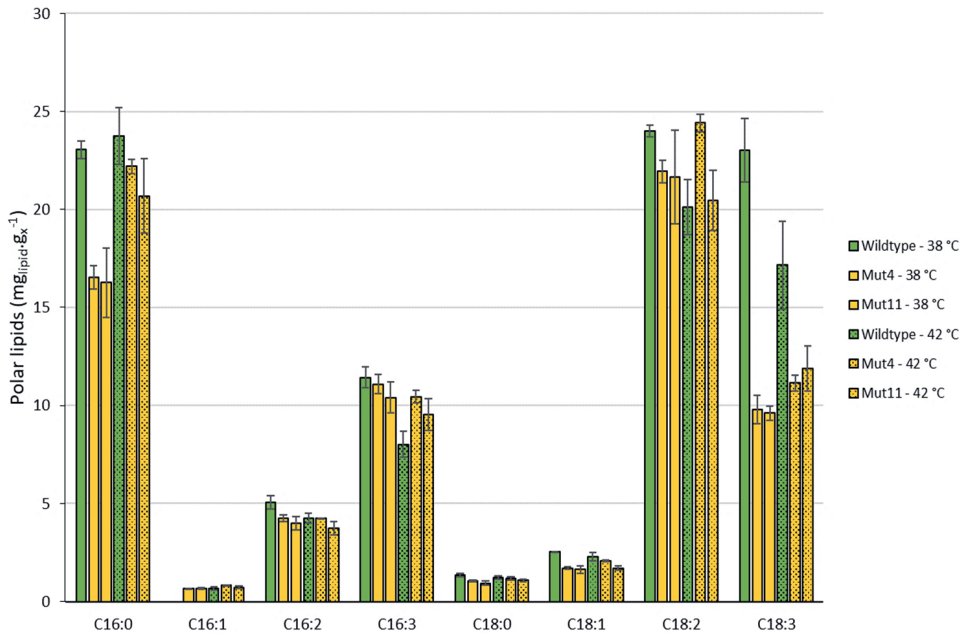
Supplementary figure 7.3: *the concentration of polar fatty acids in the wildtype and mutant cell lines at 38 °C and 42 °C.*

Neutral lipid content

Microalgae store excess energy as neutral lipids in lipid bodies. *Picochlorum sp. BPE23* maintained a very small pool of such lipid bodies under non-stressed growth conditions. The lipid pool fully consists of C16:2 when grown at 38 °C. When the temperature was increased to 42 °C the wildtype strain accumulated 0.8 wt% lipids. Previous research has shown that *Picochlorum sp. BPE23* funnels excessive energy towards fatty acid production under temperature stress to prevent formation of harmful reactive oxygen species (Chapter 7.5). Both mutant strains didn't accumulate lipids at 42 °C which indicates that there was no cellular stress.

7.5.4. Supplementary material 7.4

Pigment content plays a large role in the photosynthetic capacity. *Picochlorum sp. BPE23* utilizes both chlorophyll-a and chlorophyll-b in its photosystems. In addition to chlorophylls, photosystems contain carotenoids. Carotenoids not only fulfill a function in light harvesting but also in protection from cellular damage through quenching of excess energy, filtering of light, and scavenging of reactive oxygen species. Mut4 and mut11 showed an increased chlorophyll-a and chlorophyll-b concentration at 42 °C (Supplementary figure 7.4). The other pigments show stable concentrations.
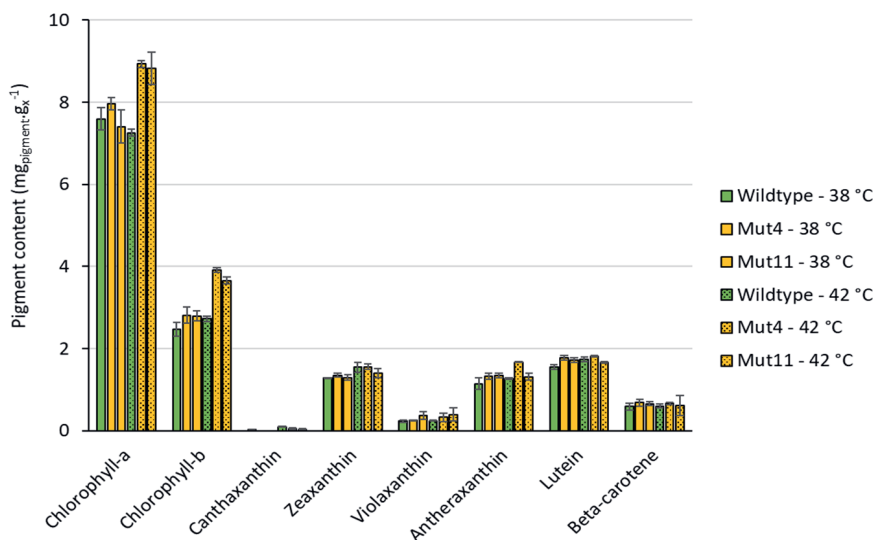
Supplementary figure 7.4: *the concentration of pigments in the wildtype and mutant cell lines at 38 °C and 42 °C.*

7.5.5. Supplementary material 7.5

The genomes of four mutant strains and the wildtype strain were sequenced by Illumina PE150 sequencing. The reads were then mapped to the phased diploid reference genome that was created through HiFi sequencing. The sequencing mapping coverage was calculated for each contig and displayed as a heatmap in Supplementary figure 7.5. The mitochondrial and plastid DNA were removed from the heatmap. Interestingly, the sequencing coverage for some of the contigs is exactly double as for others in the mutant strains, whereas the sequencing coverage of the contigs in the wildtype strain falls in a comparable range for each contig. Contigs 6, 8, and 10 had both copies doubled, whereas contig 1, 2, 3, 4, 5, 7, 9, and 11 had one of the contigs doubled. This is consistent with the findings of the HiFi sequencing (Figure 7.2). Interestingly, the same pattern was observed for each of the mutants. Only mutant 8 shows a different pattern with a very low coverage for contig 2B and a very high coverage for contig 2A.
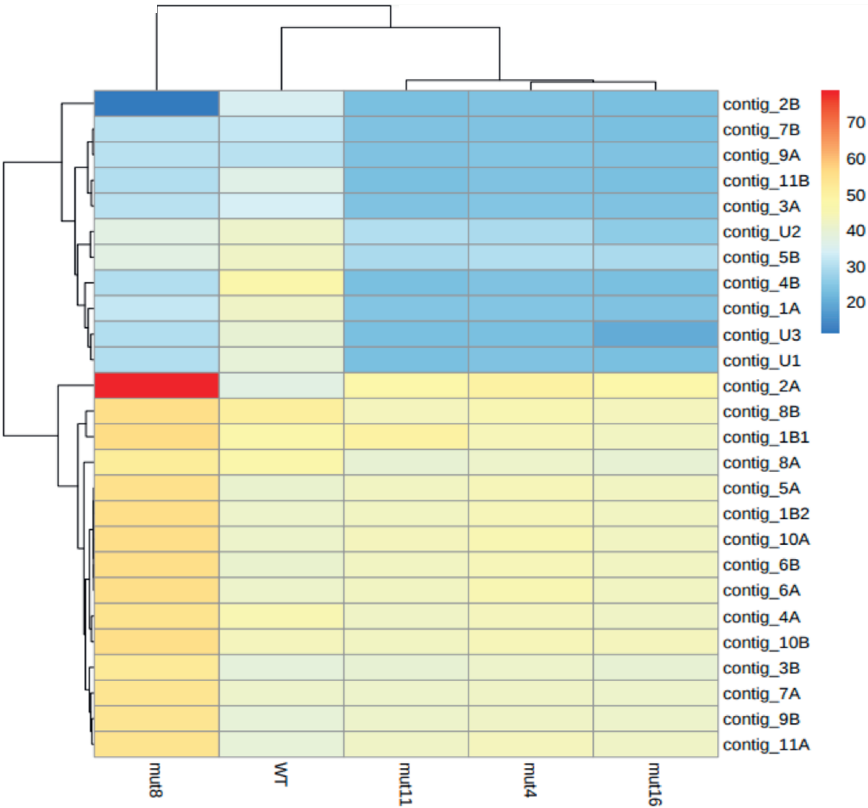
Supplementary figure 7.5: *Coverage of genome sequencing reads for the wildtype, mut4, mut8, mut11, and mut16. Sequencing was done through Illumina PE150*

7.5.6. Supplementary material 6

A principal component analysis was performed using the mRNA sequencing data for quality control and to compare major mRNA expression patterns (Supplementary figure 7.6). All samples clustered together as expected. In addition, mut4 and mut11 cluster together as well indicating comparable mRNA expression patterns. The wildtype samples are different from the mutant strains at both 38 °C and at 42 °C. Two samples were taken at 42 °C as the steady-state situation was not reached before day 19. Interestingly, the sample taken at day 9 for the wildtype is further away from the unstressed situation of 38 °C than the taken at day 19. This indicates that the mRNA expression levels were normalizing and that the hypothesized heat-shock response faded [150]. The direction of the samples in the PCA analysis in response to the temperature increase is similar for both the wildtype and the mutants, namely to the top right corner.
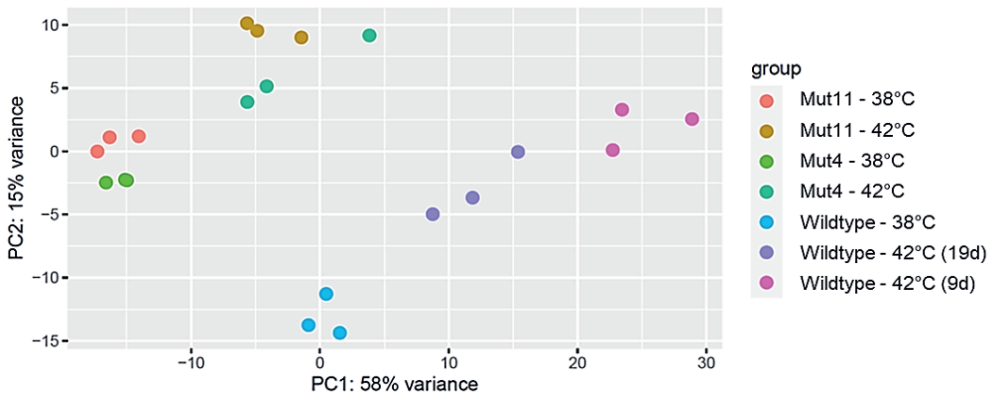
Supplementary figure 7.6: *PCA bi-plot of the sequenced mRNA samples collected from steady-state cultures at 38 °C and 42 °C. Both mut4 and mut11 were sampled in a steady-state situation. The wildtype strain was sampled twice at 42 °C, at day 9 and day 19 after the increase in temperature. The first two PCs are displayed.*

7

Chapter 8

General discussion - Robust microalgae for industrial production

8.1. Production of microalgal biomass for bulk products has potential but is currently too expensive

Microalgae have been considered a promising source for sustainable food, feed, biofuel, and specialty chemicals for decades [1, 194]. The biomass of microalgae consists mainly of protein, fatty acids, and carbohydrates. A significant advantage that microalgae have over traditional agricultural crops is their high yield on light which allows for efficient land usage [3]. In addition, microalgal biomass can be produced on non-arable land using saline water which can increase the worldwide production of food while simultaneously reducing pressure on freshwater and arable land.

Microalgae are currently commercially produced for high-value markets. Examples of such high-value microalgal products are food additives, cosmetics, health-care products, and feed for aquaculture hatcheries [194]. The bulk market is significantly larger than the specialty market and offers enormous opportunities for microalgal biomass [1, 149]. However, the commercialization of microalgal biomass for application as a bulk product such as food, feed, biofuels, biofertilizers, and chemicals has not happened yet despite significant efforts in the field. It is challenging to compete with traditional production processes on the bulk product market as such traditional processes have already been optimized significantly for cost-efficiency and new technologies such as microalgae production still need such a leap in efficiency.

The production costs of microalgal biomass should reduce significantly before successful commercialization in bulk product markets can become a reality [195]. Production costs for microalgal biomass are currently projected at 3.1 euros.kg^{-1} at commercial scale (i.e., 100 hectare scale, Turkey) [4]. The cost price is highly dependent on the chosen production location, the chosen production system and scale, and the chosen production strain [196]. Future projections indicate that the cost-price can move towards 0.5-0.7 euros.kg^{-1} in the coming years, assuming that significant process improvements will be achieved [1, 4, 149].

Photobioreactor cooling to maintain an ideal cultivation temperature currently presents a significant cost factor [4]. One of the causes for this is that microalgal strains are often selected without considering process conditions at commercial scale. In this thesis and general discussion, we plead the importance of robustness in microalgal strains to reduce production costs. Thermotolerance was the selected

robustness characteristic and focus parameter throughout this thesis. However, other factors that impact microalgal growth shouldn't be overlooked. A workflow is proposed for the rapid development of a microalgal production platform at low operational costs. Bioprospecting and adaptive laboratory evolution (ALE) are presented and discussed as effective tools to obtain robust microalgal strains. Summarizing, we present our perspective on an essential, but often overlooked aspect in microalgal biotechnology: productivity losses during microalgal cultivation due to non-optimal environmental growth conditions.

8.2. Production conditions lead to robust strains to mitigate productivity losses

8.2.1. Disturbed growth conditions cause reduced productivity

Each techno-economic study indicates photosynthetic efficiency (PE) as being the most sensitive parameter for cost price reduction of microalgal biomass [4, 149]. The maximal photosynthetic efficiency of solar energy to biomass was calculated to be 8-10% [3, 197]. Such high photosynthetic efficiencies are never observed in practice due to in-culture cell shading and metabolic maintenance. Few of the best-case scenario microalgal studies at lab scale under optimal growth conditions report a PE up to ~6%, but commonly lower PE values are reported [198]. Unfortunately, ideal growth conditions are near-impossible to achieve in an industrial production setting as weather conditions severely affect the photosynthetic efficiency of microalgal production. Microalgal growth decreases rapidly under non-ideal growth conditions [6, 199]. These environmental growth disturbances are the primary cause of the photosynthetic efficiency gap between laboratory cultivation and commercial-scale production [4, 196]. At commercial-scale, solar photosynthetic efficiencies of 2% were reached with *Chlorella* and *Dunaliella salina*, whereas an average solar photosynthetic efficiency of 2.4% was achieved in pilot-scale studies with *Nannochloropsis* [3, 62]. As observed by de Vree and co-workers, the photosynthetic efficiency fluctuates significantly between consecutive cultivation days, with maximal photosynthetic efficiencies of up to 4.2% [62].

The process parameters pH, CO_2, O_2, salinity, and temperature are relatively straightforward to control. While easy to control, the involved operational costs

8

vary depending on the parameter and location of the cultivation system. Especially temperature can become a significant cost factor due to exposure to high irradiance levels [4, 200]. Microalgal cultivation is best done in regions with high irradiance levels as higher areal productivities can be achieved. However, excessive light triggers a stress response in microalgae, ultimately leading to decreased productivity [4]. Vertical tubular photobioreactors and flat-panel photobioreactors lead to light dilution and decreased peak irradiance levels which thereby prevent photosynthetically induced stress [62]. Regions that exhibit high light levels commonly also exhibit high air temperatures. The combination of high light levels with high ambient temperatures causes photobioreactor systems to heat up to 50°C, whereas most microalgal species have a temperature optimum between 20°C to 30°C [6, 7]. Temperature control of photobioreactors is simple to perform but can become very costly. For example, on Bonaire, temperature control would constitute more than 25% of the costs for microalgal biomass production [4, 117, 196]. Therefore, temperature control presents a feasible target for cost reduction.

8.2.2. Robust microalgal strains can minimize the negative effect of disturbed growth conditions

Most of the microalgae species currently being cultivated at a commercial scale were selected for the product they make in combination with the ease of cultivation under controlled conditions. Species that are commercially cultivated at a commercial scale are *Spirulina* (cyanobacterium), *Chlorella, Dunaliella*, *Aphanizomenon flos-aquae* (cyanobacterium), *Haematococcus*, *Nannochloropsis*, and *Euglena* [201, 202]. Additional species that are currently under investigation for commercial production, or that are cultured at a smaller scale for niche applications are *Tetraselmis, Picochlorum*, *Phaeodactylum*, and *Tisochrisis lutea* [200]. *Chlamydomonas* is a particular case as it is the most studied species in algal biology and biotechnology and serves as a model organism and the production of niche products. However, it is not ideal for phototrophic cultivation at a commercial scale due to tight process control requirements. All the aforementioned species can grow in either photobioreactor or open pond systems when controlled strictly. Nevertheless, some species possess robustness characteristics that simplify cultivation, and thereby reduce the production cost-price. For example, species of *Spirulina* show a tolerance to high temperature and extreme pH levels which is beneficial for contamination control [202]. *Dunaliella* can withstand high salinity

levels, and *Chlorella* can withstand high light and temperature levels [200]. No strain exhibits robustness to all environmental stressors. However, several species of *Picochlorum* have recently gained increased attention for their robustness to multiple stressors: high light, temperature, and salinity levels [7, 21, 43]. Additionally, strains of *Picochlorum* display exceptional growth rates of up to 8 d^{-1} which is a serious advantage for strain improvement and scale-up trajectories. [21, 157].

Environmental conditions vary per region and season. Therefore, one strain might be ideal in one region or season but inefficient in another. To overcome seasonal variety, alternating between specialized summer and winter strains was proposed to maintain high productivity levels year-round. Irradiance and temperature levels also fluctuate heavily within a day and between days. A broad tolerance to a fluctuating environment and potential stressors is indispensable to reach a high level of culture stability, thereby reducing costs for process control. In addition, rapid acclimation to changing conditions is especially useful to mitigate the negative impact of day-to-day fluctuations.

Over the past decades, significant progress has been made on the improvement of photobioreactor types and optimization of growth protocols for microalgal cultivation. However, the field of microalgal biotechnology is still in its infancy compared to more developed fields such as traditional agriculture and industrial biotechnology. Microalgal biotechnology has entered an era in which selection of the ideal species followed by strain improvement is becoming increasingly important to optimize the production process further. This strain selection and improvement should be performed to conform to regional and seasonal growth conditions.

8

8.3. Strain selection and improvement

8.3.1. A methodology workflow for strain selection and improvement

Continuous strain development on robustness, photosynthetic efficiency, and product content is crucial for developing a successful microalgal platform technology [199]. Generating functional platform technology to suit specific cultivation conditions is already common for white/red biotechnology organisms such as *Escherichia coli*, *Saccharomyces cerevisiae*, and Chinese hamster ovary cells [203-205]. Strain optimization is a continuous process that should be repeated for multiple traits [195]. An overall workflow for strain selection and improvement is presented in Figure 8.1. This workflow was based on the circular principle of design, build, test, and learn, which translated to microalgal strain improvement becomes: experimental design, strain modification, strain characterization and selection, and strain evaluation [206]. Targets for strain improvement include biological growth parameters, stress tolerance, and biomass composition. Note that for each strain characteristics a specific approach is required. Steps in the workflow can be by-passed to suit individual strain improvement challenges. The success of the proposed methods heavily relies on strong selection of strains under relevant culture conditions. Specific details on strain improvement methods are elaborated in the following paragraphs. In addition, best practices and potential pitfalls are discussed.
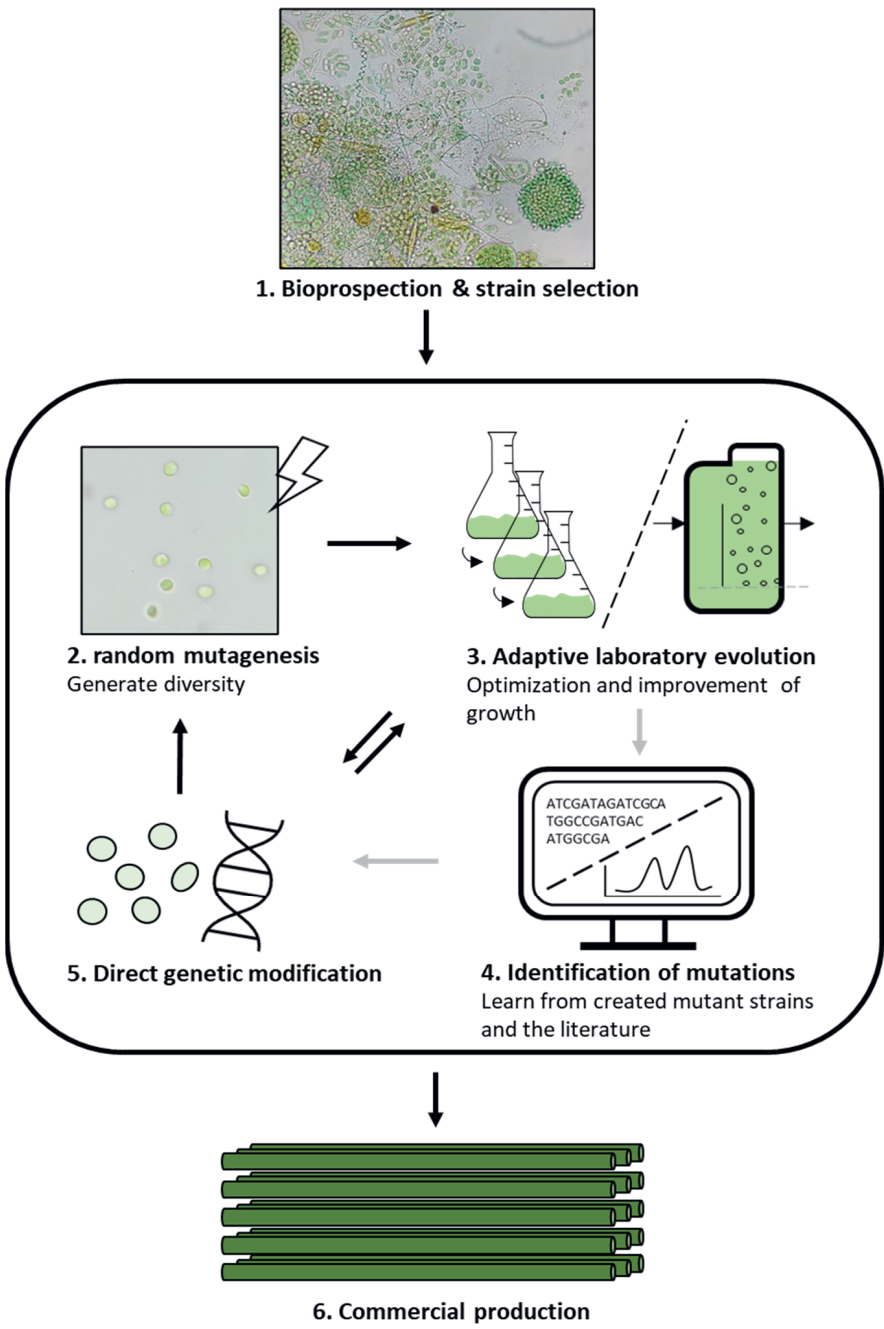
Figure 8.1: *Proposed workflow for the improvement of microalgal strains. The strain improvement workflow is displayed as a circular process to cover multiple strain characteristics in sequence. Each strain optimization step is performed through the following steps: strain modification, strain characterization and selection, and strain evaluation.*

8.3.2. Bioprospection as a method to obtain robust strains

The selection of suitable species for specific cultivation conditions is an important step that is often overlooked [7, 196, 207]. Commonly, already established organisms are chosen for strain improvement trajectories with little regard for efficient industrial production in a specific region. Obtained strains consecutively perform as desired at lab scale under ideal growth conditions but do not perform well at commercial scale due to the inability to cope with adverse climatologic conditions. Spending significant efforts on strain selection before moving onto strain improvement is a worthwhile investment as a suitable strain will prevent time spent on strain improvement and process optimization at a later stage [7, 208].

Bioprospection of new microalgal strains from nature is not new but has become increasingly relevant over the past years due to the emergence of new high throughput screening and selection technologies and due to new insights on the relevant characteristics for microalgal strains [16, 208]. Most bioprospection studies involve screening for valuable target compounds, such as fatty acids and pigments, with little regard for growth characteristics at a commercial scale. However, recently multiple bioprospection studies took place to find robust strains [7, 43, 59, 208]. It is essential to consider the location to be bioprospected. Locations with high temperatures commonly yield species tolerant to such climatologic conditions. A similar approach can be used for strains tolerant to low temperatures [209]. Furthermore, robustness to specific pH, salinity, and irradiance conditions can be looked for [21, 210]. Also, for specific applications such as the capacity of biofilm formation granule formation, and wastewater remediation, a targeted bioprospecting approach can boost chances for finding species with desired characteristics [207].

Best practice involves a screening and selection procedure in which both target product and commercial growth conditions are considered at an early stage. Following, an enrichment phase for the bioprospected samples where specific selective growth conditions are applied will ensure that only strains capable of fast growth under these conditions will remain. After the enrichment procedure, a selection based on biomass composition can be performed. In this thesis a selection of microalgal species was performed with growth at temperatures up to 45 °C as a requirement [7]. The introduction of high temperatures during the enrichment phase ensured that a wide variety of thermotolerant microalgae and cyanobacteria

were isolated. In the literature, examples are available where strains were selected based on tolerance to other environmental stressors such as high light levels, high salinity levels, and high tolerance to specific toxic compounds [207]. Ideally, the exact growth conditions of the commercial scale photobioreactor should be mimicked, combining all stress conditions into one enrichment study. By doing so, strain selection is performed for application in specific growth conditions.

8.3.3. Adaptive laboratory evolution to improve complex traits such as growth rate and robustness

Random methods for strain improvement such as ALE and random mutagenesis have been successfully applied in a wide variety of microalgal strain improvement projects, ranging from increased product yields, increased tolerance to stressors, improved substrate utilization, growth rate optimization, and improved photosynthetic efficiency [23, 30, 211]. Growth kinetics and robustness are complex traits that often involve multiple pathways [195]. Due to the complexity of these traits, direct genetic modification is still difficult in microalgae. A significant advantage to ALE over direct genetic modification is that no detailed knowledge on the metabolism or genome is necessary, which allows for the development of relatively unstudied species and traits. An additional practical advantage is that strains that are improved through ALE are not considered GMO and are therefore easier to cultivate and commercialize due to simpler legislation.

ALE experiments commonly last for hundreds of generations during which mutations accumulate and the species evolves an improved phenotype [30, 212]. Practically, cell cultures are maintained under selective pressure and continuous dilution. Examples are serially diluted Erlenmeyer cultures and bioreactor systems operated in chemostat or turbidostat [213, 214]. For Erlenmeyer cultures, it is simpler to operate parallel cultures than for bioreactor systems. Parallel cultures are an advantage for comparable genomics studies in which identification of mutational mechanisms is the key goal [151]. The emergence of multiple mutations in a single gene in parallel cultures is strong evidence that the mutation is responsible for phenotypic adaptation to the applied stress factor. A disadvantage of Erlenmeyer cultures is the continuously changing substrate concentration and cell density. Changing growth conditions are especially relevant for photoautotrophic microalgal cultivation, as dense cell cultures create in-culture cell shading, reducing the growth rate, and slowing down the emergence of mutant

8

strains. This issue is less relevant for heterotrophic cultivation. Bioreactors enable more stable, and complex growth conditions as these systems can be continuously diluted [30]. Chemostat bioreactor operation (i.e., with a constant dilution rate) presents the risk of culture-wash-out or in-culture cell shading when a non-ideal dilution rate is chosen. However, chemostat operation is not ideal for ALE experiments as the culture growth rate increases with new generations due to adaptation and decreases with increased temperature. It is better to operate bioreactors in turbidostat mode (i.e., cell density-based dilution rate) as this operation mode offers all advantages of chemostat mode, without the risk of culture wash-out [214].

All ALE studies have in common that the most significant improvement in physiology is gained within hundreds of generations, after which the rate of adaptation decreases exponentially, as shown in a study on *E.coli* for which 20000 generations of ALE were performed (Figure 8.2A)[28, 213]. Mutations continue to accumulate in time but consecutive mutations will have a reduced impact due to network complexity [30]. In addition, evolution under constant selection pressure for too many generations will yield specialist phenotypes due to the trade-off effect, which is the opposite of the desired broad tolerance [181]. Phenotypes obtained through ALE are considered to be stable as they provide a fitness advantage [215]. While ALE is effective, there are boundaries to the improvement that can be reached within a few hundred generations. Reliable ALE studies in yeast, diatoms, and cyanobacteria, with temperature as focus parameter have
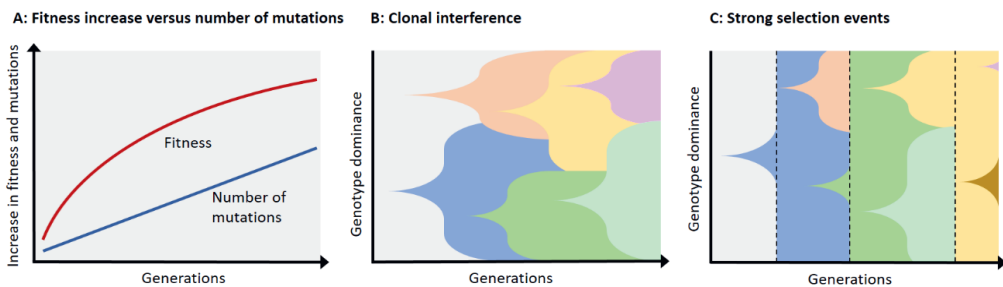
Figure 8.2*: (A) Culture fitness level and number of mutations are displayed as a function of the number of generations during an ALE experiment. The gain in fitness declines for consecutive mutations. (B/C): The strain dominance of a microalgal culture during an ALE experiment is displayed. In Figure 8.2B, a scenario is displayed where the strongest clones become dominant in a survival of the fittest scenario (i.e., clonal interference). In Figure 8.2C strong selection events provide opportunities for mutant strains to become dominant immediately as non-mutated strains are irradicated (Figure was adapted from Dragosits & Mattanovich, 2013, and Barrick & Lenski, 2013).*

repeatedly shifted the maximal growth temperature by 2 °C to 3 °C [134-136]. Comparable results were obtained in our own research (Chapter 7)[214]. Each strain characteristic has a specific plasticity that can be rapidly achieved through ALE, but is difficult to surpass [23].

The ALE process can be kickstarted by initially creating a heterogeneous mutant library through random mutagenesis before initiating ALE experiments [206]. Genetic evolution proceeds at a strain-specific mutation rate, which for microalgae is reported to be in the range of $3.23 \cdot 10^{-10}$ to $10.12 \cdot 10^{-10}$ nucleotides per generation [26, 138]. Such mutation rates correspond to 0.0062-0.0362 mutations per genome per generation for the corresponding species. Stringent selective pressure is mandatory to ensure the emergence of evolved strains within a reasonable number of generations [23]. A faster emergence of improved strains can be stimulated by providing more opportunities for mutant strains to arise. Examples of such selective occurrences are wipe-out events that eradicate non-evolved cell lines (Figure 8.2C)[188]. An alternative approach is to provide a gradient of the stressor to which mutant strains can migrate. Species of *E.coli* have been studied on such gradients with antibiotic resistance as a case study. It was found that tolerance evolved significantly faster and was gained through similar mechanisms (i.e., similar genotypes and phenotypes were found) [216]. However, on average, mutant strains obtained by such gradients displayed lower growth rates than mutants selected through slower, mixed culture selection. Combining ALE with a concurrent selection procedure involving a gradient could significantly increase the evolutionary rate while maintaining a high growth rate. As gradients are complicated to achieve within a liquid medium, an alternative approach would be to operate a separate cultivation system at a higher temperature (i.e., lethal temperature) to which culture from the ALE culture is added periodically until growth is observed, after which the process is repeated. To build upon the turbidostat approach, which was used in this thesis, the outflow of the photobioreactor could be used as the inflow of the additional photobioreactor which is operated at the higher temperature.

8

By analyzing ALE mutant strains, new mechanisms behind the improved phenotypes can be elucidated. A study on evolved *Saccharomyces cerevisiae* clones revealed that an altered sterol composition in the cell membranes rendered cells thermotolerant [134]. Also transcriptional activators and regulators are often found mutated after ALE [134, 191, 192]. In the ALE trajectory on *Picochlorum sp. BPE23*

we found several mutations in such transcriptional regulators (Chapter 7). As supra-optimal temperature induces a severe stress response with consecutive formation of ROS, scavenging enzymes such as superoxide dismutase are very important to prevent excessive cellular damage [190]. Moreover, interesting observations in chapter 7 were the improved growth rate and biomass yield on light of the mutant strains. Photosynthesis and the energy metabolism were upregulated in the mutant strains as expected based on the increased growth. In addition to adaptation to supra-optimal temperature we hypothesized that adaptation to photobioreactor growth conditions took place. Domestication of microalgae is a logical consequence when considering the fact that microalgal cells have completely different growth conditions in nature compared to photobioreactors. Processes such as nitrogen assimilation and amino acid biosynthesis have never evolved to a situation with unlimited nutrient availability. Domestication of microalgal strains through evolution and selection procedures offers considerable opportunities for strain improvement.

Elucidating mechanisms behind improved phenotypes in ALE clones involves long strain characterization trajectories. The discovery of genetic alterations depends heavily on modern bioinformatics technology, which has rapidly developed over the last years. A multi-disciplinary approach involving a combination of genomics, transcriptomics, proteomics, metabolomics, and compositional analysis is often required to fully unravel these mechanisms [215, 217]. The complexity and required investments are the most important cause that most ALE studies end after obtaining mutants with an improved phenotype without further characterization of the mechanism behind the improved phenotype. However, the characterization of such mechanisms has great potential as these could be used to directly engineer industrially relevant organisms through targeted genetic modification.

8.3.4. Targeted genetic engineering

After a robust microalgal strain with the desired growth characteristics is obtained, targeted genetic engineering strategies can be applied for further strain improvement, specifically with regard to product yield [218]. The number of microalgal species with a sequenced genome has increased significantly over the past years, enabling metabolic strain engineering approaches [219]. While strain engineering through direct genetic modification has been done in a wide variety of industrial organisms, the emergence of strain engineering tools for microalgae has only recently gained momentum [220, 221]. Knowledge on microalgal genetics and microalgal metabolism, as well as the availability of genetic tools are growing rapidly [222]. Typical targets for genetic engineering projects are lipid and fatty acid production, production of specialized biomolecules, and increased photosynthetic efficiency through manipulation of the carbon fixation and photosynthesis systems [3, 220, 221, 223, 224].

Strain engineering projects often yield positive results concerning the improvement of the target trait but modified strains often end up with reduced growth capacity or increased sensitivity to stressors due to trade-off effects [217, 225]. A targeted increase of storage compounds such as lipids naturally induces decreased growth as a larger part the intracellular energy pool is allocated to the target product instead of biomass formation. Exemplary, ALE was used to resolve the impaired state of an E.coli strain for which aromatic amino acid production was upregulated which resulted in an energy depleted metabolism and reduced growth [225]. Mutations in the glucose uptake mechanism were found after ALE which resulted in a rebalanced metabolism and consecutively, a phenotype with high aromatic amino acid production in combination with good growth capacity. The combination of targeted genetic approaches with ALE exploits the strengths of both methods while weaknesses are minimized. Re-optimization of the metabolism of impaired strains through ALE is already performed on occasion in white biotechnology and should be adopted by the microalgal biotechnologists as well [217, 226].

8

8.3.5. Strain characterization and selection

Tools for screening mutant strains are an indispensable aspect of strain improvement trajectories. After a strain improvement step such as random mutagenesis, ALE, or direct genetic modification, monoclonal cell cultures must be isolated and characterized. To obtain robust strains, culture conditions as found in commercial cultivation systems should be simulated during the screening and characterization procedure. Continuous attention to commercial culture conditions will prevent the selection of organisms that only perform under ideal growth conditions. Occasionally, follow-up studies at lab-scale and pilot-scale should be performed to verify screening results.

Modern, High throughput screening techniques such as FACS were shown to be efficient in selecting mutants with increased concentrations of target products such as lipids or pigments [227-229]. Characterizing growth is more troublesome as long and more laborious experiments are required. While the growth of heterotrophic organisms is downscaled and characterized relatively easily, characterizing the growth of phototrophic organisms is more challenging as growth is strongly dependent on light conditions supplied to each cell culture. Moreover, there is a lack of high-throughput phototrophic cultivation equipment. Most small-scale growth characterization studies, including our own research in chapter 2, chapter 6 and chapter 7, are performed using erlenmeyer flask cultures grown in incubators [7, 214]. Whereas such characterization experiments are acceptable, the light conditions in incubator systems are never uniform. In addition, the throughput of such studies is limited and the labour involved is significant [230]. Few semi-automated screening systems have been developed for less laborious and more reproducible screening [229, 231]. Upcoming technology that offers significant potential for initial strain screening and characterization studies are microfluidic culture chambers [230].

8.4. Future perspectives

Microalgae offer great potential as a sustainable lipid, protein, and carbohydrate source. However, commercial production of microalgal biomass for bulk products is still not feasible due to high operational costs. Nonetheless, techno-economic model data indicates that such production can become feasible when current challenges in microalgal biotechnology are resolved.

Fluctuating growth conditions caused by climatologic conditions result in decreased photosynthetic efficiencies. Robust microalgal strains tolerant to such conditions should be applied as an alternative to the currently used strains, which require high levels of expensive process control. Each production location offers different climatologic conditions and therefore requirements for the growth characteristics of microalgal strains vary. Multiple tailor-made microalgae platforms should be developed for growth at various production locations. Such microalgal platforms can then be customized through metabolic engineering to produce specific compounds.

Bioprospecting offers considerable potential for discovering new species with superior physiology, namely high growth in industrial cultivation systems. In addition, ALE and direct genetic modification are powerful tools for strain improvement. Combining these tools with modern high throughput screening equipment enables efficient characterization and selection procedures in which both growth characteristics and product content can be optimized concurrently.

In this thesis, the improvement of temperature tolerance was addressed to reduce cooling costs in microalgal production. A fast-growing thermotolerant marine microalgae, *Picochlorum sp. BPE23,* was isolated from Bonaire and improved through ALE to have a broader optimal growth temperature and a higher maximal growth temperature. However, improvement of temperature tolerance is only a start in creating a robust microalgal platform. Further improvements to other robustness and product formation characteristics should be induced to continue the development of *Picochlorum sp. BPE23* into a robust platform to produce bulk products.

Time has come to make a focused effort to build robust microalgal production platforms that can maintain high productivities despite climatologic disturbances. This should be done by combining knowledge on bottlenecks for outdoor production with modern strain improvement and selection methods.

8
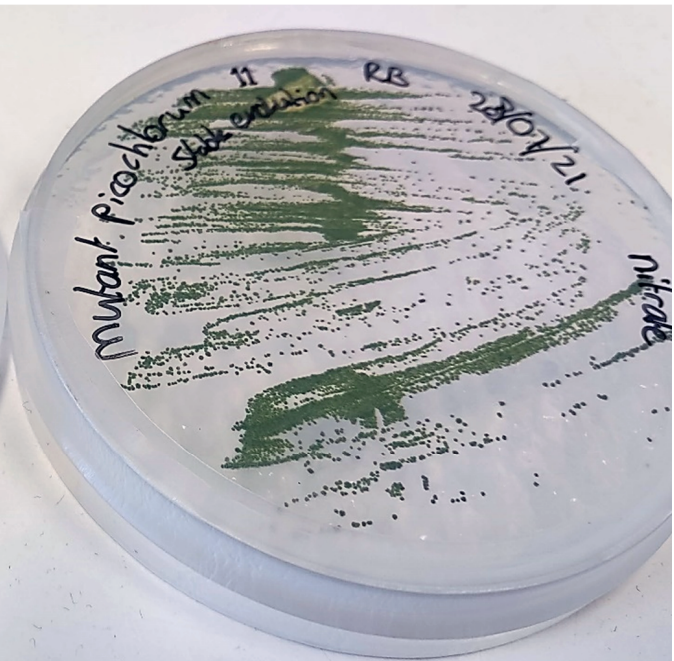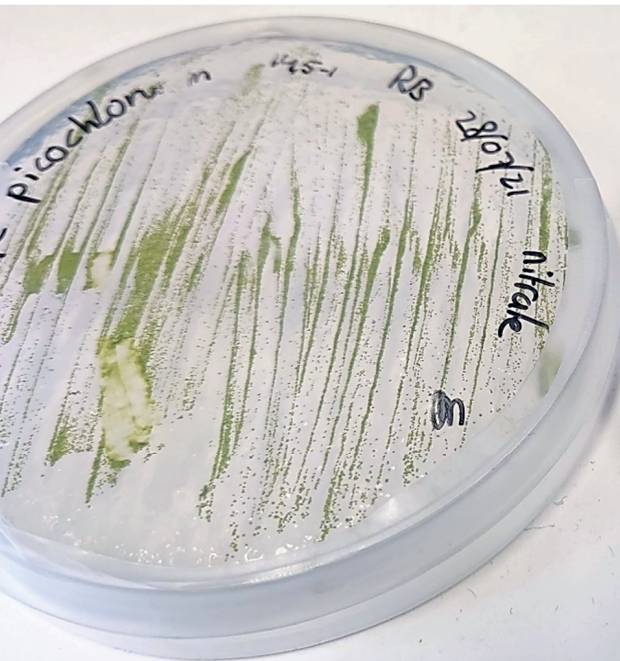
References

References

[1] R.H. Wijffels, M.J. Barbosa, An outlook on microalgal biofuels, Science, 329 (2010) 796-799.

[2] R.H. Wijffels, M.J. Barbosa, M.H. Eppink, Microalgae for the production of bulk chemicals and biofuels, Biofuels, Bioproducts and Biorefining: Innovation for a sustainable economy, 4 (2010) 287-295.

[3] A. Melis, Solar energy conversion efficiencies in photosynthesis: minimizing the chlorophyll antennae to maximize efficiency, Plant science, 177 (2009) 272-280.

[4] J. Ruiz, G. Olivieri, J. de Vree, R. Bosma, P. Willems, J.H. Reith, M.H. Eppink, D.M. Kleinegris, R.H. Wijffels, M.J. Barbosa, Towards industrial products from microalgae, Energy & Environmental Science, 9 (2016) 3036-3043.

[5] J.M. Greene, D. Quiroz, S. Compton, P.J. Lammers, J.C. Quinn, A validated thermal and biological model for predicting algal productivity in large scale outdoor cultivation systems, Algal Research, 54 (2021) 102224.

[6] M. Ras, J.-P. Steyer, O. Bernard, Temperature effect on microalgae: a crucial factor for outdoor production, Reviews in environmental science and bio/technology, 12 (2013) 153-164.

[7] R.J. Barten, R.H. Wijffels, M.J. Barbosa, Bioprospecting and characterization of temperature tolerant microalgae from Bonaire, Algal Research, 50 (2020) 102008.

[8] M. Schroda, D. Hemme, T. Mühlhaus, The Chlamydomonas heat stress response, The Plant Journal, 82 (2015) 466-480.

[9] K. Richter, M. Haslbeck, J. Buchner, The heat shock response: life on the verge of death, Molecular cell, 40 (2010) 253-266.

[10] A.K. Velichko, N.V. Petrova, O.L. Kantidze, S.V. Razin, Dual effect of heat shock on DNA replication and genome integrity, Molecular biology of the cell, 23 (2012) 3450-3460.

[11] Y. Kobayashi, N. Harada, Y. Nishimura, T. Saito, M. Nakamura, T. Fujiwara, T. Kuroiwa, O. Misumi, Algae sense exact temperatures: small heat shock proteins are expressed at the survival threshold temperature in Cyanidioschyzon merolae and Chlamydomonas reinhardtii, Genome biology and evolution, 6 (2014) 2731-2740.

[12] D. Hemme, D. Veyel, T. Mühlhaus, F. Sommer, J. Jüppner, A.-K. Unger, M. Sandmann, I. Fehrle, S. Schönfelder, M. Steup, Systems-wide analysis of acclimation responses to long-term heat stress and recovery in the photosynthetic model organism Chlamydomonas reinhardtii, The Plant Cell, 26 (2014) 4270-4297.

[13] S.I. Allakhverdiev, V.D. Kreslavski, V.V. Klimov, D.A. Los, R. Carpentier, P. Mohanty, Heat stress: an overview of molecular responses in photosynthesis, Photosynthesis research, 98 (2008) 541.

[14] R. Mittler, Oxidative stress, antioxidants and stress tolerance, Trends in plant science, 7 (2002) 405-410.

[15] C. Bowler, M.v. Montagu, D. Inze, Superoxide dismutase and stress tolerance, Annual review of plant biology, 43 (1992) 83-116.

[16] P. Steinrücken, S.R. Erga, S.A. Mjøs, H. Kleivdal, S.K. Prestegard, Bioprospecting North Atlantic microalgae with fast growth and high polyunsaturated fatty acid (PUFA) content for microalgae-based technologies, Algal research, 26 (2017) 392-401.

[17] P. Stokes, T. Hutchinson, K. Krauter, Heavy-metal tolerance in algae isolated from contaminated lakes near Sudbury, Ontario, Canadian Journal of Botany, 51 (1973) 2155-2168.

[18] F. Bleeke, V.M. Rwehumbiza, D. Winckelmann, G. Klöck, Isolation and characterization of new temperature tolerant microalgal strains for biomass production, Energies, 7 (2014) 7847-7856.

[19] F. Foflonker, D.C. Price, H. Qiu, B. Palenik, S. Wang, D. Bhattacharya, Genome of the halotolerant green alga P icochlorum sp. reveals strategies for thriving under fluctuating environmental conditions, Environmental microbiology, 17 (2015) 412-426.

[20] M. Krasovec, E. Vancaester, S. Rombauts, F. Bucchini, S. Yau, C. Hemon, H. Lebredonchel, N. Grimsley, H. Moreau, S. Sanchez-Brosseau, Genome analyses of the microalga Picochlorum provide insights into the evolution of thermotolerance in the green lineage, Genome biology and evolution, 10 (2018) 2347-2365.

[21] J.C. Weissman, M. Likhogrud, D.C. Thomas, W. Fang, D.A. Karns, J.W. Chung, R. Nielsen, M.C. Posewitz, High-light selection produces a fast-growing Picochlorum celeri, Algal Research, 36 (2018) 17-28.

[22] J.H. Janssen, P.P. Lamers, R.C. de Vos, R.H. Wijffels, M.J. Barbosa, Translocation and de novo synthesis of eicosapentaenoic acid (EPA) during nitrogen starvation in Nannochloropsis gaditana, Algal Research, 37 (2019) 138-144.

[23] A.J. LaPanse, A. Krishnan, M.C. Posewitz, Adaptive Laboratory Evolution for algal strain improvement: methodologies and applications, Algal Research, (2020) 102122.

[24] Q. Zhao, H. Huang, Adaptive evolution improves algal strains for environmental remediation, Trends in Biotechnology, 39 (2021) 112-115.

[25] M. Dragosits, D. Mattanovich, Adaptive laboratory evolution–principles and applications for biotechnology, Microbial cell factories, 12 (2013) 64.

[26] M. Krasovec, S. Sanchez-Brosseau, N. Grimsley, G. Piganeau, Spontaneous mutation rate as a source of diversity for improving desirable traits in cultured microalgae, Algal research, 35 (2018) 85-90.

[27] C.-E. Schaum, A. Buckling, N. Smirnoff, D. Studholme, G. Yvon-Durocher, Environmental fluctuations accelerate molecular evolution of thermal tolerance in a marine diatom, Nature communications, 9 (2018) 1-14.

[28] V.S. Cooper, A.F. Bennett, R.E. Lenski, Evolution of thermal dependence of growth rate of Escherichia coli populations during 20,000 generations in a constant environment, Evolution, 55 (2001) 889-896.

[29] V.S. Cooper, Experimental evolution as a high-throughput screen for genetic adaptations, MSphere, 3 (2018) e00121-00118.

[30] T.E. Sandberg, M.J. Salazar, L.L. Weng, B.O. Palsson, A.M. Feist, The emergence of adaptive laboratory evolution as an efficient tool for biological discovery and industrial biotechnology, Metabolic engineering, 56 (2019) 1-16.

[31] R.B. Draaisma, R.H. Wijffels, P.E. Slegers, L.B. Brentner, A. Roy, M.J. Barbosa, Food commodities from microalgae, Current opinion in biotechnology, 24 (2013) 169-177.

[32] O. Jorquera, A. Kiperstok, E.A. Sales, M. Embirucu, M.L. Ghirardi, Comparative energy life-cycle analyses of microalgal biomass production in open ponds and photobioreactors, Bioresource technology, 101 (2010) 1406-1413.

[33] Y. Chisti, Biodiesel from microalgae beats bioethanol, Trends in biotechnology, 26 (2008) 126-131.

[34] N.-H. Norsker, M.J. Barbosa, M.H. Vermuë, R.H. Wijffels, Microalgal production—a close look at the economics, Biotechnology advances, 29 (2011) 24-27.

[35] Q. Huang, F. Jiang, L. Wang, C. Yang, Design of photobioreactors for mass cultivation of photosynthetic organisms, Engineering, 3 (2017) 318-329.

[36] Q. Bechet, A. Shilton, O.B. Fringer, R. Munoz, B. Guieysse, Mechanistic modeling of broth temperature in outdoor photobioreactors, Environmental science & technology, 44 (2010) 2197-2203.

[37] O. Bernard, B. Rémond, Validation of a simple model accounting for light and temperature effect on microalgal growth, Bioresource technology, 123 (2012) 520-527.

[38] L. Xu, P.J. Weathers, X.R. Xiong, C.Z. Liu, Microalgal bioreactors: challenges and opportunities, Engineering in Life Sciences, 9 (2009) 178-189.

[39] B. Wang, C.Q. Lan, M. Horsman, Closed photobioreactors for production of microalgal biomasses, Biotechnology advances, 30 (2012) 904-912.

[40] M.D. Guiry, How many species of algae are there?, Journal of phycology, 48 (2012) 1057-1063.

[41] H.D. Smith-Bädorf, C.J. Chuck, K.R. Mokebo, H. MacDonald, M.G. Davidson, R.J. Scott, Bioprospecting the thermal waters of the Roman baths: isolation of oleaginous species and analysis of the FAME profile for biodiesel production, AMB Express, 3 (2013) 9.

[42] K. Lee, M.L. Eisterhold, F. Rindi, S. Palanisami, P.K. Nam, Isolation and screening of microalgae from natural habitats in the Midwestern United States of America for biomass and biodiesel sources, Journal of natural science, biology, and medicine, 5 (2014) 333.

[43] L.R. Dahlin, A.T. Gerritsen, C.A. Henard, S. Van Wychen, J.G. Linger, Y. Kunde, B.T. Hovde, S.R. Starkenburg, M.C. Posewitz, M.T. Guarnieri, Development of a high-productivity, halophilic, thermotolerant microalga Picochlorum renovo, Communications Biology, 2 (2019) 1-9.

[44] U. Nübel, F. Garcia-Pichel, G. Muyzer, PCR primers to amplify 16S rRNA genes from cyanobacteria, Applied and environmental microbiology, 63 (1997) 3327-3332.

[45] M. Wan, J.N. Rosenberg, J. Faruq, M.J. Betenbaugh, J. Xia, An improved colony PCR procedure for genetic screening of Chlorella and related microalgae, Biotechnology letters, 33 (2011) 1615-1619.

[46] L. de Winter, A.J. Klok, M.C. Franco, M.J. Barbosa, R.H. Wijffels, The synchronized cell cycle of Neochloris oleoabundans and its influence on biomass composition under constant light conditions, Algal Research, 2 (2013) 313-320.

[47] S.O. Lourenço, E. Barbarino, P.L. Lavín, U.M. Lanfer Marquez, E. Aidar, Distribution of intracellular nitrogen in marine microalgae: calculation of new nitrogen-to-protein conversion factors, European Journal of Phycology, 39 (2004) 17-32.

[48] M. Dubois, K.A. Gilles, J.K. Hamilton, P.t. Rebers, F. Smith, Colorimetric method for determination of sugars and related substances, Analytical chemistry, 28 (1956) 350-356.

[49] A.J. Klok, D.E. Martens, R.H. Wijffels, P.P. Lamers, Simultaneous growth and neutral lipid accumulation in microalgae, Bioresource Technology, 134 (2013) 233-243.

[50] C.E. Hare, K. Leblanc, G.R. DiTullio, R.M. Kudela, Y. Zhang, P.A. Lee, S. Riseman, D.A. Hutchins, Consequences of increased temperature and CO2 for phytoplankton community structure in the Bering Sea, Marine Ecology Progress Series, 352 (2007) 9-16.

[51] R. Davis, A. Aden, P.T. Pienkos, Techno-economic analysis of autotrophic microalgae for fuel production, Applied Energy, 88 (2011) 3524-3531.

[52] T.S. Abu-Rezq, L. Al-Musallam, J. Al-Shimmari, P. Dias, Optimum production conditions for different high-quality marine algae, Hydrobiologia, 403 (1999) 97-107.

[53] H.-P. Tsai, L.-T. Chuang, C.-N.N. Chen, Production of long chain omega-3 fatty acids and carotenoids in tropical areas by a new heat-tolerant microalga Tetraselmis sp. DS3, Food chemistry, 192 (2016) 682-690.

[54] Y. Liang, J. Tang, Y. Luo, M.B. Kaczmarek, X. Li, M. Daroch, Thermosynechococcus as a thermophilic photosynthetic microbial cell factory for CO2 utilisation, Bioresource technology, 278 (2019) 255-265.

[55] Z. Krupa, G. öquist, P. Gustafsson, Photoinhibition of photosynthesis and growth responses at different light levels in psbA gene mutants of the cyanobacterium Synechococcus, Physiologia Plantarum, 82 (1991) 1-8.

[56] G. Benvenuti, R. Bosma, M. Cuaresma, M. Janssen, M.J. Barbosa, R.H. Wijffels, Selecting microalgae with high lipid productivity and photosynthetic activity under nitrogen starvation, Journal of applied phycology, 27 (2015) 1425-1431.

[57] G. Breuer, P.P. Lamers, D.E. Martens, R.B. Draaisma, R.H. Wijffels, The impact of nitrogen starvation on the dynamics of triacylglycerol accumulation in nine microalgae strains, Bioresource Technology, 124 (2012) 217-226.

[58] H. Pereira, L. Barreira, L. Custódio, S. Alrokayan, F. Mouffouk, J. Varela, K. Abu-Salah, R. Ben-Hamadou, Isolation and fatty acid profile of selected microalgae strains from the red sea for biofuel production, Energies, 6 (2013) 2773-2783.

[59] K. Schipper, M. Al Muraikhi, G.S.H. Alghasal, I. Saadaoui, T. Bounnit, R. Rasheed, T. Dalgamouni, H.M.S. Al Jabri, R.H. Wijffels, M.J. Barbosa, Potential of novel desert microalgae and cyanobacteria for commercial applications and CO 2 sequestration, Journal of Applied Phycology, (2019) 1-13.

[60] L. Sakhno, Variability in the fatty acid composition of rapeseed oil: Classical breeding and biotechnology, Cytology and genetics, 44 (2010) 389-397.

[61] K.J. Mulders, P.P. Lamers, D.E. Martens, R.H. Wijffels, Phototrophic pigment production with microalgae: biological constraints and opportunities, Journal of phycology, 50 (2014) 229-242.

[62] J.H. Vree, R. Bosma, M. Janssen, M.J. Barbosa, R.H. Wijffels, Comparison of four outdoor pilot-scale photobioreactors, Biotechnology for biofuels, 8 (2015) 215.

[63] T.M. Mata, A.A. Martins, N.S. Caetano, Microalgae for biodiesel production and other applications: a review, Renewable and sustainable energy reviews, 14 (2010) 217-232.

[64] D.A. Los, K.S. Mironov, S.I. Allakhverdiev, Regulatory role of membrane fluidity in gene expression and physiological functions, Photosynthesis research, 116 (2013) 489-509.

[65] S.M. Renaud, L.-V. Thinh, G. Lambrinidis, D.L. Parry, Effect of temperature on growth, chemical composition and fatty acid composition of tropical Australian microalgae grown in batch cultures, Aquaculture, 211 (2002) 195-214.

[66] G. Markou, E. Nerantzis, Microalgae for high-value compounds and biofuels production: a review with focus on cultivation under stress conditions, Biotechnology advances, 31 (2013) 1532-1542.

[67] B. Demmig-Adams, W.W. Adams, Harvesting sunlight safely, Nature, 403 (2000) 371-373.

[68] A.K. Minhas, P. Hodgson, C.J. Barrow, A. Adholeya, A review on the assessment of stress conditions for simultaneous production of microalgal lipids and carotenoids, Frontiers in microbiology, 7 (2016) 546.

[69] T. Leya, A. Rahn, C. Lütz, D. Remias, Response of arctic snow and permafrost algae to high light and nitrogen stress by changes in pigment composition and applied aspects for biotechnology, FEMS microbiology ecology, 67 (2009) 432-443.

[70] C. Dimier, F. Corato, G. Saviello, C. Brunet, PHOTOPHYSIOLOGICAL PROPERTIES OF THE MARINE PICOEUKARYOTE PICOCHLORUM RCC 237 (TREBOUXIOPHYCEAE, CHLOROPHYTA) 1, Journal of phycology, 43 (2007) 275-283.

[71] O. Gaidarenko, C. Sathoff, K. Staub, M.H. Huesemann, M. Vernet, M. Hildebrand, Timing is everything: Diel metabolic and physiological changes in the diatom Cyclotella cryptica grown in simulated outdoor conditions, Algal Research, 42 (2019) 101598.

[72] S. Srirangan, M.-L. Sauer, B. Howard, M. Dvora, J. Dums, P. Backman, H. Sederoff, Interaction of temperature and photoperiod increases growth and oil content in the marine microalgae Dunaliella viridis, PloS one, 10 (2015).

[73] B. Tamburic, S. Guruprasad, D.T. Radford, M. Szabo, R.M. Lilley, A.W. Larkum, J.B. Franklin, D.M. Kramer, S.I. Blackburn, J.A. Raven, The effect of diel temperature and light cycles on the growth of Nannochloropsis oculata in a photobioreactor matrix, PloS one, 9 (2014).

[74] S. Willette, S.S. Gill, B. Dungan, T.M. Schaub, J.M. Jarvis, R.S. Hilaire, F.O. Holguin, Alterations in lipidome and metabolome profiles of Nannochloropsis salina in response to reduced culture temperature during sinusoidal temperature and light, Algal research, 32 (2018) 79-92.

[75] A. Converti, A.A. Casazza, E.Y. Ortiz, P. Perego, M. Del Borghi, Effect of temperature and nitrogen concentration on the growth and lipid content of Nannochloropsis oculata and Chlorella vulgaris for biodiesel production, Chemical Engineering and Processing: Process Intensification, 48 (2009) 1146-1151.

[76] W.J. Henley, J.L. Hironaka, L. Guillou, M.A. Buchheim, J.A. Buchheim, M.W. Fawley, K.P. Fawley, Phylogenetic analysis of the 'Nannochloris-like'algae and diagnoses of Picochlorum oklahomensis gen. et sp. nov.(Trebouxiophyceae, Chlorophyta), Phycologia, 43 (2004) 641-652.

[77] M. Mucko, J. Padisák, M. Gligora Udovič, T. Pálmai, T. Novak, N. Medić, B. Gašparović, P. Peharec Štefanić, S. Orlić, Z. Ljubešić, Characterization of a high lipid-producing thermotolerant marine photosynthetic pico alga from genus Picochlorum (Trebouxiophyceae), European Journal of Phycology, 55 (2020) 384-399.

[78] A. Krishnan, M. Likhogrud, M. Cano, S. Edmundson, J.B. Melanson, M. Huesemann, J. McGowen, J.C. Weissman, M.C. Posewitz, Picochlorum celeri as a model system for robust outdoor algal growth in seawater, Scientific Reports, 11 (2021) 1-13.

[79] G. Breuer, W.A. Evers, J.H. de Vree, D.M. Kleinegris, D.E. Martens, R.H. Wijffels, P.P. Lamers, Analysis of fatty acid content and composition in microalgae, JoVE (Journal of Visualized Experiments), (2013) e50628.

[80] S.J. Edmundson, M.H. Huesemann, The dark side of algae cultivation: Characterizing night biomass loss in three photosynthetic algae, Chlorella sorokiniana, Nannochloropsis salina and Picochlorum sp, Algal research, 12 (2015) 470-476.

[81] L. de Winter, I.T.D. Cabanelas, D.E. Martens, R.H. Wijffels, M.J. Barbosa, The influence of day/night cycles on biomass yield and composition of Neochloris oleoabundans, Biotechnology for biofuels, 10 (2017) 104.

[82] H.A. Frank, R.J. Cogdell, Carotenoids in photosynthesis, Photochemistry and photobiology, 63 (1996) 257-264.

[83] P. Jahns, A.R. Holzwarth, The role of the xanthophyll cycle and of lutein in photoprotection of photosystem II, Biochimica et Biophysica Acta (BBA)-Bioenergetics, 1817 (2012) 182-193.

[84] J. Masojidek, J. Kopecký, M. Koblížek, G. Torzillo, The xanthophyll cycle in green algae (Chlorophyta): its role in the photosynthetic apparatus, Plant Biology, 6 (2004) 342-349.

[85] J.E. Polle, S. Kanakagiri, E. Jin, T. Masuda, A. Melis, Truncated chlorophyll antenna size of the photosystems—a practical method to improve microalgal productivity and hydrogen production in mass culture, International Journal of Hydrogen Energy, 27 (2002) 1257-1264.

[86] J. Aussant, F. Guihéneuf, D.B. Stengel, Impact of temperature on fatty acid composition and nutritional value in eight species of microalgae, Applied microbiology and biotechnology, 102 (2018) 5279-5297.

[87] D.L. Falcone, J.P. Ogas, C.R. Somerville, Regulation of membrane fatty acid composition by temperature in mutants of Arabidopsis with alterations in membrane lipid composition, BMC plant biology, 4 (2004) 17.

[88] P. Oostlander, J. van Houcke, R.H. Wijffels, M.J. Barbosa, Microalgae production cost in aquaculture hatcheries, Aquaculture, 525 (2020) 735310.

[89] P. Darvehei, P.A. Bahri, N.R. Moheimani, Model development for the growth of microalgae: A review, Renewable and Sustainable Energy Reviews, 97 (2018) 233-258.

[90] W. Blanken, P.R. Postma, L. de Winter, R.H. Wijffels, M. Janssen, Predicting microalgae growth, Algal research, 14 (2016) 28-38.

[91] J. Quinn, L. De Winter, T. Bradley, Microalgae bulk growth model with application to industrial scale systems, Bioresource technology, 102 (2011) 5083-5092.

[92] E. Lee, M. Jalalizadeh, Q. Zhang, Growth kinetic models for microalgae cultivation: a review, Algal Research, 12 (2015) 497-512.

[93] A.M. Kliphuis, A.J. Klok, D.E. Martens, P.P. Lamers, M. Janssen, R.H. Wijffels, Metabolic modeling of Chlamydomonas reinhardtii: energy requirements for photoautotrophic growth and maintenance, Journal of applied phycology, 24 (2012) 253-266.

[94] E. Sforza, C. Calvaruso, A. Meneghesso, T. Morosinotto, A. Bertucco, Effect of specific light supply rate on photosynthetic efficiency of Nannochloropsis salina in a continuous flat plate photobioreactor, Applied microbiology and biotechnology, 99 (2015) 8309-8318.

[95] G.M. León-Saiki, N.F. Ledo, D. Lao-Martil, D. van der Veen, R.H. Wijffels, D.E. Martens, Metabolic modelling and energy parameter estimation of Tetradesmus obliquus, Algal research, 35 (2018) 378-387.

[96] X.-N. Ma, T.-P. Chen, B. Yang, J. Liu, F. Chen, Lipid production from Nannochloropsis, Marine drugs, 14 (2016) 61.

[97] Y. Li, M. Horsman, B. Wang, N. Wu, C.Q. Lan, Effects of nitrogen sources on cell growth and lipid accumulation of green alga Neochloris oleoabundans, Applied microbiology and biotechnology, 81 (2008) 629-636.

[98] T. De Mooij, M. Janssen, O. Cerezo-Chinarro, J.H. Mussgnug, O. Kruse, M. Ballottari, R. Bassi, S. Bujaldon, F.-A. Wollman, R.H. Wijffels, Antenna size reduction as a strategy to increase biomass productivity: a great potential not yet realized, Journal of applied phycology, 27 (2015) 1063-1077.

[99] J.H. de Vree, Outdoor production of microalgae, Wageningen University, 2016.

[100] S. Pirt, The maintenance energy of bacteria in growing cultures, Proceedings of the Royal Society of London. Series B. Biological Sciences, 163 (1965) 224-231.

[101] A.D. Jassby, T. Platt, Mathematical formulation of the relationship between photosynthesis and light for phytoplankton, Limnology and oceanography, 21 (1976) 540-547.

[102] S.J. Pirt, Maintenance energy: a general model for energy-limited and energy-sufficient growth, Archives of microbiology, 133 (1982) 300-302.

[103] K. Tuantet, H. Temmink, G. Zeeman, R.H. Wijffels, C.J. Buisman, M. Janssen, Optimization of algae production on urine, Algal Research, 44 (2019) 101667.

[104] B.E. Chalker, Modeling light saturation curves for photosynthesis: an exponential function, Journal of Theoretical Biology, 84 (1980) 205-215.

[105] J.-W.F. Zijffers, K.J. Schippers, K. Zheng, M. Janssen, J. Tramper, R.H. Wijffels, Maximum photosynthetic yield of green microalgae in photobioreactors, Marine biotechnology, 12 (2010) 708-718.

[106] A.M. Kliphuis, M. Janssen, E.J. van den End, D.E. Martens, R.H. Wijffels, Light respiration in Chlorella sorokiniana, Journal of applied phycology, 23 (2011) 935-947.

[107] M. Fachet, R.J. Flassig, L. Rihko-Struckmann, K. Sundmacher, A dynamic growth model of Dunaliella salina: Parameter identification and profile likelihood analysis, Bioresource technology, 173 (2014) 21-31.

[108] R. J. GEIDER, B.A. Osborne, Respiration and microalgal growth: a review of the quantitative relationship between dark respiration and growth, New phytologist, 112 (1989) 327-341.

[109] L. Gouveia, A.E. Marques, T.L. Da Silva, A. Reis, Neochloris oleabundans UTEX# 1185: a suitable renewable lipid source for biofuel production, Journal of industrial microbiology & biotechnology, 36 (2009) 821-826.

[110] M. Arumugam, A. Agarwal, M.C. Arya, Z. Ahmed, Influence of nitrogen sources on biomass productivity of microalgae Scenedesmus bijugatus, Bioresource technology, 131 (2013) 246-249.

[111] L.F. Wu, P.C. Chen, C.M. Lee, The effects of nitrogen sources and temperature on cell growth and lipid accumulation of microalgae, International Biodeterioration & Biodegradation, 85 (2013) 506-510.

[112] M. Janssen, Microalgal photosynthesis and growth in mass culture, Advances in Chemical Engineering, Elsevier2016, pp. 185-256.

[113] D. Balchin, M. Hayer-Hartl, F.U. Hartl, In vivo aspects of protein folding and quality control, Science, 353 (2016).

[114] S. Mathur, D. Agrawal, A. Jajoo, Photosynthesis: response to high temperature stress, Journal of Photochemistry and Photobiology B: Biology, 137 (2014) 116-126.

[115] V. Zachleder, I. Ivanov, M. Vítová, K. Bišová, Cell cycle arrest by Supraoptimal temperature in the alga Chlamydomonas reinhardtii, Cells, 8 (2019) 1237.

[116] M.-H. Liang, J.-G. Jiang, L. Wang, J. Zhu, Transcriptomic insights into the heat stress response of Dunaliella bardawil, Enzyme and microbial technology, 132 (2020) 109436.

[117] R. Barten, Y. Djohan, W. Evers, R. Wijffels, M. Barbosa, Towards industrial production of microalgae without temperature control: The effect of diel temperature fluctuations on microalgal physiology, Journal of Biotechnology, (2021).

[118] S. Andrews, F. Krueger, A. Segonds-Pichon, L. Biggins, C. Krueger, S. Wingett, FastQC, 2010.

[119] D. Kim, J.M. Paggi, C. Park, C. Bennett, S.L. Salzberg, Graph-based genome alignment and genotyping with HISAT2 and HISAT-genotype, Nature biotechnology, 37 (2019) 907-915.

[120] M. Kanehisa, S. Goto, KEGG: kyoto encyclopedia of genes and genomes, Nucleic acids research, 28 (2000) 27-30.

[121] P. Langfelder, S. Horvath, WGCNA: an R package for weighted correlation network analysis, BMC bioinformatics, 9 (2008) 1-13.

[122] K. Maxwell, G.N. Johnson, Chlorophyll fluorescence—a practical guide, Journal of experimental botany, 51 (2000) 659-668.

[123] M.L. Bochman, A. Schwacha, The Mcm complex: unwinding the mechanism of a replicative helicase, Microbiology and Molecular Biology Reviews, 73 (2009) 652-683.

[124] V.L. Vega, W. Charles, A. De Maio, A new feature of the stress response: increase in endocytosis mediated by Hsp70, Cell Stress and Chaperones, 15 (2010) 517-527.

[125] J. de Vries, S. de Vries, B.A. Curtis, H. Zhou, S. Penny, K. Feussner, D.M. Pinto, M. Steinert, A.M. Cohen, K. von Schwartzenberg, Heat stress response in the closest algal relatives of land plants reveals conserved stress signaling circuits, The Plant Journal, 103 (2020) 1025-1048.

[126] F.C. Streich Jr, C.D. Lima, Structural and functional insights to ubiquitin-like protein conjugation, Annual review of biophysics, 43 (2014) 357-379.

[127] F. Kumar Deshmukh, D. Yaffe, M.A. Olshina, G. Ben-Nissan, M. Sharon, The contribution of the 20S proteasome to proteostasis, Biomolecules, 9 (2019) 190.

[128] M.L. Sottile, S.B. Nadin, Heat shock proteins and DNA repair mechanisms: an updated overview, Cell Stress and Chaperones, 23 (2018) 303-315.

[129] A.E. Tjahjono, Y. Hayama, T. Kakizono, Y. Terada, N. Nishio, S. Nagai, Hyper-accumulation of astaxanthin in a green alga Haematococcus pluvialis at elevated temperatures, Biotechnology Letters, 16 (1994) 133-138.

[130] R.R. Ambati, D. Gogisetty, R.G. Aswathanarayana, S. Ravi, P.N. Bikkina, L. Bo, S. Yuepeng, Industrial potential of carotenoid pigments from microalgae: Current trends and future prospects, Critical reviews in food science and nutrition, 59 (2019) 1880-1902.

[131] S. Yao, A. Brandt, H. Egsgaard, C. Gjermansen, Neutral lipid accumulation at elevated temperature in conditional mutants of two microalgae species, Plant physiology and biochemistry, 61 (2012) 71-79.

[132] S. Hu, Y. Ding, C. Zhu, Sensitivity and responses of chloroplasts to heat stress in plants, Frontiers in plant science, 11 (2020) 375.

[133] K. Xu, B. Lv, Y.-X. Huo, C. Li, Toward the lowest energy consumption and emission in biofuel production: combination of ideal reactors and robust hosts, Current opinion in biotechnology, 50 (2018) 19-24.

[134] L. Caspeta, Y. Chen, P. Ghiaci, A. Feizi, S. Buskov, B.M. Hallström, D. Petranovic, J. Nielsen, Altered sterol composition renders yeast thermotolerant, Science, 346 (2014) 75-78.

[135] U.M. Tillich, N. Wolter, P. Franke, U. Dühring, M. Frohme, Screening and genetic characterization of thermo-tolerant Synechocystis sp. PCC6803 strains created by adaptive evolution, BMC biotechnology, 14 (2014) 1-15.

[136] D.R. O'Donnell, C.R. Hamman, E.C. Johnson, C.T. Kremer, C.A. Klausmeier, E. Litchman, Rapid thermal adaptation in a marine diatom reveals constraints and trade-offs, Global change biology, 24 (2018) 4554-4565.

[137] H. Bonnefond, G. Grimaud, J. Rumin, G. Bougaran, A. Talec, M. Gachelin, M. Boutoute, E. Pruvost, O. Bernard, A. Sciandra, Continuous selection pressure to improve temperature acclimation of Tisochrysis lutea, PloS one, 12 (2017) e0183547.

[138] R.W. Ness, A.D. Morgan, N. Colegrave, P.D. Keightley, Estimate of the spontaneous mutation rate in Chlamydomonas reinhardtii, Genetics, 192 (2012) 1447-1454.

[139] L.R. Dahlin, M.T. Guarnieri, Development of the high-productivity marine microalga, Picochlorum renovo, as a photosynthetic protein secretion platform, Algal Research, 54 (2021) 102197.

[140] P. Haldimann, Low growth temperature-induced changes to pigment composition and photosynthesis in Zea mays genotypes differing in chilling sensitivity, Plant, Cell & Environment, 21 (1998) 200-208.

[141] F.H. Arnold, P.L. Wintrode, K. Miyazaki, A. Gershenson, How enzymes adapt: lessons from directed evolution, Trends in biochemical sciences, 26 (2001) 100-106.

[142] F.A. Busch, R.F. Sage, The sensitivity of photosynthesis to O_2 and CO_2 concentration identifies strong Rubisco control above the thermal optimum, New Phytologist, 213 (2017) 1036-1051.

[143] L.J. Chakravarti, V.H. Beltran, M.J. van Oppen, Rapid thermal adaptation in photosymbionts of reef-building corals, Global Change Biology, 23 (2017) 4675-4688.

[144] M.E. Malerba, D.J. Marshall, Testing the drivers of the temperature–size covariance using artificial selection, Evolution, 74 (2020) 169-178.

[145] D. Atkinson, B.J. Ciotti, D.J. Montagnes, Protists decrease in size linearly with temperature: ca. 2.5% C− 1, Proceedings of the Royal Society of London. Series B: Biological Sciences, 270 (2003) 2605-2611.

[146] N.A. Grant, A. Abdel Magid, J. Franklin, Y. Dufour, R.E. Lenski, Changes in Cell Size and Shape During 50,000 Generations of Experimental Evolution with Escherichia coli, Journal of Bacteriology, 203 (2020) e00469-00420.

[147] R.E. Lenski, J.A. Mongold, P.D. Sniegowski, M. Travisano, F. Vasi, P.J. Gerrish, T.M. Schmidt, Evolution of competitive fitness in experimental populations of E. coli: what makes one genotype a better competitor than another?, Antonie van Leeuwenhoek, 73 (1998) 35-47.

[148] J.A. Mongold, R.E. Lenski, Experimental rejection of a nonadaptive explanation for increased cell size in Escherichia coli, Journal of Bacteriology, 178 (1996) 5333-5334.

[149] G. Benvenuti, J. Ruiz, P.P. Lamers, R. Bosma, R.H. Wijffels, M.J. Barbosa, Towards microalgal triglycerides in the commodity markets, Biotechnology for biofuels, 10 (2017) 1-10.

[150] R. Barten, M. Kleisman, G. D'Ermo, H. Nijveen, R.H. Wijffels, M.J. Barbosa, Short-term physiologic response of the green microalga Picochlorum sp.(BPE23) to supra-optimal temperature, Scientific reports, 12 (2022) 1-12.

[151] T.E. Sandberg, M. Pedersen, R.A. LaCroix, A. Ebrahim, M. Bonde, M.J. Herrgard, B.O. Palsson, M. Sommer, A.M. Feist, Evolution of Escherichia coli to 42 C and subsequent genetic engineering reveals adaptive mechanisms and novel mutations, Molecular biology and evolution, 31 (2014) 2647-2662.

[152] S. DeBolt, Copy number variation shapes genome diversity in Arabidopsis over immediate family generational scales, Genome Biology and Evolution, 2 (2010) 441-453.

[153] J. Sebat, B. Lakshmi, J. Troge, J. Alexander, J. Young, P. Lundin, S. Månér, H. Massa, M. Walker, M. Chi, Large-scale copy number polymorphism in the human genome, Science, 305 (2004) 525-528.

[154] T. Wu, L. Li, X. Jiang, Y. Yang, Y. Song, L. Chen, X. Xu, Y. Shen, Y. Gu, Sequencing and comparative analysis of three Chlorella genomes provide insights into strain-specific adaptation to wastewater, Scientific reports, 9 (2019) 1-12.

[155] P.A. da Roza, H.D. Goold, I.T. Paulsen, Picochlorum sp. SENEW3, Trends in genetics: TIG, (2021) S0168-9525 (0121) 00282-00281.

[156] F. Foflonker, D. Mollegard, M. Ong, H.S. Yoon, D. Bhattacharya, Genomic analysis of Picochlorum species reveals how microalgae may adapt to variable environments, Molecular biology and evolution, 35 (2018) 2702-2711.

[157] R. Barten, R. Chin-On, J. de Vree, E. van Beersum, R.H. Wijffels, M. Barbosa, M. Janssen, Growth parameter estimation and model simulation for three industrially relevant microalgae: Picochlorum, Nannochloropsis, and Neochloris, Biotechnology and Bioengineering, (2022).

[158] M. Kolmogorov, J. Yuan, Y. Lin, P.A. Pevzner, Assembly of long, error-prone reads using repeat graphs, Nature biotechnology, 37 (2019) 540-546.

[159] B.J. Walker, T. Abeel, T. Shea, M. Priest, A. Abouelliel, S. Sakthikumar, C.A. Cuomo, Q. Zeng, J. Wortman, S.K. Young, Pilon: an integrated tool for comprehensive microbial variant detection and genome assembly improvement, PloS one, 9 (2014) e112963.

[160] A.M. Bolger, M. Lohse, B. Usadel, Trimmomatic: a flexible trimmer for Illumina sequence data, Bioinformatics, 30 (2014) 2114-2120.

[161] M. Vasimuddin, S. Misra, H. Li, S. Aluru, Efficient architecture-aware acceleration of BWA-MEM for multicore systems, 2019 IEEE International Parallel and Distributed Processing Symposium (IPDPS), IEEE, 2019, pp. 314-324.

[162] H. Li, B. Handsaker, A. Wysoker, T. Fennell, J. Ruan, N. Homer, G. Marth, G. Abecasis, R. Durbin, The sequence alignment/map format and SAMtools, Bioinformatics, 25 (2009) 2078-2079.

[163] C.R. Gonzalez-Esquer, S.N. Twary, B.T. Hovde, S.R. Starkenburg, Nuclear, chloroplast, and mitochondrial genome sequences of the prospective microalgal biofuel strain Picochlorum soloecismus, Genome Announcements, 6 (2018) e01498-01417.

[164] C. Camacho, G. Coulouris, V. Avagyan, N. Ma, J. Papadopoulos, K. Bealer, T.L. Madden, BLAST+: architecture and applications, BMC bioinformatics, 10 (2009) 1-9.

[165] H. Li, Minimap2: pairwise alignment for nucleotide sequences, Bioinformatics, 34 (2018) 3094-3100.

[166] M. Manni, M.R. Berkeley, M. Seppey, F.A. Simão, E.M. Zdobnov, BUSCO update: novel and streamlined workflows along with broader and deeper phylogenetic coverage for scoring of eukaryotic, prokaryotic, and viral genomes, Molecular biology and evolution, 38 (2021) 4647-4654.

[167] D. Mapleson, G. Garcia Accinelli, G. Kettleborough, J. Wright, B.J. Clavijo, KAT: a K-mer analysis toolkit to quality control NGS datasets and genome assemblies, Bioinformatics, 33 (2017) 574-576.

[168] S.A. Becker, R. Spreafico, J.L. Kit, R. Brown, M. Likhogrud, W. Fang, M.C. Posewitz, J.C. Weissman, R. Radakovits, Phased diploid genome sequence for the fast-growing microalga Picochlorum celeri, Microbiology resource announcements, 9 (2020) e00087-00020.

[169] A.R. Quinlan, I.M. Hall, BEDTools: a flexible suite of utilities for comparing genomic features, Bioinformatics, 26 (2010) 841-842.

[170] M. Kokot, M. Długosz, S. Deorowicz, KMC 3: counting and manipulating k-mer statistics, Bioinformatics, 33 (2017) 2759-2761.

[171] T.R. Ranallo-Benavidez, K.S. Jaron, M.C. Schatz, GenomeScope 2.0 and Smudgeplot for reference-free profiling of polyploid genomes, Nature communications, 11 (2020) 1-10.

[172] N. Chen, Using Repeat Masker to identify repetitive elements in genomic sequences, Current protocols in bioinformatics, 5 (2004) 4.10. 11-14.10. 14.

[173] T. Brůna, K.J. Hoff, A. Lomsadze, M. Stanke, M. Borodovsky, BRAKER2: automatic eukaryotic genome annotation with GeneMark-EP+ and AUGUSTUS supported by a protein database, NAR genomics and bioinformatics, 3 (2021) lqaa108.

[174] P. Jones, D. Binns, H.-Y. Chang, M. Fraser, W. Li, C. McAnulla, H. McWilliam, J. Maslen, A. Mitchell, G. Nuka, InterProScan 5: genome-scale protein function classification, Bioinformatics, 30 (2014) 1236-1240.

[175] M. Carlson, H. Pages, AnnotationForge: Tools for building SQLite-based annotation data packages. R Packag. version 1.32. 0, 2020.

[176] E.P. Nawrocki, S.R. Eddy, Infernal 1.1: 100-fold faster RNA homology searches, Bioinformatics, 29 (2013) 2933-2935.

[177] R. Poplin, V. Ruano-Rubio, M.A. DePristo, T.J. Fennell, M.O. Carneiro, G.A. Van der Auwera, D.E. Kling, L.D. Gauthier, A. Levy-Moonshine, D. Roazen, Scaling accurate genetic variant discovery to tens of thousands of samples, BioRxiv, (2017) 201178.

[178] P. Cingolani, A. Platts, L.L. Wang, M. Coon, T. Nguyen, L. Wang, S.J. Land, X. Lu, D.M. Ruden, A program for annotating and predicting the effects of single nucleotide polymorphisms, SnpEff: SNPs in the genome of Drosophila melanogaster strain w1118; iso-2; iso-3, Fly, 6 (2012) 80-92.

[179] T. Wu, E. Hu, S. Xu, M. Chen, P. Guo, Z. Dai, T. Feng, L. Zhou, W. Tang, L. Zhan, clusterProfiler 4.0: A universal enrichment tool for interpreting omics data, The Innovation, 2 (2021) 100141.

[180] S. Kumar, G. Stecher, K. Tamura, MEGA7: molecular evolutionary genetics analysis version 7.0 for bigger datasets, Molecular biology and evolution, 33 (2016) 1870-1874.

[181] L. Caspeta, J. Nielsen, Thermotolerant yeast strains adapted by laboratory evolution show trade-off at ancestral temperatures and preadaptation to other stresses, MBio, 6 (2015) e00431-00415.

[182] J. Masojídek, K. Ranglová, G.E. Lakatos, A.M. Silva Benavides, G. Torzillo, Variables governing photosynthesis and growth in microalgae mass cultures, Processes, 9 (2021) 820.

[183] E. Kaltenegger, S. Leng, A. Heyl, The effects of repeated whole genome duplication events on the evolution of cytokinin signaling pathway, BMC evolutionary biology, 18 (2018) 1-19.

[184] A.H. Yona, Y.S. Manor, R.H. Herbst, G.H. Romano, A. Mitchell, M. Kupiec, Y. Pilpel, O. Dahan, Chromosomal duplication is a transient evolutionary solution to stress, Proceedings of the National Academy of Sciences, 109 (2012) 21010-21015.

[185] C. Jegousse, Y. Yang, J. Zhan, J. Wang, Y. Zhou, Structural signatures of thermal adaptation of bacterial ribosomal RNA, transfer RNA, and messenger RNA, PLoS One, 12 (2017) e0184722.

[186] J. Zhao, Q. He, G. Chen, L. Wang, B. Jin, Regulation of non-coding RNAs in heat stress responses of plants, Frontiers in Plant Science, 7 (2016) 1213.

[187] U.C. Jha, H. Nayyar, R. Jha, M. Khurshid, M. Zhou, N. Mantri, K.H. Siddique, Long non-coding RNAs: Emerging players regulating plant abiotic stress response and adaptation, BMC Plant Biology, 20 (2020) 1-20.

[188] J.E. Barrick, R.E. Lenski, Genome dynamics during experimental evolution, Nature Reviews Genetics, 14 (2013) 827-839.

[189] G.B. Wells, R.C. Dickson, R.L. Lester, Heat-induced elevation of ceramide in Saccharomyces cerevisiae via de novo synthesis, Journal of Biological Chemistry, 273 (1998) 7235-7243.

[190] M.B. Arriola, N. Velmurugan, Y. Zhang, M.H. Plunkett, H. Hondzo, B.M. Barney, Genome sequences of Chlorella sorokiniana UTEX 1602 and Micractinium conductrix SAG

241.80: implications to maltose excretion by a green alga, The plant journal, 93 (2018) 566-586.

[191] L.F. Thatcher, R. Foley, H.J. Casarotto, L.-L. Gao, L.G. Kamphuis, S. Melser, K.B. Singh, The Arabidopsis RNA polymerase II carboxyl terminal domain (CTD) phosphatase-like1 (CPL1) is a biotic stress susceptibility gene, Scientific reports, 8 (2018) 1-14.

[192] K.D. Jofuku, B. Den Boer, M. Van Montagu, J.K. Okamuro, Control of Arabidopsis flower and seed development by the homeotic gene APETALA2, The Plant Cell, 6 (1994) 1211-1225.

[193] F.E. Vaistij, E. Boudreau, S.D. Lemaire, M. Goldschmidt-Clermont, J.-D. Rochaix, Characterization of Mbb1, a nucleus-encoded tetratricopeptide-like repeat protein required for expression of the chloroplast psbB/psbT/psbH gene cluster in Chlamydomonas reinhardtii, Proceedings of the National Academy of Sciences, 97 (2000) 14813-14818.

[194] M.A. Borowitzka, High-value products from microalgae—their development and commercialisation, Journal of applied phycology, 25 (2013) 743-756.

[195] M.A. Alam, Z. Wang, Microalgae biotechnology for development of biofuel and wastewater treatment, Springer2019.

[196] M.A. Borowitzka, A. Vonshak, Scaling up microalgal cultures to commercial scale, European Journal of Phycology, 52 (2017) 407-418.

[197] M. Cuaresma, M. Janssen, C. Vílchez, R.H. Wijffels, Productivity of Chlorella sorokiniana in a short light-path (SLP) panel photobioreactor under high irradiance, Biotechnology and bioengineering, 104 (2009) 352-359.

[198] M. Cuaresma, M. Janssen, C. Vílchez, R.H. Wijffels, Horizontal or vertical photobioreactors? How to improve microalgae photosynthetic efficiency, Bioresource technology, 102 (2011) 5129-5137.

[199] M.J. Griffiths, S.T. Harrison, Lipid productivity as a key characteristic for choosing algal species for biodiesel production, Journal of applied phycology, 21 (2009) 493-507.

[200] T. Mutanda, D. Naidoo, J.K. Bwapwa, A. Anandraj, Biotechnological applications of microalgal oleaginous compounds: current trends on microalgal bioprocessing of products, Frontiers in Energy Research, (2020) 299.

[201] M. Olaizola, C. Grewe, Commercial microalgal cultivation systems, Grand challenges in algae biotechnology, Springer2019, pp. 3-34.

[202] R.A. Soni, K. Sudhakar, R. Rana, Spirulina–From growth to nutritional product: A review, Trends in food science & technology, 69 (2017) 157-171.

[203] X. Chen, L. Zhou, K. Tian, A. Kumar, S. Singh, B.A. Prior, Z. Wang, Metabolic engineering of Escherichia coli: a sustainable industrial platform for bio-based chemical production, Biotechnology advances, 31 (2013) 1200-1223.

[204] S. Fischer, R. Handrick, K. Otte, The art of CHO cell engineering: A comprehensive retrospect and future perspectives, Biotechnology advances, 33 (2015) 1878-1896.

[205] K.-K. Hong, J. Nielsen, Metabolic engineering of Saccharomyces cerevisiae: a key cell factory platform for future biorefineries, Cellular and Molecular Life Sciences, 69 (2012) 2671-2690.

[206] S. Lee, P. Kim, Current status and applications of adaptive laboratory evolution in industrial microorganisms, (2020).

[207] W. Barclay, K. Apt, Strategies for bioprospecting microalgae for potential commercial applications, Handbook of microalgal culture: applied phycology and biotechnology, (2013) 69-79.

[208] L.G. Elliott, C. Feehan, L.M. Laurens, P.T. Pienkos, A. Darzins, M.C. Posewitz, Establishment of a bioenergy-focused microalgal culture collection, Algal Research, 1 (2012) 102-113.

[209] C.J. Hulatt, O. Berecz, E.S. Egeland, R.H. Wijffels, V. Kiron, Polar snow algae as a valuable source of lipids?, Bioresource Technology, 235 (2017) 338-347.

[210] F. Abiusi, E. Trompetter, H. Hoenink, R.H. Wijffels, M. Janssen, Autotrophic and mixotrophic biomass production of the acidophilic Galdieria sulphuraria ACUF 64, Algal Research, 60 (2021) 102513.

[211] A.E. Sproles, F.J. Fields, T.N. Smalley, C.H. Le, A. Badary, S.P. Mayfield, Recent advancements in the genetic engineering of microalgae, Algal Research, 53 (2021) 102158.

[212] H. Mundhada, K. Schneider, H.B. Christensen, A.T. Nielsen, Engineering of high yield production of L-serine in Escherichia coli, Biotechnology and bioengineering, 113 (2016) 807-816.

[213] M. Dragosits, D. Mattanovich, Adaptive laboratory evolution–principles and applications for biotechnology, Microbial cell factories, 12 (2013) 1-17.

[214] R. Barten, T. Peeters, S. Navalho, L. Fontowicz, R.H. Wijffels, M. Barbosa, Expanding the upper-temperature boundary for the microalga Picochlorum sp.(BPE23) by adaptive laboratory evolution, Biotechnology Journal, (2022) 2100659.

[215] B. Zhang, J. Wu, F. Meng, Adaptive Laboratory Evolution of Microalgae: A Review of the Regulation of Growth, Stress Resistance, Metabolic Processes, and Biodegradation of Pollutants, Frontiers in Microbiology, (2021) 2401.

[216] L.J. Jahn, C. Munck, M.M. Ellabaan, M.O. Sommer, Adaptive laboratory evolution of antibiotic resistance using different selection regimes lead to similar phenotypes and genotypes, Frontiers in microbiology, 8 (2017) 816.

[217] C.P. Long, M.R. Antoniewicz, How adaptive evolution reshapes metabolism to improve fitness: recent advances and future outlook, Current opinion in chemical engineering, 22 (2018) 209-215.

[218] A. Hallmann, Advances in Genetic Engineering of Microalgae, Grand Challenges in Algae Biotechnology, Springer2019, pp. 159-221.

[219] E.R. Hanschen, S.R. Starkenburg, The state of algal genome quality and diversity, Algal Research, 50 (2020) 101968.

[220] G. Kumar, A. Shekh, S. Jakhu, Y. Sharma, R. Kapoor, T.R. Sharma, Bioengineering of microalgae: recent advances, perspectives, and regulatory challenges for industrial application, Frontiers in Bioengineering and Biotechnology, 8 (2020) 914.

[221] C.F. Muñoz, C. Südfeld, M.I. Naduthodi, R.A. Weusthuis, M.J. Barbosa, R.H. Wijffels, S. D'Adamo, Genetic engineering of microalgae for enhanced lipid production, Biotechnology Advances, (2021) 107836.

[222] M.I.S. Naduthodi, M.J. Barbosa, J. van der Oost, Progress of CRISPR-Cas based genome editing in photosynthetic microbes, Biotechnology journal, 13 (2018) 1700591.

[223] M.I.S. Naduthodi, N.J. Claassens, S. D'Adamo, J. van der Oost, M.J. Barbosa, Synthetic biology approaches to enhance microalgal productivity, Trends in Biotechnology, (2021).

[224] M. Cano, D.A. Karns, J.C. Weissman, M.L. Heinnickel, M.C. Posewitz, Pigment modulation in response to irradiance intensity in the fast-growing alga Picochlorum celeri, Algal Research, 58 (2021) 102370.

[225] D. McCloskey, S. Xu, T.E. Sandberg, E. Brunk, Y. Hefner, R. Szubin, A.M. Feist, B.O. Palsson, Adaptive laboratory evolution resolves energy depletion to maintain high aromatic metabolite phenotypes in Escherichia coli strains lacking the phosphotransferase system, Metabolic engineering, 48 (2018) 233-242.

[226] D. Choe, J.H. Lee, M. Yoo, S. Hwang, B.H. Sung, S. Cho, B. Palsson, S.C. Kim, B.-K. Cho, Adaptive laboratory evolution of a genome-reduced Escherichia coli, Nature communications, 10 (2019) 1-14.

[227] F. Gao, I. Teles, N. Ferrer-Ledo, R.H. Wijffels, M.J. Barbosa, Production and high throughput quantification of fucoxanthin and lipids in Tisochrysis lutea using single-cell fluorescence, Bioresource Technology, 318 (2020) 124104.

[228] H. Pereira, P.S. Schulze, L.M. Schüler, T. Santos, L. Barreira, J. Varela, Fluorescence activated cell-sorting principles and applications in microalgal biotechnology, Algal research, 30 (2018) 113-120.

[229] C. Südfeld, M. Hubáček, D. Figueiredo, M.I. Naduthodi, J. Van Der Oost, R.H. Wijffels, M.J. Barbosa, S. D'adamo, High-throughput insertional mutagenesis reveals novel targets for enhancing lipid accumulation in Nannochloropsis oceanica, Metabolic Engineering, 66 (2021) 239-258.

[230] H.S. Kim, T.P. Devarenne, A. Han, Microfluidic systems for microalgal biotechnology: a review, Algal research, 30 (2018) 149-161.

[231] H.S. Kim, T.L. Weiss, H.R. Thapa, T.P. Devarenne, A. Han, A microfluidic photobioreactor array demonstrating high-throughput screening for microalgal oil production, Lab on a Chip, 14 (2014) 1415-1425.

Thesis summary

Thesis summary

Photoautotrophic microalgal biomass production for the bulk product market is currently not commercially feasible. Nonetheless, microalgal biomass offers large opportunities due to its composition. Microalgae naturally contain high protein content and in addition accumulate lipids and carbohydrates. Some species contain valuable compounds such as polyunsaturated fatty acids and pigments. However, as mentioned before significant cost reductions must be realized to make the production of microalgal biomass commercially interesting. One factor that impacts the microalgal biomass cost price is the required cooling to maintain the photobioreactor temperature at levels suitable for microalgal growth. The microalgal species that are currently used for cultivation at pilot and commercial scale have an optimal growth temperature of 20°C to 30°C whereas photobioreactor systems heat up to 45°C to 50°C due to solar irradiation, at places with the potential to reach high microalgal productivities.

Species that are capable of growth at higher temperatures naturally reduce the requirement for cooling. In **chapter 2** we performed bioprospecting to isolate thermotolerant strains that were capable of growth at minimally 40°C, but preferably up to higher temperatures. Water samples from Bonaire were enriched with nutrients after which the cell cultures were exposed to a day temperature of 40°C. The stringent selection procedure ensured that the fifty-nine isolated and identified strains were thermotolerant. Five strains were characterized for growth rate and biomass composition to assess their potential for commercial biomass production. *Picochlorum sp. BPE23* was selected as the most promising strain due to its temperature tolerance, high growth rate, and easy cultivation.

Picochlorum sp. BPE23 was characterized for growth under diel cycles with different peak temperatures in **chapter 3**. In addition, in **chapter 4**, strain specific growth parameters were experimentally determined to allow productivity simulations using growth models. Finally, in **chapter 5**, the physiologic response to a temperature shock was studied.

In **chapter 3** we studied the physiology of *Picochlorum sp. BPE23* under four different diel cycles with peak temperatures ranging from 30 °C to 47.5 °C to investigate the potential of the microalgae in a realistic scenario as found in outdoor production. The highest growth rate was observed at a diel peak temperature of 40 °C. However, *Picochlorum sp. BPE23* was able to survive a diel

peak temperature of 47.5 °C. Pigmentation was regulated heavily and was highest at the temperature where growth was highest. In addition, it was found that the polar fatty acid content was highest at the lowest temperature and declined with increasing temperature. On the other hand, the triacylglycerol concentration increased with increasing temperature, indicating accumulation of lipids.

Microalgal growth models to predict productivity need strain specific biological growth parameters as input data. In **chapter 4** we estimated the growth parameters: maximal specific growth rate, maximal yield on light, and maintenance rate, for *Picochlorum sp. BPE23* and two other industrially relevant microalgae *Nannochloropsis sp.* and *Neochloris oleoabundans*. Among these species, *Picochlorum sp. BPE23* exhibited the highest maximal specific growth rate of 4.98±0.24 d^{-1} and the lowest maintenance rate of 0.079 d^{-1}, whereas *N. Oleoabundans* showed the highest biomass yield on light of 1.78 $g_x.mol_{ph}^{-1}$. Finally, model simulations using a pre-existing model were performed with the estimated growth parameters and light conditions as found on Bonaire. *Picochlorum sp. BPE23* displayed the highest areal biomass productivity of 32.2 $g.m^{-2}.d^{-1}$ which corresponds to a photosynthetic efficiency of 2.8%.

Supra-optimal temperature impacts nearly every cellular process and ultimately results in decreased growth or even cell death. To elucidate the physiologic stress response to supra-optimal temperatures we exposed *Picochlorum sp. BPE23* to a temperature of 42 °C for 120 hours, whereas a temperature of 38 °C is the optimal growth temperature (**chapter 5**). Throughout the experiment, we measured mRNA expression levels, cell growth, and cell composition. Two major observations in response to heat stress are decreased growth and a heat shock response, initiated to protect the cell from damage. One hour after the increase in temperature, 39% of all genes were differentially expressed which was largely reverted after 4 hours. Enrichment analysis showed that mRNA expression levels associated with pathways associated with genes acting in photosynthesis, carbon fixation, ribosome, citrate cycle, and biosynthesis of metabolites and amino acids were downregulated, whereas the proteasome, autophagy, and endocytosis were upregulated. Just as in **Chapter 3**, an accumulation of lipids was observed under stressful supra-optimal temperatures.

In **Chapter 6** and **Chapter 7** adaptive laboratory evolution (ALE) was applied to expand the maximal growth temperature of *Picochlorum sp. BPE23*. In **Chapter 6** ALE was done using diel cycles of light and temperature to mimic actual growth

conditions as found in photobioreactors. After 390 days the maximal diel peak temperature was shifted from 47.5 °C to 49 °C. Periodic tipping point experiments were performed to monitor the shift in temperature tolerance whereby we found that the maximal temperature for photosynthesis had shifted by approximately 1.5 °C. In **Chapter 7** ALE was performed under stable temperature and continuous light. After 322 days and 293 generations the cell culture showed a shifted maximal growth temperature from 42 °C to 44.6 °C. Isolated mutant strains had their maximal growth rate increased by 70.5% and their maximal biomass yield on light by 22.3%. Consecutive biomass composition and transcriptome analysis of the mutant strains revealed that they had an increased chlorophyll concentration and upregulated photosynthesis, central metabolism, and amino acid biosynthesis. Genome analysis revealed that approximately half of the genome was duplicated in addition to 21 genic mutations. Mutated genes were grouped and discussed with the following headers: adaptation to temperature stress, regulatory genes, photosynthesis, carbon fixation, and energy metabolism. This study is the first to identify microalgal evolutionary mechanisms by combining ALE with genome sequencing. The developed genome assembly and mutant strains provide a strong framework from whereupon *Picochlorum sp. BPE23* can be further developed.

In **Chapter 8** the current challenges concerning photobioreactor growth conditions, strain selection, and strain improvement are discussed within the context of this thesis and literature. Bioprospecting of robust strains and adaptive laboratory are proposed as strong methods for improvement of microalgal strain robustness.

Acknowledgements

Acknowledgements

During the four years that it took to write this PhD thesis, there were many opportunities to meet new people. Some have collaborated on the project, whereas others made life more fun socially. Regardless of their contribution, I am thankful of all these people.

First, I would like to thank my promotors. **Maria**, you taught me to look at topics from the bright side. Your enthusiasm and positive attitude made our meetings very enjoyable. I really appreciated your trust in me throughout my PhD. You gave me opportunities to develop my skills, my network, and my personality. Even when I temporarily did not enjoy the repetitive writing period, you always kept mentioning that you did not worry about my progress because I was doing great. **Rene**, thank you for giving me the opportunity to perform my PhD at BPE. I really enjoyed our annual trip to Bonaire during which we had time to enjoy the ocean in-between work activities. Although I still did not get my diving license, snorkeling on Bonaire was an amazing experience nonetheless. Your strategic input to my PhD was very useful. Especially near the end when I was actively writing papers, this was highly appreciated.

I would also like to thank the other members of the Bonaire project team. **Marcel**, you were always available whenever I needed advice on mathematical equations or photobioreactor set-ups. Your experience and critical questions really helped me to improve my experimental designs. **Rocca**, thank you for the collaboration during the project. Everything that you created was always perfect. I enjoyed our meetings and the visits to Bonaire a lot. **Iago**, I was always happy to hear when you would also join the trip to Bonaire due to your social personality. During the first years of the Bonaire project, I occasionally came to you for advice. I would like to thank you for your input in this stage of my PhD.

During my PhD, a collaboration was set up with the bioinformatics group of the plant sciences department of WUR. **Harm**, I enjoyed working with you. You always took your time to explain things. Your enthusiasm for bioinformatics and for the microalgae project reflected on others and made our meetings fun. **Dirk-Jan**, **Judith**, and **Sandra**, thank you for the amazing collaboration. It was great getting to know you. This thesis would not have been the same without your bioinformatics knowledge and contributions.

A PhD at BPE can't be completed without the great team of supporting staff. **Wendy**, we had a lot of nice talks! Also, your work on coordinating the labs and leading the lab management meeting was great. In addition, your help with HPLC and GC methods made sure that I was able to get the desired data. **Snezana**, you are the BPE mother. I very much enjoyed our talks about everything, but especially about the cats. Also, your help was great whenever I needed something to be ordered or when I needed to cryopreserved microalgae. **Fred** and **Sebastiaan**, your skills in fixing broken equipment were essential during my PhD. Even when I came by on a weekly or even daily basis to ask for help with yet another broken machine, you were always there for me. It sometimes even seemed that reactors automatically fixed themselves when you approached. **Rick**, cultivation of microalgae at AlgaePARC was always a challenge, but your help with the equipment made things manageable. **Tom** (SSB), thank you for your help with the mRNA extraction and analysis. **Marina** and **Miranda**, thank you for helping me with my administrative tasks and for the social talks.

I would like to thank all the other staff members of BPE for the courses, lectures and advice that they gave during my education and PhD: **Ruud**, **Sarah**, **Marian**, **Antoinette**, **Rafael**, **Corjan**, **Arjen**, **Sarah**, **Dirk**, **Giuseppe, Iulian**.

Furthermore I would like to thank all the members of the **WUR-Council** for the pleasant collaboration and for the experience of working in a participatory council. Working with all of you was a nice and educative distraction during the last phase of my PhD.

This thesis would not have been possible without the contributions of all the BSc and MSc students. I enjoyed working with each one of you and learned a lot at the same time. Working with you made me grow as a person. Thank you **Lidewij** and **Yovita** for helping with the first steps of this thesis by characterizing the microalgae. **Freek**, although your experiments did not go as planned, your hard work and smart mind helped to progress the research nonetheless. **Giulia**, your work with the photobioreactors and the transcriptomics analysis were very important. **Ellen**, thank you for your work on determining the growth model parameters of Picochlorum. **Fieke** and **Juliette**, unfortunately your thesis topics changed from laboratory work to theoretical work due to Covid-19. Your ideas and summaries were still very helpful for conceptualization of the theoretical part of this thesis. **Sofia**, **Emma**, **Teun**, and **Louis**, your work on adaptive laboratory evolution of microalgae and characterization of the species thereafter has become an important

part of this thesis. **Michelle**, you were essential in the bioinformatics analysis. Thank you all for your hard work.

My colleague PhD's and post-docs played an important role for the successful completion of this thesis and added a lot of fun over the past 4 years. **Barbara**, I very much enjoyed our talks about our projects, about weekend activities, and about life. Also, complaining about everything and nothing was very helpful to cope with PhD stress. **Narcis**, you were always there for everyone. The barbeques at your place were a highlight of the time at BPE. **Anna**, the partymeister of BPE. Your continuous efforts to organize borrels and other social activities kept BPE alive. **Pieter**, your happy attitude uplifted the spirits of BPE. Thank you for your support in working with the photobioreactors. I also really enjoyed our beer brewing experiments. **Camilo**, I enjoyed our discussions and talks. Your lessons on cryptocurrency and stock trading were very educative, I still hope to get rich someday. **Kylie**, we had many interesting discussions on vegan food. I hope that your start-up will become a success. **Edgar**, your friendliness, calmness, and dedication to get tasks done inspired me a lot! To Dr. Dr. **August**, it was great to work with you and to discuss microalgae cultivation. **Sabine**, our talks about work, social life, and cats were really nice. **Iris**, we always had fun talks during your time at BPE. Unfortunately you left BPE to pursue your entrepreneurial dream but I am very happy that we stayed in touch. I hope to stay friends for much longer. **Jorijn**, when I started my PhD you were one of the experienced microalgae cultivators at BPE. I could always drop by to ask for advice, thanks a lot for that! **Fabian**, whenever there was a party, you were making drinks that delivered an experience that cannot be forgotten. **Calvin**, I very much enjoyed the beers that we drank together, also your support and advice during the last phase of the PhD was very nice. I would also like to thank the other colleagues at BPE for the support and talks during coffee breaks, lunches, dinners, borrels, lab uitjes, conferences, barbecues, PhD trip and more: **Lukas**, **Rocca**, **Enrico**, **Carlos**, **Iulian**, **Chunzhe**, **Youri**, **Agi**, **Alex**, **Jin**, **Pauline**, **Renske**, **Jort**, **Henrik**, **Omnia**, **Elisa**, **Ana**, **Christian, Pedro**, **Renske**, **Marta**, **Mihris**, **Sebastian**, **Alex**, **Elisa**, **Sofia**, **Jeroen**, **Catalina**, **Wendy**, **Nicola**, **Ana**, **Nuran**, **Mels**.

During the four years of a PhD, office mates come and go. To the office mates of office 2.131: **Rocca**, **Barbara**, **Ivar**, **Camillo**, **Elisa**, **Ana**, and **Mels**, discussing projects and data was very helpful. I also really appreciated all of our social talks.

Picochlorum sp. BPE23, we encountered each other at an ocean bay where you were floating in-between seaweeds and plastic debris. It took a while before I was

convinced of our collaboration. However, this collaboration proved worthwhile as you, **Pico**, became the highlight of my PhD thesis.

Floor, my partner and best friend, you have experienced me throughout the entire PhD. The PhD came with many ups and downs during which you always supported me. I enjoyed explaining the latest status of my PhD to you as you got me thinking about what I was actually doing. Also, although I always kept saying that everything was under control, your doubts on my planning did secretly help me to finish in time :). I am super happy to have you in my life and look forward to all of our upcoming adventures.

Mijn **vrienden** uit Cuijk, Haps, en omstreken. Ik vond het altijd leuk dat jullie interesse toonden in mijn werk. En natuurlijk fijn dat jullie tijdens de weekenden zorgden voor de nodige afleiding onder het genot van een pilsje.

En natuurlijk mijn **familie**, **schoonfamilie**, en in het bijzonder **pap** en **mam**, mijn luie instelling tijdens mijn studie was vroeger was toch wel een beetje een stressfactor voor jullie. Uiteindelijk komt het toch allemaal goed! Jullie support heeft ervoor gezorgd dat ik sta waar ik nu sta. Dankjewel daarvoor.

About the author

Curriculum Vitae

Robin Barten was born on February 11th 1992, In Cuijk and Sint Agatha (Noord Brabant, The Netherlands). He attended 'Het Merletcollege' where he completed his high school (HAVO) with a course specialization in the field of nature, engineering and health. Moving forward, he obtained his bachelor degree on Biology and medical laboratory sciences at the HAN university of applied sciences with specializations in biomedical research and fermentation technology. After completing his bachelor degree, Robin joined the fermentation division of DyadicNL to work as R&D bioprocess technician. After one year of employment, Robin decided to continue his education and enrolled in a master's program at Wageningen University. The 2-year biotechnology master was completed with a specialization in process technology. Both the thesis entitled: 'Optimization of a foam-bed photobioreactor', and internship entitled: 'Production, purification, and characterization of chikungunya virus-like particles' had a strong focus on cell cultivation, cell physiology, and fermentation technology.

After obtaining his MSc degree, Robin directly continued with a PhD program at the Bioprocess engineering department at Wageningen University and Research. The challenge of this PhD program was to reduce microalgal production costs by addressing costly cooling by applying thermotolerant strains. Bioprospecting of thermotolerant strains and consecutive adaptive laboratory evolution were the chosen methods. Extensive strain characterizations were performed utilizing a wide variety of methods. The results of this PhD research are described in this thesis. In addition to the scientific part of the PhD program, Robin participated in the WUR-council as PhD-representative during the academic year of 2020/2021 where he took on the roles of chair in the Finance committee, member in the Education and Research committee, and member in the Wageningen PhD council.

Robin has a strong interest in combining biology with technology through fermentative processes to produce novel products. He plans to continue working in this research area in his future career.

List of publications

Barten, R., Peeters, T., Navalho, S., Fontowicz, L., Wijffels, R. H., & Barbosa, M. (2022). Expanding the upper-temperature boundary for the microalga Picochlorum sp.(BPE23) by adaptive laboratory evolution. *Biotechnology Journal*, 2100659.

Barten, R., Kleisman, M., D'Ermo, G., Nijveen, H., Wijffels, R. H., & Barbosa, M. J. (2022). Short-term physiologic response of the green microalga Picochlorum sp.(BPE23) to supra-optimal temperature. *Scientific reports*, *12*(1), 1-12.

Barten, R., Chin-On, R., de Vree, J., van Beersum, E., Wijffels, R. H., Barbosa, M. J., & Janssen, M. (2022). Growth parameter estimation and model simulation for three industrially relevant microalgae: Picochlorum, Nannochloropsis, and Neochloris. *Biotechnology and Bioengineering*.

Barten, R., Djohan, Y., Evers, W., Wijffels, R., & Barbosa, M. (2021). Towards industrial production of microalgae without temperature control: The effect of diel temperature fluctuations on microalgal physiology. *Journal of Biotechnology*.

Barten, R., Wijffels, R. H., & Barbosa, M. J. (2020). Bioprospecting and characterization of temperature tolerant microalgae from Bonaire. *Algal Research*, *50*, 102008.

Janoska, A., **Barten, R.**, de Nooy, S., van Rijssel, P., Wijffels, R. H., & Janssen, M. (2018). Improved liquid foam-bed photobioreactor design for microalgae cultivation. *Algal research*, *33*, 55-70.

Completed training activities

[1] Poster presentation   [2] Oral presentation

Discipline specific activities	
AlgaEurope Conference [1]	2018
Sustainable Caribbean mini-symposium	2018
Introduction to RNA-Seq and Functional Interpretation	2019
Microalgae Process Design: from cells to photobioreactors	2019
EMBL evolution and ecology Online conference	2020
Nederlandse biotechnologie conferentie [1]	2020
Bioinformatics with Linux and Python	2021
Algal Biomass, Biofuels & Bioproducts [2]	2021
ICRC2021: Prospects and challenges for the development of algal biotechnology [2]	2021

General courses	
VLAG PhD week	2018
Project and time management	2018
Supervising BSc and MSc students	2018
Introduction to R	2019
Applied statistics	2019
High Performance Computing Cluster basic course	2019
Linux basic course	2019
WUR Council training: Onderhandelen en teambuilding	2020
WUR Council training: Working online	2021
Scientific integrity session	2020
Career perspectives	2021
Scientific writing	2021

Optionals	
Preparation of research proposal	2017-2018
PhD study tour to San Diego [1&2]	2018
Weekly group meetings [2]	2017-2020
PhD peer consultation	2018
Microalgae theme meetings [2]	2017-2020
Participation WUR council	2020-2021
Participation Wageningen PhD council	2020-2021
Bonaire project meetings [2]	2017-2021